HYBRID PROPULSION TECHNOLOGY PROGRAM

Volume I
CONCEPTUAL DESIGN PACKAGE

15 October 1989
Final Report

Contract No. NAS 8-37778

Prepared by

G. E. Jensen
A. L. Holzman
S. O. Leisch
J. Keilbach
R. Parsley
J. Humphrey

Prepared for

GEORGE C. MARSHALL SPACE FLIGHT CENTER
NATIONAL AERONAUTICS AND SPACE ADMINISTRATION
MARSHALL SPACE FLIGHT CENTER, AL 35812

by

P.O. Box 49028
San Jose, CA 95161-9028

CONTENTS

CONTENTS (Continued)

ILLUSTRATIONS

ILLUSTRATIONS (Continued)

ILLUSTRATIONS (Continued)

ILLUSTRATIONS (Continued)

ILLUSTRATIONS (Continued)

TABLES

TABLES (Continued)

1.0 INTRODUCTION AND SUMMARY

Future launch systems of the United States will require improvements in booster safety, reliability and cost. In order to increase payload capabilities, performance improvements are also desirable. The hybrid rocket motor (HRM) offers the potential for improvements in all of these areas. By virtue of separation of its inert solid fuel and liquid oxidizer, a hybrid booster offers improved ground and flight safety. Even in the event of a major vehicle structural failure, a propellant explosion or major fire remains a highly improbable occurance with the hybrid system. Moreover, the hybrid booster offers launch abort capability, throttleability to increase launch trajectory performance, and insensitivity to grain anomalies during operation, all of which are not available with solid rocket motor boosters. The safety aspects of the hybrid would allow for modifying manufacture and launch operations, thereby resulting in a reduction of payload-to-orbit costs. Another important benefit associated with the development of large HRM technology is that it provides the means to test critical components, such as nozzles and insulation, under actual operating conditions with full capability to stop and restart the motor. This capability permits evaluating the components at various stages throughout a given operating duration.

Volume I of this report presents the designs for two sizes of hybrid boosters, one duplicating the Advanced Solid Rocket Motor (ASRM) vacuum thrust-time profile and the other a smaller one-quarter thrust level booster. The large booster would be used in tandem, while eight small boosters would be used for the same total thrust. These preliminary designs have been generated as part of NASA contract No. NAS8-37778, Hybrid Propulsion Technology Program. This program is the first phase of an eventual three-phase program culminating in the demonstration of a large subscale engine. The objectives of the Phase I program are to: (1) define preferred hybrid concepts and configurations, (2) identify the concepts and technologies required to enable development of an HRM booster, (3) plan for acquisition of this technology in Phase II, and (4) plan for demonstration of a large subscale HRM in Phase III. Objectives 2 through 4 are discussed in volume II of this report.

The program schedule and program logic for the 6-month Phase I study program are presented in Figures 1-1 and 1-2. The concept definition task was conducted over the entire 6-month period, starting in early March 1989. Since the findings of the design efforts provide the basic input for the Phase II and Phase III programs, the Task 2 technology definition effort was conducted in parallel with the design studies.

As indicated in Figure 1-2, the key features of the CSD Phase I study plan are as follows:

- Full use of the extensive CSD hybrid propulsion database to select and design the hybrid components and booster engines
- Use of CSD analytical models to design and predict performance of hybrid motors
- Use of Pratt and Whitney expertise in the area of oxidizer turbo-pump/feed system technology
- Use of United Technologies Research Center (UTRC) expertise in the area of liquid injection, controls, combustion diagnostics, and health monitoring systems
- Inclusion of the Acurex/Aerotherm oxygen-rich gas generator concept in the system trade studies plus their expertise in the areas of computational fluid dynamics (CFD) modeling and insulation materials
- Use of Space Flight Systems expertise in the areas of vehicle system integration, component design and life cycle costs.

As indicated in Table 1-1, the primary requirement for the large hybrid booster is to meet the ASRM vacuum thrust-time profile depicted in Figure 1-3. The small hybrid booster meets the one-quarter thrust requirement. Booster designs and major subcomponents designs have been completed for both sizes of hybrid booster. The designs were generated using the other design requirements summarized in Table 1-1.

After completing initial studies to select the oxidizer (liquid oxygen) and potential fuel systems, trade studies were performed with the CSD hybrid

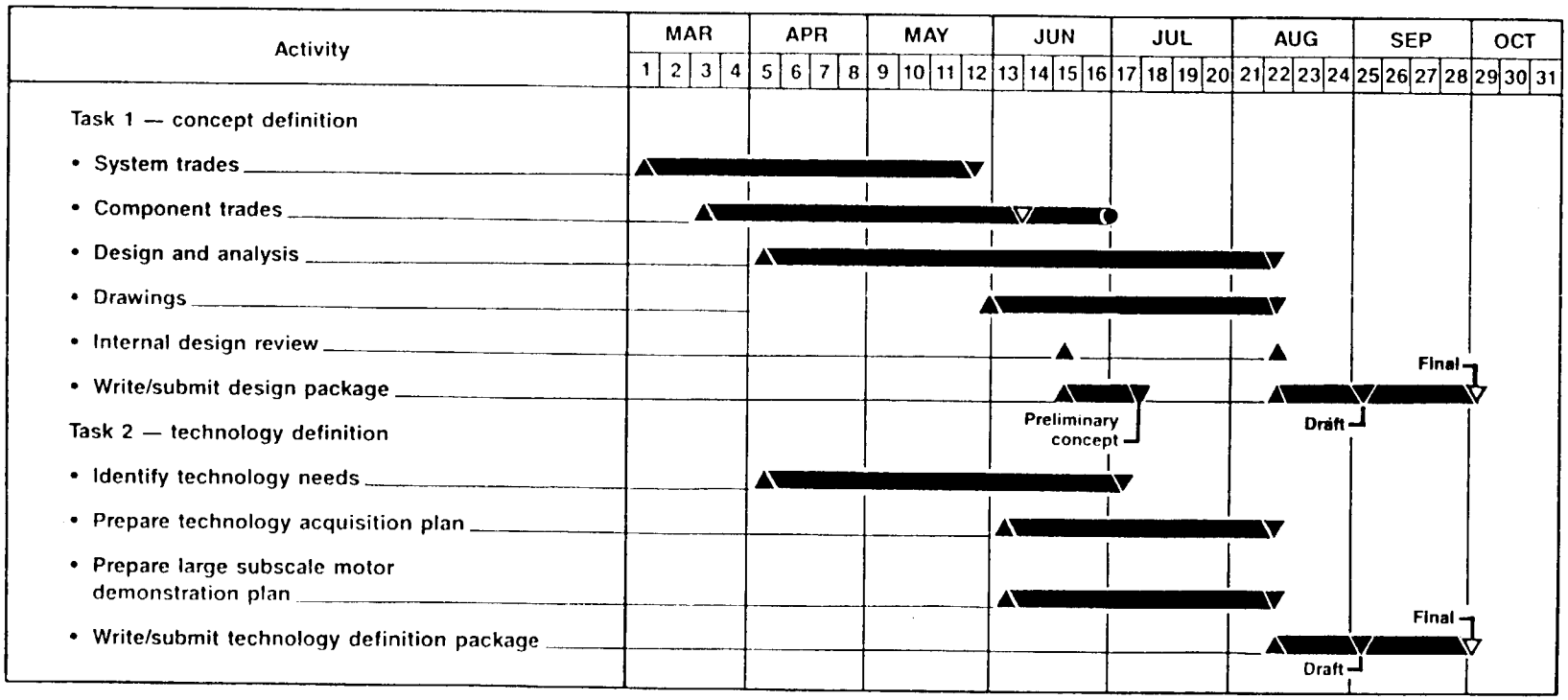

Figure 1-1. Hybrid Propulsion Technology Program Schedule

50478

design/performance model. Fuel performance tables were calculated and representative fuel regression rate data were used to evaluate the effect of fuel composition, motor diameter, number of fuel ports, port geometry, oxidizer delivery system (pump versus pressure feed), oxidizer flow rate, and operating pressure upon booster configuration and weight. These initial studies were nonspecific as to component design with only general size and weight models. In all cases the designs met the thrust-time profile and total impulse requirements of Figure 1-3. Because the hybrid can be throttled to always meet the nominal thrust time curve, the minimum and maximum thrust time limits are not germane. The booster design study was therefore performed using the nominal thrust time curve and a total nominal impulse of 1.44×10^9 N-sec (324,000,000 lb-sec), which corresponds to an action time of 134 sec.

The initial trade and sizing studies resulted in preferred motor diameters, operating pressures, nozzle geometry and fuel grain systems for the large and small boosters. The data were then used for specific performance predictions in terms of payload and for definition and selection of the requirements for the major components: oxidizer feed system, nozzle and thrust vector system. All of these parametric studies were performed using realistic fuel regression models based upon specific experimental data or interpoplated data.

The parametric and sizing studies resulted in the selection of a 4.57-m (180-in.) diameter large booster and a 2.44-m (96-in.) diameter small booster. An average operating pressure of 5.17-MPa (750 psi) was fixed for pump-fed oxygen feed systems, while an average pressure of 3.45-MPa (500 psi) was selected for pressure-fed systems. These values were selected on the basis of minimizing booster weight. Given more precise performance requirements, additional optimization studies would result in slightly different values, but the differences would have minor effects upon the basic designs.

A second design effort was performed using preliminary weight and size requirements for alternative oxygen feed systems, fuels, injector designs, case designs, and nozzle and thrust vector systems. These studies were also

FOLDOUT FRAME 1

FOLDOUT FRAME 2

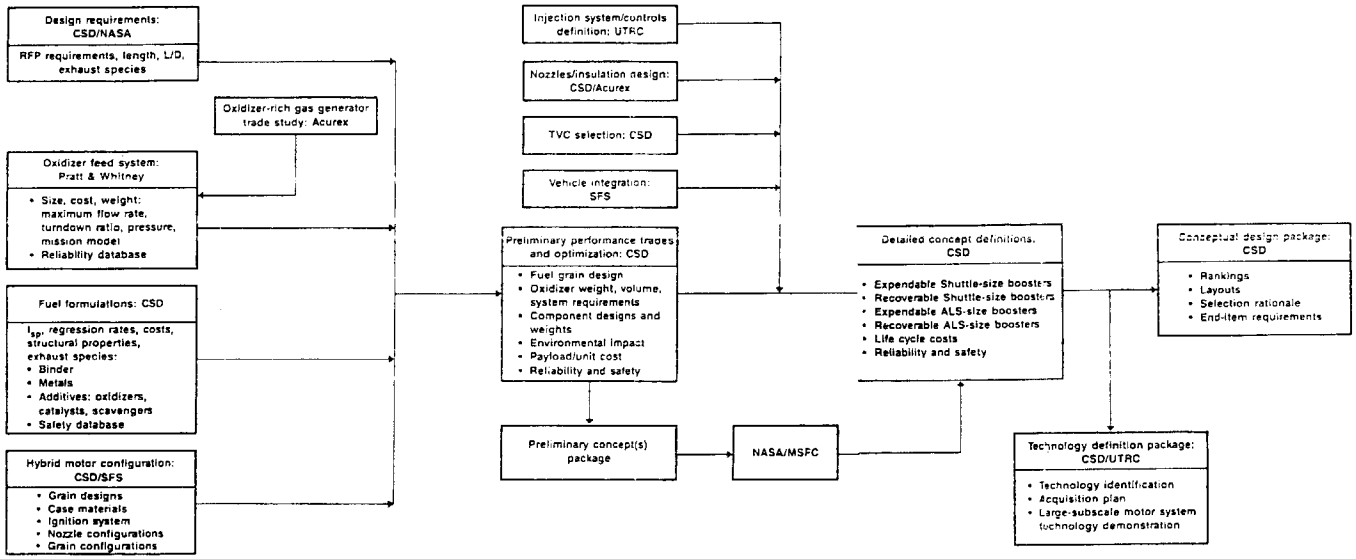

Figure 1 2. Program Flow Diagram
46337

TABLE 1-1. REQUIREMENTS AND TRADES

T16916

Parameter	Requirements/Trades
Thrust-time profile	Table 1 of SOW (March 31, 1989)
Impulse values	Figure 1 (March 31, 1989 SOW)
Motor size	• Two-booster: Shuttle • Eight-booster: Advanced Launch System (ALS)
Thrust vector control	Utilize TVC
Asbestos-containing materials	None allowed
Control systems	Active control: • Performance • Thrust imbalance • Propellant utilization • Transients
Environmentally degrading exhaust products	Minimize
Shelf life	Maximize
Extinguishability	• Goal: extinguish upon fluid flow termination • Required: thrust < 0.7 weight
Safety and reliability	Identical for manned and unmanned
Life cycle costs	• 14-year operational phase • 4-year linear growth • 10-year constant rate: - 1 flight per month - 1 flight per week
Utilization	Expendable-reusable

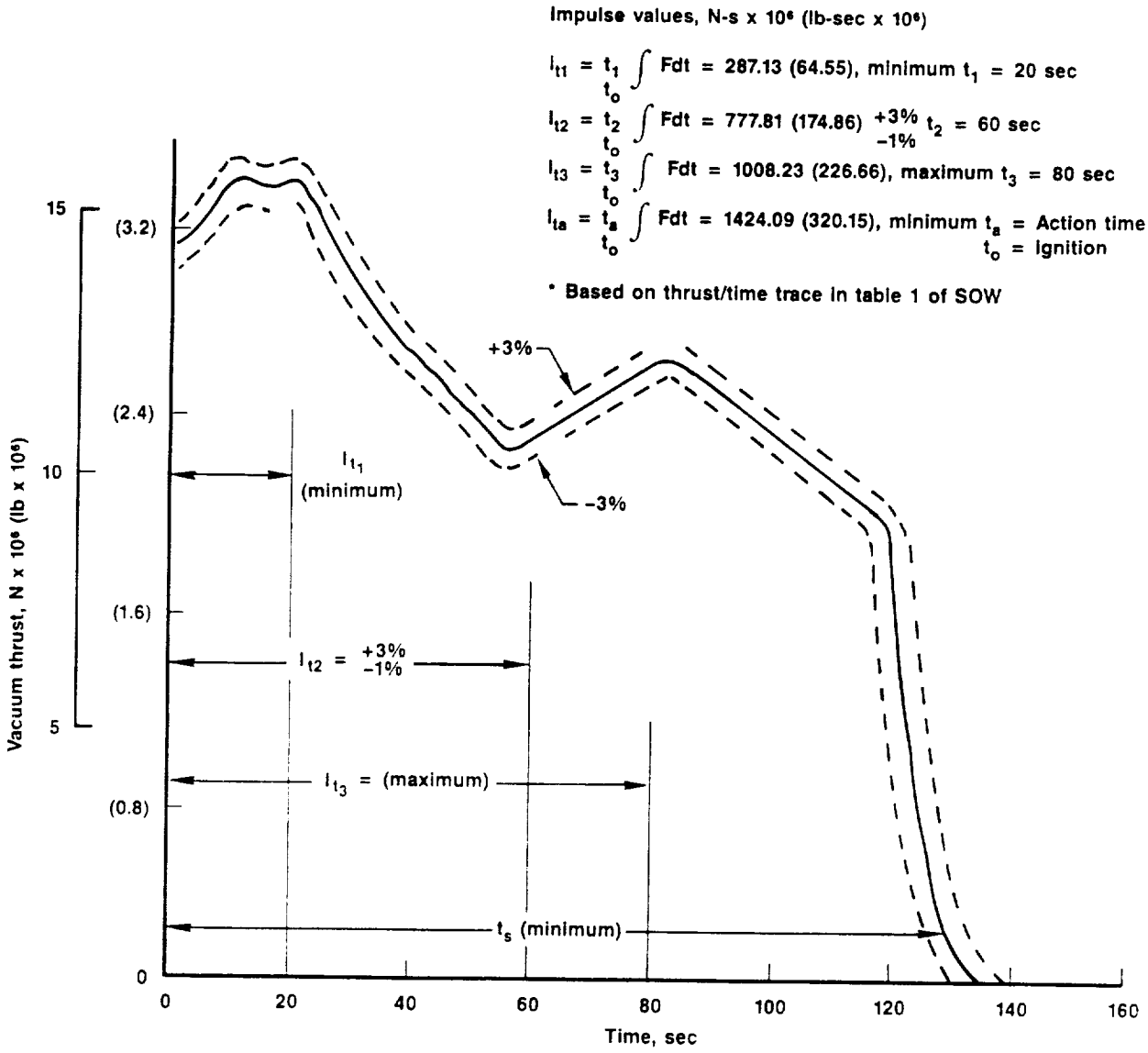

Figure 1-3. ASRM Reference Vacuum Thrust-Time Trace and Impulse Values at 60°F

50448

used to generate performance requirements for the subsystems, which could be used to refine their designs. This second effort generated two large booster designs: a baseline 4.57-m (180-in.) diameter, inert-fuel-grain design and an alternative (3.96-m (156-in.) diameter booster using a high-regression (oxidized) fuel grain. Both systems utilize a pump-fed (3) GOX delivery system. Additionally, a large booster configuration was designed using four parallel 2.44-m (96-in.) diameter combustors (quad design) and a single LOX

tank. A fundamental advantage of this system is that, with individual GOX pumps, the system has engine-out capability thereby significantly improving abort capability.

An inert-fuel, 2.44-m (96-in.) diameter booster with a single pump-fed GOX delivery system was designed for the small booster application as well as the quad design. These designs, discussed in detail in the preliminary design report,[1] served as the preliminary designs for the detailed final engine design and selection studies as well as serving to identify critical technology issues.

Following the generation of the preliminary design concepts, additional sizing and trade studies were performed using detailed subsystem weights and geometries to finalize the designs of the large and small boosters. The baseline large booster is the 4.5-m (180-in.) diameter design, while the small booster is the 2.44-m (96-in.) diameter design. Both contain a HTPB/Escorez hydrocarbon fuel grain which is completely inert and permits thrust termination. The 34-port large fuel grain is cast into two steel cartridges using a continuous mix operation. The two cases are connected with RSRM type field joints, and the segments are also connected to the forward and aft domes using the same type of joint. Based on cost and performance trades, the large case would be recoverable. A recoverable gaseous oxygen (GOX) turbine/pump and injector system has also been baselined for the large hybrid. The large booster utilizes a flexseal moveable nozzle in accordance with the statement of work (SOW) requirement that thrust vector capability be provided.

The small 2.44-m (96-in.) diameter hybrid design is less specific. Life-cycle cost trades favor a nonrecoverable composite overwrapped grain design with a pressure-fed oxygen feed system, if the launch rate is 12 per year. This system would utilize liquid oxygen injection into one quadrant of a fixed nozzle. At the rate of 52 launches per year, a recoverable steel case, pump-fed oxygen feed system motor has the highest overall score considering life-cycle costs, development risk, and performance. However, based on costs per pound of payload an expendable, pump-fed, flexseal nozzle motor is preferred

at either launch rate. Actually, either liquid oxygen injection or a gimballed nozzle could be used for thrust vector control in this system. If the ultimate application were for the advanced launch system (ALS), then a fixed nozzle would be preferred.

The details of both sizes of booster as well as the alternative large booster systems are discussed in the following sections. The following sections also identify the primary technology issues. The proposed plan for acquiring these technologies is supplied in volume II. A major thrust of this study was to identify these limiting technologies through the design of the two boosters. While the RSRM solid propellant booster and the Shuttle mission were used to define delta payload capabilities and were used to a limited extent in the trade and selection processes, there was not a major systems analysis to quantify the performance potential of the hybrid system for different applications. It is felt that this is premature at this time due to the lack of identified missions. The studies do indicate that the hybrid offers extreme design flexibility, has a higher potential performance level than solid boosters, and offers significantly higher safety and abort capabilities. For these reasons, it warrants further analysis as well as technology acquisition studies.

2.0 DESIGN SUMMARY

The sizing studies showed that hybrid boosters offer significant configurational flexibility. Typical sizing trends for the large liquid oxygen (LOX)/hybrocarbon fuel hybrid booster are presented in Figure 2-1. Payload capability is relatively insensitive to diameter over the range of 3.81 to 5.8 m (150 to 200 in.), which corresponds to booster L/Ds of 8 to 18. This is the preferred booster diameter range for the Shuttle-compatible thrust and impulse values defined in the requirements. For the specified requirements, boosters smaller than 3.81 m (150 in.) begin to get too long and lose payload. Boosters larger than 5.08 m (200 in.) in diameter require an increasing number of ports and also lose payload. For the quarter-scale thrust booster requirements, boosters smaller than 1.78 m (70 in.) begin to get too long and those larger than 3.05 m (120 in.) in diameter require numerous ports. This preferred diameter range is driven by the performance requirements and would

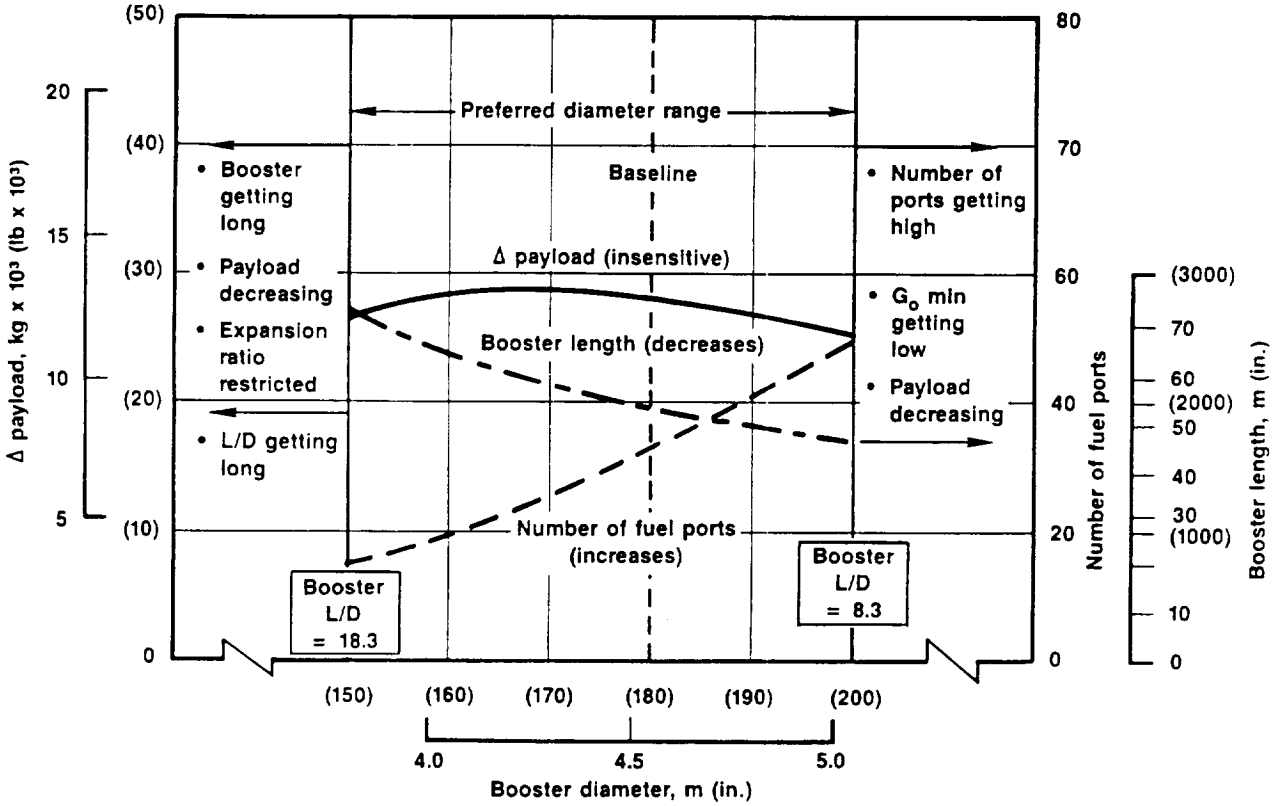

Figure 2-1. Hybrid Booster Sizing Trends

50352

change in response to changes in required performance. This trend also holds for the other hybrid fuel systems.

Figures 2-2, 2-3, and 2-4 summarize the selected configurations for the large and one-quarter-scale hybrid booster applications. All of the hybrid systems use oxygen as the oxidizer because of its commonality at the launch bases, cost, ease of use, and general safety in comparison to other oxidizers. In general, performance comparisons of the optimum pump-fed and pressure-fed systems favored selection of a pump-fed system. The preferred pump system actually produces gaseous oxygen (GOX), which is injected into the forward dome through a manifold injector system.

The booster selections were made partially on the basis of the largest improvement in possible payload capabilities. The method of additional payload analysis is discussed in subsection 3.2.1. If lower payload requirements were specified, the motor weights and lengths could be reduced from the values presented. Also, if the advantages of hybrid throttleability were fully used, the engines could be down sized.

The booster designs are discussed in the following subsections. These designs have been generated for two types of fuels which are discussed in more detail, along with the other system characteristics, in the following sections.

2.1 LARGE MOTOR DESIGN

For the large motor application, three designs have been selected. These include: a baseline single 4.57-m (180-in.) diameter booster; a 3.96-m (156-in.) diameter booster; and a combination system that has four parallel 2.44-m (96-in.) diameter grains with a common oxidizer tank. This latter combination offers definite advantages over the single large booster since it has engine-out capabilities and permits abort of the mission.

The analysis results for the large booster indicate that within the constraints of port L/D and oxidizer mass velocity on hybrid operation, there

FOLDOUT FRAME

FOLDOUT FRAME

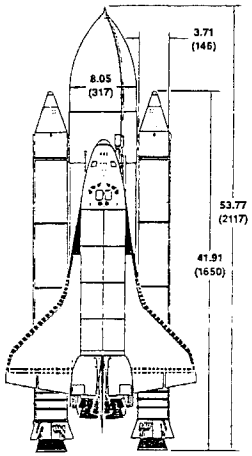

Note: Dimensions are in meters (inches) RSRM

Fuel No.	Solid propellant
Composition	HTPB/AP/Al
Classification	Class B
No. of boosters	2
OD, m (in.)	3.71 (146)
L_{grain}, m (in.)	—
L_{betr}, m (in.)	41.91 (1650)
No. of ports	1
Δpayload, kg (lb)	Reference

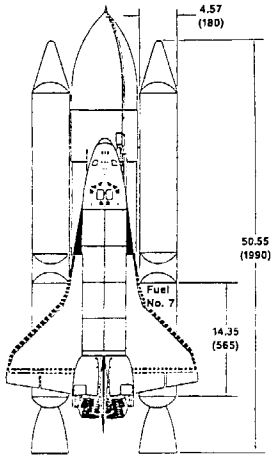

Large Hybrid
(A)

Fuel No.	Hybrid No. 7
Composition	HTPB/Escorez
Classification	Inert
No. of boosters	2
OD, m (in.)	4.57 (180)
L_{grain}, m (in.)	14.35 (565)
L_{betr}, m (in.)	50.55 (1990)
No. of ports	34
Δpayload, kg (lb)	11,533 (25,425)

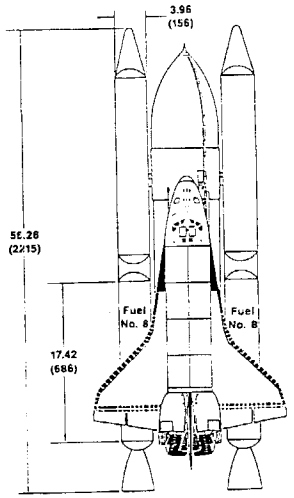

Large Hybrid
(B)

Fuel No.	Hybrid No. 8
Composition	HTPB/Escorez/AP
Classification	Class B
No. of boosters	2
OD, m (in.)	3.96 (166)
L_{grain}, m (in.)	17.42 (686)
L_{betr}, m (in.)	56.26 (2215)
No. of ports	9
Δpayload, kg (lb)	9959 (21,955)

Figure 2-2. Full-Scale Boosters
50466

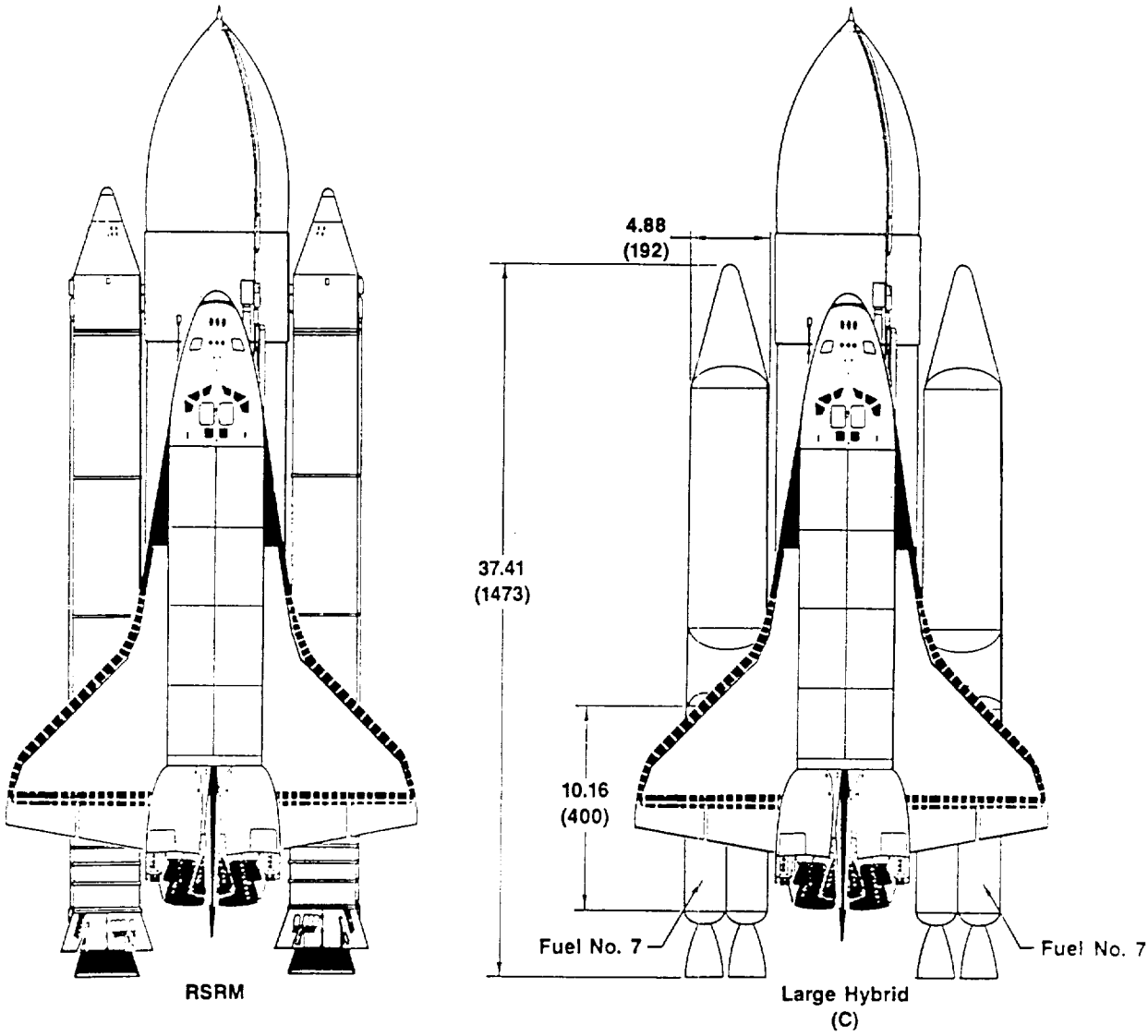

Fuel No.	Solid propellant
Composition	HTPB/AP/Al
Classification	Class B
No. of boosters	2
OD, m (in.)	3.81 (150)
L_{grain}, m (in.)	—
L_{bstr}, m (in.)	41.91 (1650)
No. of ports	1
Δpayload, kg (lb)	Reference

Fuel No.	Hybrid No. 7
Composition	HTPB/Escorez
Classification	Inert
No. of boosters	8
OD, m (in.)	2.44/4.88 (96/192)
L_{grain}, m (in.)	10.16 (400)
L_{bstr}, m (in.)	37.41 (1473)
No. of ports	18
Δpayload, kg (lb)	12,746 (28,100)

Note: Dimensions are in meters (inches)

Figure 2-3. Full-Scale Booster/Quad Combustor

50464

is a large variety of fuels and motor diameters that can be made to perform. Therefore, the selection process was based upon factors other than performance alone; these other factors included reliability, life cycle costs, development risk, fabrication requirements, and transportation issues. These factors were used to select the baseline 4.57-m (180-in.) diameter large booster and the 2.44-m (96-in.) diameter small booster systems.

2.1.1 4.57-m (180-in.) Diameter Booster.

The preliminary design studies show that minimum system weight and best packaging were achieved at a diameter of 4.57-m (180-in.). At this diameter, launch pad modifications would be required if the ultimate application of the hybrid booster were to be a Shuttle SRM replacement. Without this constraint, the 4.57-m (180-in.) diameter is optimum and was selected as the baseline design.

The grain preferred by CSD for the 4.57-m (180-in.) motor is based upon an inert, all-hydrocarbon fuel, (designated fuel No. 7) which provides the highest improvement in payload increment, as well as the highest system safety. The fuel consists of a hydroxyl-terminated polybutadiene (HTPB) binder and a polycyclopentadiene reinforcing agent (Escorez). To achieve the necessary fuel flow, over 30 fuel ports are required. These are arranged in two rows with a central port. While an open dome is used, an equivalent number of oxygen injectors would be used. To increase the system reliability, this booster would have multiple GOX pumps (3) with one-out capability. These feed into a common manifold which supplies the injectors.

Figure 2-2 shows the large booster relative to the shuttle with RSRM boosters. Performance is summarized in Table 2-1, along with that for the alternative 3.96-m (156-in.) diameter large booster and the 2.44-m (96-in.) diameter small booster. As noted, performance is indicated to be higher than that for the solid propellant RSRM booster. However, it should be emphasized that these values are based on RSRM performance partials and the RSRM as a reference. Ultimate performance potential must be based on specific hybrid mission requirements.

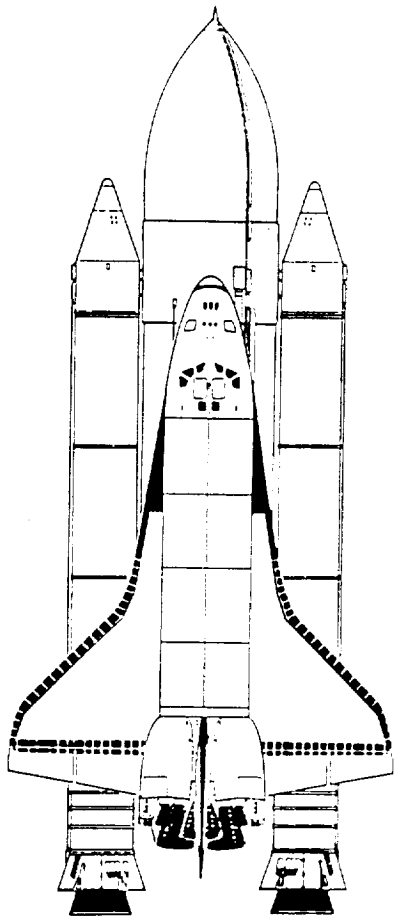

RSRM

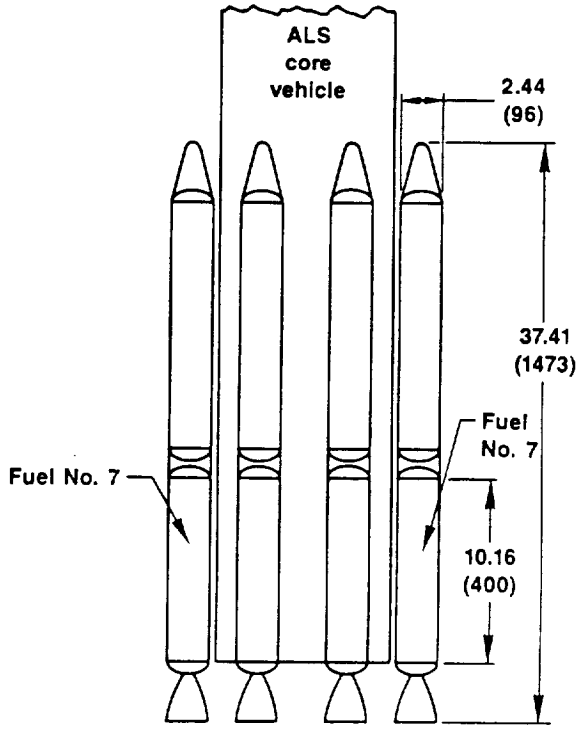

1/4 Scale Hybrid
Booster

Fuel No.	Solid propellant
Composition	HTPB/AP/Al
Classification	Class B
No. of boosters	2
OD, m (in.)	3.81 (150)
L_{grain}, m (in).	—
L_{bstr}, m (in.)	41.91 (1650)
No. of ports	1
Δpayload, kg (lb)	Reference

Fuel No.	Hybrid No. 7
Composition	HTPB/Escorez
Classification	Inert
No. of boosters	8
OD, m (in.)	2.44 (96)
L_{grain}, m (in).	10.16 (400)
L_{bstr}, m (in.)	37.41 (1473)
No. of ports	18
Δpayload, kg (lb)	12,746 (28,100)

Note: Dimensions are in meters (inches)

Figure 2-4. Quarter-Scale Hybrid Booster

50465

TABLE 2-1. HYBRID BOOSTER PERFORMANCE SUMMARY

T17021

Parameter	Booster Size		
	4.57-m (180-in.) Diameter*	3.96-m (156-in.) Diameter†	2.44-m (96-in.) Diameter*
Booster weight, kg (lb)	569,503.1 (1,255,546)	592,016.1 (1,305,179)	141,228.9 (311,358)
Length, m (in.)	50.5 (1990)	56.3 (2215)	37.4 (1473)
Δ payload, kg (lb)	11,532. (25,425)	9976.8 (21,995)	12,745.9 (28,100)
$\overline{O/F}$	2.64	1.84	2.76
$\overline{I_{sp}}$ (vacuum), N-s/kg (sec)	2965 (302.3)	2825 (288.1)	2947 (300.5)
$\overline{P}$, MPa (psi)	5.18 (750)	5.18 (750)	5.18 (750)
MEOP, MPa (psi)	7.01 (1027)	7.14 (1035)	7.27 (1053)
Mass fraction, %	85.3	86.1	86.6
Life cycle cost, $ x 10^6			
One launch per month	6008	Not determined	8757
One launch per week	18,468	Not determined	27,178
$ per pound payload			
One launch per month	2032	Not determined	2252
One launch per week	1943	Not determined	2082

* HTPB/Escorez fuel
† HTPB/Escorez AP/Al fuel

Figures 2-5 and 2-6 show layouts of the 4.57-m (180-in.) hydrocarbon booster and hybrid case, while Table 2-2 provides a weight breakdown. System trades favor a metal two-segment case with separate forward and aft domes. The oxidizer manifold is located above the forward dome with the oxygen being fed in through full cone injectors located above and in-line with the fuel ports. Because of the large number of ports (34), an open dome design has been chosen that permits the use of a common ignition system consisting of supplemental fuel injectors and redundant pyrogen initiators. Individual ports with fuel cast to the injector face would result in lower reliability because of the potential for non-ignition in one or more ports and failure of the grain due to pressure differences between the fuel ports.

Clevis pin field joints similar to the RSRM design for the case segments have been selected on the basis of better performance, lower weight and lower cost. As will be discussed in more detail later, the fuel grains would be processed to eliminate exposure of the joints completely, thereby avoiding any of the problems encountered with the solid propellant solid rocket motors (SRMs).

The steel cases and aft nozzle dome are insulated with strip-wound Kevlar filled EPDM insulation. The forward dome is insulated with a trowelable EPDM insulation that covers the dome and the sides of the oxygen injectors. Because of termination grain stresses, the fuel grains are slotted at the upper end of the forward grain and the lower end of the aft grain. This is done by using release strips installed in the course of the continuous mix operations selected for casting the fuel grains. The two segments are bonded together to eliminate any leak paths to the middle field joint. This is done by installing a preformed fuel gasket between the segments as they are assembled together. The fuel gasket is bonded to the surfaces of both segments using a catalyzed liner system. The forward and aft field joints are insulated with additional thickness of EPDM insulation as well as the fuel grain which extend past the joints.

A flexseal nozzle with hydraulic actuators has been baselined for this application on the basis of proven technology and performance. However, the

performance improvements due to LOX injection were not fully considered in analyzing the alternative liquid injection TVC system shown in Figure 2-3. This is an area requiring further review upon more precise mission requirements and TVC requirements in particular.

At this time, the preferred oxidizer feed system consists of three pumps located in the interstage space between the fuel grain and a composite overwrapped LOX tank. The feed system is based upon a version of the Acurex integral oxidizer-rich burner turbine and LOX pump. This system provides the highest performance with the burner products being added to the oxygen delivery. This is not a critical design issue as alternative pump systems could be used, but at the expense of about 544.3 kg (1200 lb) in delivered payload.

2.1.2 Alternative 3.96-m (156-in.) Diameter Booster

To promote compatibility with the current processing and launch facilities, the preliminary sizing studies show the booster diameter could be reduced to minimize launcher impacts if required. Figure 2-2 shows a 3.96-m (156-in.) diameter version of the large-thrust hybrid booster. For this version, three fuel systems were evaluated. The CSD selection for this size is designated fuel No. 8 and is a high-regression fuel (30% AP/HTPB) which provides a shorter booster length than the inert fuel formulation. Overall safety is compromised, however, by the use of the oxidized fuel. To increase the system reliability, this booster would also have multiple LOX pumps with one-out capability.

2.1.3 Alternative Full-Scale Booster/Quad Combustor

The hybrid booster system studies have also led to a multiple chamber design option. This configuration (Figure 2-3) clusters four of the 1/4-scale fuel grains with a single oxidizer tank to perform the large motor mission. To minimize the size of the combustion chamber/solid fuel case and to provide increased system safety, an all hydrocarbon fuel was selected. Each chamber is either self-contained with its own oxidizer feed pump and thrust vector control system TVC. Alternatively, for increased pump and system reliability, a common feed system consisting of three (3) pumps could be used. The central

FOLDOUT FRAME 1

FOLDOUT FRAME 2

FOLDOUT FRAME 2

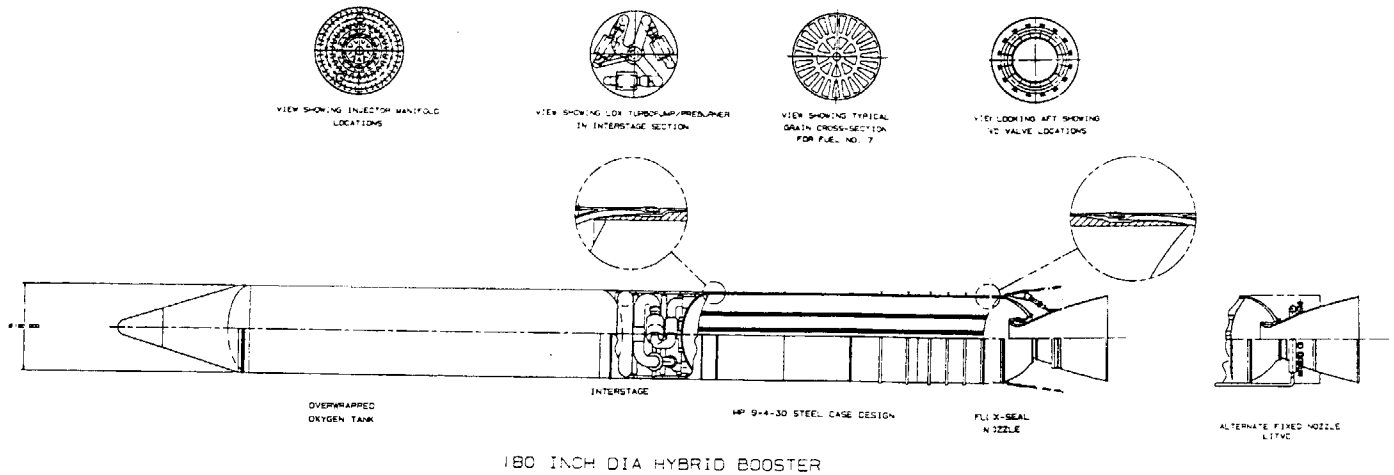

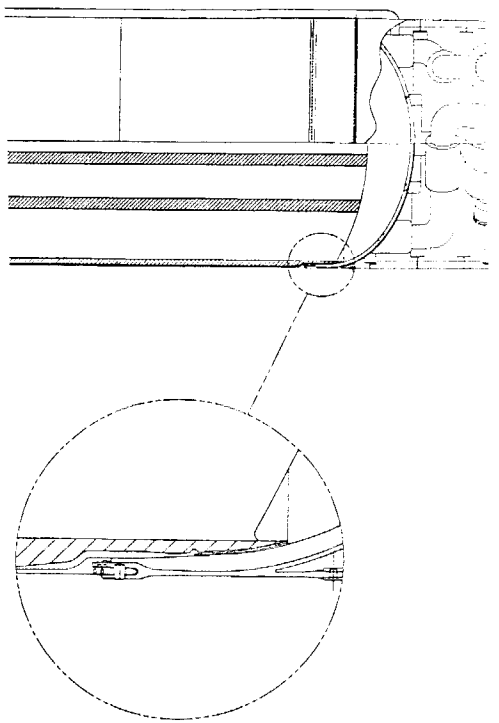

Figure 2-5. 4.57-m (180-in.) Hybrid Booster Motor

50392

2-11

FOLDOUT FRAME 1

FOLDOUT FRAME 2

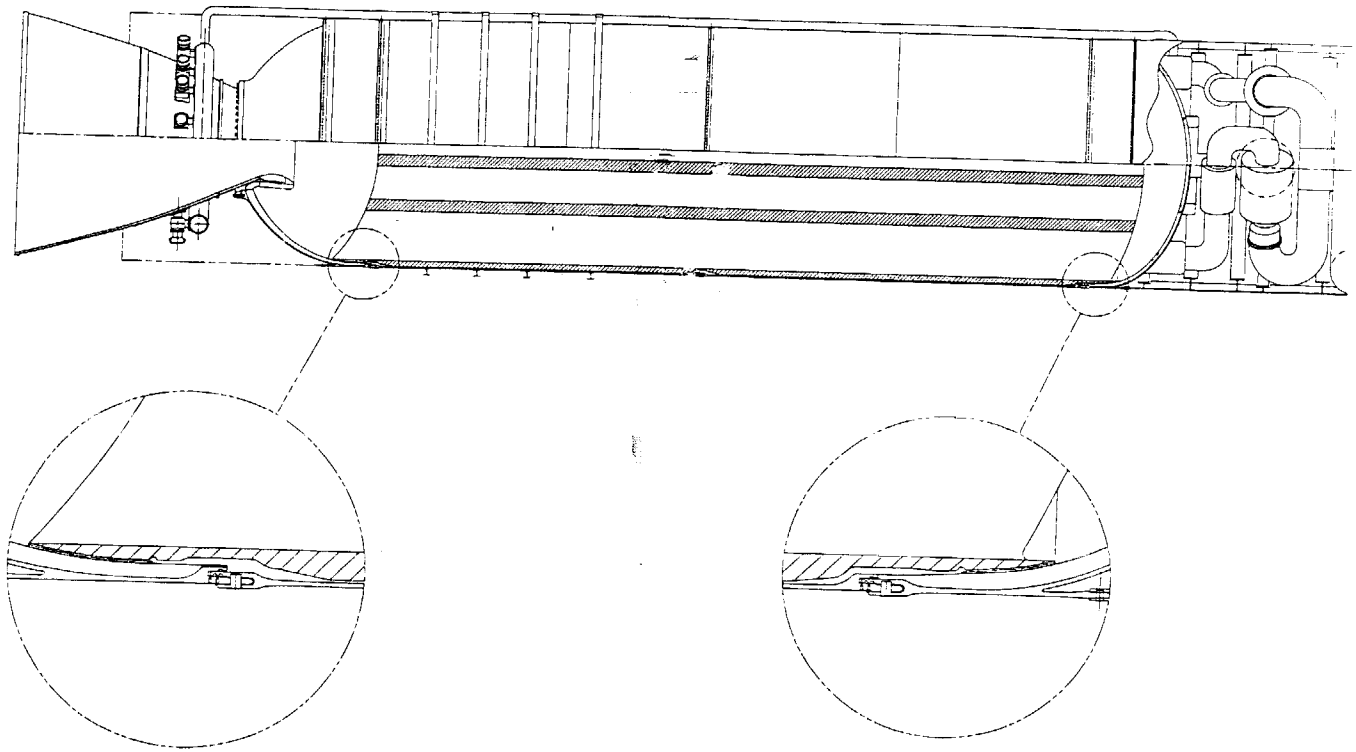

Figure 2-6. 4.57-m (180-in.) Hybrid Case
50393

TABLE 2-2. FINAL DESIGN WEIGHT SCHEDULE - FUEL NO. 7
PUMP FED LOX FLEXSEAL TVC

T16937

Item	Weight, kg (lb)	
	4.57-M (180-in.) Diameter	2.44-M (96-in.) Diameter One Quarter Scale
Hybrid rocket motor	569,506.1 (1,255,546)	141,229.6 (311,358)
Fuel (including 6% residual)	138,068.5 (304,389)	33,645.2 (74,175)
Oxidizer - hybrid (including 0.5% residual LOX and 0.53% residual GOX)	355,790.6 (784,384)	90,689.9 (199,937)
Subsystems, recovery separation motors, standard structures	16,500.3 (36,377)	5150.5 (11,355)
LOX tank (composite with metal liner)	2702.5 (5958)	984.7 (2171)
Interstage structure	1425.2 (3142)	422.7 (932)
Ignition system	226.8 (500)	68 (150)
Motor case	26,912.1 (59,331) (steel)	2766 (6098) (composite)
Case insulation	31,812.7 (70,135)	1794 (3955)
Flexseal nozzle	9867 (21,753)	2502.9 (5518)
Mass fraction	0.387 (0.853)	0.393 (0.866)
Total propellant (fuel, oxidizer	497,620.8 (1,097,066)	125,242.3 (276,112)
Total inerts (does not include residual propellants)	72,837.9 (160,580)	18,209.5 (40,145)

space between the chambers may be used for a common propane tank to drive the four LOX pumps. The single oxidizer tank diameter can be selected to achieve the desired attachment length to the external tank (ET) in the case of the Shuttle or other core vehicle structure. For the large hybrid booster application, the multiple-chamber option offers several advantages. The most important advantage is enhanced manned flight safety achieved through continuous engine-out capability. Normally, command shutdown in response to detected failures or impending failures provides enhanced safety only for the portion of the booster flight during which the orbiter can safely land following booster shutdown or jettison.

The multiple-chamber design is sized to maintain an adequate thrust-to-weight ratio following single chamber shutdown on each booster for shutdown at any time from ignition through booster burnout. This enables the hybrid booster to achieve single engine (pair) failure capability throughout the flight, thereby expanding to multiple failure capability as the flight progresses, a significant enhancement in manned flight safety.

The multiple-chamber option also offers reduced development costs, design simplicity, and enhanced operational flexibility. Using the small motor chamber obviates the need to develop a single large chamber. The small motor can be used singly or in clusters of two, three, or five for other missions without additional chamber development. Each chamber has roughly 1/2 the number of fuel ports as the large motor, which enhances the design simplicity and reduces grain processing costs. Finally, the reduced size of the small motor simplifies recovery if so desired.

2.2 SMALL MOTOR DESIGN

Figure 2-4 shows how eight of the small 1/4-scale hybrid boosters would be clustered around an Advanced Launch System (ALS)-size payload. The inert fuel grain is the same as was selected for the multiple chamber design discussed in the previous subsection. Figure 2-7 shows a layout of the 2.44-m (96-in.) hydrocarbon quarter-scale booster, while Table 2-2 summarizes the weight breakdown. The system definition is less precise for the small

FOLDOUT FRAME 1

FOLDOUT FRAME 2

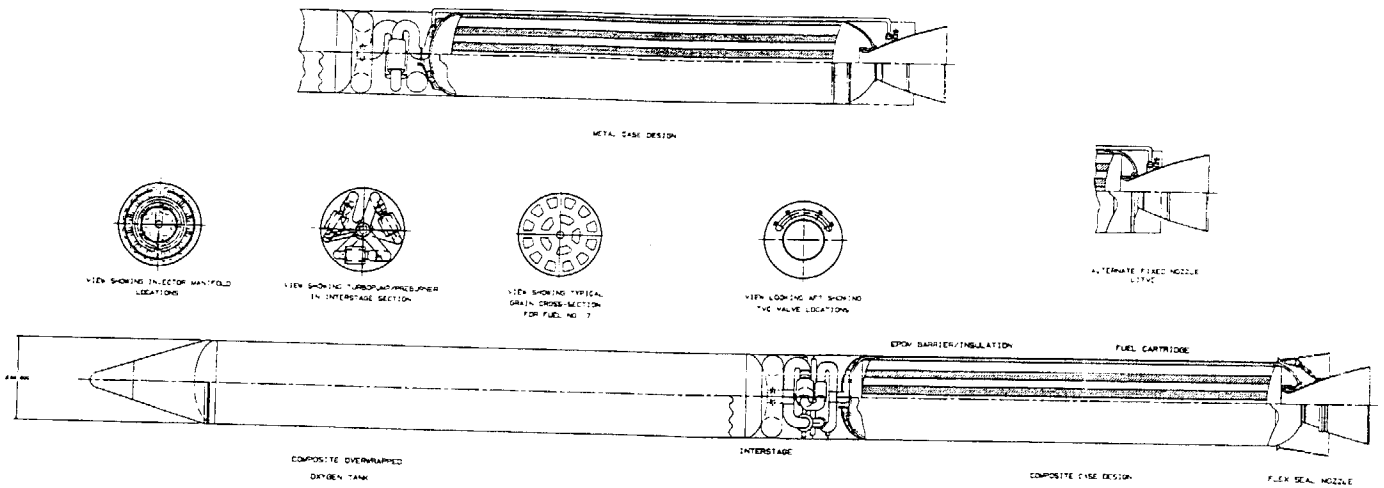

Figure 2-7. 2.44-m (96-in.) Quarter-Scale Booster

50394

2-15/2-16

booster. The low launch rate overall preferred design is pressure fed with LITVC. This is primarily due to a lower life-cycle cost. Highest performance is achieved with a pump-fed system, a flexseal nozzle and a composite combustor case. At the high launch rate the preferred design has three integral GOX burner/turbine/pump units in the interstage. These units use the same basic design as that of the units used in the large motor. GOX is fed into a manifold that is an integral part of the dome. On the basis of reliability and costs, an expendable composite case overwrapped on the precast fuel grain has been selected for the low launch rate application. At the high rate a recoverable steel case is preferred. Also, the trade studies resulted in the selection of either liquid injection fixed nozzles or flexseal nozzles for the small booster, as it was specified that both size boosters have TVC capability. If the application were truly for ALS, it is likely no TVC would be required and the performance of the system would be improved.

A unique feature of the expendable small booster design is that the fuel grain is cast into a cartridge using consumable, nonremovable mandrels. After cure, the cartridge is overwrapped with the forward dome and nozzle polar boss. This facilitates the overwrap process and eliminates mandrel withdrawal problems.

Better definition of the small booster requires further specification of cost and performance. Highest performance is obtained with a composite case, pump-fed, flexseal nozzle design with a delta payload of 28,100 lb, but a low launch rate (LCC) of $\$9438 \times 10^6$ and a high launch rate (LCC) of $\$30,148 \times 10^6$. Using a recoverable steel case and LITVC the delta payload is reduced by about 6000 lb, but the costs are reduced to $\$8775 \times 10^6$ and $\$26,199 \times 10^6$ for the low and high rates. This is the cheapest approach for the high launch rate. If a pressure-fed system is used with an expendable composite case and LITVC, the delta payload drops to 16,915 lb, but the life-cycle costs are the cheapest for the low launch rate at $\$7941 \times 10^6$.

Based on dollars per pound of payload, the small expendable booster with pump fed and the flexseal nozzle is the preferred system. Preliminary calculations show a cost of $2252 per pound of payload at 12 launches per year and $2082 per pound at 52 launches per year. These costs are significantly lower than for any other system.

2.3 BALLISTIC PERFORMANCE SUMMARY

Details of the large booster ballistic performance levels are shown in Figures 2-8 through 2-11. These are essentially the same as for the small booster except for the thrust and oxygen flow rate which are one-quarter the values of the large hybrid.

The pump-fed designs were optimized to a preselected average pressure of 5.17 MPa (750 psi). Consequently, the peak value is approximately 40% higher than the average. Figure 2-8 shows the variation of chamber pressure as a function of burn time. This curve shape is the same independent of average pressure level or booster size. Figure 2-9 plots the thrust profile which meets the revised SOW nominal thrust-time schedule for the large booster. The action time integrated total impulse is 1.44 x 109 N-sec (324 million lb-sec). This exceeds the specified minimum integrated value of 1.42 x 109 N-sec (320.15 million lb-sec). As the hybrid can be throttled to meet the nominal thrust level, the minimum value is not significant.

For the large 4.52-m (180-in.) diameter booster using the all-hydrocarbon inert fuel No. 7, the oxygen flow rate schedule is shown in Figure 2-10 as a function of time. Except for the tailoff after 120 sec, there is less than a 2-to-1 turndown in the oxidizer flow, easily achievable with turbine-driven pumping systems. This head-end oxidizer flow variation will result in a minor varition in the propellant mixture ratio passing through the nozzle. Figure 2-10 shows that there is only a ±5% variation in mixture ratio, which eliminates the need for any aft-end oxidizer injection or more complicated injection distribution scheme. This variation in mixture ratio does not seem to vary

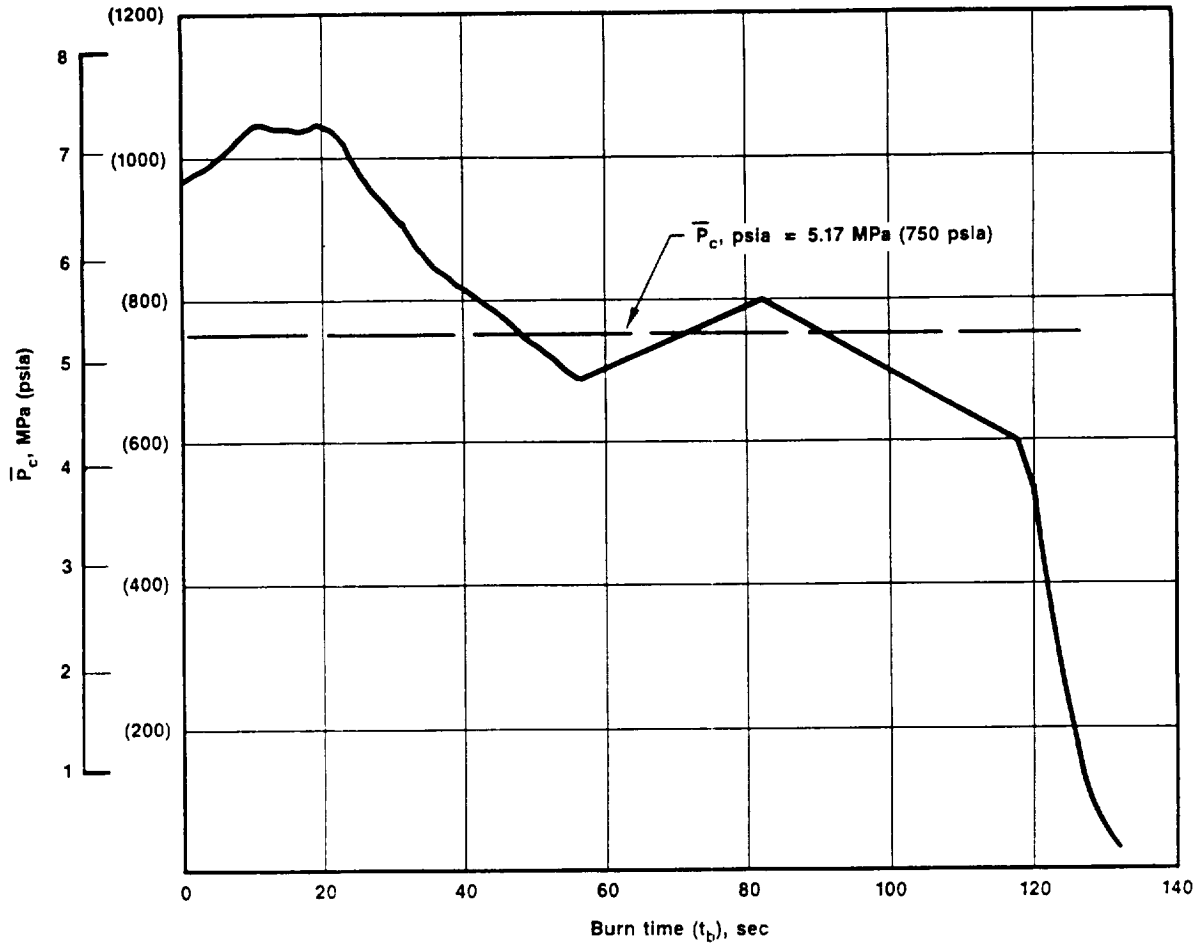

Figure 2-8. Large Hybrid Booster Chamber Pressure as a Funciton of Time
50315

with motor size or total impulse. Note that the supplied total impulse schedule is the same as that to which the ASRMs were designed and does not reflect the optimum shape for the hybrid capabilities. The ASRM curve shape is limited by the ability to design a solid propellant motor to change surface area for producing changes in thrust level. Since the hybrid can be throttled like a bi-propellant liquid rocket, the thrust-time curve can be prescribed with much greater freedom.

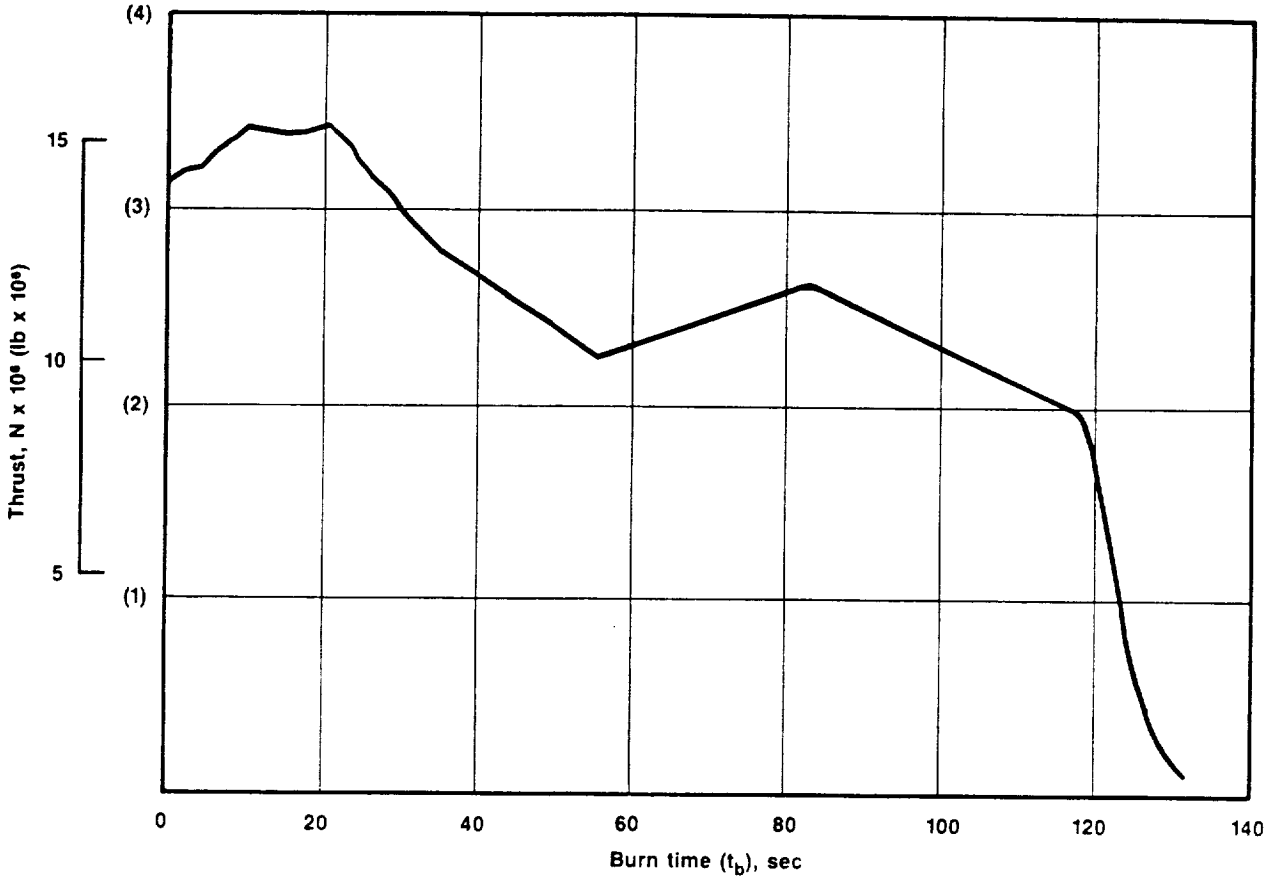

Figure 2-9. Large Hybrid Booster Thrust-Time Schedule

50314

2.4 PERFORMANCE UPDATE

The designs shown in the previous sections do not take advantage of the hybrid throttleability. An item of particular importance to large size boosters is their thrust-energy time distribution. Large launch vehicles have a relatively low thrust-to-weight ratio, which results in lower overall accelerations requiring a steeper trajectory. Such trajectories are characterized by dominating gravity flight losses. A significant reduction of these losses can therefore have a correspondingly consequential effect on payload improvement. Gravity flight losses can be reduced by preparing a proper rocket motor thrust profile that reduces burn time and/or the average flight path angle, while complying with trajectory, aerodynamic and structural load limits. The Space Transportation System (STS) solid rocket boosters (SRBs) have been

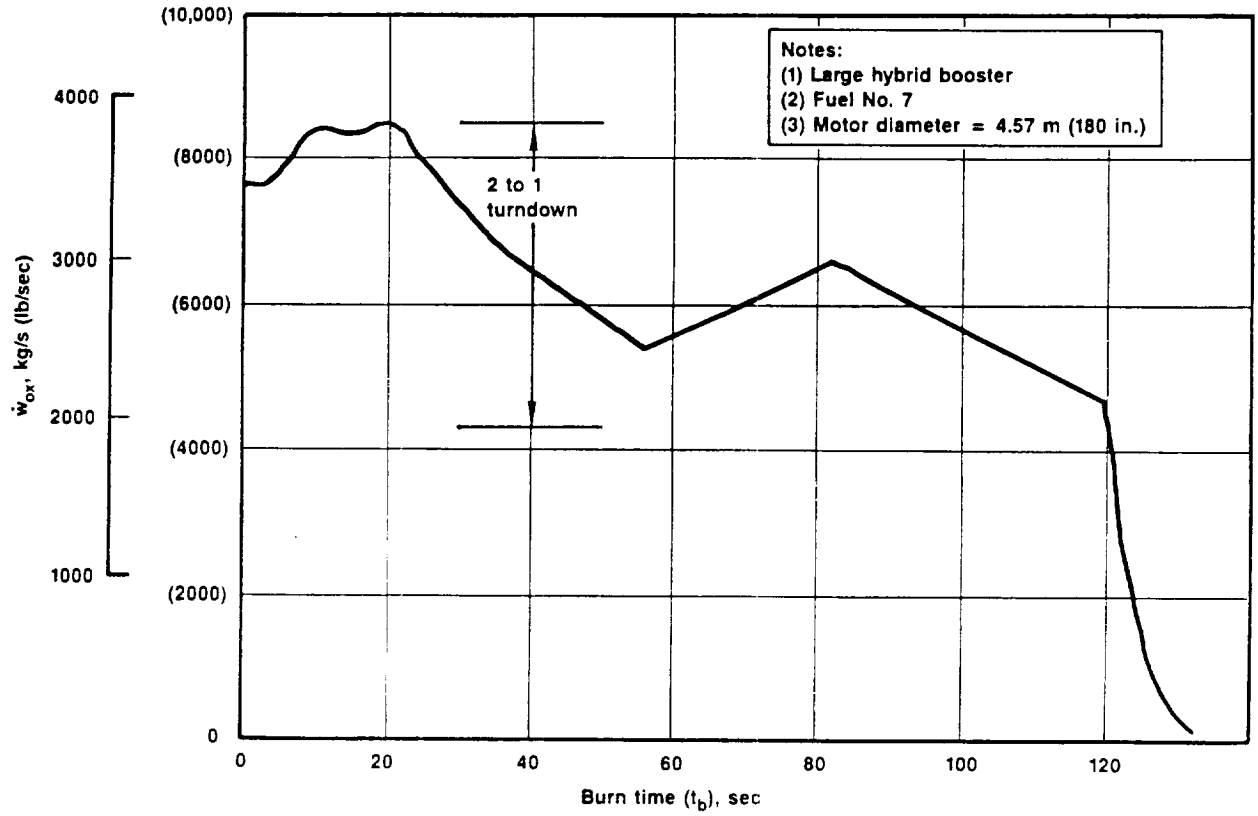

Figure 2-10. Oxygen Flow Rate as a Function of Time

50316

designed to have a saddle-shaped thrust profile for this reason (see Figure 2-9). High up-front thrust decreases the average flight path angle; the saddle section is designed to reduce aerodynamic loading during the period of maximum dynamic pressure. The linear gradual thrust decreasing section (before tail-off) was designed to minimize the burn time while subjecting the structure to their load limits throughout this period. However, this profile has been limited by solid fuel grain ballistic limitations. These limitations impede an enhanced thrust profile that can result in further performance gains. Since the hybrid rocket motor is throttleable, it doesn't have the thrust management limitations inherent to the solid fuel system. A trajectory study was conducted to quantify the payload lift advantage that can be realized from this hybrid feature. The mission trajectory consisted of a

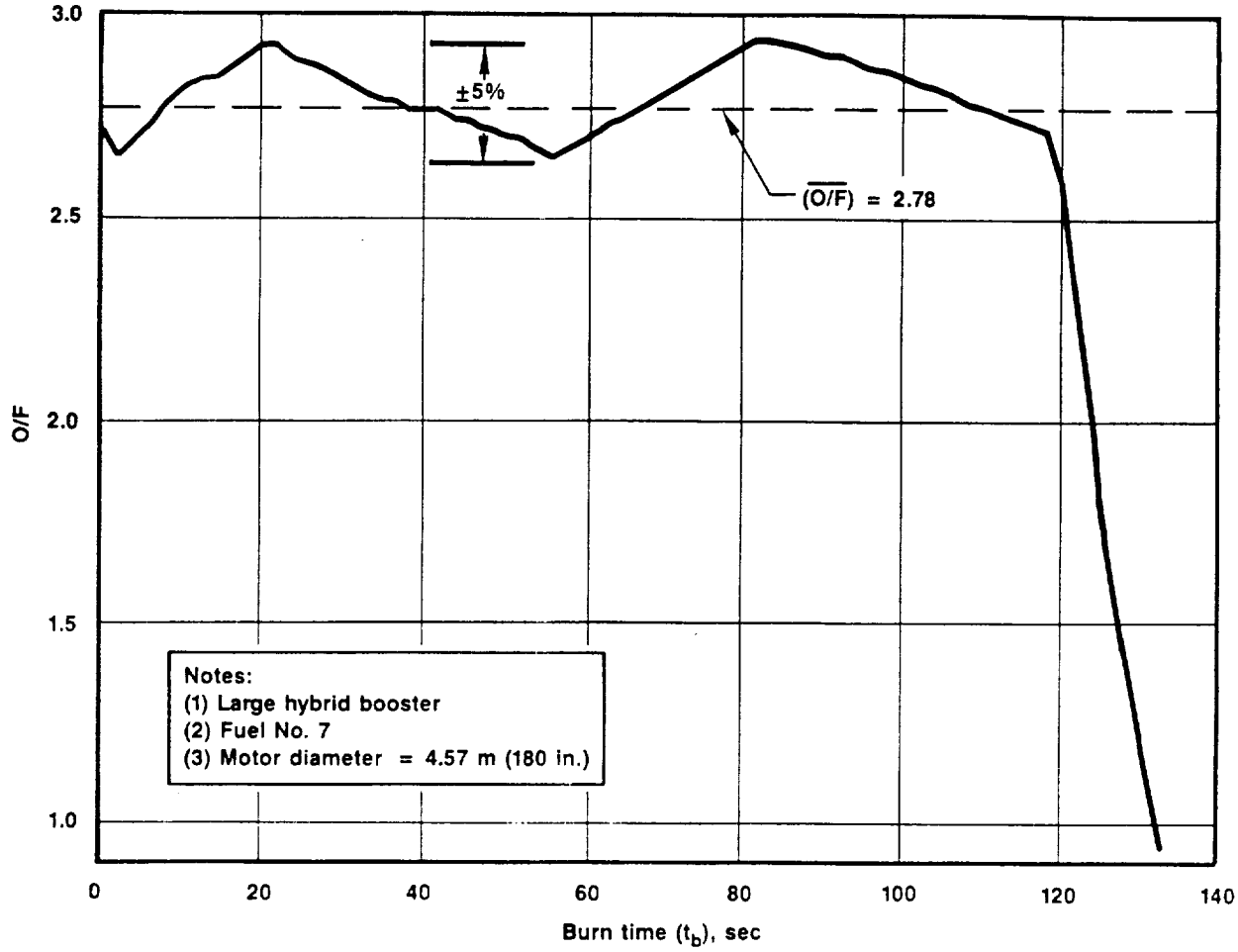

Figure 2-11. Mixture Ratio as a Function of Time

50317

launch out of the Eastern Test Range (ETR) to a 28.5-deg inclination orbit with a 296 km (160 nmi) altitude. Trajectory constraints were obtained from Rockwell International and used to guide the shape of the hybrid motor thrust shape. Three booster motors were looked at: (1) a NASA straw man ASRM design that was used as a guideline during the ASRM phase B study contract No. NT018; (2) a hybrid booster that matched the aforementioned study contract's thrust shape; and (3) the same hybrid motor with an enhanced thrust profile.

The enhanced thrust profile was arrived at by a manual interactive procedure wherein performance was maximized while adhering to the trajectory limits. This profile is not the desired optimum, but serves to illustrate the

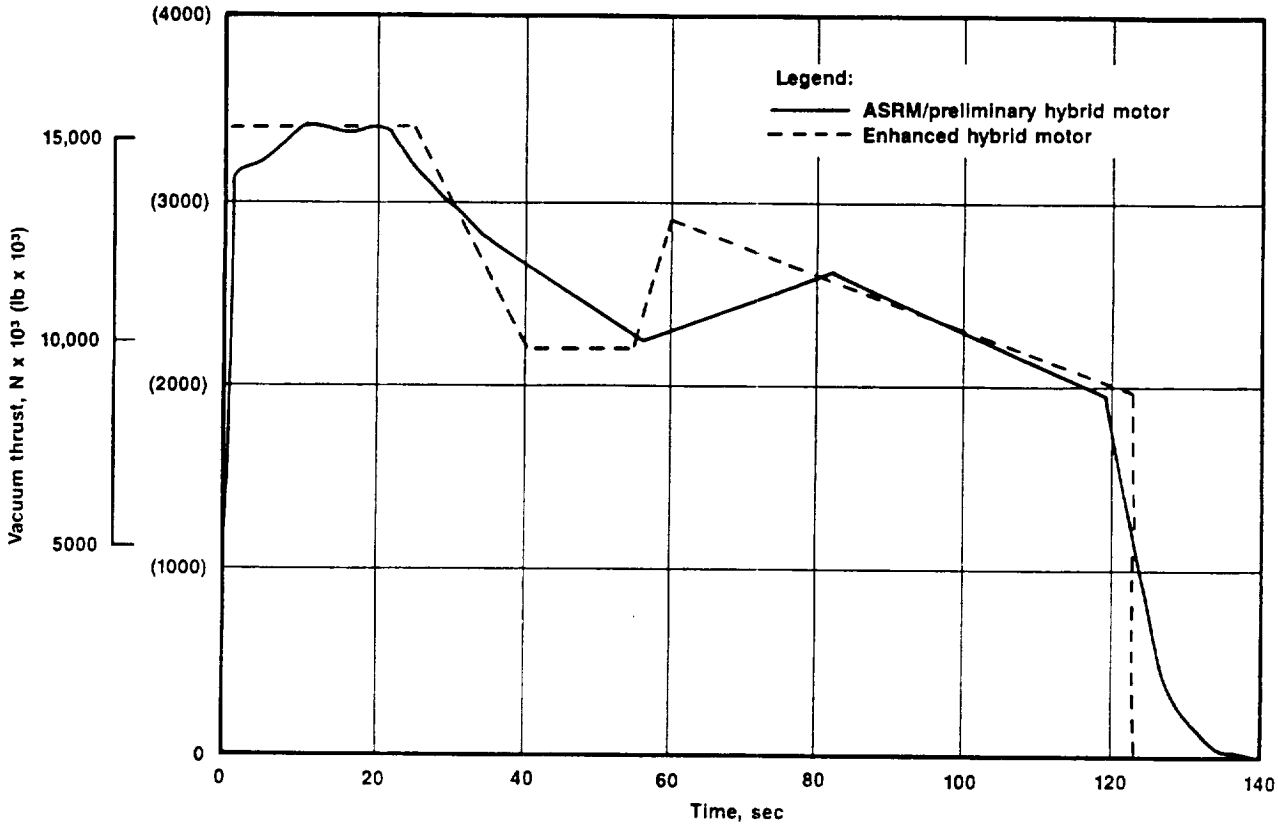

Figure 2-12. Thrust Profile

50435

performance advantage of the hybrid booster. Figures 2-12 through 2-14 show the improved hybrid booster performance within the operational limits.

Table 2-3 summarizes the weight and propulsive characteristics of these boosters and the calculated main engine cut-off (MECO) weight from the trajectory simulation. This weight represents the remaining weight of the system after the boost phase has been completed, and as such is an indication of the performance achieved from the boosting system (SSMEs and boosters). Since the core (SSMEs) propulsion is the same in each case, any changes in MECO weight are due to changes in the characteristics of the boosters. MECO weight changes representing changes in useful payload lift capability are also shown in Table 2-3. Based upon the booster characterics used in the study, the throttle-ability feature enhances hybrid payload capability by approximately 3175 kg (7000 lb).

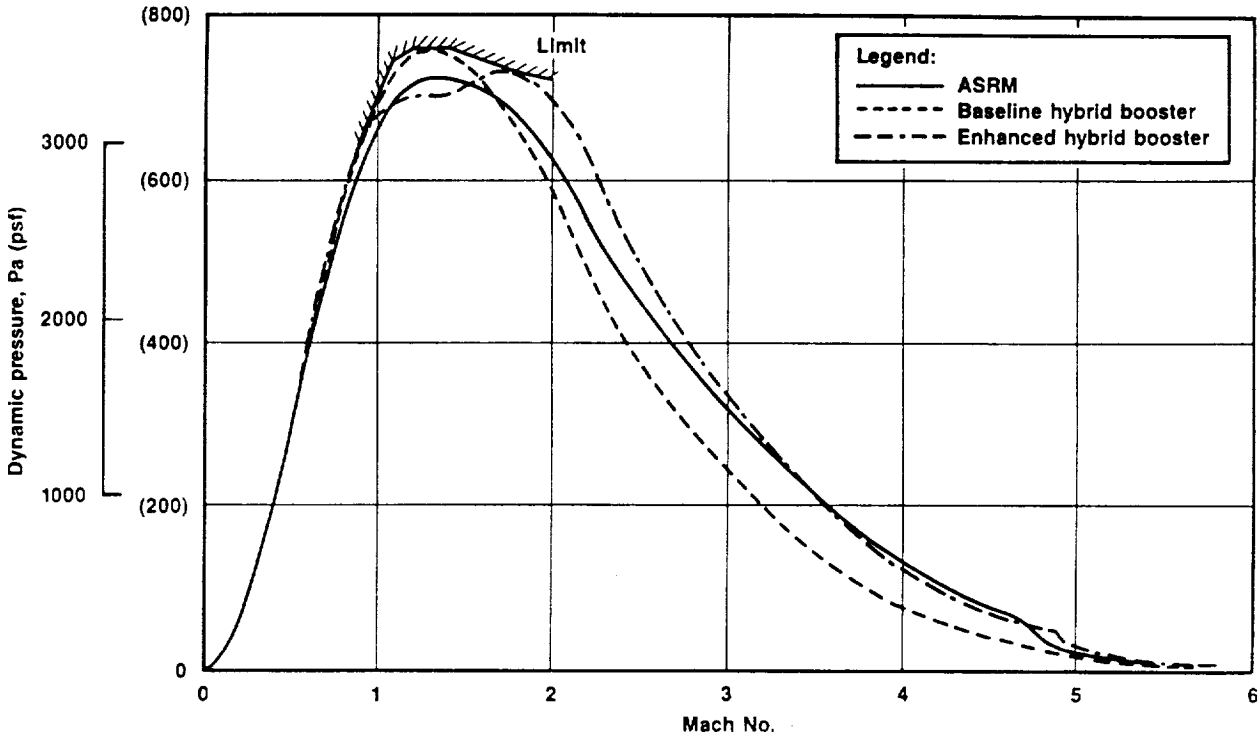

Figure 2-13. Dynamic Pressure vs Mach No.

50433

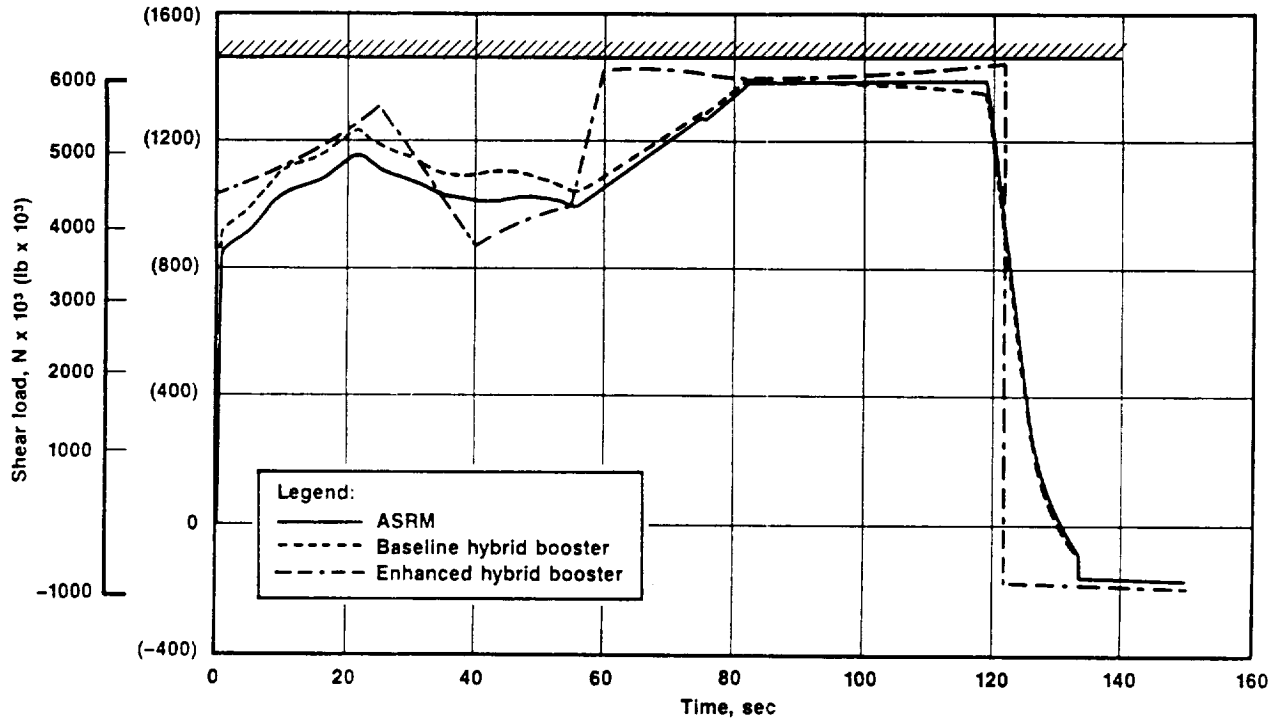

Figure 2-14. Booster Shear Load

50432

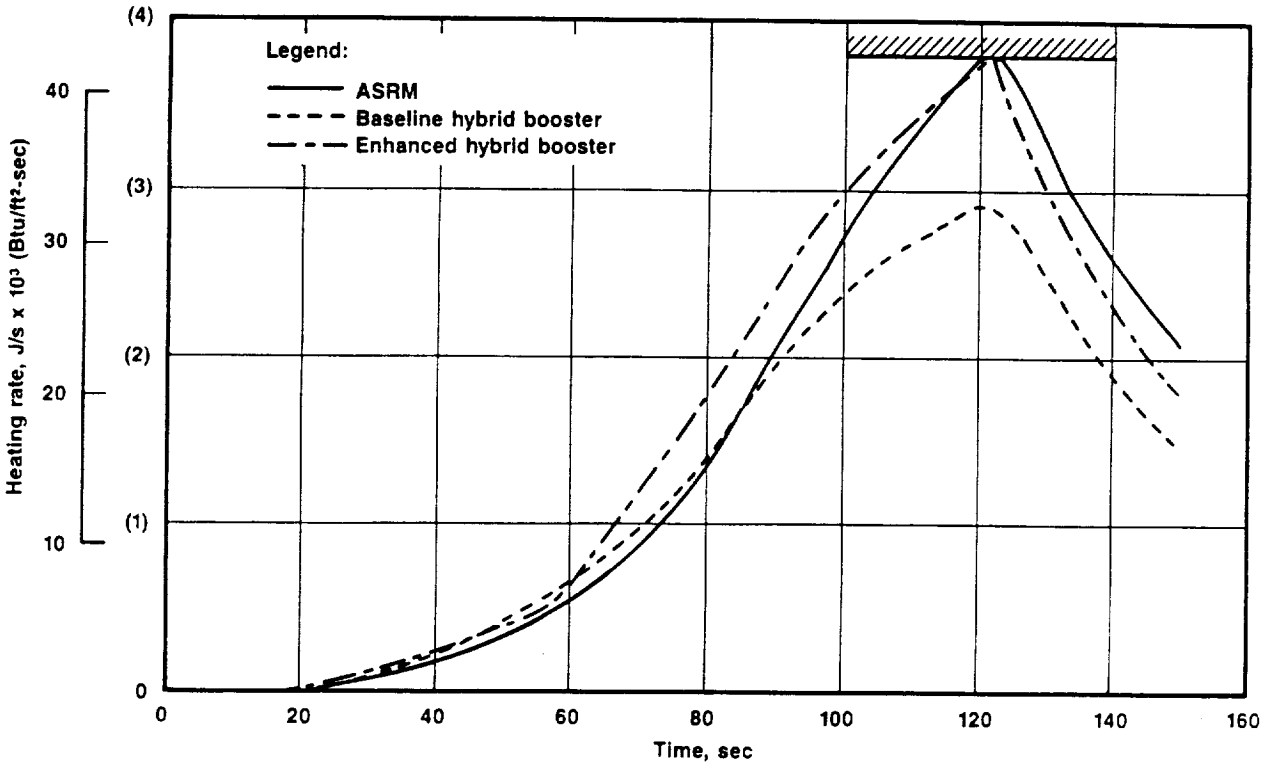

Figure 2-15. Aerodynamic Heating Rate

50434

TABLE 2-3. PERFORMANCE COMPARISON OF SOLID AND HYBRID BOOSTERS

T16987

Parameter	NASA's ASRM	Hybrid 1*	Hybrid 2†
Burnout weight, kg (lb)	75,323.1 (166,059)	85,074.9 (187,558)	85,074.9 (187,558)
Expanded weight, kg (lb)	548,285.7 (1,208,763)	490,970.2 (1,082,404)	490,970 (1,082,404)
Total weight, kg (lb)	623,608.8 (1,374,822)	576,045.1 (1,269,962)	576,045 (1,269,962)
Effective I_{sp}, N-s/kg (sec)	2023 (267.45)	2929 (298.67)	2929 (298.67)
Total impulse, N-sec (lb-sec)	1.43803×10^9 (323,283,664)	1.43802×10^9 (323,281,603)	1.43802×10^9 (323,281,603)
MECO weight, kg (lb)	166,624.4 (367,344)	168,387.6 (371,231)	171,568.2 (378,243)
Payload improvement, kg (lb)	-	1763.1 (3887)	4939.2 (10,889)

* Duplicates ASRM's thrust profile
† Enhanced thrust profile that uses the HRB's throttleability

3.0 MOTOR DESIGN STUDIES

The three areas of comparison of chemical rocket propulsion systems are safety and reliability, their propulsion performance or specific impulse, and their size or volume. The solid propellant systems have a lower maximum specific impulse using practical propellants than either the hybrid or bi-propellant systems. The attainable specific impulses of the latter two systems are comparable except for the propellant combination of oxygen-hydrogen, for which there is no equal in the hybrid system.

When comparing system density, the solid propellant rocket has the best system density. Except for the initial port area, there is very little volume not filled with the high density solid propellant. The liquid and hybrid oxidizers are the same, so that portion of the system is the same volume. While the hybrid fuel can be of higher density than the liquid fuel, the liquid fuel can usually be packaged in a smaller volume and lighter weight case. The volume of the bi-propellant combustion chamber is less than that required in the hybrid mainly because the combustion chamber consists of passages in the fuel grain plus the aft end internal dome volume. The overall volume of the hybrid system is not markedly different from the all-liquid system.

The major advantages for the hybrid are reliability and safety. Like the all-liquid system, the hybrid can be shut down and even restarted. Its fuel is not volatile and is generally inert. It thus presents no explosive hazards during processing, assembly, launch activities or flight. To increase the system density without increasing the hazards, metals can be added to the inert solid fuel. Even if solid oxidizer is added to the solid fuel to increase the overall regression or burning rate, it does not have to cause the fuel to become a solid propellant unless the oxidizer content is greater than approximately 30%.

The complexity of the hybrid system is half of that of the liquid system since only one of the propellants is in the liquid phase. The cost of the hybrid is potentially less than a liquid system because the separate combustion chamber and one fuel flow system are eliminated from the design.

The hybrid design study was performed using the CSD hybrid ballistics and design model to define both large and small hybrid boosters to meet the specified thrust-time profile provided in the statement of work (SOW). To define preferred operating pressure and motor diameter the initial parametric sizing studies were performed with preliminary weight and size models for the various hybrid components. As the study progressed, the models were improved to reflect more accurate assessments of the actual weights and dimensions. Finally, detailed weight size and performance analysis data were used for the final trade and selection studies. The following subsections describe the fundamentals of the hybrid ballistics, the CSD performance model, the various fuels used in the evaluation, and the results of the initial and subsequent design studies.

3.1 DESIGN BASIS

3.1.1 Oxidizer Selection

A variety of liquid oxidizers could be used for this booster system. Initially the oxidizers: inhibited red fuming nitric acid (IRFNA), nitrogen tetroxide, liquid oxygen (LOX), and hydrogen peroxide were all considered as potential propellants. However, all of the oxidizers except LOX are corrosive or mono-propellants and, because of safety considerations, were eliminated from consideration for these booster systems. LOX is used extensively at the nation's launch facilities and in this effort was assumed as the hybrid oxidizer. It is available at all launch sites and is the least expensive oxidizer available.

3.1.2 Hybrid Motor Ballistics

This subsection presents the development of the hybrid ballistic relationships used for generating the hybrid fuel grain designs. The fundamentals of hybrid combustion are presented first, followed by experimental laboratory-scale regression rates for the candidate fuels and fuel regression rate scaling relationships[2-10] used for the design. Hybrid fuel ballistics are controlled by the interaction of forced convection and radiative heat transfer to the fuel grain surface and volumetric heat of vaporization of the fuel. This process, shown in Figure 3-1, results in a fuel-rich boundary layer with a thin flame zone.

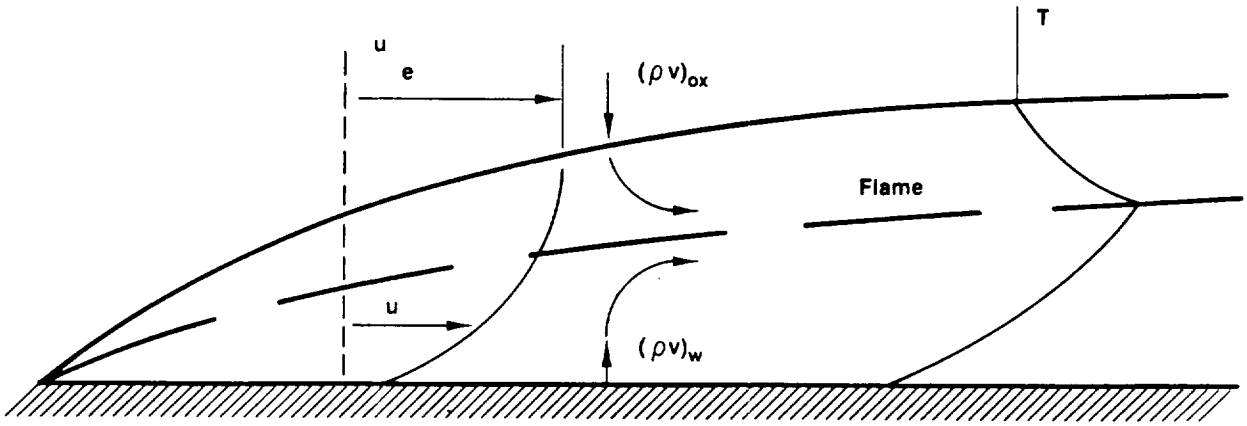

Figure 3-1. Hybrid Combustion Model

50353

Extensive work with hybrid combustion has led to a good theoretical understanding of hybrid fuel ballistics. Although these theoretical relationships require calibration for unique designs, they provide a physical understanding of the interaction of different combustion parameters on hybrid fuel regression rates. Equation 1 relates the fuel regression rate, r, to the total heat flux to the fuel surface:

$$\dot{r} \cdot \rho_f \cdot hv = Q_w \qquad (1)$$

where ρ_f = fuel density and hv = fuel heat of vaporization. In the absence of radiation, the regression rate due to forced convection is given by

$$\dot{r} = 0.036\ G^{0.8}\ B^{0.23}/\rho_f\ X^{0.2} \qquad (2)$$

where G = gas mass flux ($\rho \cdot V$) and B = the "mass transfer number" approximately equal to the $\Delta hc/hv$.

Several effects are worth noting:

- The fuel regression rate is driven by the mass flux.
- The fuel regression rate is insensitive to hv because decreases in hv that would be expected to directly increase $\dot{r}$ (per equation 1),

increase the blowing effect of mass flow from the surface resulting in a much smaller increase in convective heat transfer.

- The fuel regression rate is insensitive to ρ_f; therefore, addition of solid particles such as metals allow a higher mass flow rate for the same volumetric flow of gas from the fuel surface.
- Although the fuel regression rate is only weakly size-dependent, these effects can be important in using subscale data.

Addition of metal to the fuel also increases the heat flux by significantly increasing radiation. However, the blowing effect of the resulting higher fuel regression rate reduces the convective heat flux. The coupled effects of radiative heat flux (Q_R) and forced convection (Q_C) without radiation is given by:

$$\dot{r} = (1/\rho_f \cdot hv)[Q_c e^{-Q_R/Q_C} + Q_R] \qquad (3)$$

Experimental results show that the fuel regression rate relationship can be simplified to $r = aG_{ox}^{n}$ for convection controlled conditions, where G_{ox} is the head-end oxidizer mass flux.

A key objective of hybrid fuel grain design is to achieve the desired oxidizer-to-fuel ratio (O/F) throughout the firing. This requires that the perimeter increase as the A_{port}^{n}. A circular port perimeter increases as $A_p^{0.5}$ and pie-shaped grains are less progressive. Since typical hybrid "n" values are 0.5 or greater, constant oxidizer flow results in an O/F increase during the firing. The regressive thrust trace required for this application minimizes this O/F shift by the throttling of the oxidizer flow during the firing.

Subscale test data for several fuels were used for the ballistic characterization of the candidate hybrid fuel formulations. The subscale test results, together with previous theoretical and experimental work, provide a sufficient basis for preliminary design and hybrid regression rate relationships.

The principal adjustments from subscale data to full-scale data involve size and pressure adjustments. For turbulent convection, the regression rate varies as size to the -0.2 power. Therefore, the measured regression rates in large motors would be reduced by $(D_{fullscale}/D_{subscale})^{0.2}$.

Pressure has two effects on hybrid fuel regression. If oxidizer is present in the fuel, the rate of fuel decomposition is pressure-sensitive. This typically adds a weak pressure sensitivity to the regression rate. If radiation effects are present, but not controlling as is expected over the preliminary design mass flux range, the regression rate will also show a weak pressure sensitivity. These pressure effects have been modeled by multiplying the subscale fuel regression rates by $(P/P_{subscale})^{0.13}$.

3.1.3 Selected Candidate Fuels

Although oxygen was considered to be the preferred oxidizer, numerous hybrid fuel formulations were evaluated as possible solid fuels in this booster study. Table 3-1 summarizes nine fuels initially considered. CSD's vast experimental and analytical background in hybrids and solid fuel ramjets, a hybrid with diluted oxygen (air as the oxidizer), includes experience with hundreds of fuel formulations potentially appropriate for this booster application. As can be seen from the table, the stoichiometric mixture ratios ranged from 1.14 for the aluminized and oxidized fuel grains to 3.23 for 100% hydrocarbon fuel grains. Fuel No. 1 contains AN (ammonium nitrate) oxidizer, which eliminates hydrochloric acid (HCl) from the exhaust flow species. Fuel Nos. 3, 5, and 6 have most of the HCl formed from the AP (ammonium perchlorate) scavenged by combining it with sodium nitrate to form non-hazardous sodium chloride. These three fuel systems have HCl concentrations in the exhaust plume of less than 0.9% by weight as compared to a standard solid propellant which produces about 22% HCl by weight. Fuel No. 8 was developed for solid fuel ramjets and incorporates 30% AP to increase the regression rate. Because of dilution with oxygen in the combustion process, the exhaust HCl level is reduced to 2.5% by weight. Although this might be a problem, this fuel represents the maximum enhanced regression rate that might be obtained while using a fuel that will not burn as a solid propellant.

TABLE 3-1. HYBRID BOOSTER FUELS WITH LOX
(Sheet 1 of 2)

T17085

Fuel No.	wt-%										O/F Stoichiometric	Heat of Combustion, cals/g (Btu/lb)	wt-% HCl In Exhaust at ϕ = 1.17
	HTPB	AI	AP	$NaNO_3$	AN	Escorez	Fe_2O_3	KNO_3	HAN	p, g/cc			
1	30	30	-	-	36	-	-	4	-	1.350	1.14	5331 (9595)	0
2	50	30	-	-	-	-	-	-	20	1.318	1.80	7294 (13,130)	0
3	30	20	12	8.7	-	28.3	1.0	-	-	1.310	1.97	7245 (13,041)	0.72
4	30	30	-	-	-	40.0	-	-	-	1.23	2.53	9168 (16,503)	0
5	30	-	20	14.4	-	34.6	1.0	-	-	1.228	1.95	6362 (11,451)	0.88

TABLE 3-1. HYBRID BOOSTER FUELS WITH LOX
(Sheet 2 of 2)

T17085

Fuel No.	wt-%										O/F Stoichiometric	Heat of Combustion, cals/g (Btu/lb)	wt-% HCl In Exhaust at ϕ = 1.17
	HTPB	AI	AP	$NaNO_3$	AN	Escorez	Fe_2O_3	KNO_3	HAN	p, g/cc			
6	30	-	12	8.7	-	48.3	1.0	-	-	1.142	2.45	7729 (13,912)	0.60
7	40	-	-	-	-	60.0	-	-	-	1.009	3.23	9912 (17,841)	0
8	40	-	30	-	-	30.0	-	-	-	1.19	2.10	7057 (12,702)	2.5
9	30	40	-	-	-	30.0	-	-	-	1.33	2.28	8926 (16,068)	0

Note: HAN = hydroxylamine-nitrate, B = explosive class B

Fuels Nos. 4, 7, and 9 are completely inert and free of any possible hazards. The other oxidized fuels are considered Class B explosives by the DOT even though they do not have an explosive hazard as compared to solid propellants. A formulation is considered to be explosive if there is any solid oxidizer mixed with the fuel.

The major reason for adding oxidizer to the fuel is to increase the fuel regression rate, which in turn reduces the number of ports and the geometric complexity of the grain. Aluminum is added to increase the density of the fuel grain. The effect of adding oxidizer and/or aluminum is to reduce the stoichiometric mixture ratio and increase the weight of the solid fuel required in respect to the required weight of LOX. This in itself is not an advantage unless the regression rate is increased, since the larger fuel grain weight requires larger ports to keep the port L/D to an acceptable level.

After an initial sizing study, the nine fuels were re-examined and the number used in this study was reduced to five. Figure 3-2 shows curves of relative fuel regression rate for those five fuels as a function of gaseous oxygen mass velocity. The data were obtained in the course of CSD FR and D tests with small-scale connected-pipe test hard-ware. As can be seen, the aluminized, oxidized fuel No. 1 has a higher slope than the other non-metallized fuels. When these data were used in the initial preliminary sizing and trade studies, corrections were not made to the regression rate equations for port diameter and pressure effects. Corrections were made to the motors shown in the preliminary configuration studies and in the later optimization studies.

3.2 PRELIMINARY SIZING AND TRADE STUDIES

There is a regular progression used to design a hybrid system. A fuel and oxidizer combination is selected and theoretical thermodynamic values of vacuum, specific impulse, and characteristic exhaust velocity, c^*, are calculated as functions of chamber pressure and O/F ratio. The usual procedure requires estimating motor diameter from a specific port configuration, oxidizer mass flow rate, and web thickness based upon the integrated regression

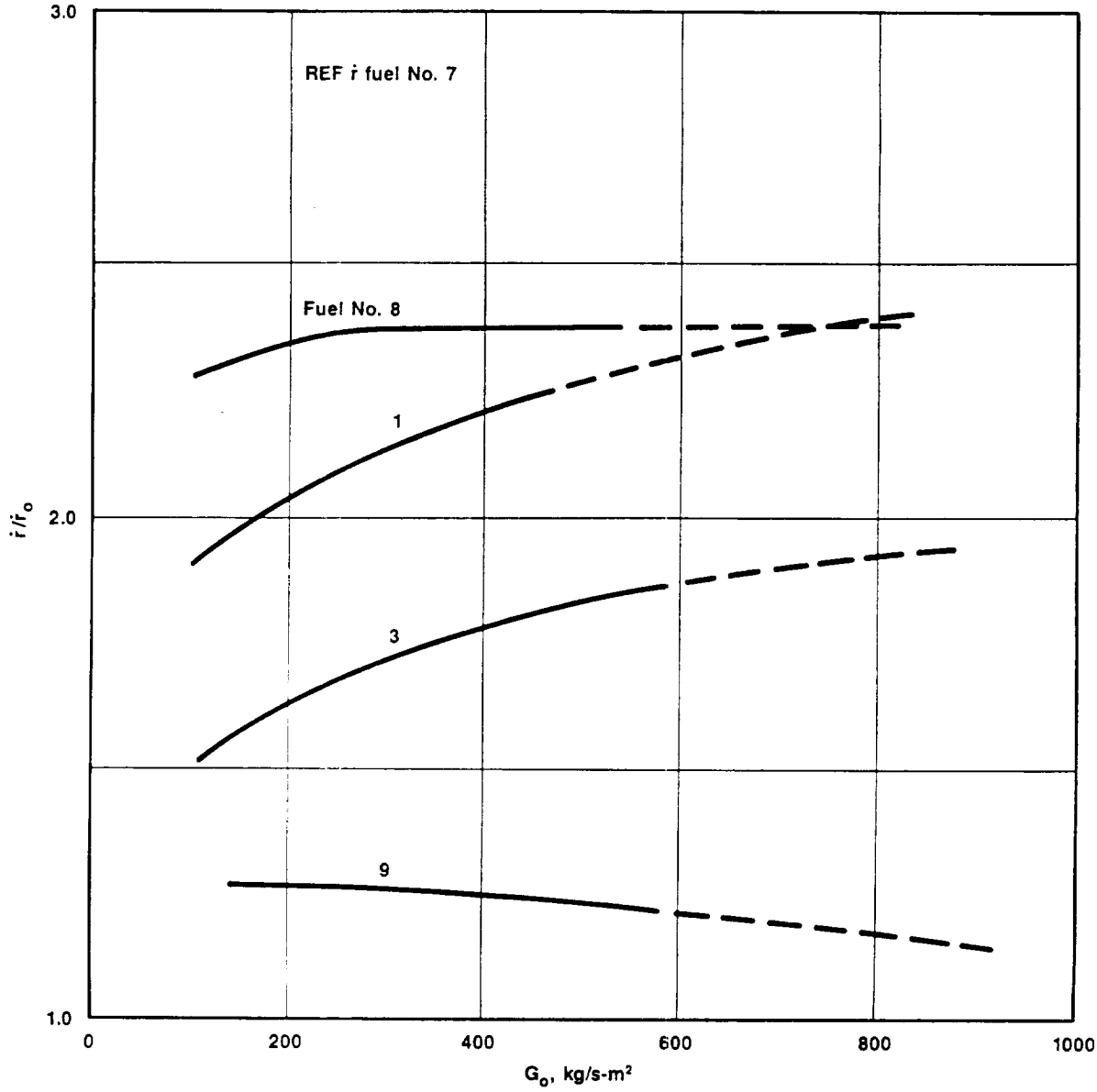

Figure 3-2. Fuel Regression Rate Data

50477

rates and burn time. Then the length of the grain is determined based upon the limitations of port L/D. This gives an overall mixture ratio which fixes the amount of oxidizer required and the nozzle area required to produce the desired chamber pressure. The nozzle expansion ratio then gives the attainable vacuum impulse. If there is a throat area-to-port area ratio limitation, it may not be possible to obtain a design. Then the number of ports

have to be varied to obtain a solution. From these sizes and pressures, using a safety factor of 1.4 for manned systems, the tank and chamber sizes, wall thicknesses and weights can be calculated. Component and subsection weights such as the TVC system, insulation, and valves and pumps are added to the system weight.

3.2.1 Design Approach and Models

The primary approach used in selecting a hybrid fuel and the design of a hybrid rocket system for this hybrid booster program was the use of a computer program specifically designed to size a hybrid rocket motor to meet a specified total impulse schedule.

Of primary interest was determinating what specific properties the hybrid fuel should have to meet the booster thrust requirements. Ideally, the fuel should have the same regression rate as the burning rate of solid propellants now in use for such booster applications. With such high regression rates, there would be a single central port and the overall design would be simple. However, the hybrid fuel regression rates are 1/6 to 1/3 of those of solid propellants, so the port design in the hybrid fuel grain becomes of significantly greater importance.

The hybrid's solid phase is designated a fuel since it normally would not be considered a solid propellant, even if it contains low levels of oxidizer. At the low oxidizer levels under evaluation, it would not sustain combustion without additional oxidizer present. Because of the large increase of surface area required in the hybrid grain compared to the solid propellant grain for the same thrust application, it was decided to use multiple separate ports rather than a high perimeter factor, spoked grain configuration. Determinating the final grain configura-tion during the intermediate test program will be made easier by testing single ports and then increasing the number of required ports rather than by scaling up a spoked configuration.

In the hybrid motor design program, the primary design variables are: solid fuel grain diameter, length and web thickness and nozzle throat area for

a specific type of fuel, grain shape, average combustion chamber pressure and thrust versus time throttling curve.

The grain shape design options include cylindrical, slotted and wagon wheel designs. The configuration that is most useful with low regression rate hybrid fuels is the wagon wheel shape with either one or more circumferential arrays of ports. The number of ports must be specified along with their general positioning. The program will then size the grain diameter, length, web and throat for a required total impulse and thrust-time profile. Some constraints to the design include port-length-to-hydraulic diameter ratio, required average chamber pressure, limits of mixture ratio, and limits on oxidizer mass flux. The design of the fuel grain is then optimized to the maximum change in payload capability, minimum booster weight, or minimum length assembly.

The regression rate is computed by the law:

$$\dot{r} = a\, G_o^{n} (P_c/P_{co})^{p} (D_h/D_{ho})^{d} \qquad (4)$$

Coefficients and exponents used in the equation are determined empirically from test data. The last terms are used to correct the small-scale test data to full-scale motors. G_o is the oxidizer mass flux and $\dot{r}$ is the regression rate in inches per second. The combustion chamber/solid fuel case is sized to accommodate the maximum expected operating pressure (MEOP) times a safety factor. The oxidizer tank can be sized by pressure requirements or the input of minimum practical wall thicknesses, depending on whether the system is pressure-fed or pump-fed. The nozzle weight is computed as a function of half angle and throat and exit diameter. Other weights are accounted for as miscellaneous input weights.

Fuel characteristics are input as tables of specific impulse ($I_{\overline{sp}}$) and characteristic exhaust velocity (c^{*}) as a function of mixture ratio, O/F, and combustion pressure, P_c. I_{sp} and required thrust are used to compute the necessary mass flow rate for each specified thrust. The fuel and oxidizer

flow rates are computed as functions of mixture ratio, which are iteratively adjusted by the program until their sum matches the total required mass flow. Chamber pressure is then computed using c^* and W:

$$P_c = c^* \cdot W/(A_t \cdot g) \tag{5}$$

In order to have the program optimize a motor design, a merit function that can be minimized must be defined. The merit function used for these studies is the improvement in payload weight compared to the reference mission corresponding to the input total impulse and thrust-time history.

Payload weight improvement was determined by using performance exchange ratios and partials that amounted to an approximated change in payload lift capability given a booster characteristic perturbation. These perturbations consisted of changes in: (1) inert weight, (2) propellant weight, (3) vacuum delivered specific impulse ($I_{\overline{sp}}$) and, (4) cross-sectional area. The source of the first three partials is NASA's request for proposal for the phase B ASRM study contract, in which these Rockwell-defined partials were to be used to assist the ASRM design exercise. Two partials for propellant weight were given; a propellant density partial that assumes a change in propellant density only and a propellant volume partial that assumes a change in propellant web only. Both these partials coupled propellant weight and action time effects on payload. Since new candidate booster designs can independently vary weight and action time, CSD developed a propellant weight partial independent of action time. In addition, a booster cross-section area partial was calculated from trajectory simulations to approximate the effect of diameter change on payload weight. These partials are summarized in Table 3-2.

These same partials were also applied to the small booster combination. It is recognized that the hybrid booster and the small booster in particular are quite different from the RSRM and that the partials are inexact. While new partials should be generated for the hybrid boosters and specific missions, the present approach allows comparisons of different hybrid designs and provides a good evaluation of potential performance gains. The same

TABLE 3-2. PAYLOAD PARTIALS - BASED ON SRM BOOSTER

T16915

Variable	Reference Value	$\frac{\partial \text{ Payload}}{\partial \text{ Variable Increase}}$
Inert weight (including residual propellant), kg, (lb)	90,112 (198,660)	-0.2 kg PL/kg inert (-0.2 lb PL/lb inert)
Propellant weight, kg, (lb)	502,203.4 (1,107,169)	0.143 kg PL/kg propellant (0.143 lb PL/lb propellant)
Vacuum I_{sp}, N-s/kg (sec)	2607 (265.8)	401.4 kg PL/sec (885 lb PL/sec)
Motor cross-section area m^2, (ft^2) drag	10.8 116.3	-76.2 kg PL/m^2 (-15.6 lb PL/ft^2)
Note: PL = payload		

reference values have been used for all comparisons, so any changes in those values will not change the ranking of the selected fuel systems. In the initial studies, the only inert weights included in the inert partial comparison were the weights of the SRM case and nozzle. As the database on the weights of feed systems, insulation and other inerts improved, CSD added those applicable inert weights from the SRM for an improved comparison.

To obtain the maximum payload weight increase that satisfies the total impulse requirement and all of the constraints, the program progressively varies such allowable variables as motor diameter, grain length, fuel web thickness and throat area. The resulting motor design parameters are printed out along with a time history of the global combustion parameters such as pressure, thrust, O/F, G_o (oxidizer mass flux), regression rate, web thickness and expected nozzle area change due to erosion. Certain assumptions are made in the design; the propellant residuals were initially limited to 5% for the solid fuel and 0.5% for the LOX. This amount was later increased to 6% for the fuel and 1.5% for the oxidizer (to account for GOX in the storage tank after shutdown). The I_{sp} combustion efficiency was limited to 93% of theoretical. The nozzle expansion ratio was limited to 12.0 or no more than with an

nozzle exit cone outside area equal to the motor case diameter. An expansion ratio of 12 was selected since that gave the maximum total impulse over the estimated flight trajectory without having separated flow in the nozzle at launch. The nozzle diameters for both size units were sized to give the desired average chamber pressure. This gave a specific throat-to-port area ratio. As the chamber pressure is reduced, the port area approaches the throat area and the port velocities become excessive. An example of a computer printout showing the input file and the output file is shown in Appendix A.

3.2.2 Preliminary Sizing Study

The preliminary efforts were geared toward determining what hybrid fuels were acceptable for the two booster applications, what size motors maximized the payload potential, and preferred operating conditions. The hybrid design computer program described earlier was used to compare fuels and booster diameter. In performing these studies, approximate oxidizer fuel system and inert weights were used. The combustor case weight was based on the use of a steel tank while an aluminum oxygen tank was used. Weights were determined by sizing the walls as a function of maximum pressure. Figures 3-3, 3-4, and 3-5 show the variation in booster length for the large hybrid booster as a function of motor diameter and increasing throat-to-port area ratio for three different fuel systems. The port-to-throat area ratio is considered one of the more important variables since it determines the initial oxidizer mass velocities and volumetric loading of the fuel grain. In this early work, the regression rate for fuel No. 6 was assumed to have a coefficient of 0.18 (the fuel regression rate at a oxidizer port mass flux of 1.0), and an exponent of 0.65.

After some experimental testing of various fuels, the regression rate data for fuel No. 6 were changed to a coefficient of 0.096 and an exponent of 0.45. There seemed to be no incentive to continue working with fuel No. 6 as it did not offer any specific advantages over the other fuels. Hence, further calculations were suspended after the initial effort.

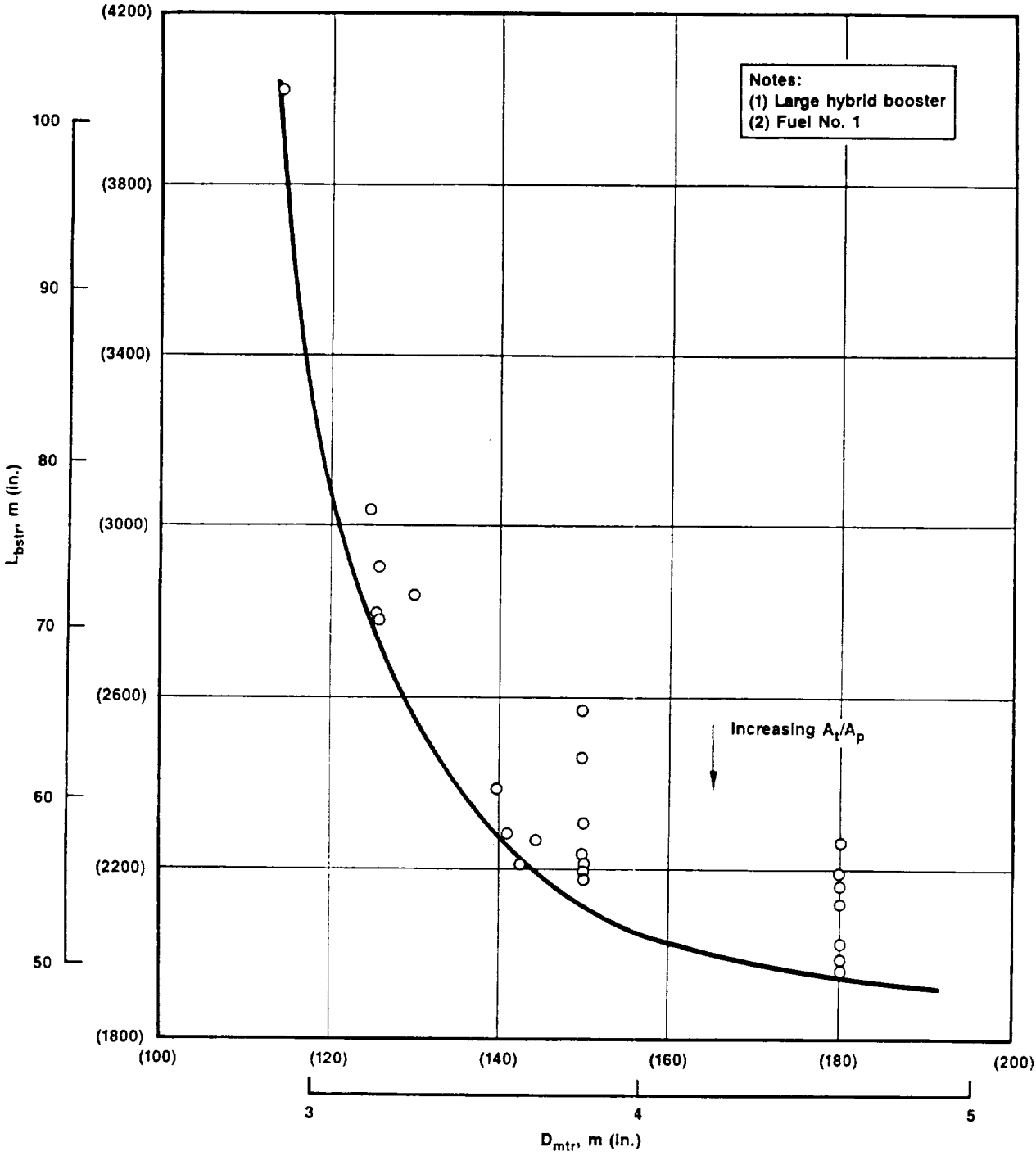

Figure 3-3. Effect of Large Hybrid Booster Diameter on Booster Length - Fuel No. 1

50280

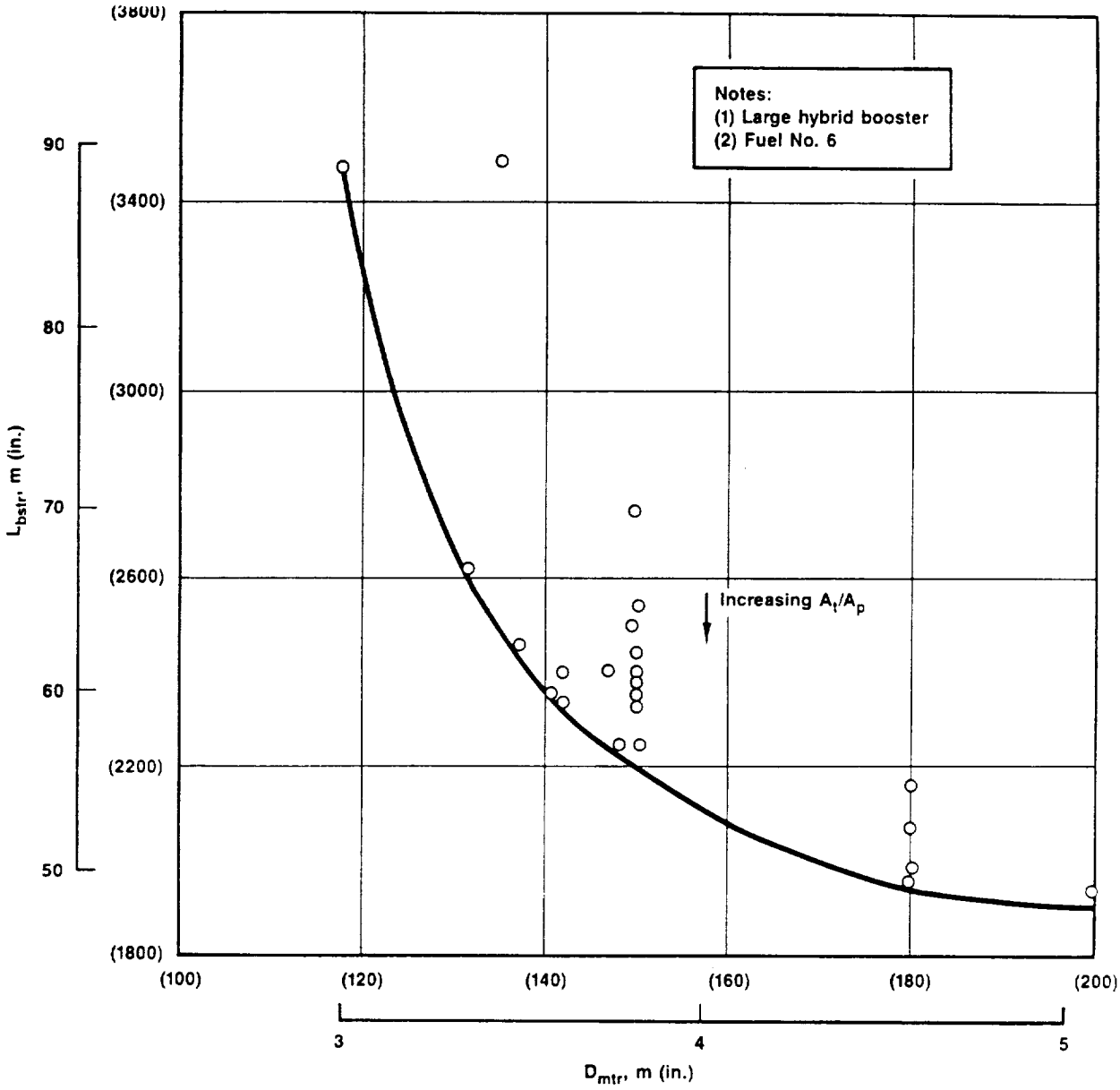

Figure 3-4. Effect of Large Hybrid Booster Diameter on Booster Length - Fuel No. 6

50279

Figure 3-6 shows that, for both fuels Nos. 1 and 7, there is not an appreciable variation in large booster system weight as a function of motor diameter. When the port L/Ds are compared in Figure 3-7, the all-hydrocarbon fuel No. 7 is shown to require many more ports than the aluminized, oxidized fuel No. 1. However, since the high values of port L/D exceeded the available

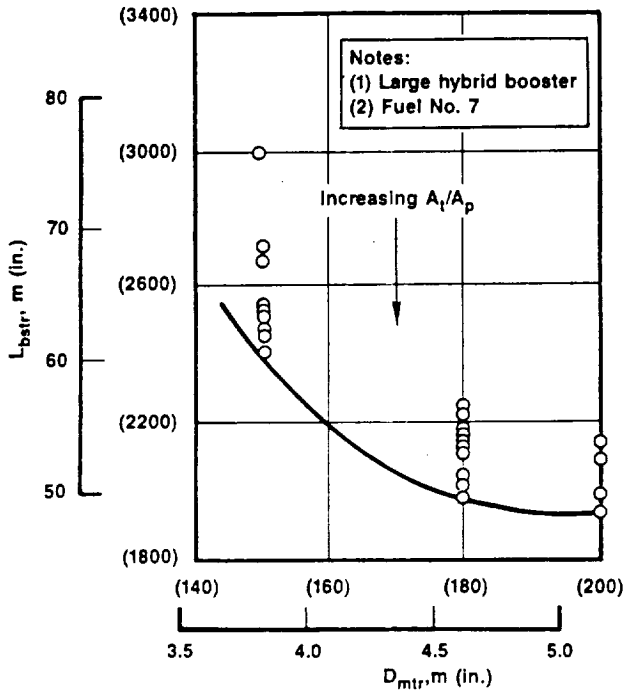

Figure 3-5. Effect of Large Hybrid Booster Diameter on Booster Length - Fuel No. 7

50278

data on hybrid fuels, it was decided to limit the L/Ds to approximately 40. This is a critical design issue. Previous efforts used a port L/D of 25 as an upper limit for uniform regression. This value is derived from theoretical considerations and limited tests have been conducted in small motors at higher levels of L/D. Experimental data are needed in longer, larger diameter motors to fully quantify the allowable limit as a function of fuel composition and operating conditions.

It can be seen from the results of Figure 3-6 a and b that the motor weight is a minimum between 4.57 and 5.08 m (180 and 200 in.) for these fuels. As there were no constrains on motor diameter, a diameter of 4.57 m (180 in.) was selected for the large diameter booster.

When the port L/D's are plotted against the throat-to-port area ratio, it can be seen in Figure 3-8 that for the all-hydrocarbon fuel No. 7, the effect is to limit the throat-to-port area ratios drastically.

As previously mentioned, hybrid fuels can be either oxidized or have aluminum or some other added metal. Adding these materials will increase the density of the solid fuel but will reduce the mixture ratio at which the system will optimally operate. This reduction will increase the ratio of solid phase to liquid phase required and will usually result in a heavier system because the motor case/combustion chamber is appreciably heavier than the tank for a pump-fed oxidizer. The advantage of adding metals to the fuel is to slightly increase the regression rate. The addition of solid oxidizers

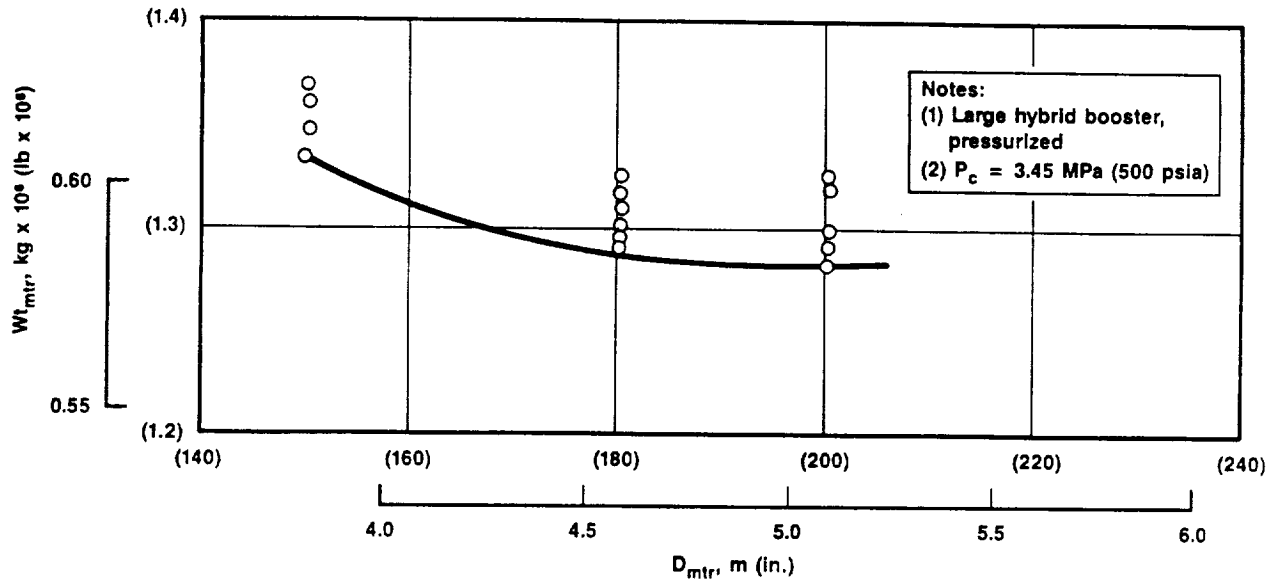

A. Fuel No. 7

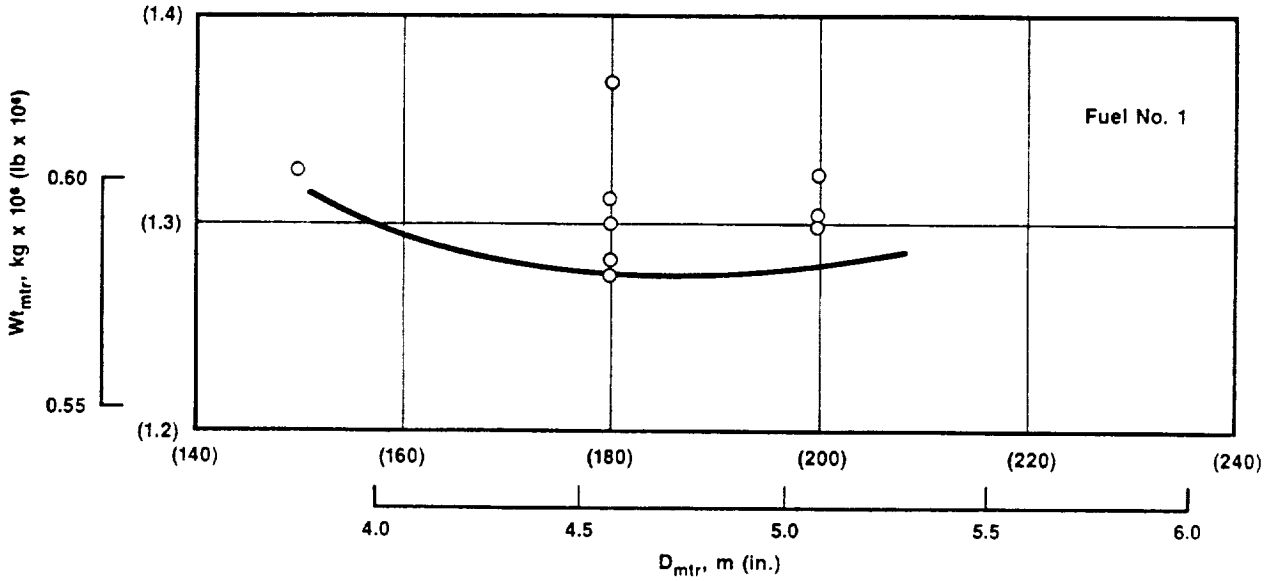

B. Fuel No. 1

Figure 3-6. Effect of Diameter of Large Hybrid on Motor Weight

50277

has a major impact on increasing the regression rate. Increases in regression rate reduce the number of fuel ports required in the grain and make it possible to operate at lower port L/Ds. However, metallized exhausts are much hotter and more erosive than non-metallized combustion systems, and oxidizer in the grain increases the safety hazards and the cost of handling and fabrication.

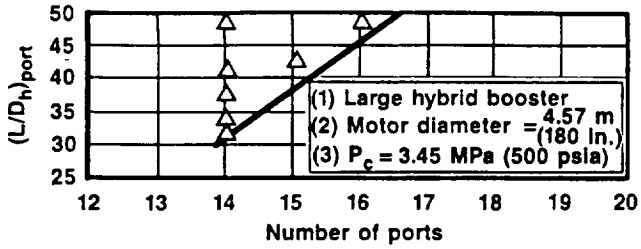

A. Fuel No. 1

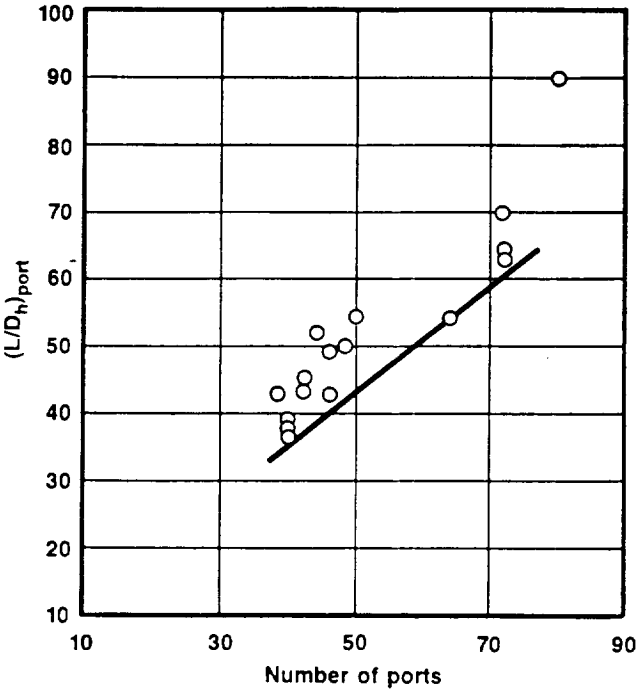

B. Fuel No. 7

Figure 3-7. Port L/D_h Variation with Number of Ports for Large Hybrid

50276

The major effect on booster weight shown in Figure 3-9 is the combustion pressure. Since the motor case is, in fact, the combustion chamber, its weight has a large effect on overall weight. For the pressurized system, the operating pressure seemed to optimize at 3.45 MPa (500 psia) average, while later studies optimized the large pump fed-system to about 5.17 MPa (750-psia) average chamber pressure. This is much lower than for bi-propellant liquid boosters because of the effect of pressure on the weight of the larger fuel case/combustion chamber. The average pressures of 5.17 and 3.45 MPa (750 and 500 psia) result in MEOPs of approximately 7.69 and 5.14 MPa (1115 and 745 psia) respectively, depending on the oxygen-to-fuel ratio of the fuel system.

For this evaluation, a parallel design effort was performed for the quarter-scale booster and the full-scale design thrust-time curve was reduced by three-quarters. Figures 3-10 and 3-11 show the port L/D variation with the number of ports and throat-to-port area ratio for the all-hydrocarbon fuel. The observations are the same as for the large booster. The initial diameter considered was 3.05 m (120 in.) since that size hardware was available from Titan booster development. Figures 3-12 and 3-13 show the variation of fuel grain length and overall booster length, respectively, as a function of throat-to-port area ratio. As the design evaluation continued, the diameter of the quarter-scale boosters was varied from the originally selected 3.05 m

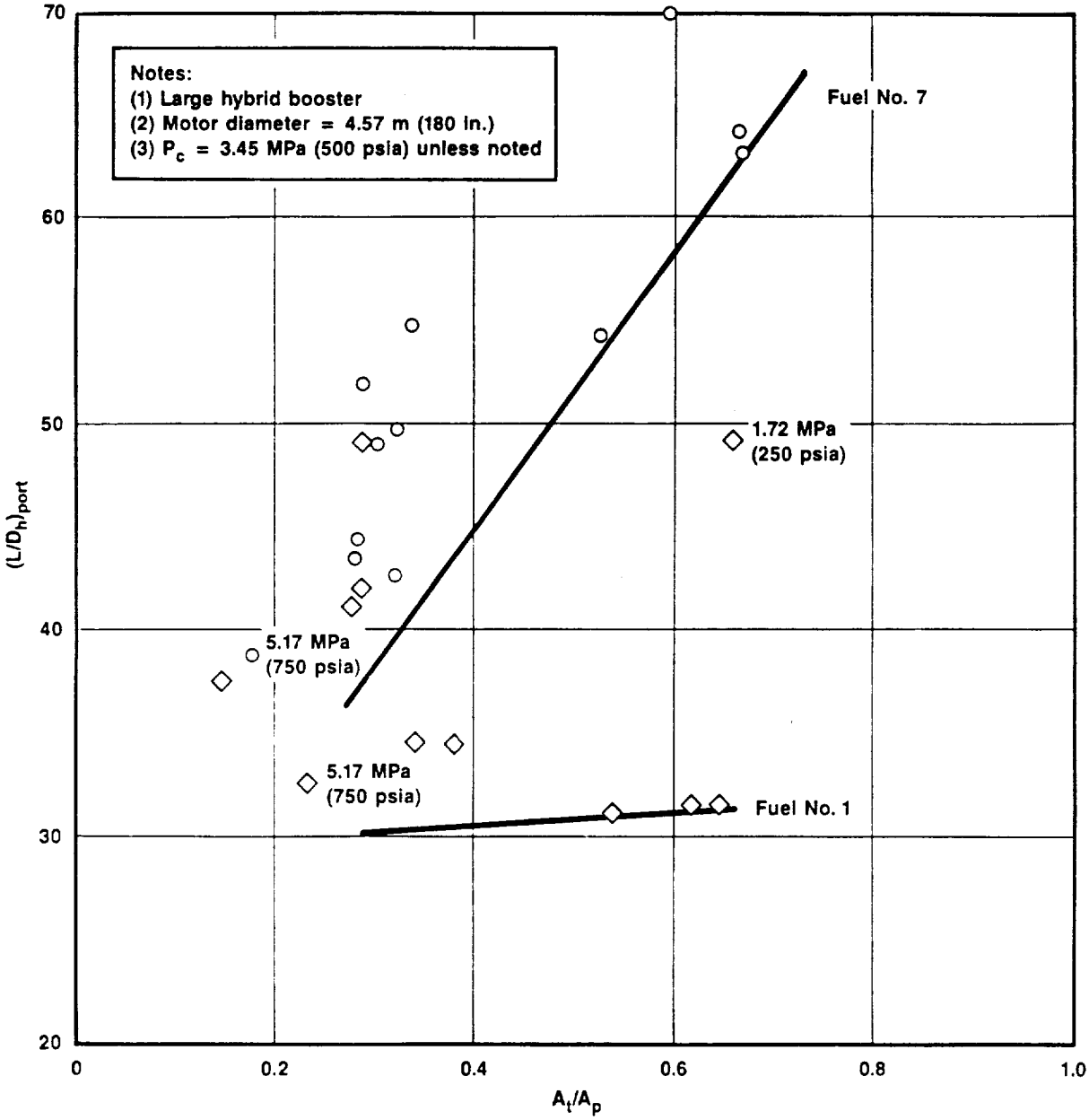

Figure 3-8. Variation of Large Hybrid Port L/D_h with Throat to Port Area Ratio
50275

(120 in.) to the 2.03 to 3.05 m (80 to 120 in.) range. Figure 3-14 shows that the booster weight does not vary appreciably in the 2.29 to 3.05 m (90 to 120 in.) range. For a specific number of ports in the fuel grain, the variations in length of the fuel grain and diameter of the motor and payload increment with throat-to-port area ratio are shown in Figure 3-15.

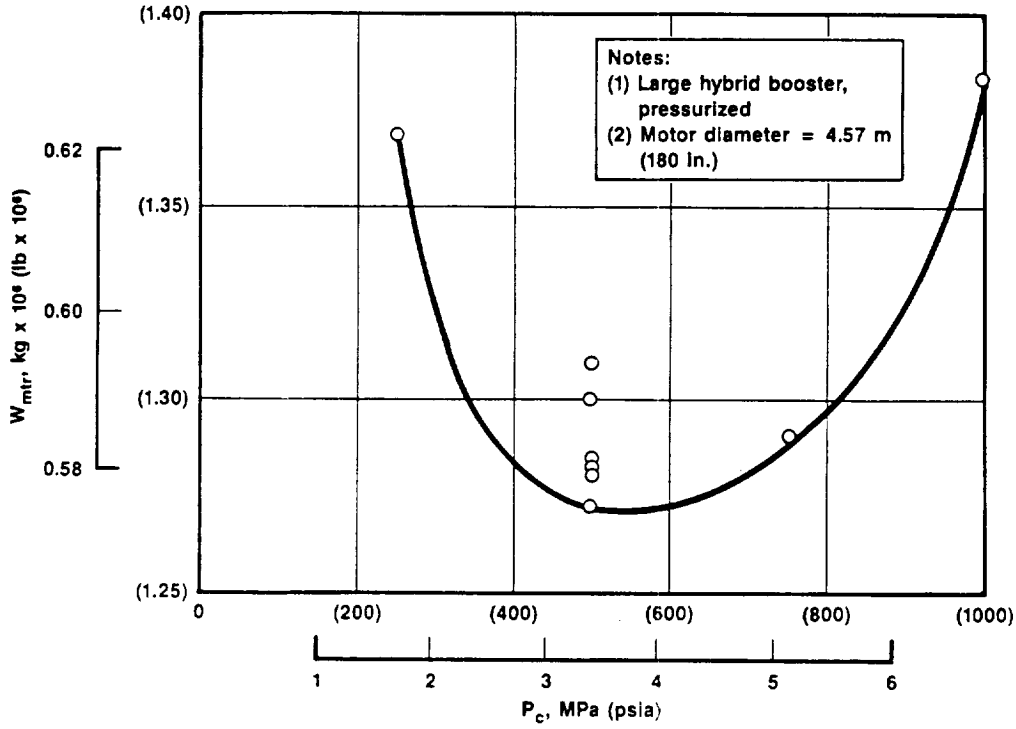

A. Fuel No. 1

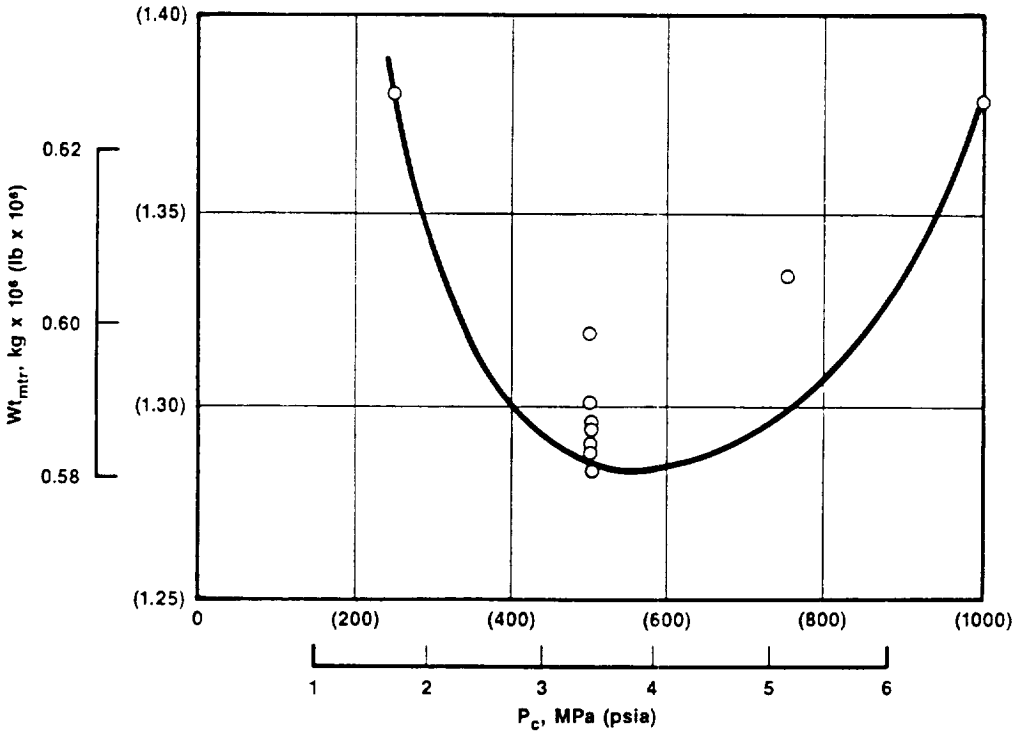

B. Fuel No. 7

Figure 3-9. Effect of Average Combustion Pressure on Large Hybrid Motor Weight

50274

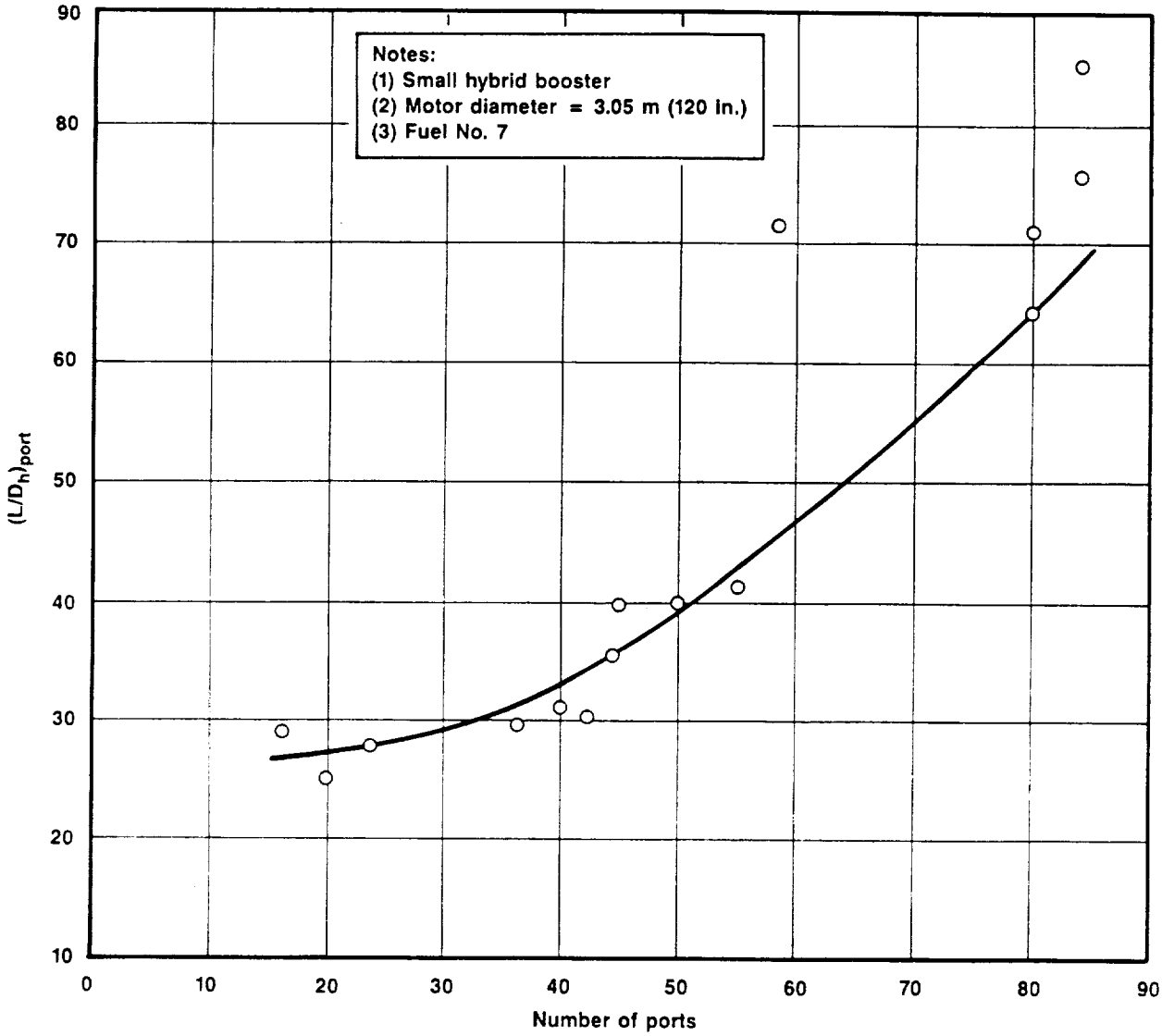

Figure 3-10. Port L/D_h Variation with Number of Ports for Small Hybrid

50273

The quarter-scale booster configuration was selected to be 2.29 to 2.44 m (90 to 96 in.) in diameter, dependent upon the fuel formulation. This is mainly because the number of fuel ports and the overall length of the booster were considered reasonable. Any size under 3.05-m (120-in.) diameter offered the same advantages as far as fabrication and shipment were concerned.

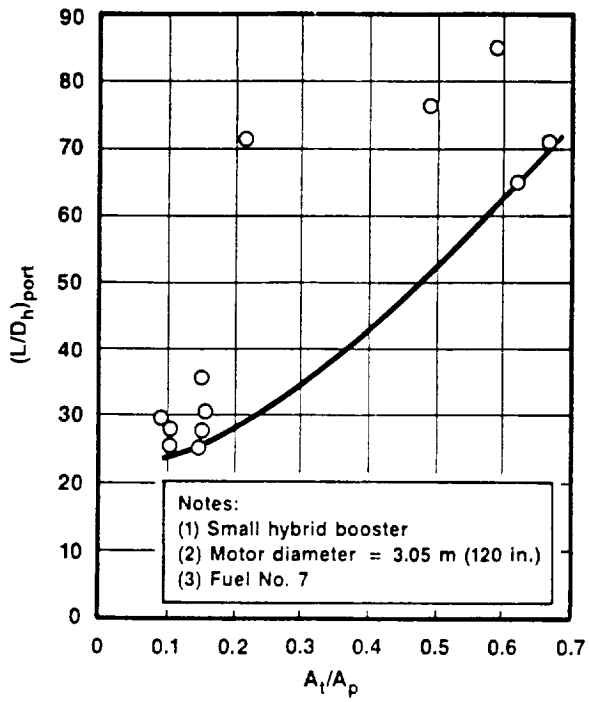

Figure 3-11. Variation of Small Hybrid Port L/D_h with Throat to Port Area Ratio

50272

3.3 PRELIMINARY CONCEPT DESIGN STUDY

The full-scale and quarter-scale design efforts were continued with updated component weight information and TVC design considerations. The preliminary concept designs[1] offered reflected the impact of improved weight estimates. In evaluating the large-scale booster, it became evident that it was possible to package such a unit in as small a diameter as 3.96 m (156 in.) and up to a unit of more than 5.08 m (200 in.) in diameter. The variation in total weight was not large and the major factor was the overall booster length. At 3.8 m (156 in.), it was found that with fuel No. 7 the length is excessive for shuttle usage based upon the desire to have the booster length such that the shock cone off the Shuttle tankage does not intersect the boosters. If the payload is not the existing Shuttle, then the 3.96 m (156-in.) diameter unit may be quite acceptable. However, on the basis that length is important, a diameter of 4.57 m (180 in.) was selected for the baseline design.

Figure 3-16 summarizes the preliminary single booster designs for the pump-fed systems, while Figure 3-17 shows them in relation to the Shuttle and RSRM. The initial analysis of pump-fed versus pressure-fed boosters indicated that the pressure-fed systems had two major drawbacks and one advantage: a higher tank weight by a factor of 5 to 6, and a factor of 10 in residual GOX weight in the tank, but a lighter weight pressurization system compared to the weight of LOX pumps and fuel required to drive the turbine. There was no measurable increase in reliability or safety to justify the additional weight.

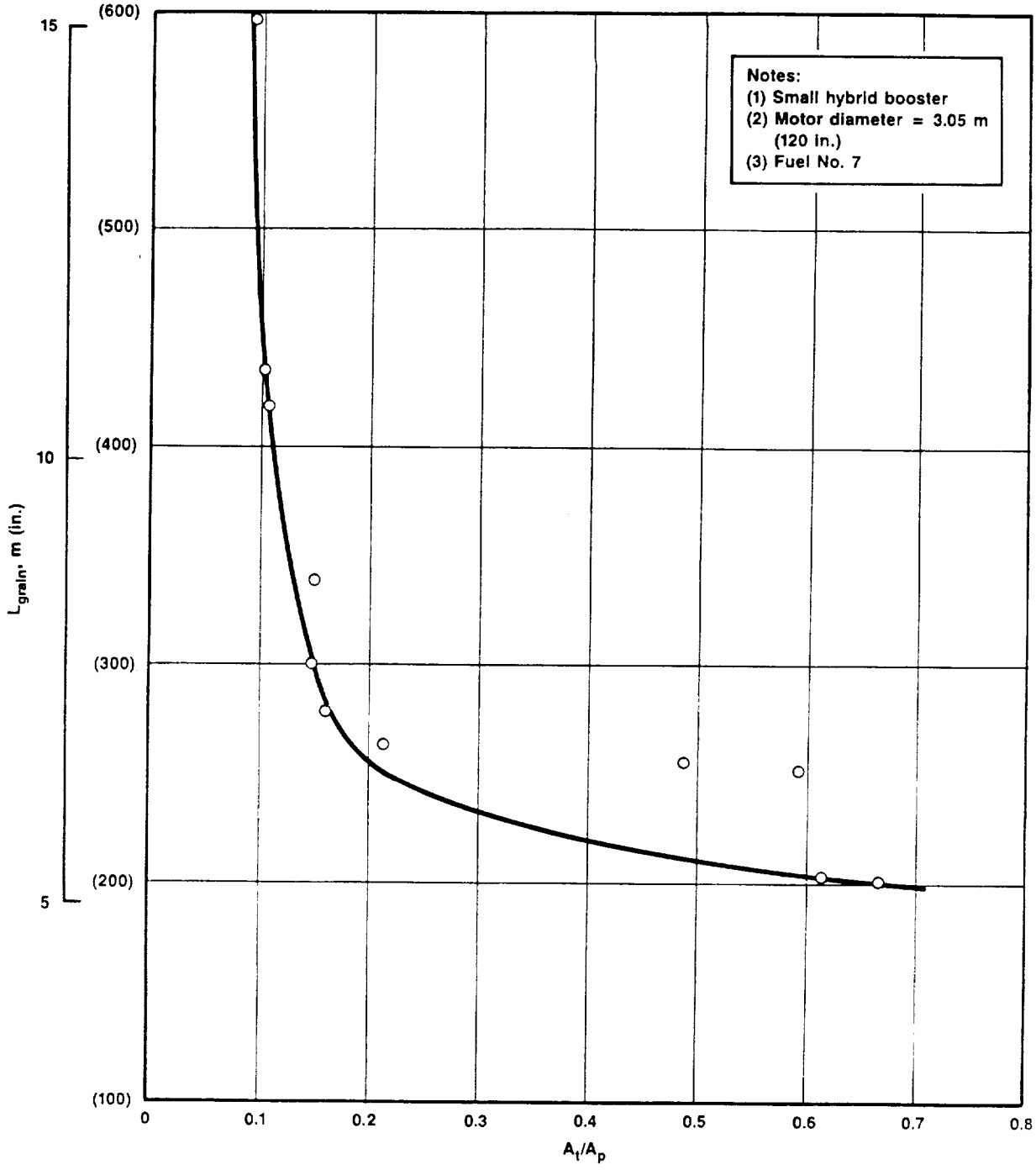

Figure 3-12. Small Hybrid Grain Length as a Function of Throat to Port Area Ratio

50271

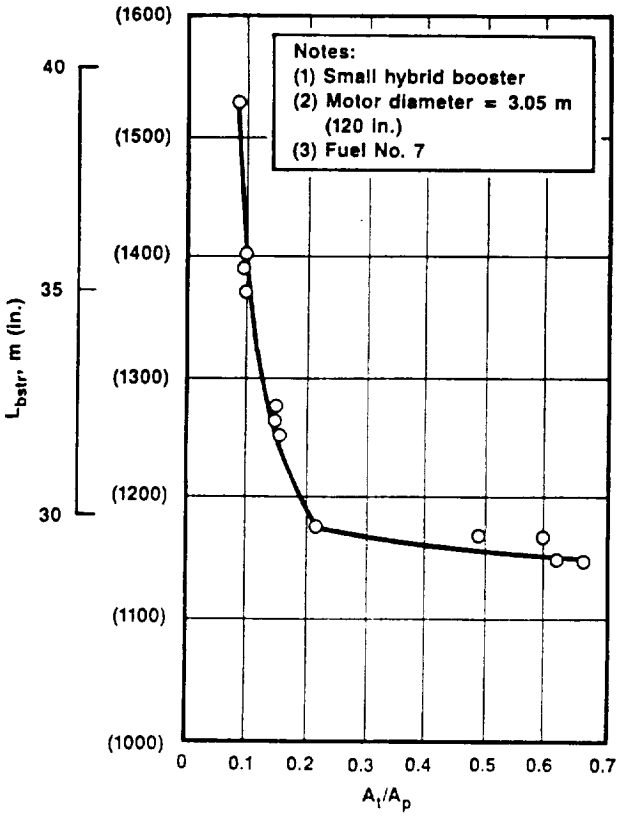

Figure 3-13. Small Hybrid Booster Length as a Function of Throat to Port Area Ratio

50270

As can be seen from Figure 3-16, all of the pump-fed designs provided the required total impulse, with the major differences being in overall length. The 3.96 m (156-in.) diameter unit using fuel No. 8 had the smallest overall volume but used a solid fuel-containing oxidizer that made it a Class B explosive. The insensitivity of the hybrid booster design to size and fuel considerations made it difficult to select the "best" configurations. This fact can also make the hybrid an excellent booster choice since the design can be selected based upon other considerations than a specific required diameter.

Figure 3-18 summarizes the preliminary concept quarter-scale booster designs for pump-fed systems. The higher regression rate fuel No. 8 makes a more compact system, but since it contains AP, the 2.44-m (96-in.) diameter inert fuel design was selected as the preliminary baseline design. Liquid injection (LOX) TVC in one quadrant of the fixed nozzle was selected a the baseline approach.

3.4 FINAL DESIGN STUDY

The preliminary designs were used to update the subsystem and component weights for the final design update and concept selection studies. Subsystem weights used in the final studies are shown in Table 3-3. The numbers were evolutionary so that individual studies showed some differences, but comparisons for any particular system study were made on the same basis.

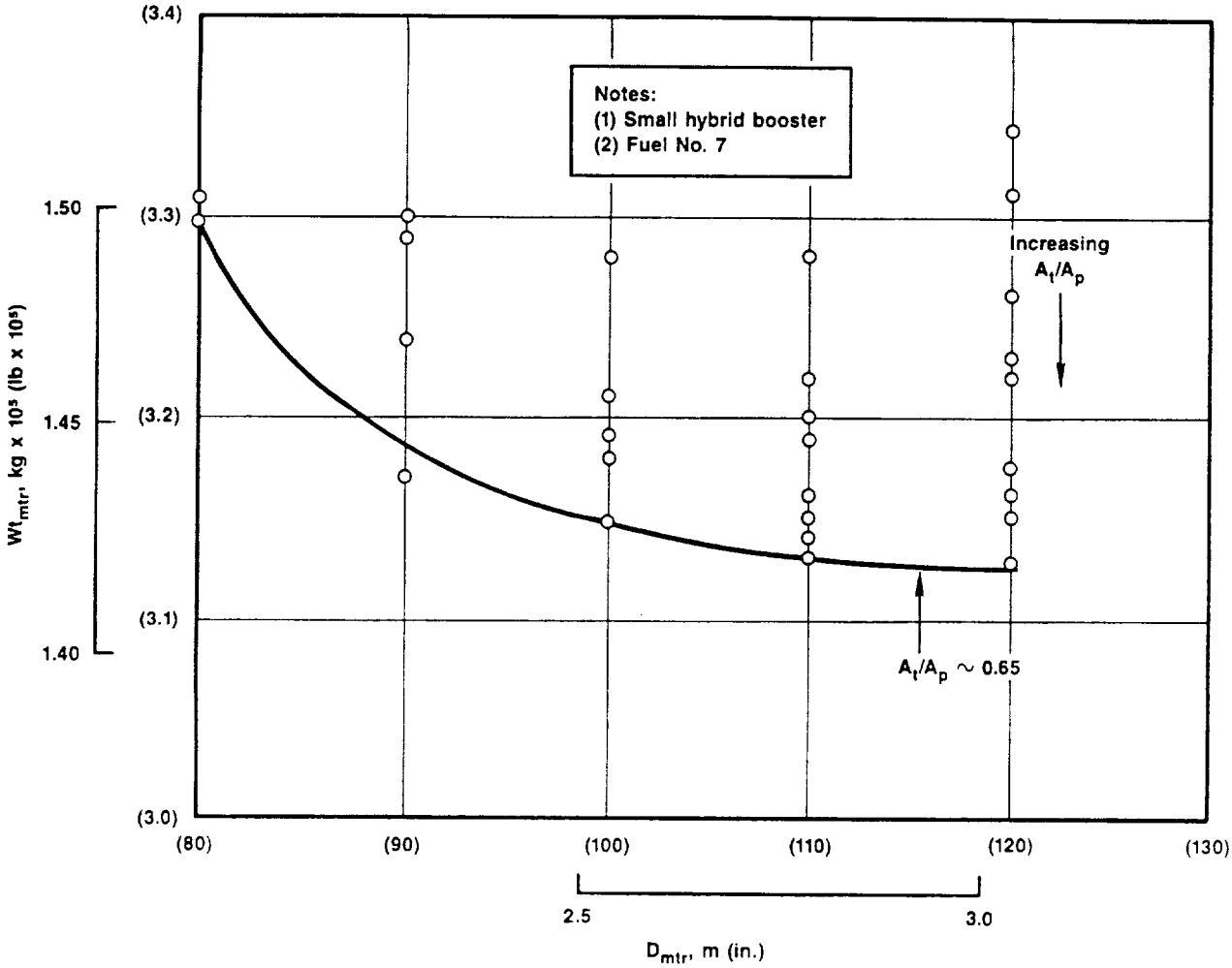

Figure 3-14. Effect of Diameter of Small Hybrid on Motor Weight

50269

The initial update study re-examined the effect of motor diameter for the pump-fed system using either fuel No. 7 (inert) or the aluminized AN fuel (fuel No. 1). The results of these studies are shown in Table 3-4. As may be seen, a number of viable designs can be used, all of which meet the required thrust-time profile and provide positive delta payloads relative to the RSRM. Within the limits shown, the delta payloads do not demonstrate a great variation for diameters of 4.06 to 4.57 m (160 to 180 in.). The major differences are that performance improves with an increase in the number of fuel ports for a given diameter, and the length of the booster decreases with increasing diameter. While not necessarily an optimum, the 4.57 m (180-in.) diameter inert fuel grain provides equivalent performance and the shortest

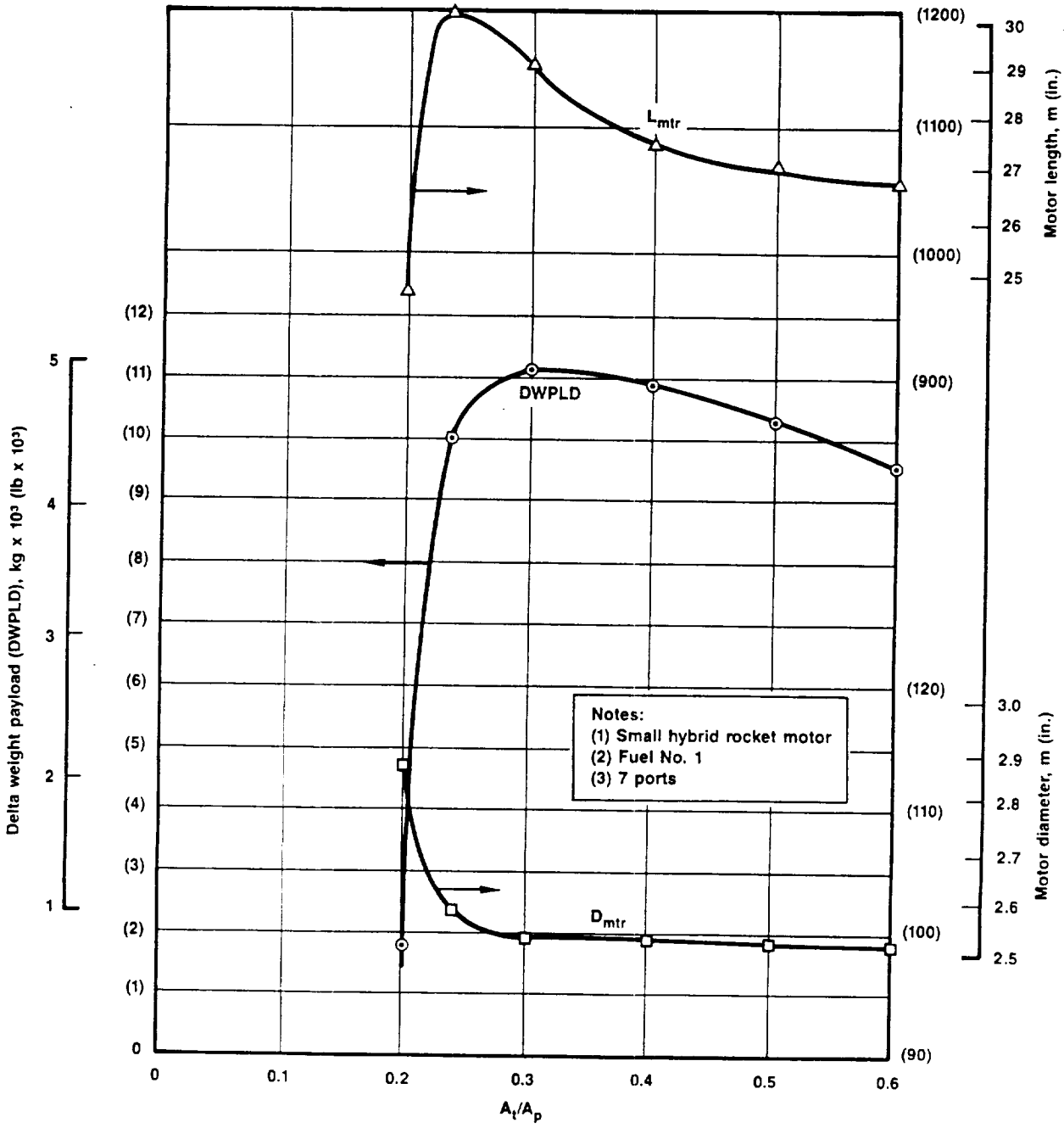

Figure 3-15. Design Variables as a Function of A_t/A_p for the Small Hybrid Booster

50318

Parameter	Fuel No.				
	1	7	7	9	8
LOX feed	Pump	Pump	Pump	Pump	Pump
Total impulse, N-s (lb-sec)	1.44×10^9 (3.24×10^8)	1.44×10^9 (3.24×10^8)	1.44×10^9 (3.24×10^8)	1.44×10^9 (3.24×10^8)	1.44×10^9 (3.24×10^8)
Motor diameter, m (in.)	4.57 (180)	4.57 (180)	3.96 (156)	3.96 (156)	3.96 (156)
No. of ports	8 | 10	10 | 24	5 | 15	5 | 14	3 | 8
Area/port, m^2 ($in.^2$)	0.38 | 0.35 (588 | 544)	0.19 | 0.20 (299 | 303)	0.26 | 0.27 (401 | 415)	0.26 | 0.25 (399 | 391)	0.23 | 0.24 (354 | 370)
R1, m (in.)	1.40 (55.13)	1.13 (44.58)	0.85 (33.28)	0.87 (34.31)	0.76 (30.11)
R2, m (in.)	1.73 (67.94)	1.35 (53.19)	1.10 (43.17)	1.16 (45.55)	1.34 (52.91)
R3, m (in.)	2.12 (83.59)	2.16 (85.13)	1.84 (72.27)	1.82 (71.59)	1.69 (66.53)
L/D_h	39.2	38.0	40.9	39.9	37.9
A_t/A_p	0.187	0.187	0.231	0.263	0.55
Web, m (in.)	0.16 (6.41)	0.11 (4.30)	0.13 (4.94)	0.14 (5.62)	0.29 (11.40)
Volume fraction	0.60	0.59	0.56	0.60	0.81
G_o, maximum, kg/m^2 (lb/$in.^2$-sec)	330 (0.47)	520 (0.74)	689 (0.98)	689 (0.98)	1287 (1.83)
ε	12.0	12.0	10.0	10.0	9.4
O/F	0.88	2.73	2.89	1.90	1.75
I_{sp}, N-s/kg (sec)	2832 (288.8)	2994 (300.2)	2879 (293.6)	2817 (287.3)	2841 (289.7)
P_c, MPa (psia)	5.16 (749)	5.16 (749)	5.21 (755)	5.16 (749)	5.16 (749)
W_{ox}, maximum, kg/s (lb/sec)	2479.8 (5467)	3856 (8501)	4042 (8910)	3671 (8093)	3485 (7671)
W_{motor}, kg (lb)	0.590×10^6 (1.301×10^6)	0.557×10^6 (1.229×10^6)	0.569×10^6 (1.254×10^6)	0.579×10^6 (1.276×10^6)	0.569×10^6 (1.254×10^6)
DWLPD, kg (lb)	3998 (8814)	8557 (18,864)	7752 (17,090)	6786 (14,960)	8032 (17,708)
L_{grain}, m (in.)	21.49 (846)	14.1 (555)	19.00 (781)	19.3 (758)	16.6 (652)
L_{LOX}, m (in.)	13.67 (538)	20.5 (806)	28.0 (1101)	25.2 (991)	23.9 (939)
L_{noz}, m (in.)	5.74 (226)	5.77 (227)	5.05 (199)	5.13 (202)	4.98 (196)
L_{NC}, m (in.)	5.61 (221)	5.61 (221)	4.88 (192)	4.88 (192)	4.88 (192)
L_{dome}, m (in.)	1.32 (52)	1.32 (52)	1.14 (45)	0.99 (39)	1.14 (45)
L_{bstr}, m (in.)	49.48 (1948)	48.9 (1925)	60.2 (2370)	58.1 (2286)	52.8 (2078)

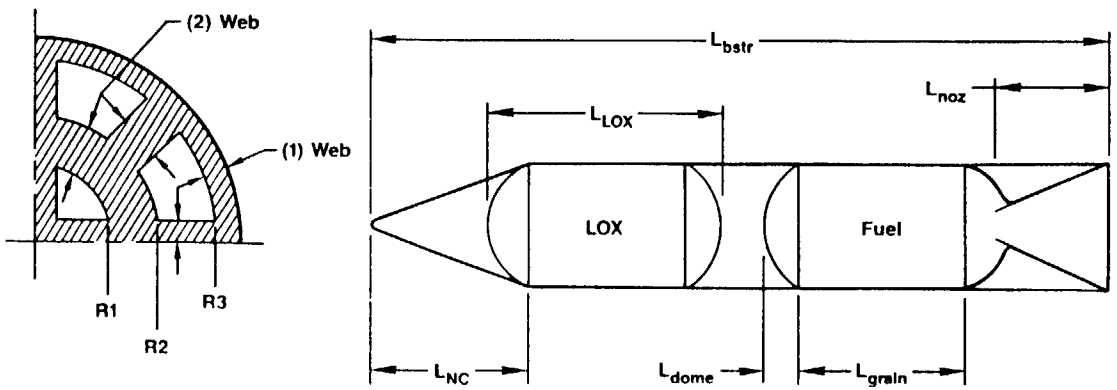

Figure 3-16. Preliminary Concept Large Hybrid Booster Design Parameters

50327

booster length, but requires 33-34 fuel ports. The number of fuel ports can be reduced by using the higher regression fuel, but at the expense of delta payload performance. Based on these findings, the baseline design remained the 4.57-m (180-in.) diameter inert fuel system.

Design details were explored further with the studies summarized in Figures 3-19, 3-20, 3-21 and 3-22. It can be seen that with fuel No. 7, the booster length decreases as the number of ports increases, and that the payload increases with 34 ports providing the best overall performance (Figures 3-20). It can also be seen that the ratio of grain length to hydraulic diameter affects performance. In the case of 28 ports (Figure 3-4), delta payload peaks at a ratio of 36. With 34 ports, the performance peak ratio is at 40 to 41. As indicated earlier, increasing the regression ratio permits fewer ports but at the expense of performance and safety. This is shown in Figure 3-22 for fuel No. 8 containing 30% AP. Eighteen ports provide a nearly equivalent performance and a shorter booster length. Without a clear length restraint, fuel No. 7 is preferred on the basis of higher safety.

Fewer ports are required in the case of the 2.44-m (96-in.) diameter booster. As shown in Figures 3-23 and 3-24, near minimum length and near maximum performance are achieved with 18 ports. Although not shown, fuel No. 9, containing aluminum, resulted in a slightly shorter length but with a reduction in delta payload.

The final design comparison is summarized in Table 3-5 for the large booster and Table 3-6 for the small booster. In these studies quantitative comparisons were made of the effect of the oxygen-fed system and thrust vector control, as well as fuel type and booster diameter. Material trades were also examined. As a result of these studies and the life cycle costs discussed in the following sections, the baseline large booster and small booster systems were selected. Details of these studies are summarized in Tables 3-5, 3-6 and 3-7. However, the effects of the different components and design parameters is better seen in the following figures. Figure 3-25 shows the booster length for the different large configurations. It can be seen that as

expected, all the boosters are longer than solid propellant ASRM. However, the 4.57-m (180-in.) booster with either the inert fuel No. 7, the aluminized inert fuel No. 9 or the oxidized fuel provide the shortest lengths. Figure 3-20 shows that the inert fuel system, a flexseal nozzle and a pump-fed oxidizer delivery system provides the highest performance. This is also shown in Figure 3-21.

Figure 3-22 shows that a composite overwrapped metal LOX tank is preferable for either the pump-fed or pressure-fed systems, and for either the 4.57 m (180 in.) or 2.44 m (96-in.) diameter boosters.

In the case of the 2.44-m (96-in.) booster, the shortest length (using fuel No. 7) is with the use of the flexseal nozzle and pump-fed oxygen delivery. The highest delta payload is achieved with the same system and a composite overwrapped metal LOX tank.

While these results show clear length and performance preferences with regards to the oxygen feed system, oxygen tank composition, thrust vector control, etc., they do not address the impact of these parameters on life cycle costs, launch rate and issue of recoverable or nonrecoverable systems. These items are addressed in the following section.

FOLDOUT FRAME /

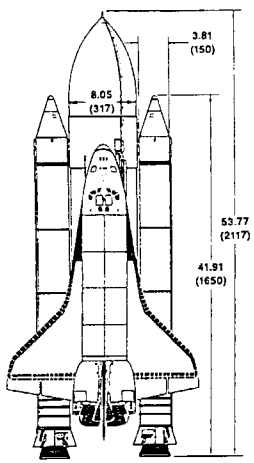

ASRM

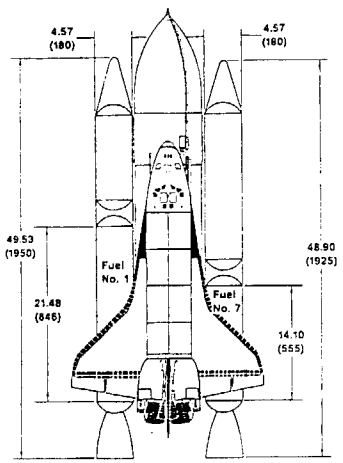

Large Hybrid
(A)

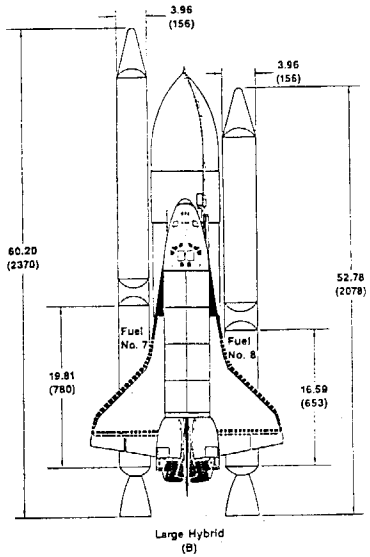

Large Hybrid
(B)

Note: Dimensions are in inches

Fuel No.	Solid propellant	1	7	7	9	8
No. of boosters	2	2	2	2	2	2
Classification	Class B	Class B	Inert	Inert	Inert	Class B
OD, m (in.	3.81 (150)	4.57 (180)	4.57 (180)	3.96 (156	3.96 (156)	3.96 (156)
L_{grain}, m (in.)	—	21.48 (846)	4.57 (555)	1981 (780)	19.25 (758)	16.59 (653)
L_{bstr}, m (in.)	41.91 (1650)	49.53 (1950)	48.90 (1925)	60.20 (2370)	58.17 (2290)	52.78 (2078)
Δpayload, kg (lb)	Reference	3991 (8800)	8550 (18,850)	7711 (17,000)	6781 (14,950)	8029 (17,700)
No. of ports	1	18	34	20	19	11
O/F	—	0.88	2.73	2.89	1.90	1.75
Preliminary CSD selection	—	—	X	—	Similar to No. 7	X

Figure 3-17. Preliminary Large Booster Configurations

50241

Parameter	Fuel No.	
	8	7
LOX feed	Pump	Pump
Total impulse, N-s (lb-sec)	3.60×10^8 (0.81×10^8)	3.60×10^8 (0.81×10^8)
Motor diameter, m (in.)	2.29 (90)	2.44 (96)
No. of ports	1 | 4	6 | 12
Area/port, m^2 ($in.^2$)	0.077 | 0.143 (119 | 222)	0.088 | 0.077 (137 | 119)
R1, m (in.)	0.16 (6.17)	0.62 (24.41)
R2, m (in.)	0.68 (26.68)	0.84 (32.92)
R3, m (in.)	0.88 (34.78)	1.10 (43.33)
L/D_h	38.2	40.4
A_t/A_p	0.500	0.226
Web, m (in.)	0.26 (10.26)	0.11 (4.25)
Volume fraction	0.84	0.68
G_o maximum, kg/m^2-s ($lb/in.^2$-sec)	1097 (1.56)	584 (0.83)
$\bar{\varepsilon}$	12.0	12.0
$\overline{O/F}$	1.66	2.57
$\bar{I}_{sp}$, N-s/kg (sec)	2912 (297.0)	2973 (303.3)
$\bar{P}_c$, MPa (psia)	5.16 (748)	5.16 (749)
$\dot{w}_{ox}$, maximum, kg/s (lb/sec)	821 (1811)	(2062)
W_{motor}, kg (lb)	1.41×10^5 (3.11×10^5)	1.384×10^5 (3.051×10^5)
DWPLD, kg (lb)	6713 (14,800)	6547 (14,433)
L_{grain}, m (in.)	12.0 (471)	11.2 (439)
L_{LOX}, m (in.)	16.9 (667)	17.0 (671)
L_{noz}, m (in.)	2.95 (116)	2.97 (117)
L_{NC}, m (in.)	2.82 (111)	3.00 (118)
L_{dome}, m (in.)	0.66 (26)	0.71 (28)
L_{bstr}, m (in.)	36.12 (1422)	36.71 (1406)

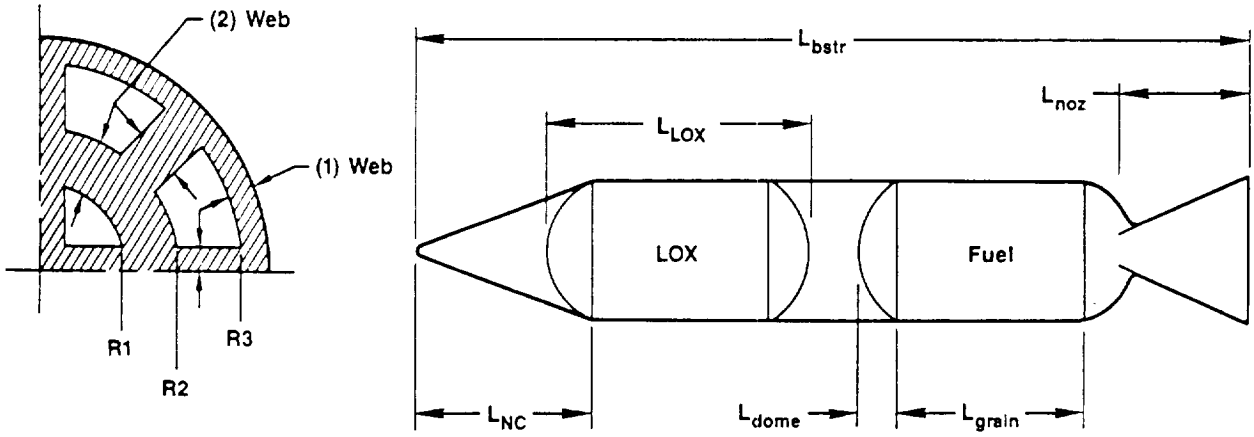

Figure 3-18. Preliminary Concept for Small Hybrid Booster Design Parameters
50326

TABLE 3-3. SUBSYSTEM WEIGHTS FOR HYBRID BOOSTER MOTORS

T17023

Function Code	Description TVC	SRM Flexseal, kg (lb)	4.57-m (180-in.) HBM LI, kg (lb)	4.57-m (180-in.) HBM Flexseal, kg (lb)	2.44-m (96-in.) HBM LI, kg (lb)	2.44-m (96-in.) HBM Flexseal, kg (lb)
3.1/3.2	Nosecap and frustum	1886 (4158)	1886 (4158)*	1886 (4158)*	537 (1184)*	537 (1184)*
3.3	Forward skirt	2888 (6367)	817 (1800)†	817 (1800)†	454 (1000)†	454 (1000)†
3.5	Aft skirt	4997 (11,016)	5443 (12,000)	5443 (12,000)	1588 (3500)	1588 (3500)
3.5.5	Hold-down posts	1227 (2705)	1225 (2500)	1225 (2700)	-	-
3.6	Attach structure	679 (1497)	-	-	-	-
3.7	Systems tunnel	338 (746)	396 (873)	396 (873)	338 (746)	338 (746)
3.9	Separation ring	71 (157)	-	-	-	-
4.1	Thermal protection	812 (1790)	771 (1700)	771 (1700)	386 (850)	386 (850)
4.3/4.4	Paint and sealants	67 (148)	68 (150)	68 (150)	45 (100)	45 (100)
5.1.2	Deceleration system	4302 (9485)*	3742 (8250)*	3742 (8250)*	862 (1900)*	862 (1900)*
5.3/26.6	Separation motors	609 (1342)	609 (1342)	609 (1342)	181 (400)	181 (400)
9.2	Batteries/generator/ conductor	20 (45)	54 (120)	54 (120)	54 (120)	54 (120)
10.	Electrical/ instrumental	447 (985)	354 (780)	354 (780)	354 (780)	354 (780)
-	Avionics and flight controls	-	11 (25)	11 (25)	11 (25)	11 (25)
-	HMS (data base)	-	3 (6)	3 (6)	3 (6)	3 (6)
11.	TVC control system	1056 (2329)	930 (2050)	1056 (2329)	128 (283)	272 (600)
16.	Range safety and abort	65 (144)	65 (144)	65 (144)	65 (144)	65 (144)
	Subsystem weight	19,466 (42,914)	16,374 (36,098)	16,501 (36,377)	5007 (11,038)	5150 (11,355)
	Interstage structure	-	1425 (3142)	1425 (3142)	423 (932)	423 (932)
	Total subsystem weight	19,466 (42,914)	17,799 (39,240)	17,926 (39,519)	5430 (11,970)	5573 (12,287)

* Recoverable (use 50% for recoverable)
† Attach ring structure ratio to Titan

TABLE 3-4. LARGE MOTOR TRADE STUDY
(Sheet 1 of 2)

T16917

Fuel No.	Number of Ports	Motor Diameter, m (in.)	Preliminary Booster Length, m (in.)	$(L/D_h)_{port}$	Δ payload, kg (lb)	Booster Weight kg x 10^6 (lb x 10^6)	Volumetric Loading, %	Residual Fuel, %	Meets Total Impulse
A. Hydrocarbon Fuel									
7	18	3.86 (152)	63.9 (2514)	40	8436.8 (18,600)	0.558 (1.231)	52	35	Yes
7	23	4.06 (160)	58.4 (2298)	40	8754.3 (19,300)	0.555 (1.224)	54	6	Yes
7	23	4.57 (180)	54 (2124)	40	-5579.2 (-12,300)	0.625 (1.378)	63	35	Yes
7	33	4.57 (180)	48.1 (1895)	40	9065 (19,270)	0.552 (1.218)	62	6	Yes
7	32	4.57 (180)	47.7 (1878)	40	8740.7 (19,270)	0.548 (1.209)	63	6	No (-1%)
7	31	4.57 (180)	50.9 (2003)	40	8377.9 (18,470)	0.553 (1.219)	53	6	Yes
7	34	4.57 (180)	49.1 (1932)	34/40	9003.8 (19,850)	0.551 (1.215)	59	6	Yes
7	23	4.57 (180)	51.2 (2014)	25	-1340.4 (-2955)	0.523 (1.152)	37	6	No (-11%)
7	23	5.46 (215)	51.8 (2040)	25	2041.2 (4500)	0.586 (1.293)	27	6	Yes

TABLE 3-4. LARGE MOTOR TRADE STUDY
(Sheet 2 of 2)

T16917

Fuel No.	Number of Ports	Motor Diameter, m (in.)	Preliminary Booster Length, m (in.)	$(L/D_h)_{port}$	Δ payload, kg (lb)	Booster Weight kg x 10^6 (lb x 10^6)	Volumetric Loading, %	Residual Fuel, %	Meets Total Impulse
B. Aluminized/AN Fuel									
1	15	4.57 (180)	55.9 (2200)	39	1254.2 (2765)	0.605 (1.333)	49	6	Yes
1	15	4.50 (177)	55 (2165)	39	2057 (4535)	0.602 (1.327)	53	6	Yes
1	18	4.57 (180)	51.8 (2041)	39	2644.4 (5830)	0.599 (1.321)	57	6	Yes
1	21	4.57 (180)	49.3 (1942)	39	3517.6 (7755)	0.596 (1.313)	64	6	Yes
1	22	4.57 (180)	48.7 (1916)	39	2649.9 (5842)	0.583 (1.286)	64	6	No (-2%)

Note: Composite LOX tank, propane LOX pump, ϵ = 12

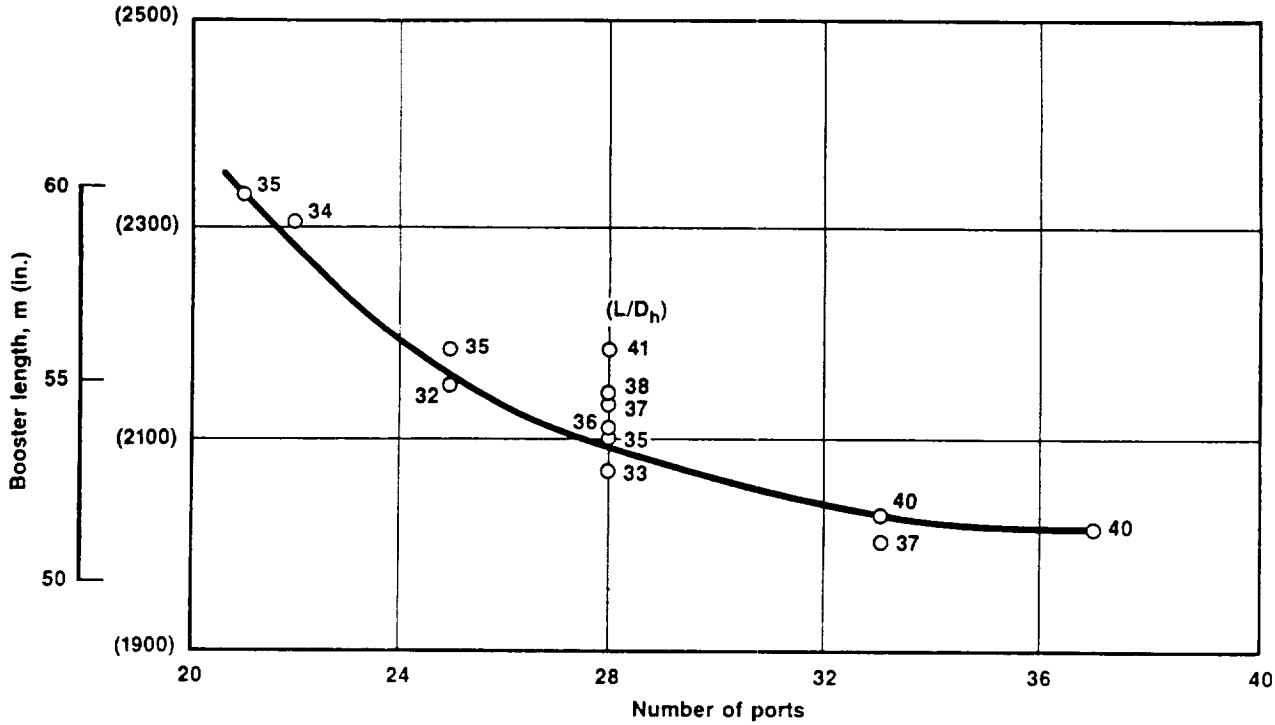

Figure 3-19. Variation of Booster Length with No. of Fuel Ports - Fuel No. 7, 4.57-m (180-in.) OD, Composite LOX Tank/Pump-Fed

50413

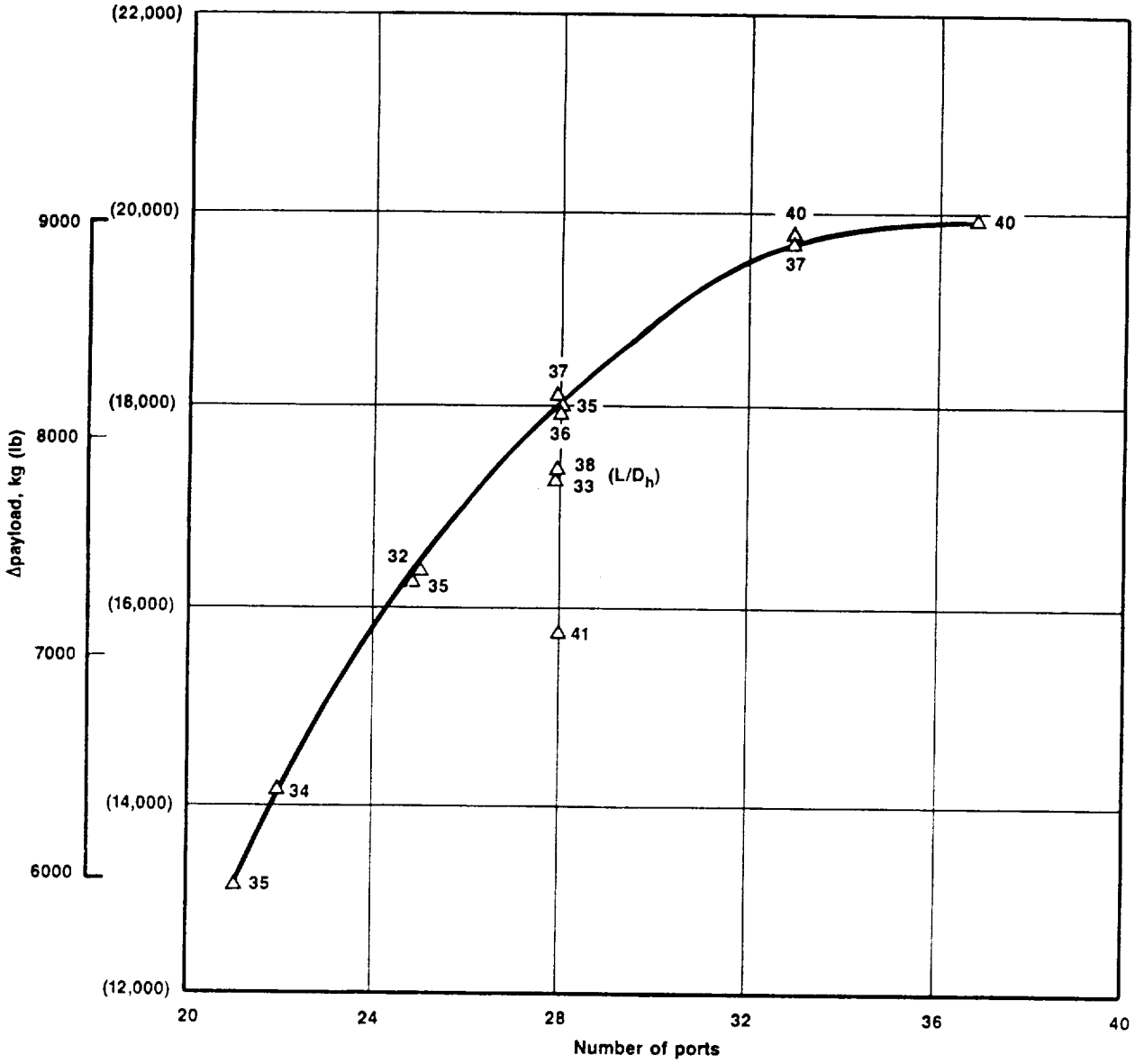

Figure 3-20. Variation of Delta Payload with Number of Fuel Ports - Fuel No. 7, 4.57-m (180-in.) OD, Composite LOX Tank

50467 467

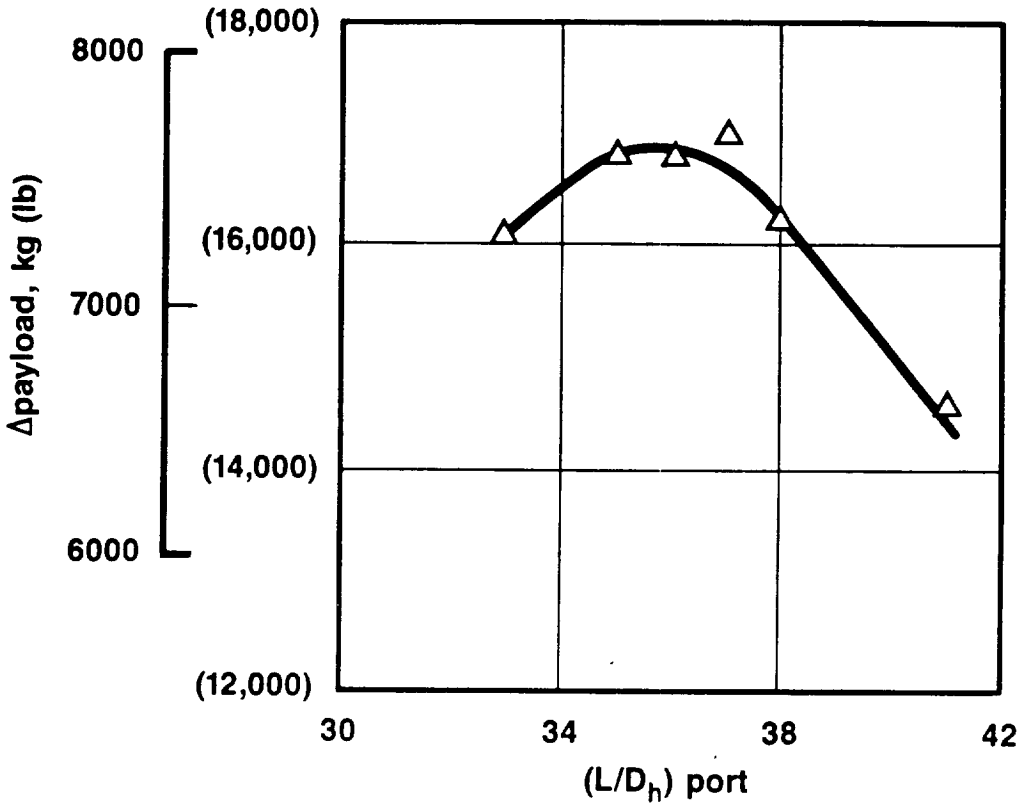

Figure 3-21. Variation of Delta Payload with Port (L/Dh) for 28 Ports - Fuel No. 7, 4.57-m (180-in.) OD, Composite LOX Tank

50468

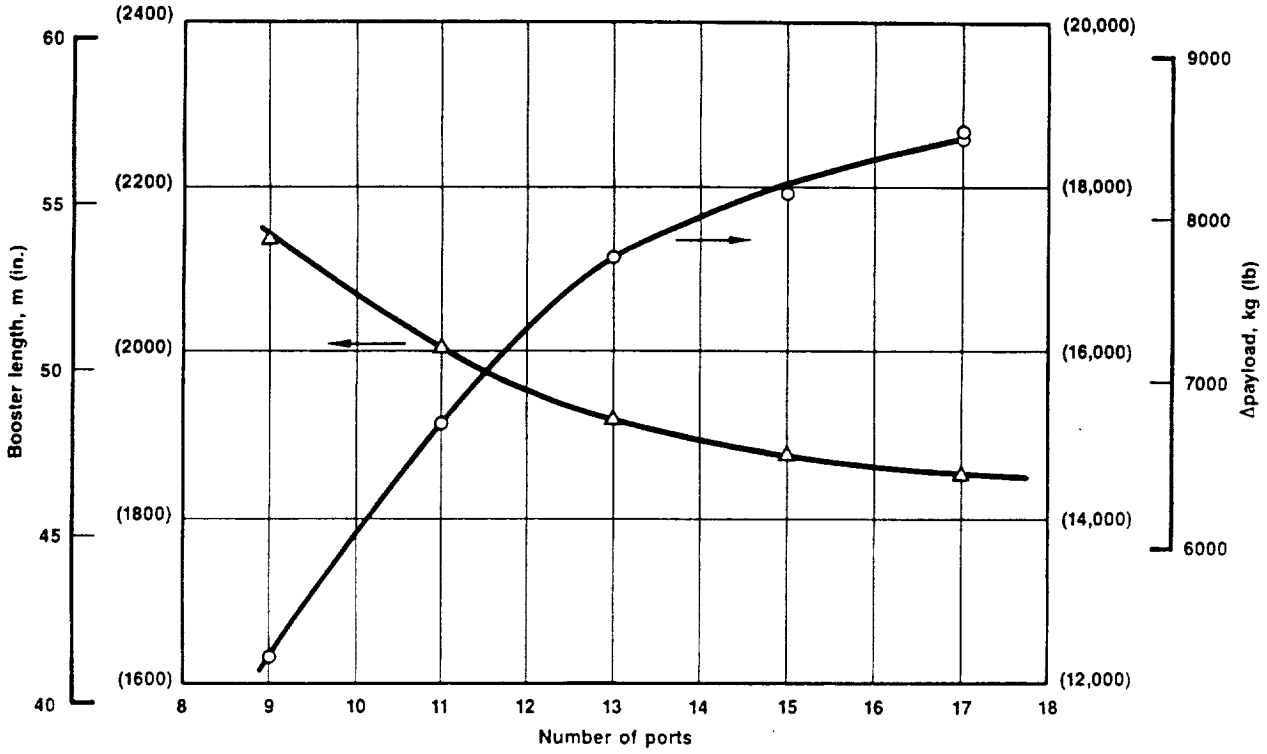

Figure 3-22. Variation of Delta Payload and Booster Length with Number of Fuel Ports - Fuel No. 8, 4.57-m (180-in.) OD, Composite LOX Tank

50469

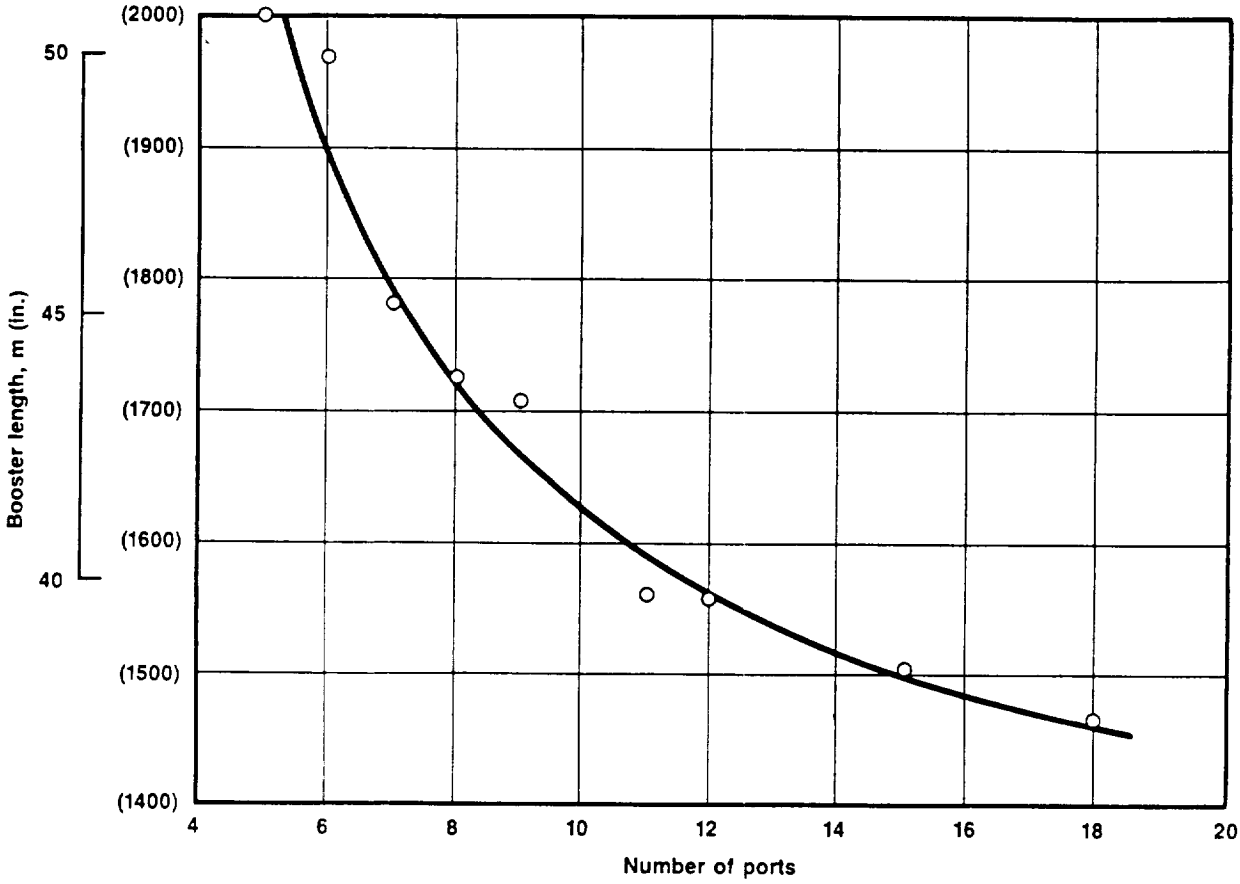

Figure 3-23. Variation in Booster Length with No. of Ports - Fuel No. 7 2.44-m (96-in.) OD, Composite LOX Tank

50417

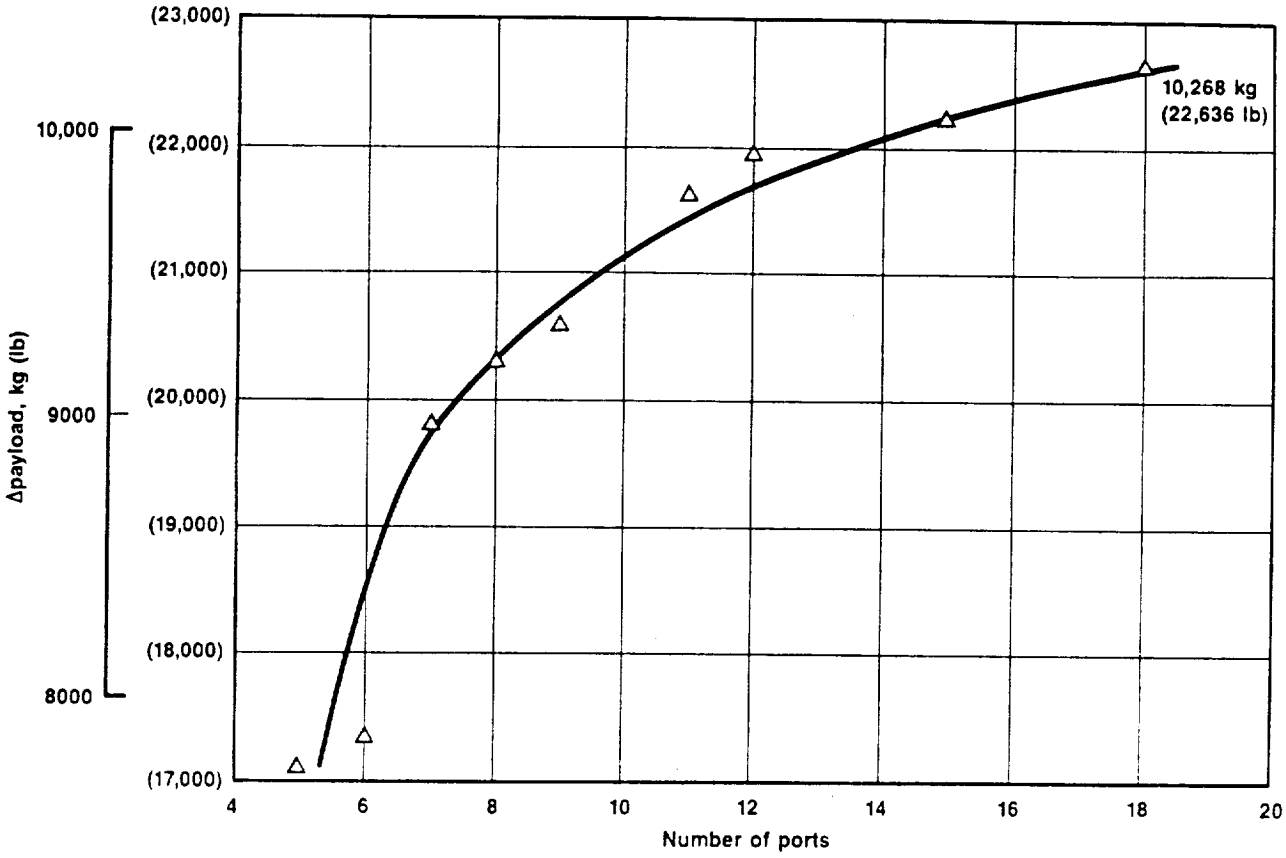

Figure 3-24. Variation in Δ Payload with No. of Fuel Ports - Fuel No. 7, 2.44-m (96-in.) OD, Composite LOX Tank

50470

FOLDOUT FRAME 1

FOLDOUT FRAME 2

TABLE 3-5. LARGE HYBRID BOOSTER DESIGN SUMMARY

T17022

Total Impulse, N-s (lb-sec)	14.40 X 10^8 (3.24 X 10^8)									
Run No.	-934	-935	-955	-961	-940	-937	-939	-942	-976	-992
Fuel No.	7	8	1	9	7	7	7	8	8	7
Diameter, m (in.)	4.57 (180)	4.57 (180)	4.57 (180)	4.57 (180)	.57 180)	4.96 (180)	4.57 (180)	3.96 (156)	3.96 (156)	3.96 (156)
TVC	LI	LI	LI	LI	.I	Flexseal	Flexseal	LI	Flexseal	Flexseal
Pump/press	Pump	Pump	Pump	Pump	Press (He)	Pump	Press (He)	Pump	Pump	Pump
W_{motor}, kg (lb)	562,617.2 (1,284,-51)	580,312.4 (1,301,-16)	628,793.5 (1,381,843)	599,391.5 (1,321,432)	505,213.8 (1,334,268)	569,506.1 (1,255,546)	590,019.8 (1,300,771)	603,65E.9 (1,330,840)	592,019.3 (1,305,179)	584,824.4 (1,289,317)
$W_{propellant}$, kg (lb)	511,675 (1,128,050)	522,960.3 (1,152,930)	545,094.3 (1,201,727)	528,446.5 (1,165,025)	532,897.6 (1,174,838)	497,620.8 (1,097,066)	517,675.1 (1,141,719)	537,922.2 (1,185,916)	524,493.4 (1,156,310)	516,3+7.6 (1,138,352)
$W_{burnout}$, kg (lb)	97,121.8 (214,117)	94,667 (208,705)	11,253.1 (24-5,227)	98,473.6 (217,097)	97,447.5 (214,835)	83,852 (184,862)	82,538 (18-,965)	93,808.3 (206,822)	82,259.9 (181,352)	80,305.7 (177,043)
$W_{propellant\ expendable}$, kg (lb)	485,495.4 (1,070,334)	495,645.4 (1,092,711)	515,560.4 (1,136,616)	500,918 (1,104,335)	507,766.3 (1,119,433)	485,608.8 (1,070,584)	507,482 (1,118,806)	509,895.1 (1,124,135)	509,759.4 (1,123,827)	504,519 (1,112,274)
MF	0.833	0.860	0.822	0.836	0.839	0.853	0.860	0.845	0.861	0.863
L_{grain}, m (in.)	14.45 (569)	12.9 (508)	20.42 (804)	14.66 (577)	15.01 (591)	14.35 (565)	15.04 (592)	17.45 (687)	17.42 (686)	17.75 (669)
No. ports	34+1+9+24	17+1+4+12	21+1+7+13	29+1+8+20	34+1+9+24	34+1+9+24	34+1+9+24	9+2+7	9+2+7	24+1+7+16
VF	0.60	0.77	0.64	0.59	0.58	0.59	0.58	0.76	0.76	0.61
(L/D)port	34.4/40.7	28.9	39.2	34.2	36.7/41.0	34.2/40.3	36.9/41.0	33.3	33.2	41.0
Area/port m^2 ($in.^2$)	0.139/0.145/0.210 (215/225/326)	0.156/0.264/0.201 (242/409/312)	0.213/0.282/0.272 (330/437/422)	0.144/0.201/0.241 (223/311/373)	0.132/0.155/0.219 (204/240/339)	0.138/0.146/0.211 (214/226/327)	0.130/0.156/0.219 (202/242/340)	0.376/C.304 (583/471)	0.377/0.306 (585/474)	0.147/0.194/0.203 (228/301/315)
Web, m (in.)	0.109 (4.30)	0.252 (9.91)	0.177 (6.95)	0.125 (4.94)	0.106 (4.18)	0.109 (4.29)	0.106 (4.17)	0.285 (11.21)	0.284 (11.19)	0.130 (5.11)
O/F	12.0	12.0	12.0	12.0	8.5	12.0	8.5	9.4	9.4	9.4
I_{sp}, N-s/kg (sec)	2.60 2968.5 (302.7)	1.75 2905.7 (296.3)	0.91 2793.9 (284.9)	1.83 2874.3 (293.3)	2.81 2838 (289.4)	2.64 2964.6 (302.3)	2.81 2839 (289.5)	1.83 2826.3 (288.2)	1.84 2825.3 (288.1)	2.98 2854.7 (291.1)
G_o, max kg/m^2/sec (lb/$in.^2$/sec)	513.2 (0.73)	836.7 (1.19)	393.7 (0.56)	485.1 (0.69)	527.3 (0.75)	513.2 (0.73)	527.3 (0.75)	1089.8 (1.55)	1082.7 (1.54)	773.4 (1.10)
P_c, MPa (psi)	5.17 (750)	5.17 (750)	5.17 (750)	5.17 (750)	3.45 (500)	5.17 (750)	3.45 (500)	5.17 (750)	5.17 (750)	5.17 (750)
LIS	120	120	120	120	240	120	240	110	110	110
L_{BSTR}, m (in.)	51.28 (2019)	47.73 (1879)	51.23 (2017)	49.96 (1967)	55.88 (2200)	50.55 (1990)	55.12 (2170)	57.23 (2253)	56.26 (2215)	60.12 (2367)
WPLD, kg (lb)	9003.8 (19,850)	8455 (18,640)	3517.6 (7755)	7255.73 (15,830)	7323.25 (16,145)	11,532.6 (25,425)	10,267.5 (22,680)	7690.7 (16,955)	9958.6 (21,955)	10,738.8 (23,675)
Motor case	Steel	Steel	Steel	Steel	Steel	Steel	Steel	Steel	Steel	Steel

TABLE 3-6. ONE-QUARTER SCALE HYBRID BOOSTER

T17024

Total Impulse N-s (lb-sec)	(4 X(3.60 X 10^8)) 4 X(0.81 X 10^8))				
Run No.	943	944	933	931	946
Fuel No.	7	7	7	7	7
Diameter, m (in.)	2.44 (96)	2.44 (96)	2.44 (96)	2.44 (96)	2.44 (96)
TVC	LI	Flexseal	LI	Flexseal	LI
Pump/press	Pump	Pump	Press (He)	Press (He)	Pump
W_{motor}, kg (lb)	144,329.9 (318,193)	141,229.6 (311,358)	150,071.1 (330,850)	146,839.7 (323,726)	147,978 (326,235)
$W_{propellant}$, kg (lb)	128,852 (284,070)	125,242.3 (276,112)	132,019.9 (291,054)	128,337.2 (282,935)	129,685 (285,907)
$W_{burnout}$, kg (lb)	22,052.3 (48,617)	18,952.9 (41,784)	24,258.6 (53,481)	21,016.8 (46,334)	25,718 (56,699)
$W_{propellant\ expendable}$, kg (lb)	122,277.6 (169,576)	122,276.7 (269,574)	125,812.5 (277,369)	125,823 (277,392)	122,713 (270,536)
MF	0.847	0.866	0.838	0.857	0.829
L_{grain}, m (in.)	10.2 (400)	10.2 (400)	10.6 (418)	10.6 (418)	10 (392)
No. ports	18=1+5+12	18=1+5+12	18=1+5+12	18=1+5+12	18=1+5+12
VF	0.74	0.74	0.72	0.72	0.72
$(L/D)_{port}$	41.0	41.0	41.0	41.0	39.0
Area/port, m^2, ($in.^2$)	0.048/0.068/0.062 (75/105/96)	0.048/0.068/0.062 (75/105/96)	0.052/0.074/0.068 (81/114/105)	0.052/0.074/0.068 (81/114/105)	0.051/0.072/0.066 (79/111/102)
Web, m (in.)	0.122 (4.80)	0.122 (4.80)	0.117 (4.59)	0.117 (4.59)	0.122 (4.79)
ϵ	0.30 (12.0)	0.30 (12.0)	0.25 (10.0)	0.25 (10.0)	0.30 (12.0)
$\overline{O/F}$	2.76	2.76	2.93	2.93	2.82
I_{sp}, N-s/kg (sec)	2946.9 (300.5)	2946.9 (300.5)	2865.5 (292.2)	2864.5 (292.1)	2938.1 (299.6)
G_o, max, $kg/m^2/sec$ ($lb/in.^2/sec$)	766.4 (1.09)	766.4 (1.09)	738.2 (1.05)	738.2 (1.05)	731.2 (1.04)
P_c, MPa (psi)	5.18 (750)	5.18 (750)	3.45 (500)	3.45 (500)	5.18 (750)
LIS	83	83	112	112	83
LBSTR, m (in.)	38.1 (1501)	37.4 (1473)	40.3 (1586)	39.5 (1557)	37.6 (1479)
AWPLD, kg (lb)	10,267.1 (22,635)	12,746 (28,100)	7672.5 (16,915)	10,253.5 (22,605)	7568.2 (16,685)
Motor case	Composite	Composite	Composite	Composite	Steel

TABLE 3-7. BOOSTERS WEIGHT SCHEDULE FOR LOX PUMP FED, FLEXSEAL NOZZLE SYSTEMS

T17025

Parameter	Hybrid Booster Motor					
Diameter, m, (in.)	4.57	(180)	3.96	(156)	2.44	(96)
Hybrid fuel, No.	7				7	
Total impulse, N-m (lb-sec)	14.41×10^8	(3.24×10^8)	14.41×10^8	(3.24×10^8)	3.60×10^8	(0.81×10^8)
Weight, kg (lb)						
Hybrid rocket motor	569,503	(1,255,546)	592,016.1	(1,305,179)	141,228.9	(311,358)
Total solid fuel (including residual)	138,272.7	(304,839)	187,487.9	(413,340)	33,645.2	(74,175)
Fuel residual	8296.7	(18,291)	11,249.1	(24,800)	2018.5	(4450)
Total oxidizer (including (residual)	355,790.6	(784,384)	333,668.9	(735,614)	90,689.4	(199,937)
Oxidizer residual	3679.1	(8111)	3450.5	(7607)	937.6	(2067)
Subsystems (recovery, separation interstage structure, nose cone)	17,925.5	(39,519)	17,925.5	(39,519)	5573.3	(12,187)
LOX tank, (composite with metal liner and insulation)	2702.5	(5958)	2861.7	(6309)	984.8	(2171)
LOX pump and hardware	2766.9	(6100)	2766.9	(6100)	1587.6	(3500)
Pump fuel	3558	(7844)	3336.6	(7356)	906.7	(1999)
Pump fuel tank	204.1	(450)	204.1	(450)	56.3	(124)
Helium tank	112.5	(248)	112.5	(248)	32.2	(71)
Helium	39.5	(87)	39.5	(87)	10.4	(23)
Injector	635.03	(1400)	623.7	(1375)	612.4	(1350)
Ignition system	226.8	(500)	226.8	(500)	68.04	(150)
Motor case (metal with three joints)	31,810.9	(70,131)	28,578.7	(63,025)	-	-
Motor case (composite)	-	-	-	-	2766	(6098)
Case insulation	5595.1	(12,335)	4787.2	(10,554)	1794	(3955)
Flexseal nozzle	9867	(21,753)	9390.3	(20,702)	2593.6	(5718)
Total weight inerts	485,606.2	(1,070,584)	509,756.7	(1,123,827)	122,276.1	(269,574)
MF (expended weight/initial weight	0.39	(0.853)	0.39	(0.861)	0.39	(0.866)

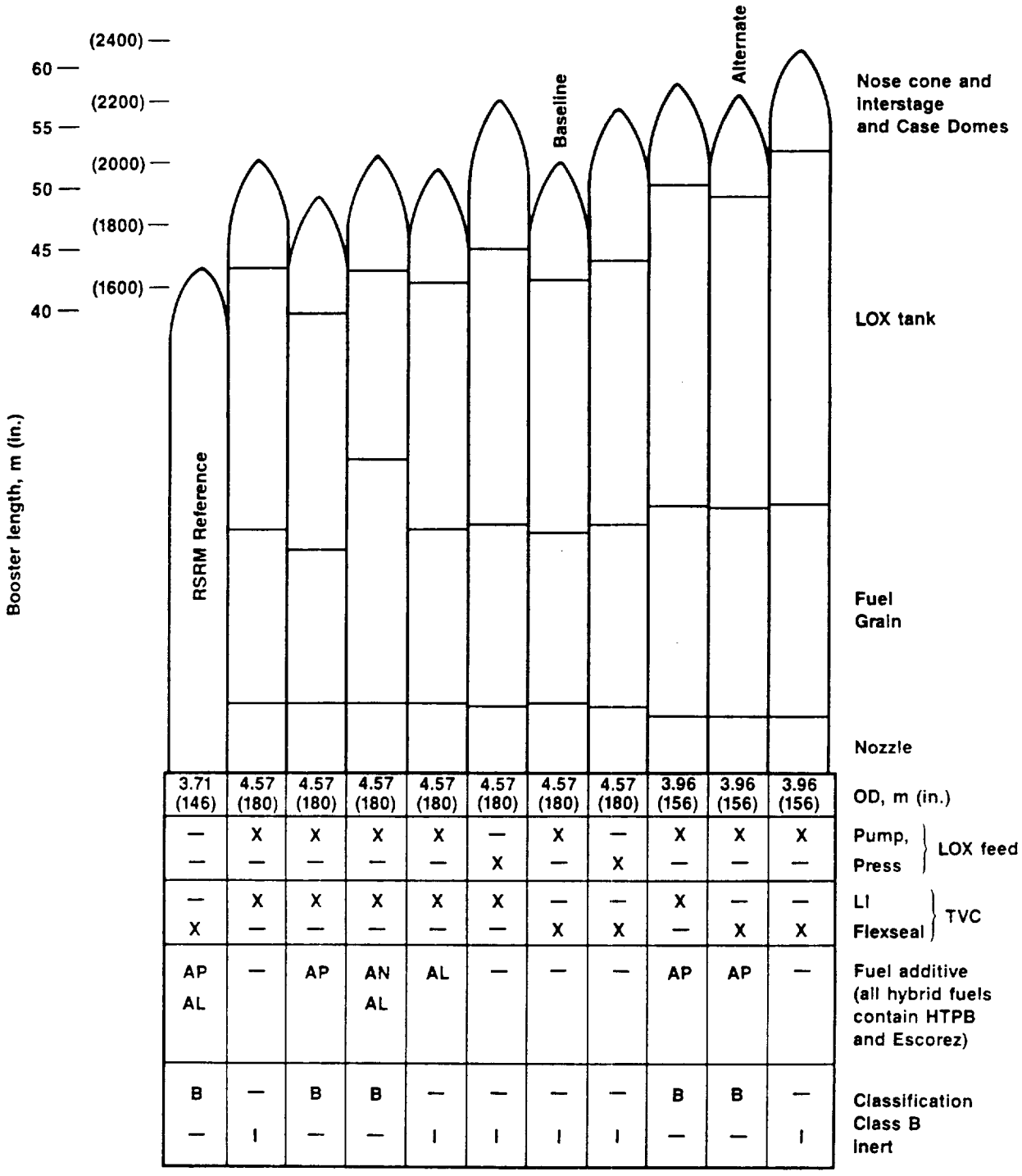

RSRM Reference	Baseline						Alternate			
3.71 (146)	4.57 (180)	4.57 (180)	4.57 (180)	4.57 (180)	4.57 (180)	4.57 (180)	4.57 (180)	3.96 (156)	3.96 (156)	3.96 (156)
—	X	X	X	X	—	X	—	X	X	X
—	—	—	—	—	X	—	X	—	—	—
—	X	X	X	X	X	—	—	X	—	—
X	—	—	—	—	—	X	X	—	X	X
AP AL	—	AP	AN AL	AL	—	—	—	AP	AP	—
B	—	B	B	—	—	—	—	B	B	—
—	I	—	—	I	I	I	I	—	—	I

Figure 3-25. Large Booster Length Comparisons

50449

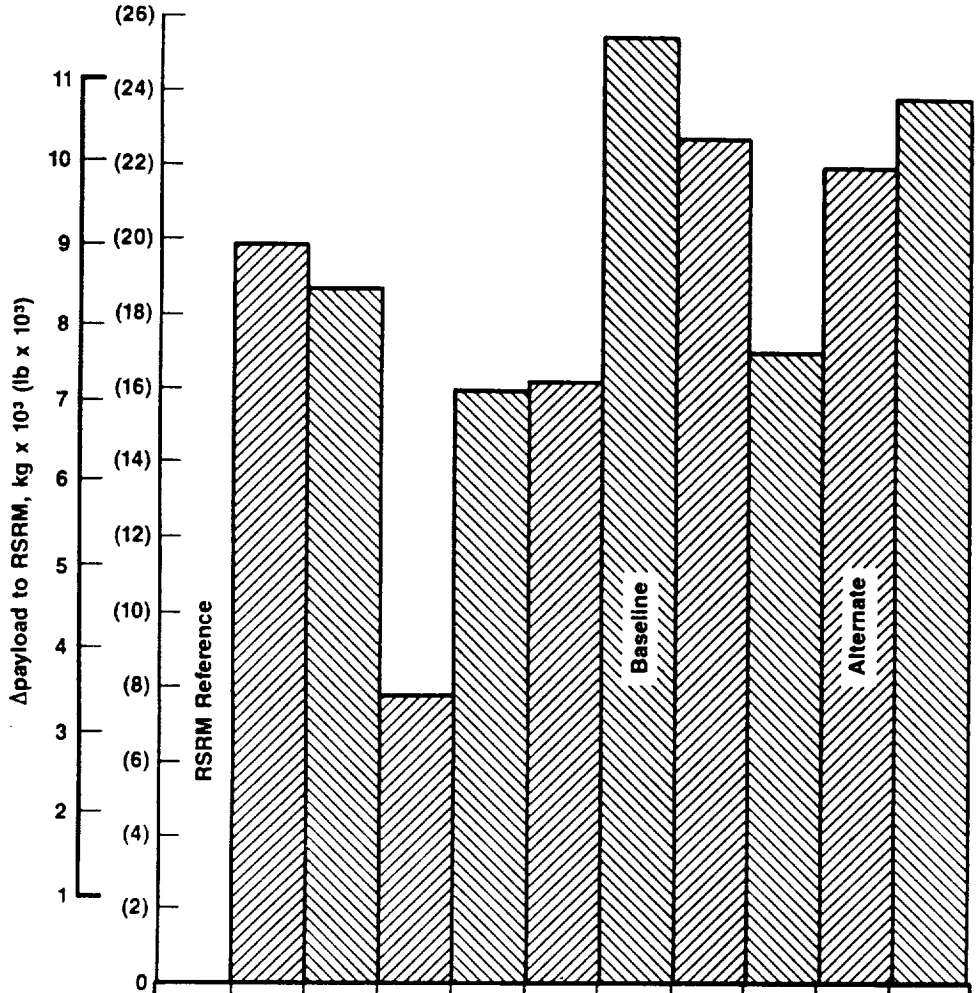

3.81 (150)	4.57 (180)	4.57 (180)	4.57 (180)	4.57 (180)	4.57 (180)	4.57 (180)	4.57 (180)	3.96 (156)	3.96 (156)	3.96 (156)	OD, m (in.)
—	X	X	X	X	—	X	—	X	X	X	Pump, LOX feed
—	—	—	—	—	X	—	X	—	—	—	Press LOX feed
—	X	X	X	X	X	—	—	X	—	—	LI TVC
X	—	—	—	—	—	X	X	—	X	X	Flexseal TVC
AP AL	—	AP	AN AL	AL	—	—	—	AP	AP	—	Fuel additive (all hybrid fuels contain HTPB and Escorez)
B —	— I	B —	B —	— I	— I	— I	— I	B —	B —	— I	Classification Class B Inert

Figure 3-26. Large Booster Payload Comparisons

50459

C-2

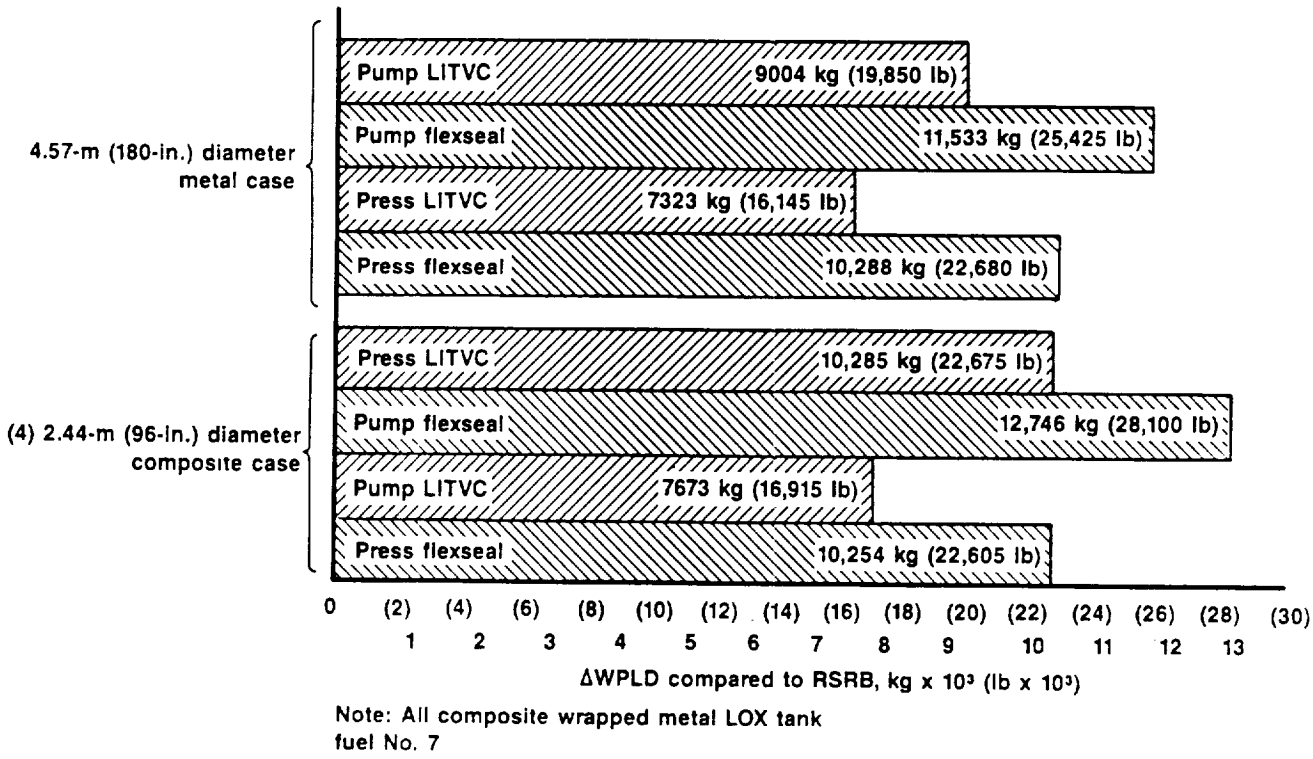

Figure 3-27. Effect of Nozzle/TVC System on Performance

50463

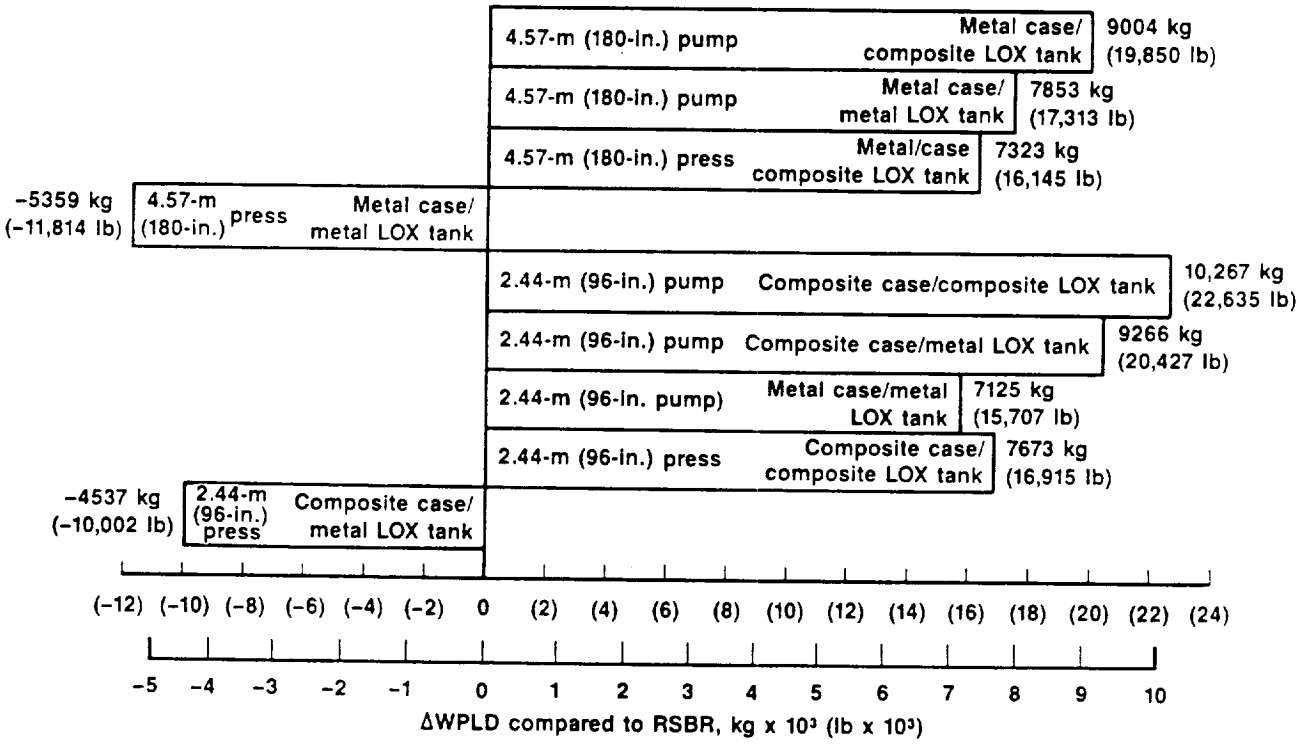

Figure 3-28. Effect of Oxidizer Tank Design and Load System on Performance

50462

4.0 COMPONENT DESIGN STUDIES

Trades and selections of the subcomponents (i.e., insulation materials, igniters, etc.) were made in conjunction with the preliminary concept and the final design studies, and are reported in the following sections. Selections of preferred and alternative major components, i.e., thrust vector control, oxidizer feed system, etc., have been made, but the ultimate selection must be made upon specific mission requirements. Consequently, the following section presents alternative designs and trade considerations as well as the preferred designs.

4.1 OXIDIZER FEED SYSTEMS

Hybrid rocket boosters have the potential to provide the optimum balance between cost and performance with significantly improved reliability and safety relative to conventional all-solid or all-liquid boosters. For a hybrid rocket, the fuel is in a solid state just as in a conventional solid booster. However, unlike a solid rocket all the oxidizer is not in a solid form integral with the fuel. Even if there is some solid oxidizer mixed with the fuel, the weight fraction is low enough to eliminate the possibility of an accidental ignition as with conventional solid propellants. For a hybrid the majority of all of the oxidizer, in this case liquid oxygen, is contained in a separate tank and must be made available to the fuel at various flow rates and pressures throughout the mission.

The purpose of this study was to conduct conceptual design studies to identify the optimum oxidizer supply system philosophy and configuration for the two different hybrid design sizes; an ASRM thrust size motor and a quarter-scale version of the same. Two different philosophies of supplying high-pressure oxygen to the hybrid have been examined. One option was to maintain a moderate pressure in the oxygen supply tank 0.69 MPa (100 psia) and pump the required flow to the 6.89+ MPa (1000+ psia) chamber pressure levels with a pump package. For this option, several pumping system thermodynamic and hardware options have been identified and examined. Based on preliminary booster option studies, the maximum desirable chamber pressure for the pump

fed configuration is about 7.69 MPa (1115 psia). Chamber pressures higher than this level begins to reduce payload capability as the combustion/fuel grain case starts to become excessively heavy.

An alternate to the pump-fed system is a pressure-fed system where the LOX supply tank is pressurized to a sufficient level to push the LOX flow into the hybrid combustion chamber. For this configuration, since the entire LOX tank gets heavier along with the combustor/fuel grain case, the payload begins to decrease if the peak chamber pressure exceeds about 5.17 MPa (750 psia). Several hardware options to maintain adequate LOX tank pressure have been examined. The major drivers to be considered in the pressure-fed system are the weight and cost of the large high-pressure LOX tank and the residual weight of the high pressure 3.24 MPa (≈470 psia) medium, used to displace the LOX remaining in the tank at shutdown.

Detailed thermodynamic and hardware investigations have been completed for several pump-fed and pressure-fed oxidizer supply system configurations. Based on these initial screening studies, one pump-fed and one pressure-fed configuration were identified for further evaluation. These two options were then evaluated with respect to weight, cost and reliability. The results of these studies were used to support an overall configuration recommendation for both the large and small booster applications.

Several tank design alternatives were considered for this hybrid study. Feasible design alternatives range from all metal tanks to all composite tanks, with the use of metal spray liners to prevent leakage and reaction with the propellants to tanks constructed as thin shells, then wrapped with composite to carry the structural load. After review of several cryogenic tankage studies for which no clear conclusions were reached, primarily due to unknowns about cost, it was decided that the thin metal shell concept with composite structural wrap would be used as a baseline for this study. Without extensive use of composites to minimize weight, the high-pressure LOX tank for the pressurized oxidizer supply systems would become extremely heavy and be totally uncompetitive from a performance standpoint with the pump-fed systems.

Also, several vendors contacted during this study were familiar with this concept of tank construction and were able to provide current cost information. Although it may not be optimum in each case, this type of construction was used to size all the tanks for all configuration evaluated during this study.

4.1.1 Pump-Fed Cycle Description

For the pump-fed system, a range of cycles were screened and three were selected for further examination. Thermodynamic cycle calculations were generated for each of these systems, then exercised to generate cycle matching trends based on a range of pump pressures, fuel flows, and turbine expansion ratios. These cycle trends were required to support hardware integration studies for each cycle. A fourth cycle was also identified and discussed but not examined in detail. The level of detail required to ensure feasibility was beyond the scope of this investigation.

A small separate fuel system is required for each of the three cycles examined. For this study it was assumed that the fuel supply system was pressure-fed. In each case the fuel tanks are relatively small and the weight penalty for a pressure-fed fuel system driven by a stored high-pressure gas (helium or nitrogen) has been accounted for and is considered acceptable relative to the cost and reliability implications of a pump-fed fuel system.

Various fuels were considered for the turbine drive systems. These included hydrogen, propane, and jet propellant (JP). Hydrogen, while the cleanest and highest heat content fuel available, does not package well, and requires a very large and heavy storage tank. Since JP does not lend itself to auxiliary use as a hybrid ignition fuel, the final decision was to use propane.

The four cycles identified are illustrated in Figures 4-1, 4-2, 4-3 and 4-4. The diagrams are simplified in that they show only one branch of a multi-branch pumping system. As will be discussed in the hardware integration section (4.1.3) three pumps operating in parallel have been selected as a baseline configuration for both the large and small boosters. Each "branch"

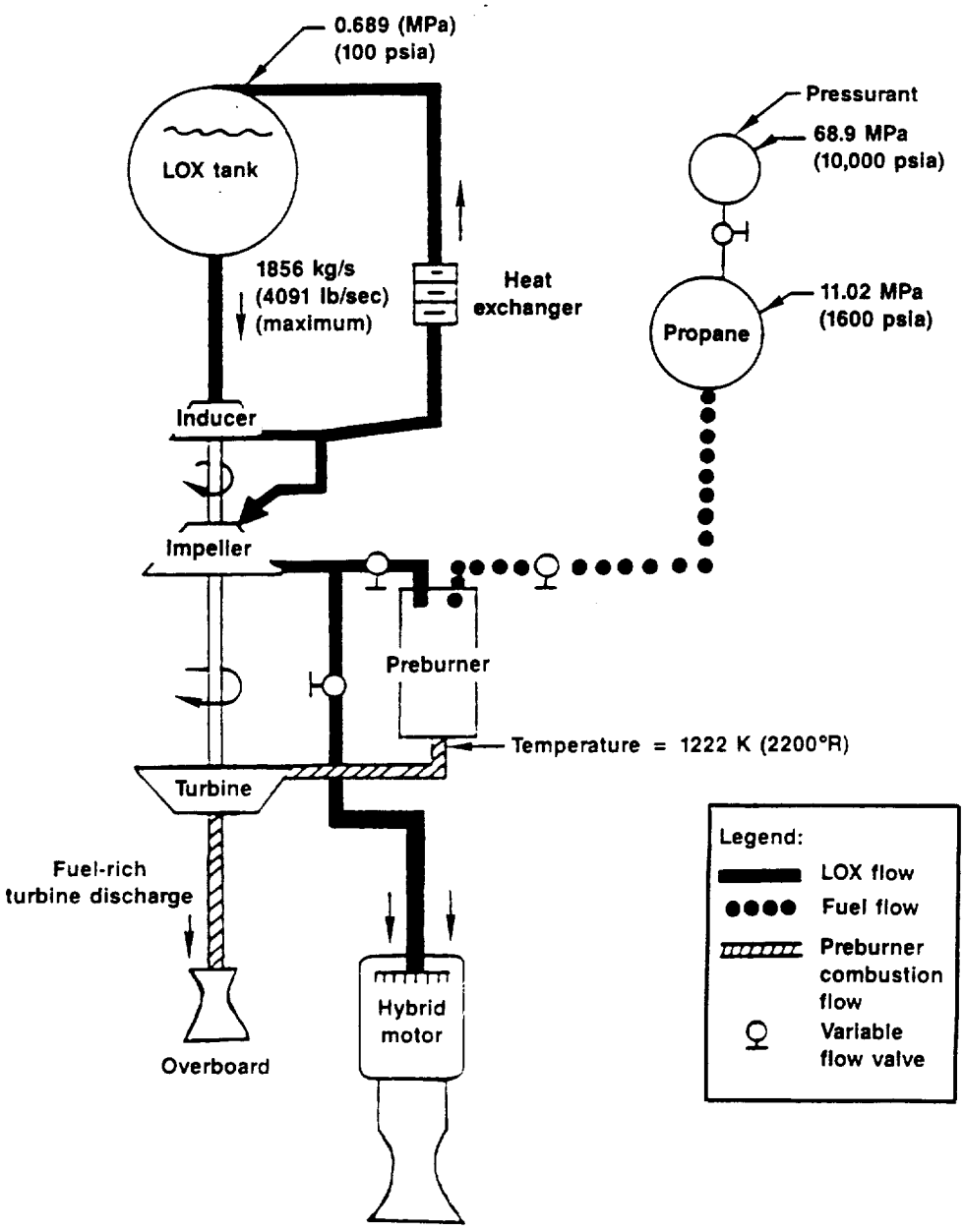

Figure 4-1. Fuel-Rich Turbine Drive to Overboard Discharge

50373

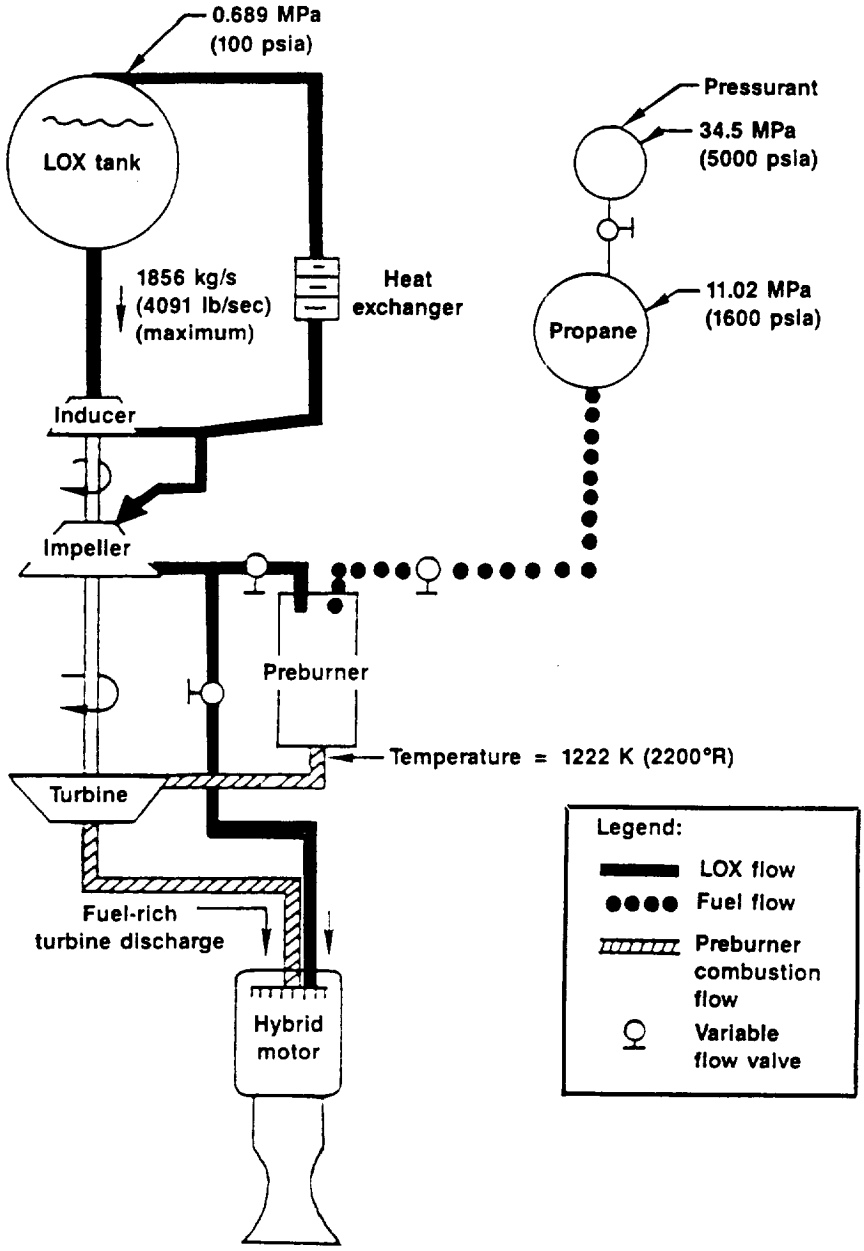

Figure 4-2. Fuel-Rich Turbine Drive with Discharge to Hybrid

50374

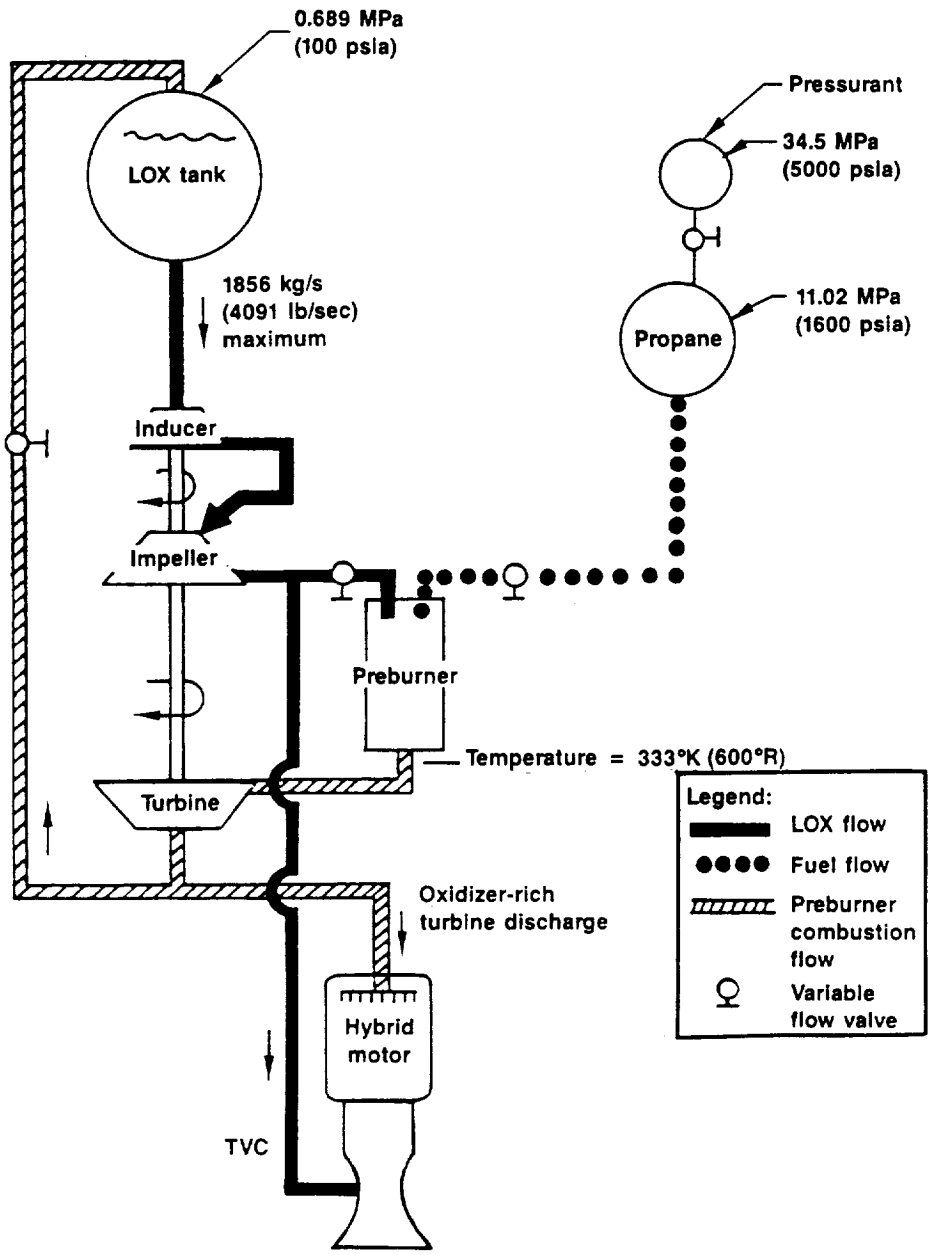

Figure 4-3. Oxidizer-Rich Turbine Drive with Discharge to Hybrid

50375

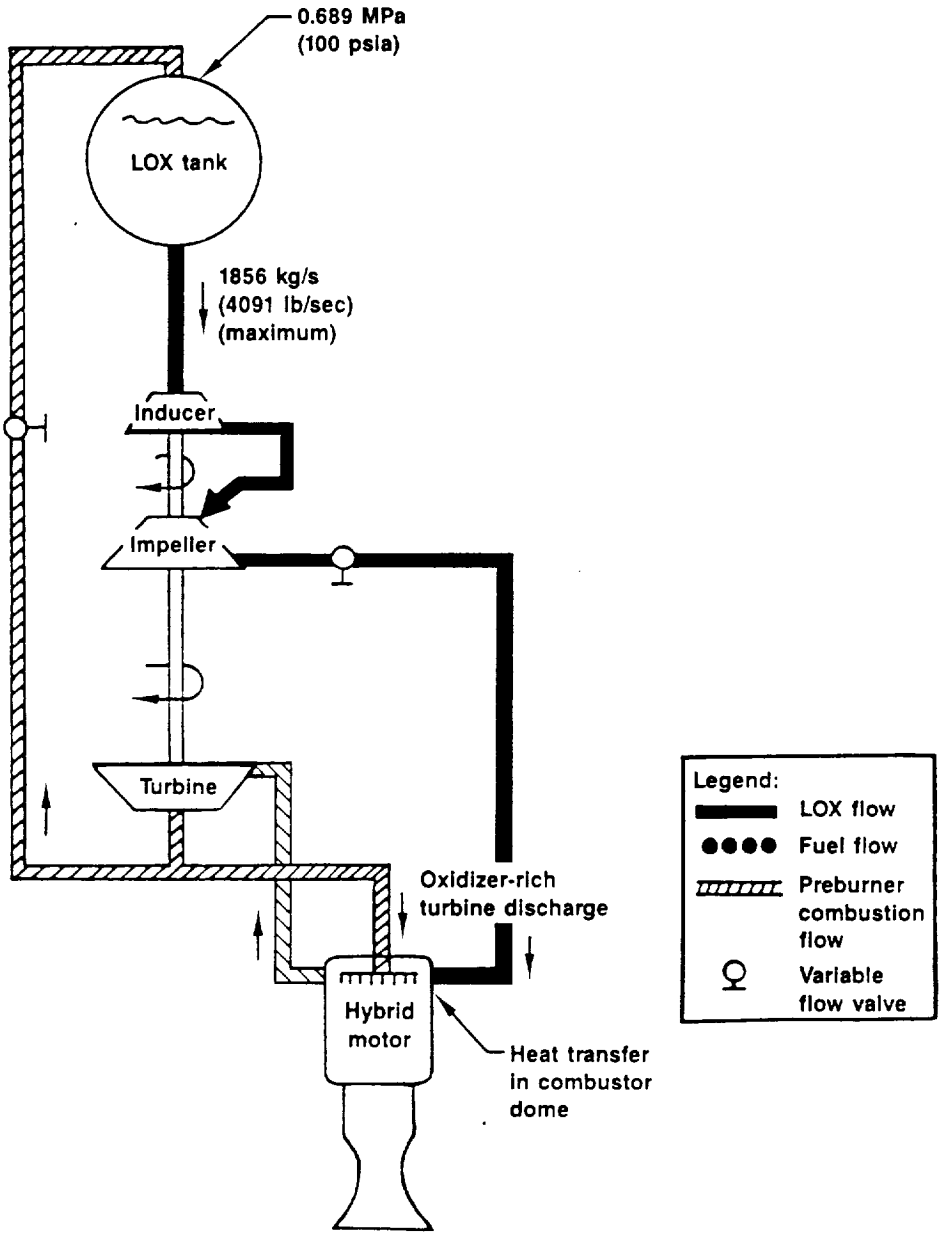

Figure 4-4. Pump-fed Oxygen Expander Cycle

50423

of the system has been designed to operate with 50% flow margin to allow for an emergency pump-out condition. Each pump is also capable of throttle-down to the 50% flow rate required for minimum thrust operation with all pumps operating. This overall throttling ratio from minimum flow divided by maximum flow of about 0.35 is well within Pratt and Whitney experience and is not a concern.

Cycle option 1 is depicted in Figure 4-1. This cycle provides for each pump to be driven by a fuel-rich combustion mixture which then discharges overboard to ambient pressure. The advantage of this cycle is that since the turbine discharges to a low pressure, high turbine expansion ratios can be achieved with minimum LOX pump discharge pressures. This will maximize turbine work per pound of turbine flow, which helps minimize the volume of pump-system fuel required for the mission. One disadvantage is that the energy of this overboard flow must be recovered in separate nozzles in order to avoid a loss in specific impulse. The drive turbines for this option 1 are limited to a maximum of 1.222°K (2200°R) at the maximum-thrust emergency (one pump-out) condition by the material properties of the turbine rotors. Another concern for this cycle is that the turbine and LOX impeller must be isolated by a reliable shaft seal to prevent mixing of the LOX with the hot fuel-rich turbine flow. These interpropellant seals packages are complicated and require an additional medium such as helium be used as a buffer.

Cycle option 2 is shown in Figure 4-2. This cycle is similar to the first cycle except that the fuel-rich turbine discharge flow is directed into the high pressure hybrid combustion chamber instead of overboard. The advantage of this cycle is that there is no performance impact since the turbine discharge flow is expanded through the main hybrid nozzle. It is also possible that the high-energy turbine discharge flow could be useful in gasifying part or all of the main LOX flow entering the hybrid if this is required. This high-energy flow may also be useful in "starting" the hybrid. Since the turbine for this cycle must discharge to a higher pressure which is now set by chamber pressure instead of ambient pressure, turbine work will be reduced.

In order to restore adequate turbine work, turbine fuel flow requirements will increase. This will increase the volume and weight of the fuel storage and helium pressurant tanks. For this cycle the maximum turbine inlet temperature is also limited to 1222°K (2200°R), and since this turbine is operating fuel-rich, an interpropellant seal package is also required for each pump.

Cycle option 3 is shown in figure 4-3. Although schematically similar to options 1 and 2, this option is quite different thermodynamically. For options 1 and 2, only a fraction of the main LOX flow is used in the preburner and expanded through the drive turbine. In each case, the amount of fuel that is added is limited in order to maintain the fuel-rich preburner combustion temperature at or below the 1222°K (2200°R) turbine limit. The remainder of the main LOX flow bypasses the drive turbines and is delivered to the hybrid combustion chamber as a liquid. For cycle option 3, proposed by Acurex, all of the main LOX flow is directed through the preburner, significantly increasing the turbine mass flow. Sufficient fuel flow is added such that the oxygen-rich preburner exit temperature is maintained at or below a very cool 333°K (600°R). Although operating turbines in an LOX-rich environment is not common, the very benign conditions imposed by this cycle (333°K and <10.3 MPa (600°R and <1500 psia)) are felt to reduce the those of the fuel-rich configurations (options 1 and 2) operating at 1222°K (2200°R). Operation of the preburners at the necessary mixture ratio of about 40, depending on final cycle optimization, is within flamability limits and is not considered a problem.

For option 3 the turbine discharge flow, which contains all the oxygen required by the hybrid, is directed into the high-pressure hybrid combustion chamber. Unlike options 1 and 2, where the oxidizer was supplied as LOX, option 3 supplies the oxidizer flow as GOX. If there is a requirement to maintain a fraction of the oxidizer as LOX, (for hybrid combustion control or thrust vector control (TVC)), this could be accomplished by bypassing the flow around the preburners and turbines. Options to allow up to 30% of the oxidizer to be bypassed and supplied as LOX have been examined and the impact on the cycle configuration is minimal.

Cycle option 4 is similar to option 3 except that the oxygen is heated in the thrust chamber cooling jacket instead of being burned with a small amount of fuel. This option is shown in Figure 4-4. Cycle option 4 would eliminate the preburner and separate fuel system required by option 3. There could, however, be a significant increase in injector dome complexity in order to achieve adequate heat transfer with minimum pressure loss. This cycle does introduce some concerns about "starting" the turbo-machinery, which must be supported entirely by the "ambient" energy in the combustor dome, since the hybrid is not yet operating.

The detailed transient heat transfer analysis and involved combustor dome configuration studies could not be performed within the scope of this program to the level of depth required to ensure concept feasibility. Based on the potential merits, however, it should be considered as an alternative to option 3 should this pump-fed configuration be the eventual configuration of choice.

4.1.2 Pump-Fed Cycle Integration Results

Operational characteristics were established for the three options: (1) fuel-rich operation/overboard, (2) fuel-rich preburner cycle, and (3) oxidizer-rich preburner cycle. These characteristics were based on the oxidizer flow profile required to meet the overall hybrid thrust versus time curve for either the large or small booster.

For either the large of small thrust application, the basic design of the inducer and impeller design is essentially the same regardless of the thermodynamic cycle option being considered. There are some slight differences due to the different discharge pressures required, depending on the cycle option, but the weight and packaging differences are trivial at this point. The designs will differ, however, between the large and small thrust applications due to the differences in inlet design flow. A summary of critical pump design parameters for the maximum discharge pressure application (options 2 or 3) is shown in Table 4-1.

TABLE 4-1. OPERATION CHARACTERISTICS

T16945

Parameter	Large Hybrid		Small Hybrid	
Nominal LOX flow rate, kg/s (pps)	1237	(2727)	313	(691)
Maximum LOX flow rate, kg/s (pps)	2223	(4901)	470	(1037)
Maximum volume flow rate, gal/min	97.9	(25,857)	24.9	(6547)
Inlet temperature, K (°R)	91	(164)	91	(164)
Inlet pressure, MPa (psia)	0.69	(100)	0.69	(100)
Maximum exit pressure, MPa (psia)	16.8	(2435)	16.8	(2435)
Maximum headrise, m (ft)	1304.9	(4281)	1304.9	(4281)
Maximum shaft speed, rpm		(6272)		(12,466)
Efficiency		(0.803)		(0.803)
Maximum shaft horsepower, Mwatts (shp)	29.6	(39,673)	7.5	(10,045)
Inducer hub diameter, m (in.)	0.11	(4.4)	0.06	(2.2)
Inducer tip diameter, m (in.)	0.37	(14.4)	0.18	(7.2)
Impeller diameter, m (in.)	0.54	(21.2)	0.27	(10.6)
Inducer suction specific speed		21,971		21,971

For each of the pump-fed cycle options requiring a separate fuel supply, a cycle parametric study was performed to investigate the interaction between drive turbine fuel flow rate and turbine expansion ratio. The required drive, turbine expansion ratio will drop if the turbine flow rate is increased. This lowers the peak operating system pressures and the number of turbine stages required, but increases the required oxidizer-drive system fuel flow requirements.

Based on these thermodynamic cycle studies, along with turbine aerodynamic and structural screening criteria, an optimum combination of turbine expansion ratio and number of turbine stages was selected for each cycle. The objective was to identify the most practical combination to minimize pump impeller diameter and fuel flow requirements, thus minimizing fuel storage volume and weight oxidizer supply system. Table 4-2 is a summary of the turbine configuration study results for the large booster application. These results are very similar for the small thrust application except that the rotational speeds are higher and the diameters smaller. Table 4-3 details a

TABLE 4-2. TURBINE PARAMETERS

T16946

Parameter	Option 1	Option 2	Option 3
No. of turbine stages	3	2	1
Expansion ratio	1.35	1.29	1.31
Mean diameter, m (in.)	0.45 (17.8)	0.48 (18.9)	0.46 (18.1)
Efficiency	0.741	0.812	0.833
Rotational speed, rpm	5060	6874	6272
Maximum inlet temperature, K (°R)	1222 (2200)	1222 (2200)	333 (600)

comparison between the turbines for the large and small thrust applications for the LOX-rich preburner cycle (option 3), which requires only one turbine stage. At this point pump impeller dimensions, turbine dimensions and rotational speeds have been identified. Based on these parameters, a preliminary pump assembly drawing was generated to ensure mechanical feasibility, assembly, thrust balance, etc. This drawing was also required in order to establish external dimensions to be considered in the overall vehicle integration. The premilinary pump assembly is shown in Figure 4-5. Based on this assembly sketch and similar design studies for the burner, preliminary weight estimates were generated for the large and small booster application which are listed in Table 4-4. Preliminary hardware configuration studies indicate that only one shaft with an inducer and one impeller is required to achieve the desired cycle pressures. This restricts the impeller rotational speed to be the same as the suction limited inducer, resulting in the relatively large impeller tip diameter of 0.54 m (21.2 in.) and 0.27 m (10.6 in.) for the respective applications indicated in Table 4-1. This diameter could be reduced somewhat if an additional shaft were configured into the pump, allowing a higher rotational speed to be selected for the impeller. A schematic of the Acurex, twin-shaft, integrated burner/turbine/pump is shown in Figure 4-6. However, since no packaging problems were encountered in the overall vehicle integration and since two shafts increase the complexity of the pump system, the single shaft approach has been selected as the baseline.

TABLE 4-3. LARGE VS SMALL TURBINE COMPARISON (CYCLE OPTION 3)

T16944

Parameter	Large	Small
Maximum flow rate, kg/s (lb/sec)	1867 (4116)	467 (1029)
Shaft power, Mwatts (hp)	24.5 (32,800)	6.2 (8300)
Speed, rpm	6272	11,330
Efficiency	0.833	0.827
Inlet temperature, K (°R)	320 (576)	320 (576)
Exit temperature, K (°R)	306 (550)	306 (551)
Inlet pressure, MPa (psi)	11.1 (1610)	11.1 (1610)
Exit pressure, MPa (psi)	8.5 (1225)	8.5 (1225)
Expansion ratio	1.3	1.3
Exit Mach No.	0.35	0.35
Velocity ratio	0.67	0.67
Tip diameter, m (in.)	0.59 (23.1)	0.29 (11.6)
Δ enthalpy, Kjoules/kg (Btu/lb)	13.6 (5.84)	13 (5.59)

Each cycle examined requires a different fuel flow rate to drive the oxidizer supply system. Table 4-5 details the fuel supply differences between cycle options 1, 2 and 3. In each case, the total fuel volume and associated pressurant volume requirements were obtained by integrating the fuel flow rate versus time required by the pumping system to support the required hybrid thrust versus time profile.

Either nitrogen or helium could be used as a pressurant for the fuel supply system. The advantage of helium is that is requires less volume although it is more expensive. However, in the small volumes being considered for the pump-fed systems, the cost differences would be insignificant. The overall selection will be driven by the vehicle packaging limitations and overall vehicle support and operational impacts. For this study, helium has been used as the baseline pressurant.

As indicated by the fuel tank volumes in Table 4-5, the average fuel flow rate for the fuel-rich overboard cycle (option 1) is nearly three times larger than that for the oxidizer-rich preburner cycle (option 3), and the fuel-rich preburner cycle (option 2) is nearly an order of magnitude larger than option 3.

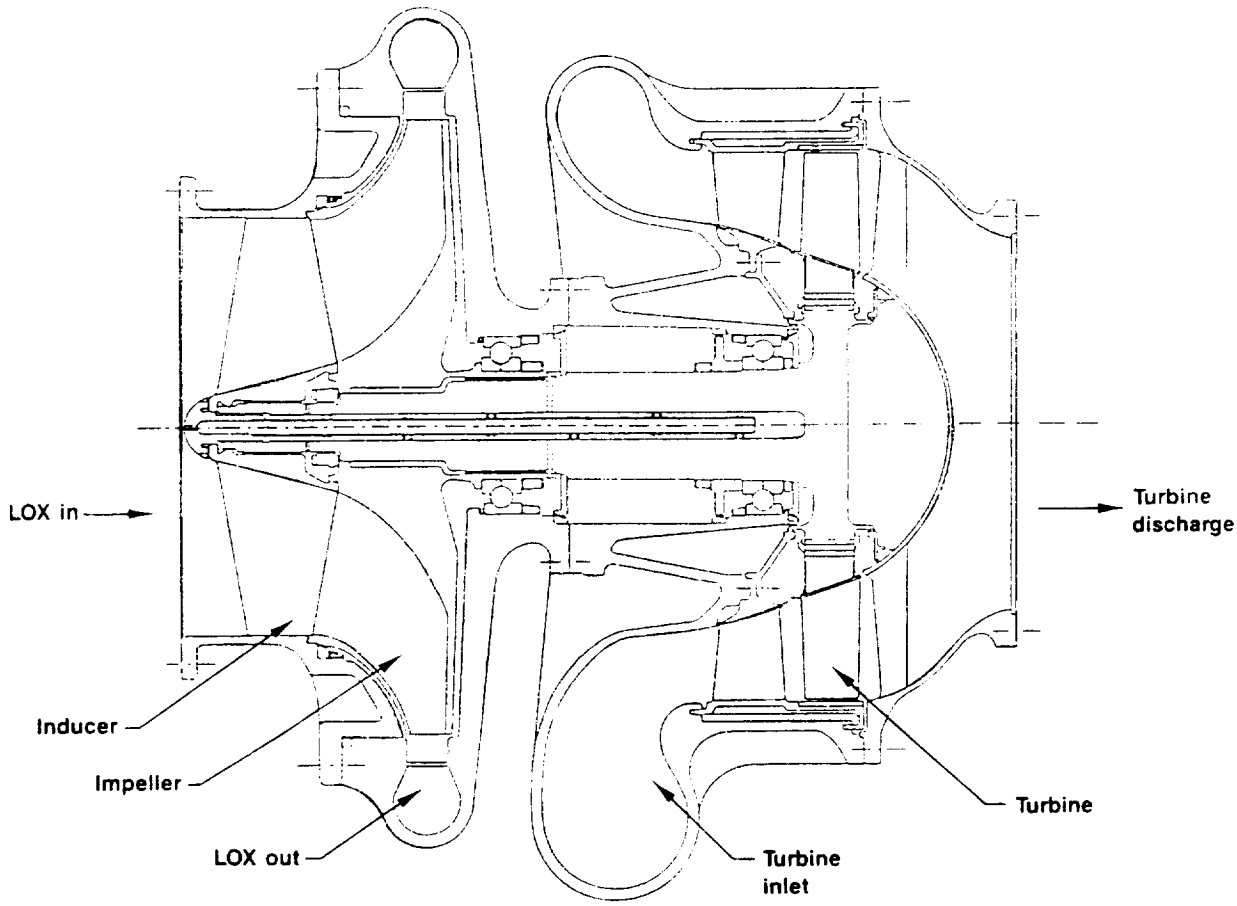

Figure 4-5. Single-Shaft Oxidizer Supply Turbopump Assembly

50424

TABLE 4-4. TURBO MACHINERY WEIGHT SUMMARY

T16982

Equipment	Large Booster, kg (lb)	Small Booster, kg (lb)
Turbopump (3)	1234.7 (2722)	740.3 (1632)
Burner (3)	315.7 (696)	168.7 (372)
Miscellaneous Hardware (3)	1174.4 (2589)	704 (1552)
Controller (1)	27.2 (60)	27.2 (60)
Total	2752 (6067)	1640.2 (3616)

Tables 4-6 and 4-7 summarizes the total oxidizer supply system weights for each of the pump-fed cycles (large and small boosters. In each case, the weight of the fuel required to drive the pumps has not been included. It has been assumed that this fuel contributes to total hybrid thrust and would simply offset hybrid solid fuel weight. This assumption is valid for both pre-burner cycles (options 2 and 3), but is only valid for the overboard cycle (option 1) if separate nozzles are provided to recover thrust from the turbine discharge flow.

Of the pump-fed cycle options examined in detail, the oxidizer-rich pre-burner cycle (option 3) is the recommended cycle for the following reasons:

- Equivalent reliability
- Lowest cost (one-stage turbine, no interpropellant seal)
- Lowest weight
- Lowest volume
- High efficiency (no overboard flow).

It should be emphasized however, that either of the other two options could be used with only minimal impact upon performance.

In addition to the weight of each system, the packaging volume has also been considered. Figure 4-7 illustrates packaging of the three turbopump burner packages, along with the propane and helium pressurant tanks in the region between the bottom of the LOX tank and the top of the hybrid combustion

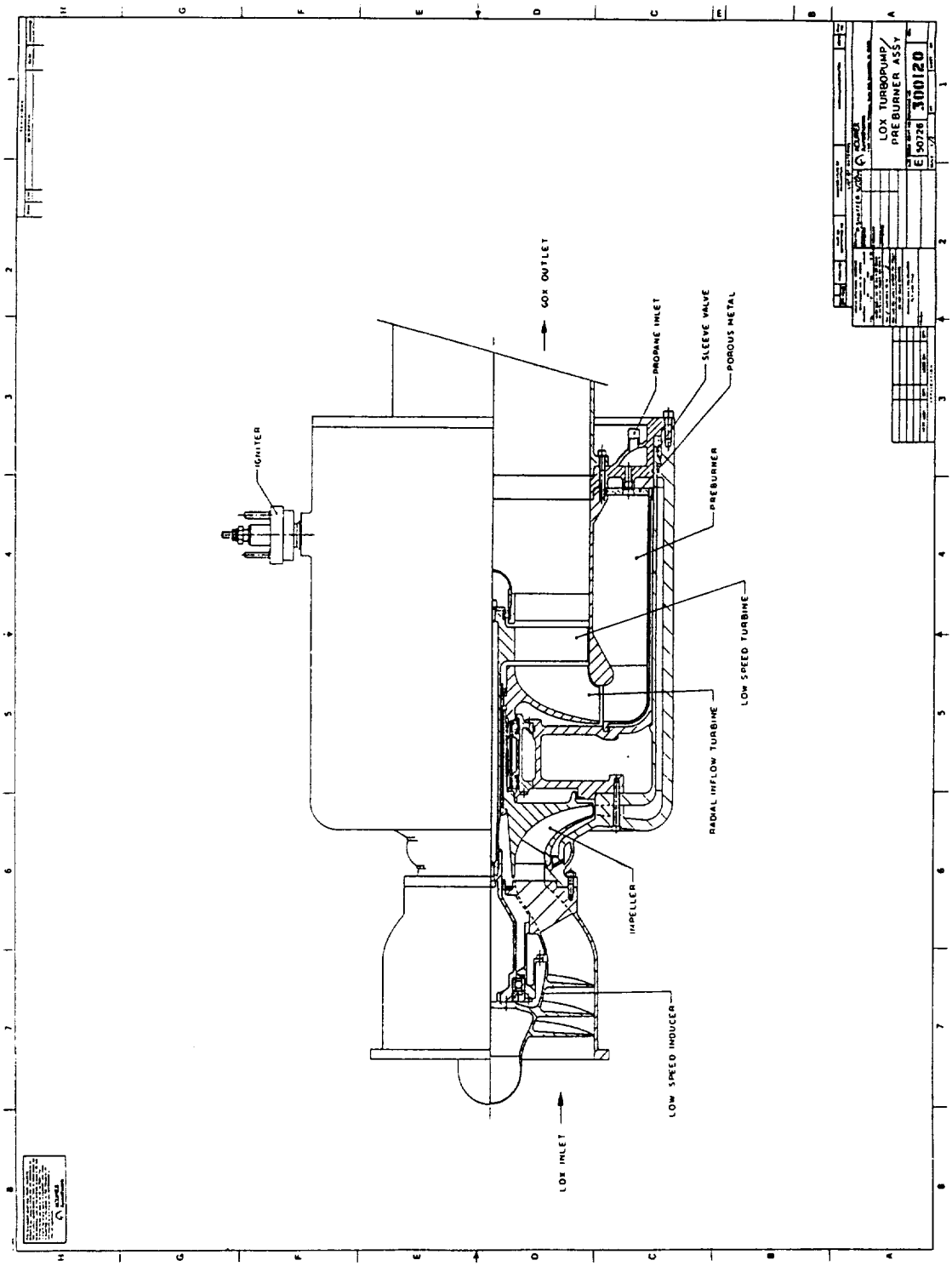

50376

Figure 4-6. Acurex LOX Turbopump/Preburner Assembly

TABLE 4-5. OXIDIZER SUPPLY SYSTEM FUEL REQUIREMENTS

T16943

Parameter	Cycle Option 1	Cycle Option 2	Cycle Option 3
Fuel tank volume, m^3 (ft^3)	12.2 (430)	35.1 (1240)	4.3 (150)
Fuel tank diameter, m (in.)	2.8 (112)	4.1 (160)	2.0 (80)
Fuel tank weight, kg (lb)	290.3 (640)	1642 (3620)	204.1 (450)
Helium tank volume, m^3 (ft^3)	1.4 (48)	5.2 (184)	0.85 (30)
Helium tank diameter, m (in.)	1.4 (54)	2.2 (85)	1.2 (46)
Helium tank weight, kg (lb)	167.4 (369)	1208.4 (2664)	112.5 (248)
Helium weight, kg (lb)	63.1 (139)	242.2 (534)	39.5 (87)
Total fuel tank, helium tank and helium weight, kg (lb)	520.7 (1148)	3092.6 (6818)	356.1 (785)

TABLE 4-6. PUMP-FED SUPPLY SYSTEM WEIGHT SUMARY, KG (LB)
(LARGE BOOSTER)

T16939

Item, kg (lb)	Cycle Option 1	Cycle Option 2	Cycle Option 3
LOX tank	2357.3 (5197)	2357.3 (5197)	2357.3 (5197)
Residual LOX	830.3 (4035)	830.3 (4035)	830.3 (4035)
Residual GOX	2027.6 (4470)	2027.6 (4470)	2027.6 (4470)
Fuel tank	290.3 (640)	1642 (3620)	204.1 (450)
Helium tank	167.4 (369)	1208.4 (2664)	112.5 (248)
Helium	63.1 (139)	242.2 (534)	39.5 (87)
Turbo pump and hardware	2721.6 (6000)	2857.6 (6300)	2766.9 (6100)
Total	9457.4 (20,850)	12,165.4 (26,820)	9338.1 (20,587)

TABLE 4-7. PUMP-FED OXIDIZER SUPPLY SYSTEM WEIGHT SUMMARY, KG (LB) (SMALL BOOSTER)

T16983

Item, kg (lb)	Cycle Option 1	Cycle Option 2	Cycle Option 3
LOX tank	846.4 (1866)	846.4 (1866)	846.4 (1866)
Residual LOX	458.1 (1010)	458.1 (1010)	458.1 (1010)
Residual GOX	507.1 (1118)	507.1 (1118)	507.1 (1118)
Fuel tank	79.8 (176)	452.7 (998)	56.6 (124)
Helium tank	48.1 (106)	346.1 (763)	32.2 (71)
Helium	16.8 (37)	64 (141)	10.4 (23)
Turbo pump and hardware	1564.9 (3450)	1642 (3620)	1587.6 (3500)
Total	3521.2 (7763)	4316.4 (9516)	3498.1 (7712)

chamber dome. It was discovered during this packaging exercise that it was more volume efficient to package the pressurant in a cylinder as opposed to a sphere.

4.1.3 Pressure-fed Configuration Study Result

Three pressure-fed options to supply oxidizer flow to the hybrid combustion chamber have been examined. These options are shown in Figures 4-8 through 4-10. For each of these options, the significant parameters to be considered during initial screening is the weight associated with the high pressure (6.03 MPa (875 psia)) LOX tank, and the associated pressurant weight and pressurant tankage weight that remains with the system until shutdown. Other considerations include the complexity of the hardware associated with each option as well as the cost and availability of helium quantities required to sustain the projected launch rate. Unlike in the pump-fed systems where helium or nitrogen could be used as a fuel pressurant (at ambient conditions), the thermodynamic properties of nitrogen deem it unsuitable for cyrogenic liquid.

A GOX recirculation pressure-fed option (option 5) is shown in figure 4-9. For this option a medium-sized pump and turbine configuration is required to recirculate adequate LOX through a heat exchanger, to be supplied

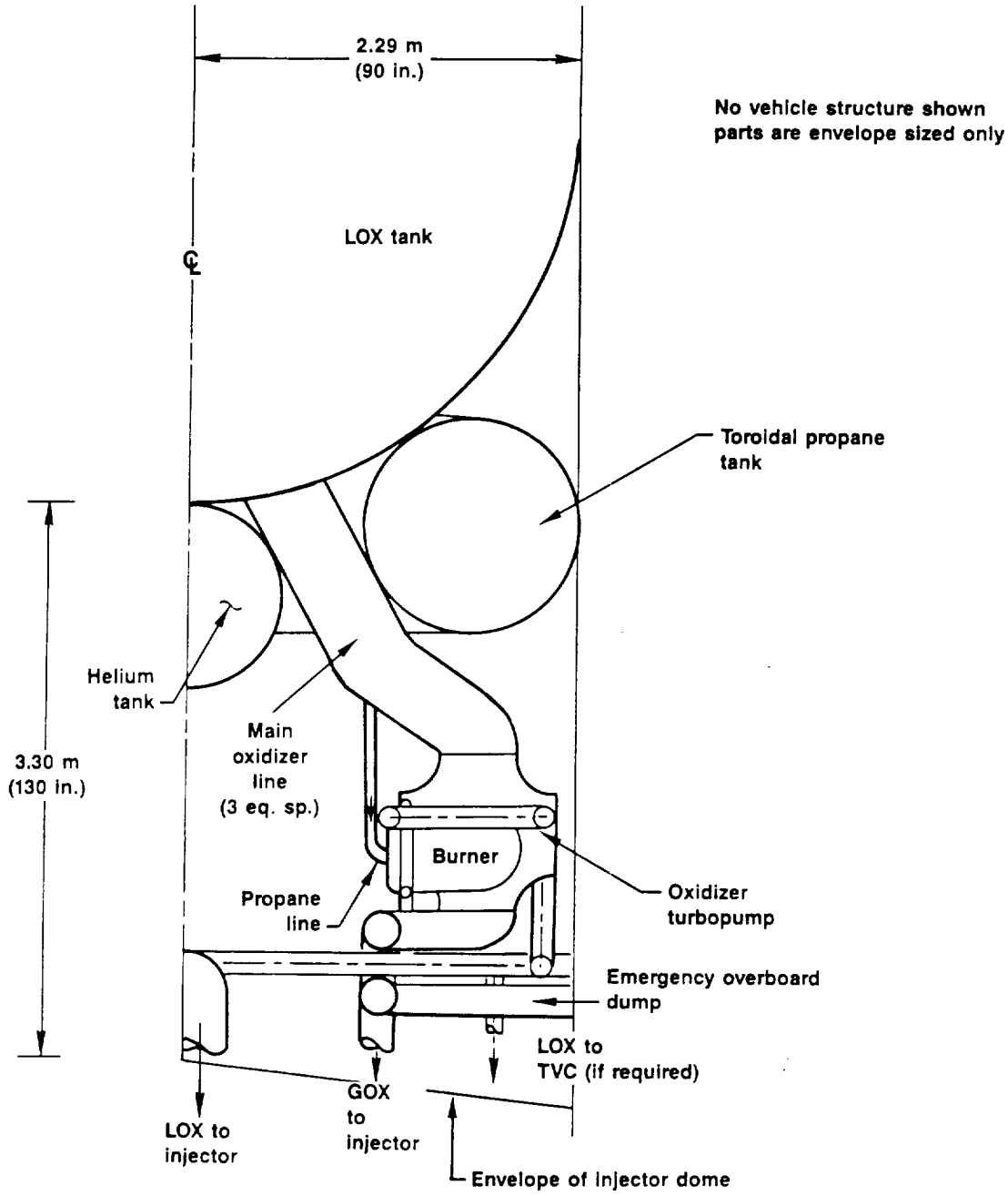

Figure 4-7. Conceptual Pump Integration for Large Hybrid

50426

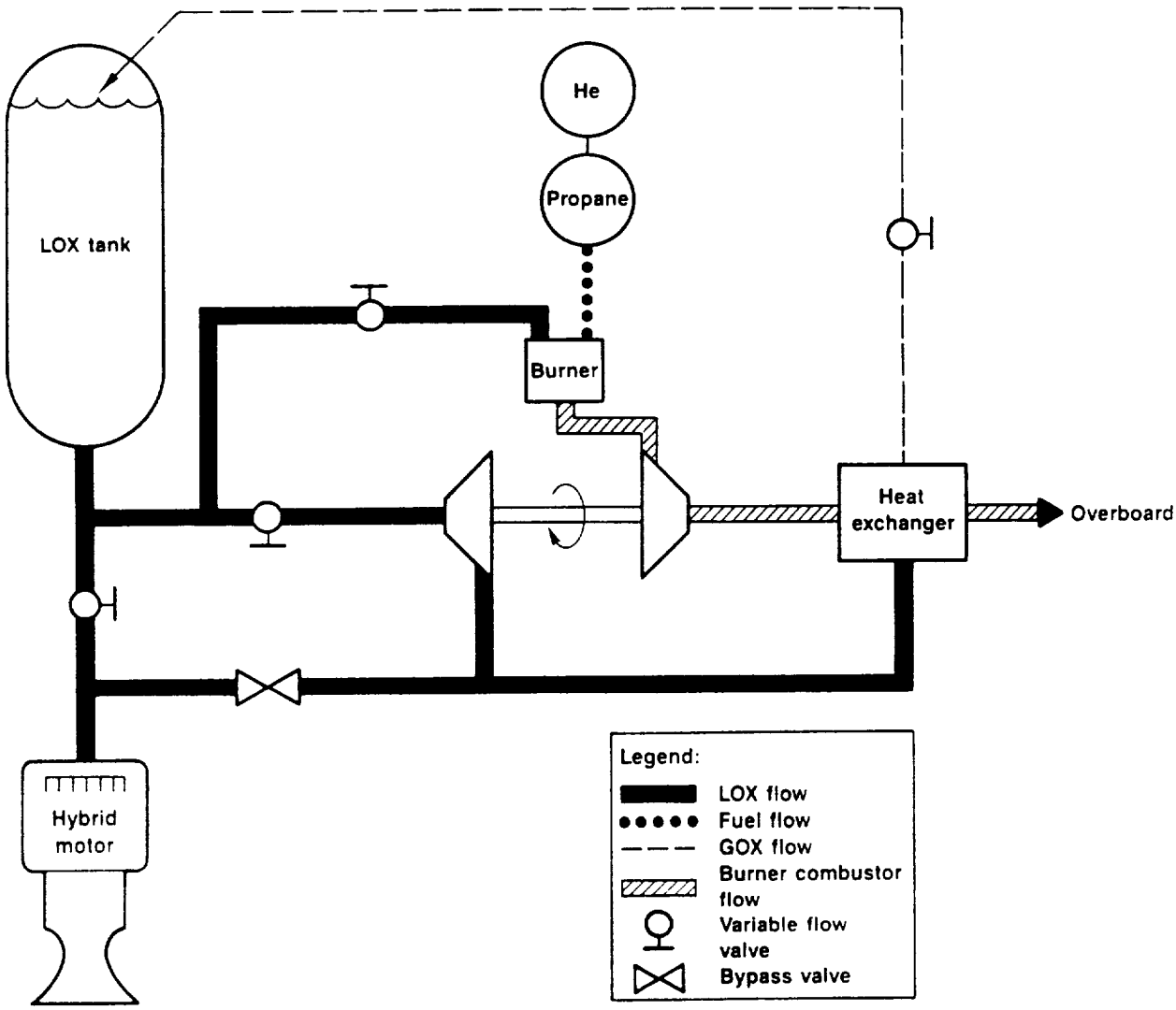

Figure 4-8. Pressure-Fed via GOX Recirculation

50427

back to the LOX tank as GOX. As indicated, a separate fuel supply is required to burn with a small amount of LOX, supplying turbine power and providing energy to gasify the LOX via a heat exchanger.

For this option the LOX tank must be oversized to store the LOX that will remain with the system as GOX at shutdown. Without much comtemplation, it becomes obvious that the complexity of this system is nearly equal to the much lighter pump-fed options described in section 4.1.1.

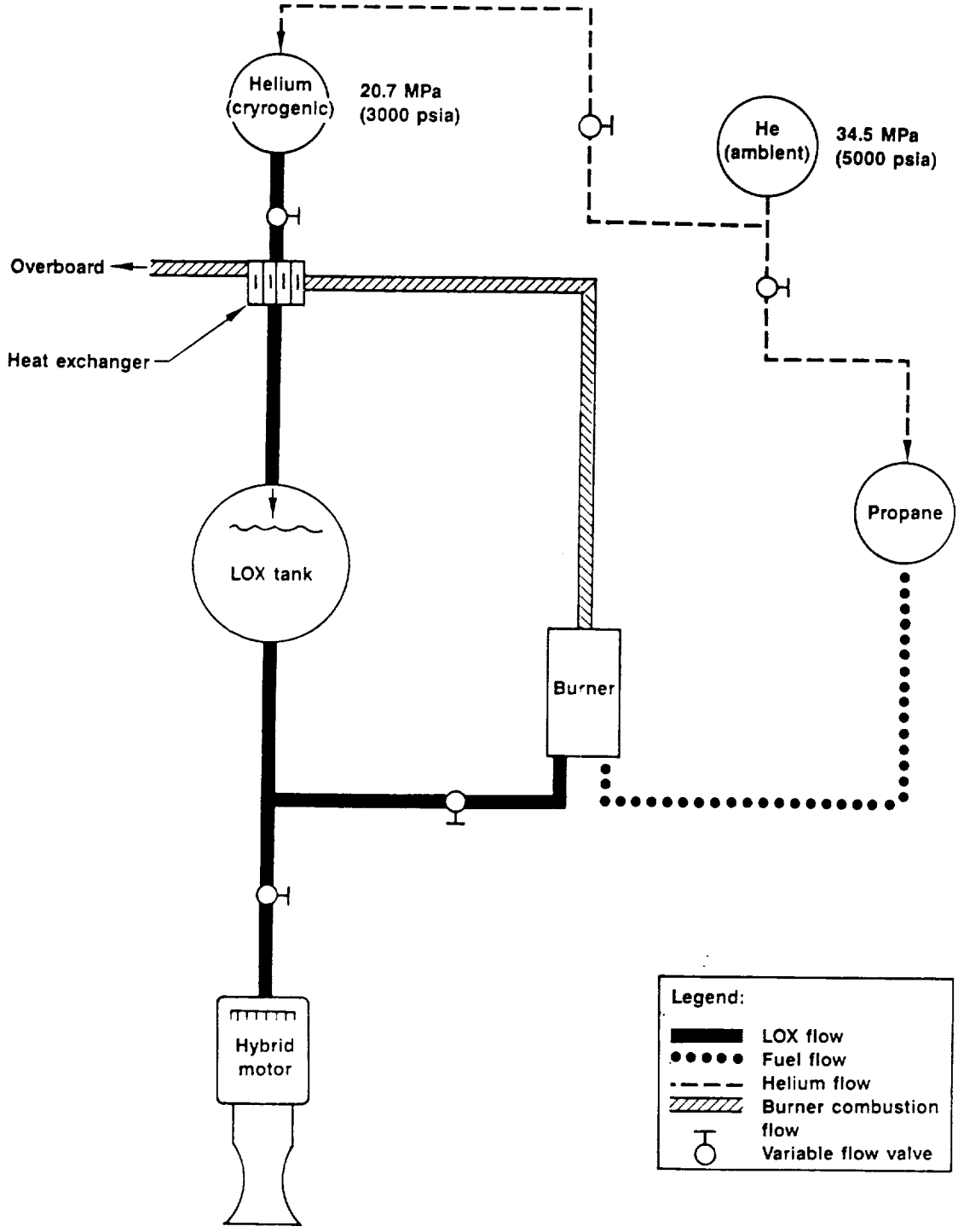

Figure 4-9. Pressure-Fed via Heated Helium

50428

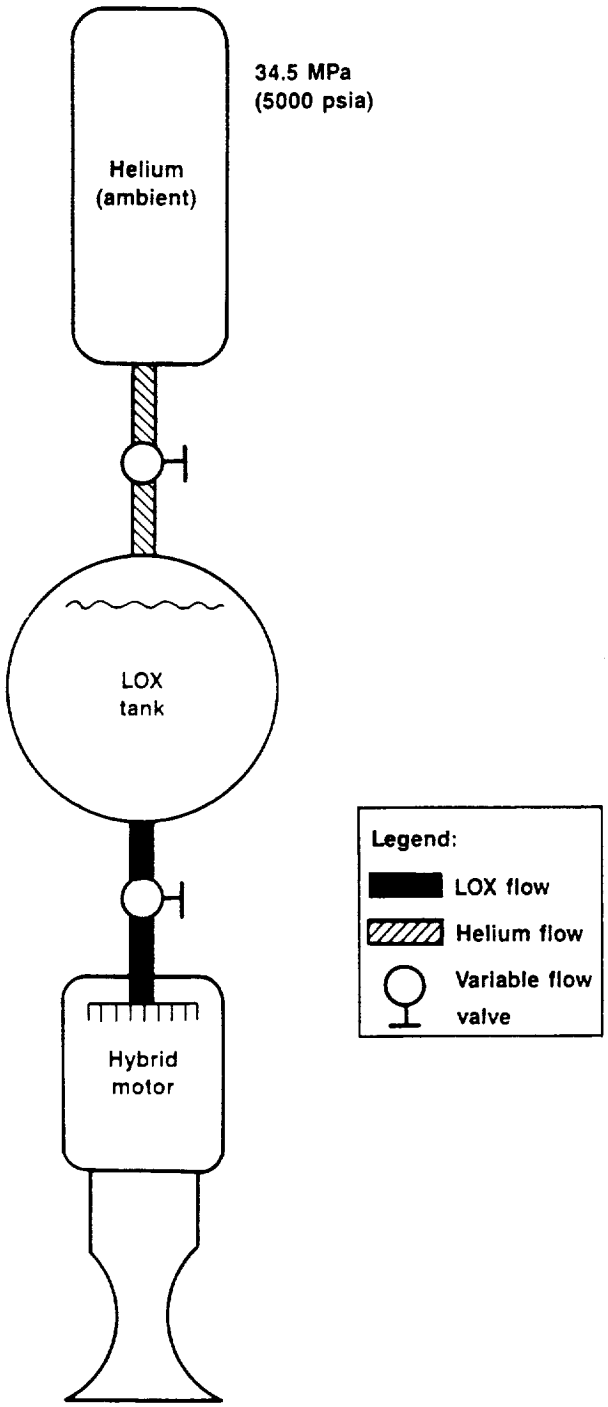

Figure 4-10. Pressure-Fed via Ambient Helium

50429

In order to maintain the high level of system reliability desired, full redundancy for this GOX recirculation system is required.

Pressure-fed cycle option 6 is shown in Figure 4-9. For this option, helium is stored at a moderate pressure as a cryogenic liquid to conserve volume. However, in order to provide adequate displacement capability in the LOX tank, the helium must be heated. A separate smaller volume of helium gas pressurant is required to maintain adequate pressure in the cryogenic helium tank as well as maintain fuel pressure to the burner required to heat the cyrongenic helium.

This option eliminates all turbo-machinery requirements but is still burdened with three moderate-to-high pressure tanks, including extra fuel to be dumped overboard after heating the helium. There is also the ground support problems associated with handling and additional cyrogenic substance. And again, the pressure-fed simplicity which is sought after to improve reliability and reduce cost to offset the known weight penalties is absent.

Figure 4-10 shows the pressure-fed system of choice (option 7). For this option, helium is stored as a gas in a high-pressure tank above the pressurized LOX tank. During the mission helium is released, entering the LOX tank as required to maintain adequate LOX tank pressure.

A detailed comparison of the associated tankage weight, residual pressurant weight and associated hardware weights estimates were summarized for both the large and small booster applications and are shown in Tables 4-8 and 4-9.

4.1.4 Reliability and Cost Comparison

Based on detailed design studies described in sections 4.1.1-3, recommended pump-fed and pressure-fed configurations have been identified for further investigation. The final configuration selection will be heavily weighted toward reliability, safety and system cost, in addition to performance and weight (Δ payload). To support this selection, a comprehensive investigation with respect to reliability and cost has been performed.

TABLE 4-8. LARGE BOOSTER PRESSURE-FED WEIGHT SUMMARY

T16984

Item, kg (lb)	Cycle Option 5 - GOX (recirculated)	Cycle Option 6 - Helium (cryogenic)	Cycle Option 7 - Helium (gas)
LOX tank	13,912.1 (30,671)	10,849 (23,918)	10,849 (23,918)
Helium tank (gas)	0 (0)	879.1 (1938)	6259.6 (13,800)
Helium tank (cryogenic)	0 (0)	845.5 (1864)	0 (0)
Propane tank	92.1 (203)	7.3 (16)	0 (0)
Propane	2003.1 (4416)	98.9 (218)	0 (0)
Residual GOX	23,344.1 (51,465)	0 (0)	0 (0)
Residual LOX	2365.5 (5215)	1830.3 (4035)	1830.3 (4035)
Residual helium	13.6 (30)	2509.7 (5533)	2373.7 (5233)
Miscellaneous hardware	1814.4 (4000)	680.4 (1500)	226.8 (500)
Total	43,544.9 (96,000)	17,700.1 (39,022)	21,539.3 (47,486)

TABLE 4-9. SMALL BOOSTER PRESSURE-FED WEIGHT SUMMARY

T16985

Item, kg (lb)	Cycle Option 5 - GOX (recirculated)		Cycle Option 6 - Helium (cryogenic)		Cycle Option 7 - Helium (gas)	
LOX tank	3740.78	(8247)	2921.6	(6441)	2921.6	(6441)
Helium tank (gas)	0	(0)	230	(507)	2507.9	(5529)
Helium tank (cryogenic)	0	(0)	227.7	(502)	0	(0)
Propane tank	28.1	(62)	3.2	(7)	0	(0)
Propane	538	(1186)	25	(55)	0	(0)
Residual GOX	5887.2	(12,979)	0	(0)	0	(0)
Residual LOX	596.5	(1315)	458.1	(1010)	458.1	(1010)
Residual helium	3.2	(7)	631	(1391)	547.9	(1208)
Miscellaneous hardware	1043.3	(2300)	390.1	(860)	131.5	(290)
Total	11,837	(26,096)	4886.6	(10,733)	6567.1	(14,478)

Figures 4-11 and 4-12 are relatively detailed schematics of the two configurations being evaluated. Considerations such as starting, system response, throttling, emergency shutdown, etc., helped provide insight into the operational hardware required for each concept. Based on these diagrams a critical parts list was compiled for each option. The individual elements of this list was then compared to similar hardware catalogued in Pratt and Whitney's rocket hardware reliability database. This allowed a projected reliability to be assigned to each part based on historical failure rate data. The database used to estimate hardware reliability for all the parts, except the tankage, was compiled from development and operational failure data from the SSME F-1 and RC-10 rocket programs. Since limited failure rate data is available for high pressure tankage, the projected tank failure rates were based on Advanced Launch System (ALS) study projections.

The individual hardware rates were then used to generate mission reliability for the entire oxidizer supply system. Table 4-10 summarizes projected mission reliability for both the pump-fed and pressure-fed options. Since the amount of hardware is the same but with size differences, these projections are valid for both the large and small booster applications.

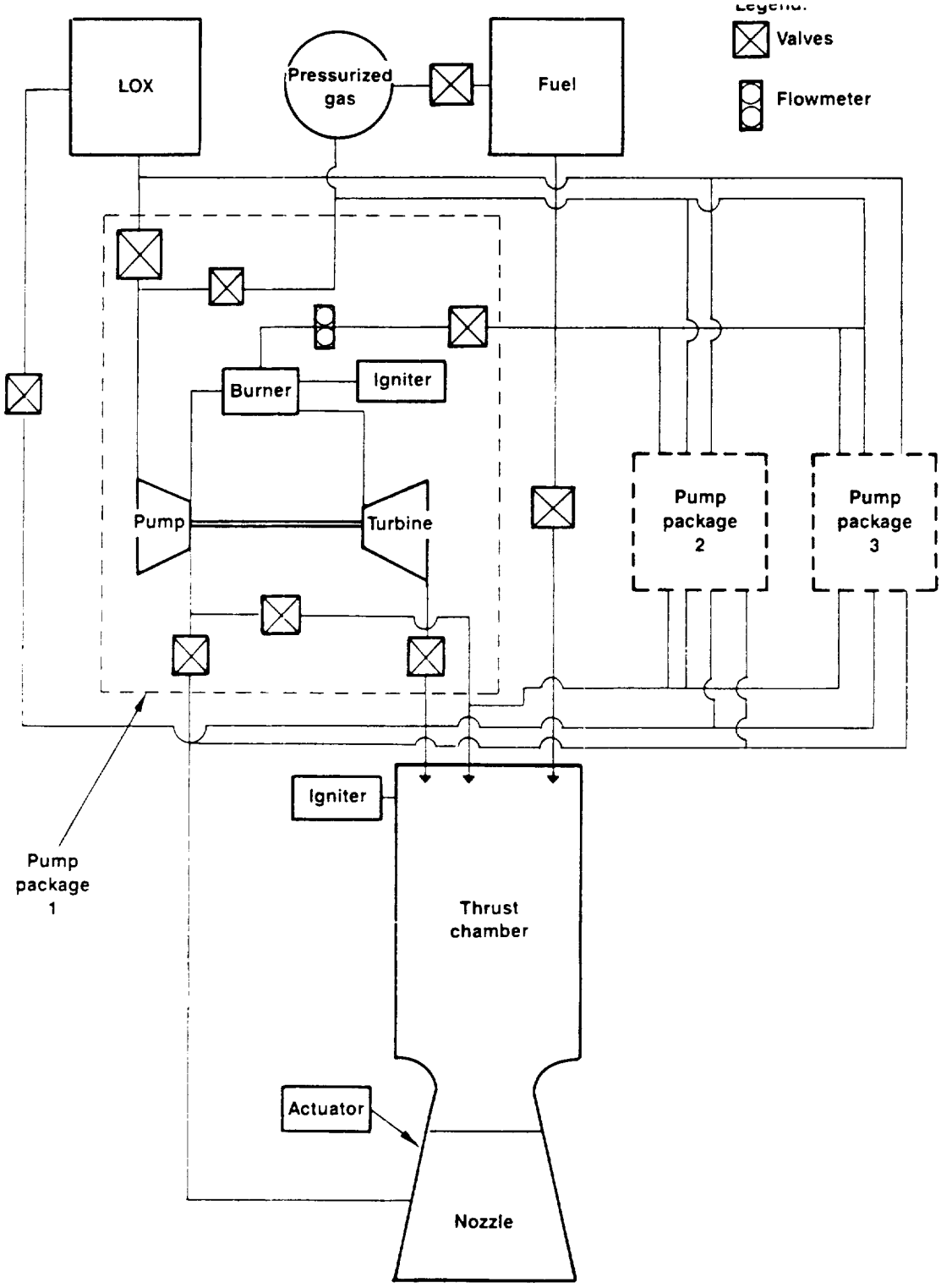

Figure 4-11. Pump-Fed Booster Flow Schematic with Redundancy

50430

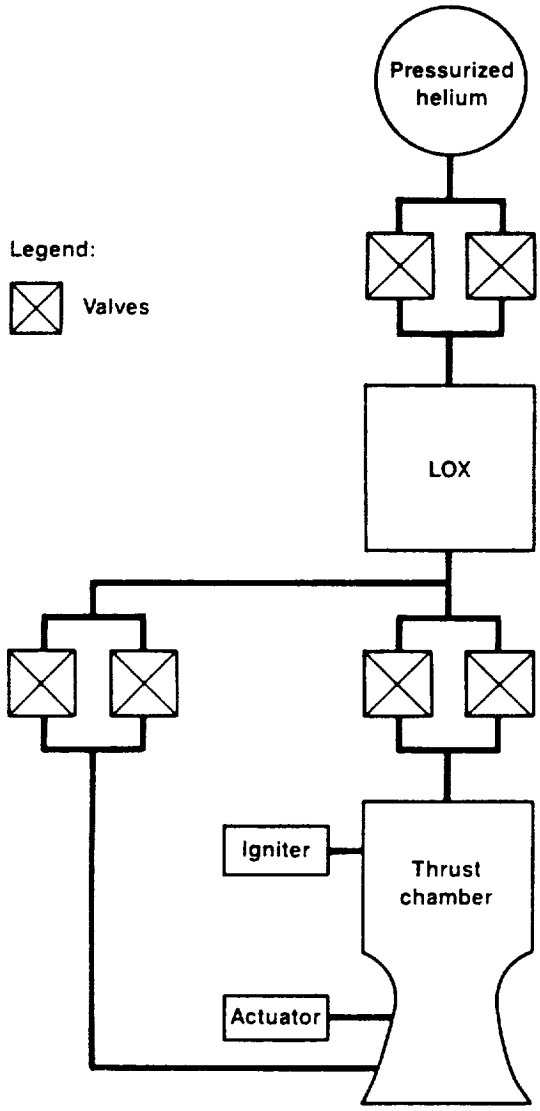

Figure 4-12. Pressure-Fed Booster Hardware Schematic with Valve Redundancy

50431

4.2 INJECTION SYSTEM

The oxidizer can be injected into the hybrid fuel system as either a gas or a liquid. An advantage of liquid injection over gaseous oxygen injection is that the valves and feed lines are smaller in size and weight. An additional advantage is that the effective gas velocities at the head end of the motor can be controlled by staging the vaporization along the port. The disadvantages of liquid injection include (1) the requirement for orders of magnitude more injection ports or high injection pressure drops to reduce the distance required for liquid vaporization, (2) the possibility of liquid quenching of the initial combustion process with the solid fuel, (3) the need for cryogenic hardware (4) and the difficulty in getting uniform LOX distribtion over the entire head end of the fuel grain. While sacrifical splash plates can be used to promote vaporization, this is less desirable than using turbine-driven exhaust gases and/or injector design to promote vaporization. The advantages of GOX injection include more uniform mass velocity in the fuel ports; large, less costly injector ports; and reduction of possible quenching problems. Either the Acurex turbine/LOX pump (cycle 3) or the fuel-rich cycle 2 pump system can be designed to promote GOX. As the cycle 3 pump is now designed,

TABLE 4-10. PROJECTED MISSION RELIABILITY

T16986

Option	Reliability	Comments
Option 3 - pump fed	0.999942	Requires one - pump out capability
Option 7 - helium pressurized	0.999999	Assumes all valves are redundant

the LOX is converted to 306 to 333°K (550 to 600°R) GOX by the oxygen/propane combustion products. However, by redesign, supercritical oxygen could be the pump effluent and temperatures as low as 172°K (310°R) could be achieved. In Phase II, it will be determined if LOX or GOX is the better injectant. As discussed in volume II, new technology requirements will be dependent upon the choice of either LOX of GOX injectant for a large hybrid booster.

4.3 HYBRID BOOSTER MOTOR CASE DESIGN

The baseline motor case configurations for the two hybrid booster concepts are shown in Figures 2-5 and 2-7. Increased reliability and reduced cost were the primary objectives in establishing case configuration selection criteria. Both configurations were based on an MEOP of 7.69 MPa (1115 psig) assuming a pump-fed system and a factor-of-safety of 1.4.

A reusable segmented metallic case is the baseline selection for the 4.57-m (180-in.) diameter motor. This approach was selected for the large motor to minimize program cost and risk. The technologies involved in designing, producing, handling and refurbishing this type of case are common to both solid rocket motors and hybrid rocket motors. Production facilities and processes developed for Shuttle, Titan and ASRM programs could be used for this case.

An expendable, monolithic, filament-wound case is the first choice for the 2.44-m (96-in.) diameter motor. This motor's smaller size and relatively high production volume, along with physical characteristics of the hybrid

motor provide the potential to significantly reduce the overall cost of motor fabrication through filament winding. The baseline fabrication approach involves winding directly over the motor fuel and injector system. These operations would require developing new technologies beyond those currently used in SRM case fabrication.

An alternate design for the 2.44-m (96-in.) diameter case would be a segmented metallic case similar to the 4.57-m (180-in.) diameter design, but without a middle joint. Cost and schedule would drive the decision for reusability.

4.3.1 Large Booster Case Design

The selected motor case design is a reusable, segmented HP 9-4-30 steel case with roll-formed cylinders and die-formed domes. HP 9-4-30 (9% nickel, 4% cobalt, 0.30% carbon) steel was selected for its high strength (1517 MPa (220 ksi)) and good stress corrosion properties (KISCC > 1.12 MPa * m $\sqrt{m}$ (40 ksi * in. $\sqrt{in.}$)).

Two casting segments are mated with field joints to form the case cylinder. Each segment consists of two roll-formed cylinders joined by a plasma arc weld. ASRM reliability studies indicated that a welded joint provides increased reliability over a mechanical factory joint. For the cavity collapse water impact loads that occur during booster splashdown, the external water pressure stability of the motor case is increased by reinforcing the aft segment with removable stell stiffening rings. These rings are attached through stub rings integrally machined with the case.

The base wall thickness is 9.09 x 10-3 m (0.358 in.) and is constant along the length of the motor. Wall thicknesses are based on 1.4 x MEOP with allowances of $\pm 2.54 \times 10^{-4}$ m (±0.010 in.) for manufacturing tolerances and +2.29 x 10-4 m (+0.009 in.) for a refurbishment allowance (20 reuses). Local build-ups are provided for welds assuming 90% efficiency. Local build-ups are provided in the aft segment for cavity attach stiffener attachment.

The forward dome is an oblate spheroid based on a 1.5:1 ellipse. The aft dome is hemispherical. Both closures are attached to cylinders with field joints to facilitate grain fabrication, and injector processing will eventually allow the use of welded joints between the domes and segments.

The design and construction of the forward closure differs from that for a solid propellant motor only by incorporating the oxidizer-injectant system. The aft closure and segment designs are identical to those that would be used in a SRM.

Forward and aft structural interfaces are integral stub skirts that are the same diameter as the case cylinder and are machined at the closure dome tangent points.

The recommended design of these joints is based upon ASRM joint design requirements. This maximizes seal reliability. All joints have redundant pressure seals. Face seals are used wherever possible and all seal gaps are designed to preclude gap opening under pressure.

The nozzle closure joint shown in Figure 2-6 uses an internal radial shear lip to provide a mechanism for primary seal gap closure. The effective rotation restraint from the shear lip, as well as the closure flange flexural rigidity, provide seal gap control at the redundant seals.

The baseline segmented motor case has three field assembly joints. The selected configuration is a clevis joint using a capture feature similar to that on the ASRM joint. The primary factor leading to the selection of a clevis/bore seal configuration over a bolted/face seal joint was the undesirable impact on fuel port design from the internal envelope intrusion required for a bolted joint. During ASRM design studies, developing a clevis joint with bore seal gaps that close during pressurization was shown to be analytically feasible. Continued work on the recommended joint concepts will be required to eliminate the internal joint capture flange and reduce the displacement of fuel by the joint.

4.3.2 Small Booster Case Design

The proposed Hybrid Advanced Launch Vehicle (ALV) combustor case design and the critical attendant materials process and nondestructive evaluation (NDE) technologies are shown in Figure 4-13. The motor case is a monolithic, helically-wound, double-domed motor case with wound-in end fittings. All joints are designed so that the O-ring gaps close under pressure and incorporate redundant and verifiable O-ring seals. The skirt rings also are riveted/bolted to the skirts.

The selected fiber, Fortafil 3(C), is a commercially available, low-cost, PAN-based carbon fiber with a 227.5 GPa (33 million psi) modulus/3792 MPa (550 ksi) strength. Since the Fortafil 3(C) has the largest tow area by a factor of four and largest spool size 23 kg (50 lb) of any of the competitive fibers, it effectively allows cutting the number of layers to be wound by a factor of four.

The selected wet winding resin is a non-carcinogen, non-hazardous, all-liquid system consisting of a conventional bisphenol-A epoxy, DER-332; a diluent, neopentyl glycidyl ether, WC-68; and a hardener, diethylotoluene diamine, Ethacure 100A-1. This system is available in large quantities (90,720 to 362,880 kg (100 to 400 tons) per year). To prevent dome failure, the selected resin also has a long pot life. The selected design hoop fiber stress is 2758 MPa (400 ksi) and the selected helical fiber stress is 1517 MPa (220 ksi) at 1.25 x MEOP. In IR&D testing done to date by CSD, this system has delivered up to 3199-MPa (464-ksi) hoop fiber stresses.

The motor case is wound over the head-end oxidizer injector and fuel grain cartridge and cocured with a wound-on EPDM pressure seal liner to improve both insulator-to-case bond and leakage reliability, and to lower process costs. The skirts are layed up in repetitive sequences of ±45/0/±45 deg preplied layers, hoop-over wound, and cocured. The selected fiber is the Fortafil 3(c) fiber and the selected resin is Fiberite 948A1 commercial epoxy resin. Both undirectional, ±45 deg bias cloth, and preplies are available in standard 1.52-m (60-in.) wide rolls.

FOLDOUT FRAME 1

FOLDOUT FRAME 2

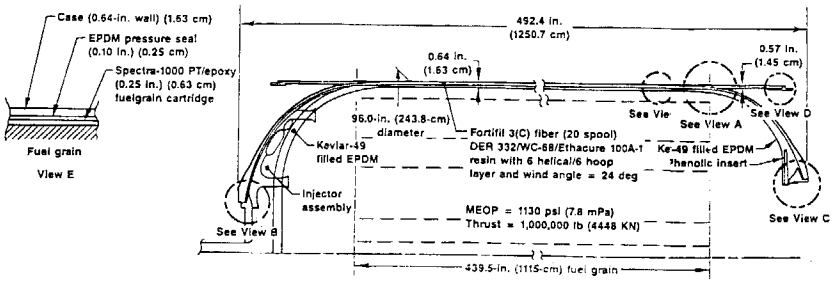

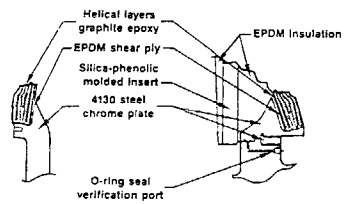

View B — Typical Wrap Pattern, Forward Boss

View C — Typical Wrap Pattern, Aft Boss

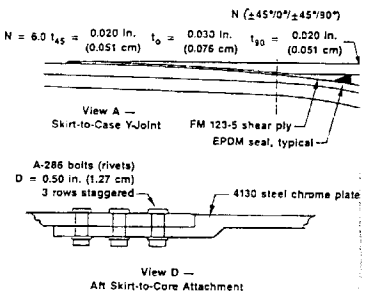

View D — Aft Skirt-to-Core Attachment

Process and Product Verification Enhancements

Process
- Vertical wind aft end down
- Wound in and on reinforced fuel cartridge and insulated forward dome injector
- Aft dome supported by reusable segmented metal mandrel
- Multiple winding heads
- Automated tensioning
- Automated mix wet wind
- Co-cure case and insulator using embedded dielectric sensors, fiber optics and pulse echo ultrasonics

NDE
- In-process automated record
- Fiber optics
- Pulse echo ultrasonic
- "Super proof"
- Health monitors — fiber optics and pulse echo ultrasonic

Figure 4-13. Combustor Case Design
30525

The skirt-to-case structural joint is made from cold-molded FM 123-5 adhesive, which has been shown by CSD to possess the ability to withstand very high skirt line loads, with shear strengths of over 28 MPa (4000 psi) and co-cured. The resulting choice is an order of magnitude better than if conventional rubber shear plies were used. CSD has used this material since the mid-1970s on all filament-wound motor case products (IUS, KEW, Small ICBM, PK, Orbus 1, ISMS, and Sentry).

The selected materials and their identifed backups are shown in Table 4-9 along with the supporting rationale.

4.3.3 Design Trade Studies

As part of ongoing CSD studies into low-cost, high-reliability motor case technology, many trade studies have been conducted. Among these was the case design study summarized in Figure 4-14. In addition to trades between a low-risk steel weldment case design and composite cases, a detailed study was conducted comparing a monolithic fiber dominated with no-cut fiber and minimum machining to various combinations of segmented cases. This study addressed one or more joints, leakage concerns, cut fiber and primary failure modes dependent upon resin properties, extensive machining and NDE requirements. For reliability and cost reasons, the monolithic design was selected.

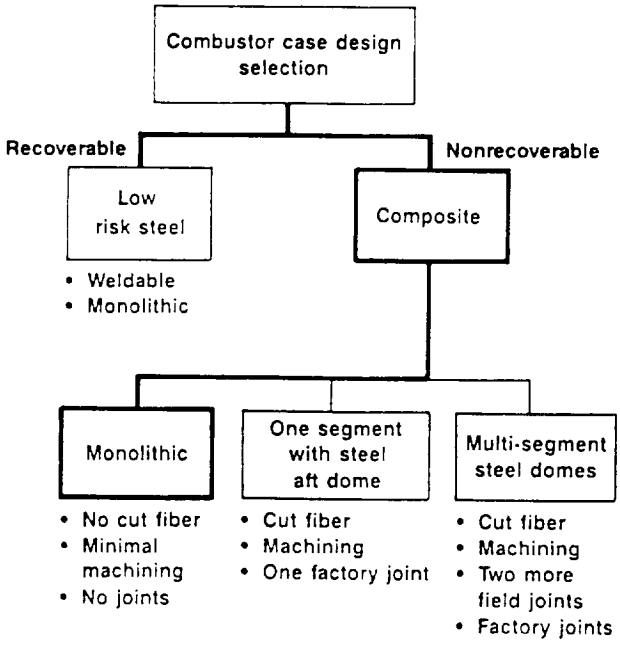

Figure 4-14. Combustor Case Design Trade Study

50321

Next a winding pattern, dome contour, and dome reinforcement study was conducted. Owing to the size, L/D and desire for minimum winding operations, a helically-wound, balanced dome contour with no local dome reinforcement was selected. CSD

has shown that for PAN-based carbon fiber and helical-to-hoop fiber stress ratios up to 0.60, the helical dome strength can be maintained with nozzle port diameters of 50% of the case diameter without added reinforcement. S-glass case designs can achieve stress ratios of up to 0.93 with nozzle ports up to 45% of the case diameter. The hybrid ALV nozzle port diameter is expected to be between 0.40 and 0.50 times the case diameter.

A skirt design trade study is summarized in Figure 4-15. Based on past design experience, available material forms, and ability to automate and demonstrated reliability, the co-processed ±45/0/±45 deg, 1.52-m (60-in.)-wide preply and hoop overwound approach was selected. This trade should be revisited in later studies when the core attachment and resultant skirt loads are better defined. Higher skirt loads may favor prefabricated braided or pultruded channel sections stacked side by side on the skirt tooling and hoop, overwinding to achieve the required strength and stiffness at a minimum of cost.

The core attachment trade study is shown in Figure 4-16. The selected approach, patterned after the DELTA-2 GEM configuration, is to react the generated moment and thrust on the core in order to minimize SRB aft skirt load and structure complexity. The alternative approach is patterned after the Titan-34D, -4 where the thrust and moment are reacted on the SRB aft skirt, making it a more complex and expensive structure.

Next, the metal-end fitting or polar boss design was evaluated, resulting in the selection of a design that provides O-ring gap closure under pressure, allows dual verifiable O-rings, and utilizes low-cost fasteners with high structural reliability. Figure 4-17 summarizes the results and baseline selection.

4.3.4 Material Trade Studies

The composite material trade studies began with the basic materials used in a filament-wound motor case, via the resin and fiber. The primary resin properties and associated requirements are low cost, availability, ease of

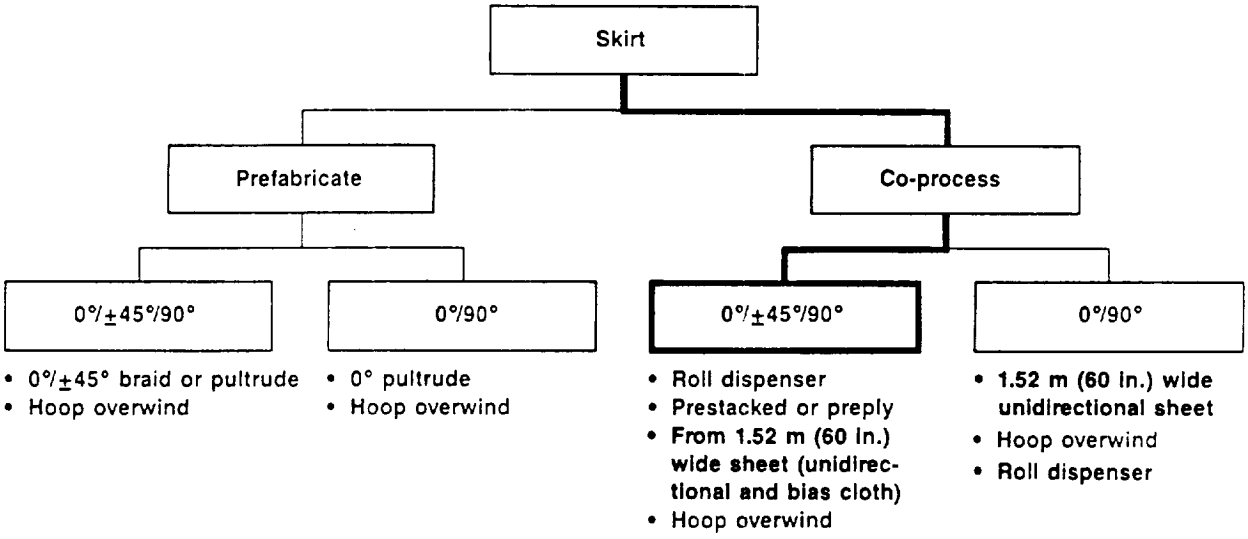

Figure 4-15. Skirt Design Trade Study

50322

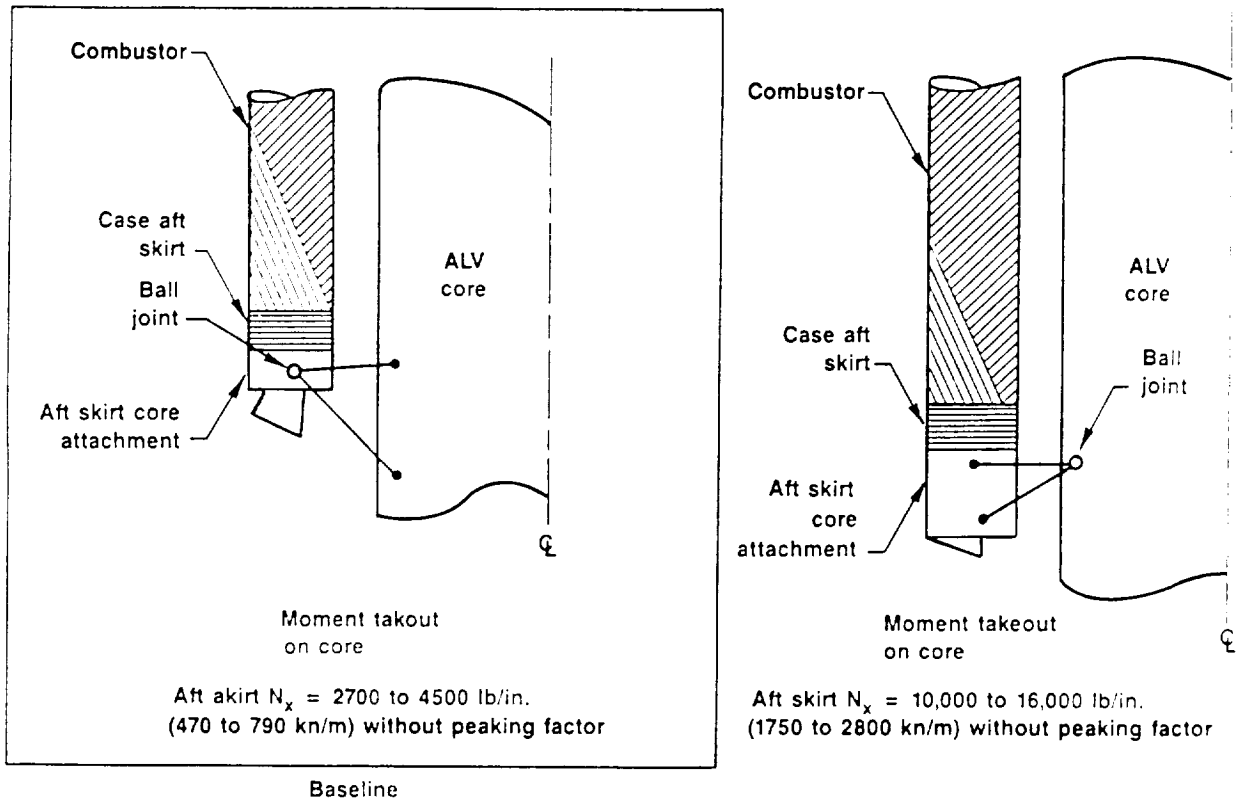

Figure 4-16. Core Attach Trade Study

50323

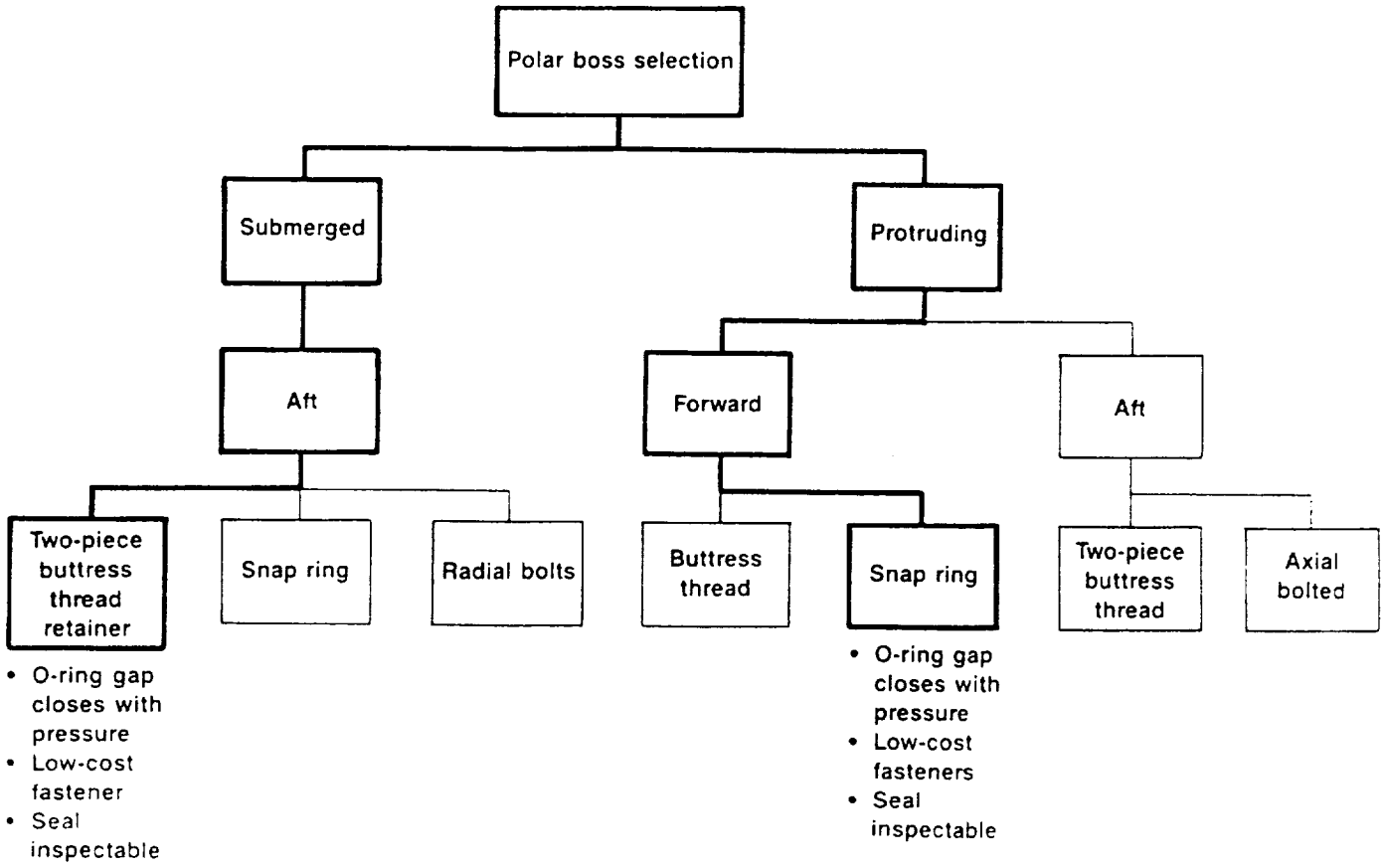

Figure 4-17. Polar Boss Design Trade Study

49870

processing, and absence of health hazards (non-carcinogenic). These properties are particularly relevant because of the quantities used (based on size and production rate). Process and cost evaluations were conducted for wet winding resins versus prepreg and amine cure versus polyester or anhydrides cure. Based on cost, ease of processing, process tolerance to environment and health hazards, a non-toxic, all-liquid, amine, wet winding, long pot life epoxy resin was selected. The baseline resin and its properties are shown in Table 4-10 as well as the backup resin and the current CSD SOTA production resin, which contains vinyl clorohexane and MDA, both known carcinogens. The processing and mechanical properties of the chosen resins have been tailored to match the SOTA resin and have been extensively characterized by CSD for the ALV program.

The next critical trade study was for the fiber (see Table 4-11). Three classes were considered: PAN-based carbon fibers, Aramids, and glass fibers. Aramid fibers were deleted because of poor shear, compressive, and moisture absorption characteristics, and moisture-affected, matrix-dominated properties. The decision between glass and carbon fiber would normally be based on cost alone; however, stiffness concerns favor the low-cost carbon fiber, or a hybrid combination. Previous studies by CSD on stiffness-driven cost per pound to orbit resulted in the selection of S-2 glass. However, any stiffness constraints resulted in selection of the low-cost carbon fiber. CSD has elected Fortafil 3(c) (as shown in Table 4-12) based on life cycle cost studies conducted for the ALV solid strap-on boosters. The combustor case is a very similar structure considering performance design and manufacturing technologies.

The Y-joint shear ply trade study is summarized in Figure 4-18. The chosen film adhesive materials are based on anticipated high skirt axial line loads and demonstrated experience. CSD has selected FM 123-5 based on a long history of use by both CSD and Brunswick and its demonstrated shear strength of over 928 MPa (4000 psi).

The metal components (end fitting and skirt attach rings) were traded as indicated in Figure 4-19. Based on cost, low-alloy, annealed steels available in plate and simple rings were selected over aluminum alloys and composites. The steel will be chrome-plated for corrosion resistance, a process that is routinely performed for production tooling where weight is not a constraint.

4.4 NOZZLES

Two nozzle configurations, a movable nozzle and a fixed nozzle with liquid injection thrust vector control (LITVC), are being studied for both the large and the small motors. With the exception of size, the nozzles for the large and small motors are the same; that is, they have the same design features and materials. The nozzle configurations are shown in Figures 4-20 and 4-21. Both configurations are based on the use of ablative insulators.

TABLE 4-11. FIBER SELECTION TRADE STUDY

T16904

Property	Kevlar 49	(Baseline) Fortafil 3(C)	(Backup) AS-4W Grafil 33-650 T-500	T650/42 IM-6G G40-700	IM7 T-40 T-800 G40-800	S-2 Glass, MIL-R-60346, Type III	E-Glass, MIL-R-60346, Type 1
Tensile strength, ksi (mPa)	550 (3800)	550 (3800)	580 to 650 (4000 to 4480)	720 to 785 (4960 to 5400)	800 to 820 (5500 to 5650)	500 (3800)	385 (2650)
Modulus, msi (GPa)	19 (131)	33 (228)	33 to 35 (130 to 240)	40 to 44 (270 to 300)	39 to 43 (250 to 280)	12.4 (85)	10.5 (72)
Denier, gr/9000m	4560	35,300	7600 to 8100	3900 to 4100	4005	18,220	18,220
Density, g/cc	1.4	1.8	1.77 to 1.81	1.74 to 1.81	1.81	2.49	2.60
Tow area, $in.^2 \times 10^4$ ($cm^2 \times 10^{-4}$)	5.452 (35.2)	33.5 (216)	6.9 to 7.7 (45 to 50)	3.8 to 4.1 (24.5 to 26.5)	3.8 (24.5)	12.46 (80.4)	9.97 (64.3)
Cost, $/lb ($/kg)	22.50 (49.60)	13.00 (28.66)	21.00 to 25.00 (46.30 to 55.10)	40 to 45 (88 to 99)	50 to 55 (110 to (120)	4 to 6 (8.80 to 13.22)	0.75 (1.65)
Spool size, lb (kg)	10 (4.5)	50 (22.7)	10 (4.5)	5 to 9 (2.2 to 4.1)	5 to 9 (2.2 to 4.1)	15 (6.8)	35 (15.9)
Delivered fiber strength, ksi (mPa)	350 to 400 (2400 to 2760)	420 to 460 (2895 to 3170)	420 to 560 (2895 to 3860)	680 to 710 (4690 to 4900)	730 (5030)	400 to 430 (2760 to 2965)	300 (2070)
Interlaminar shear, psi (mPa)	4500 (31)	8000 to 10,000 (55 to 70)	8000 to 10,000 (55 to 70)	8000 to 10,000 (55 to 70)	8000 to 10,000 (55 to 70)	8000 (55)	8000 (55)

TABLE 4-12. ALV BOOSTER SYSTEM CASE FIBER COST TRADE STUDY

T16905

Item	Case 1	Case 2 (Baseline)	Case 3	Case 4
Fiber	T-40, 12K tow	Fortafil-3C, 50K tow	Grafil 33-650, 12K tow	Glass S-2, 60 end tow
Relative strength	1.0	0.67	0.67	0.67
Relative density	1.0	1.0	1.0	1.30
Relative cost	1.0	0.34	0.75	0.34
Motor weight, kg (lb)	155,355.4 (342,500)	160,798.5 (354,500)	160,798.5 (354,500)	168,056 (370,500)
Case length, m (in.)	16.9 (664)	17.5 (687)	17.5 (687)	18.1 (712)
Case diameter, m (in.)	2.7 (105)	2.7 (105)	2.7 (105)	2.7 (105)
Bending natural frequency, Hz	9.2	10.1	10.1	6.2
Recurring cost, $M*	1542	1416	1530	1463
Life cycle cost, $M*	2047	1932	2046	1993
Cost/SRB, $M*	2.97	2.72	2.94	2.81

*10 launches/year for 13 years; four boosters/ALS vehicle; 1987 dollars; 95% learning curve

Preliminary trades indicated reliability and cost favored this approach rather than using regeneratively cooled nozzles using LOX or GOX.

The selected movable nozzle design uses a conservative approach, including (1) redundant features such as bondline O-rings and backside insulators, (2) well-characterized graphite-phenolic material in the entrance and throat rings, helping eliminate "pocket erosion," and (3) manrated safety factors (2.0 erosion + 1.25 char + 1.0 insulation), were used to establish

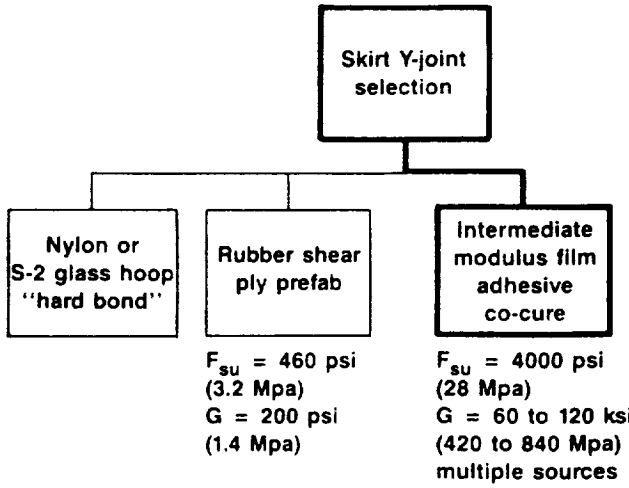

Figure 4-18. Y-Joint Shear Ply Material Selection Trade Study

50319

minimum thicknesses. The nozzle configuration is simplified, as compared to the existing RSRM nozzle, with a reduced number of joints, giving better structural support to insulators and making nozzle structures more producible. As part of the reconfiguration, the nozzle boot ring, a source of continued problems, has been replaced by a flexible thermal barrier (thermal seal) mounted on the flexseal. All joints use face seals as primary seals, and close under applied loading for superior seal displacement control.

The same conservative approach was used in arriving at the fixed nozzle design. With one notable exception, the materials, redundant features and safety factors used are the same as those for the movable nozzle. The exception is the use of silica phenolic as the aft exit cone liner material in

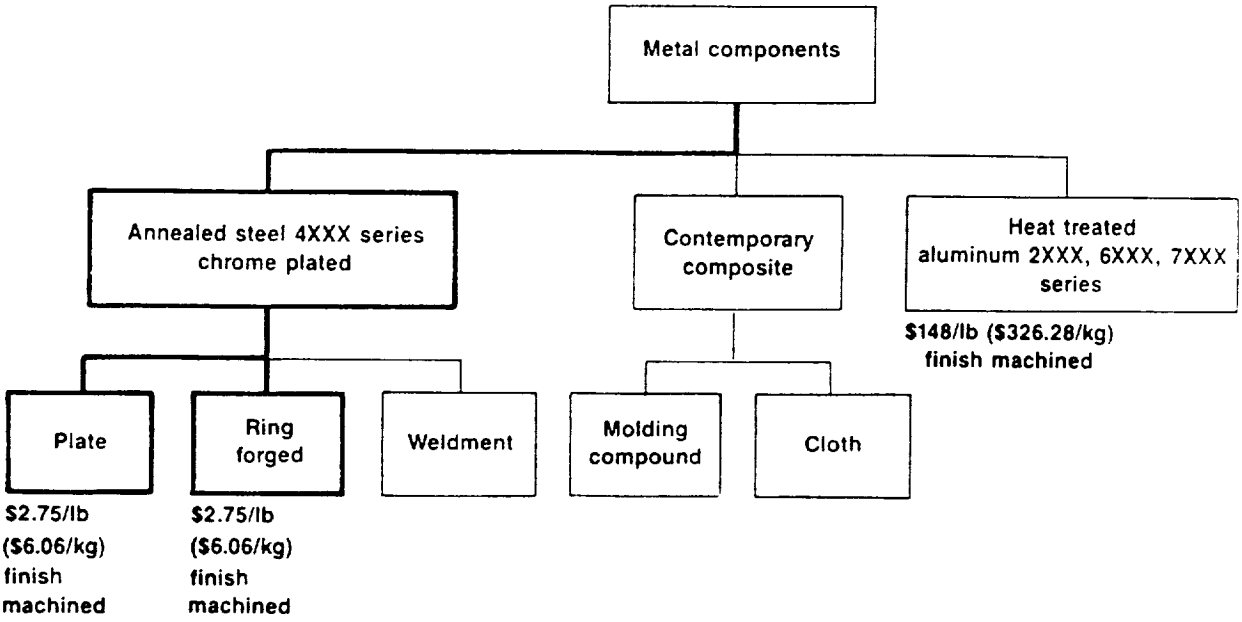

Figure 4-19. Metal Component Material Selection Trade Study

50320

FOLDOUT FRAME 1.

FOLDOUT FRAME 2.

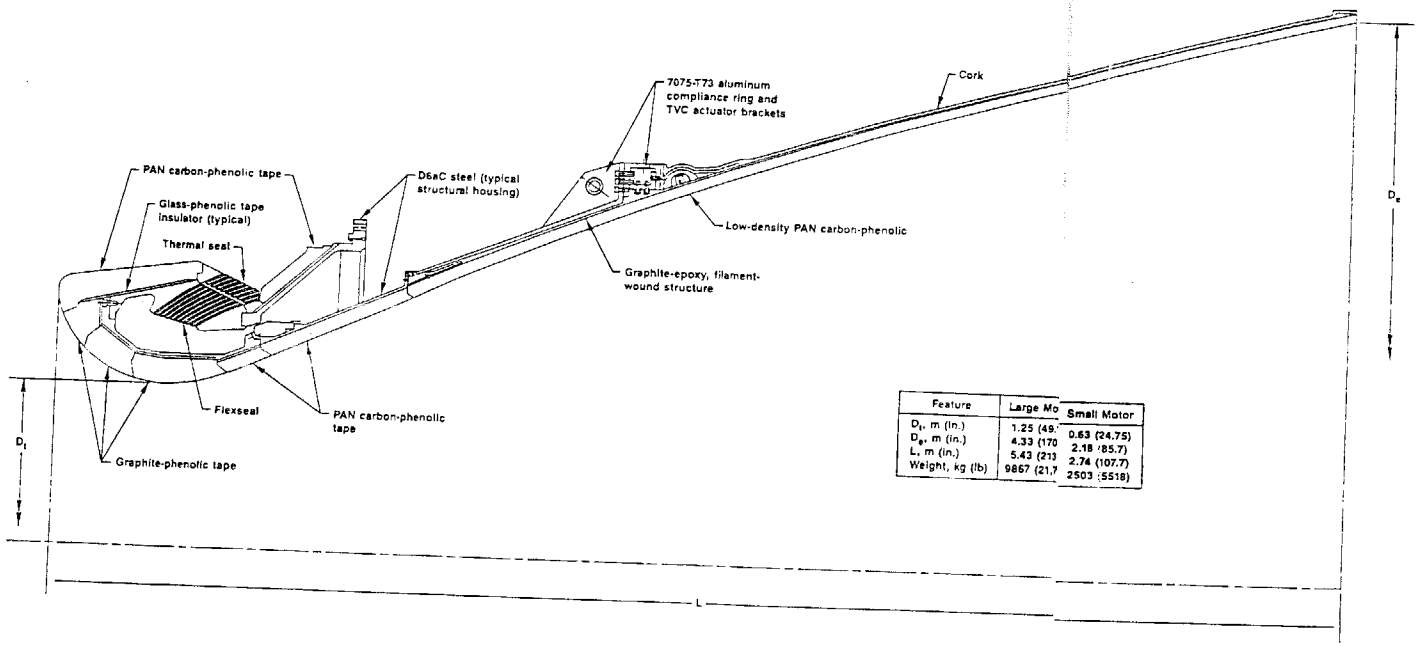

Feature	Large Mo	Small Motor
D_i, m (in.)	1.25 (49.	0.63 (24.75)
D_e, m (in.)	4.33 (170	2.18 (85.7)
L, m (in.)	5.43 (213	2.74 (107.7)
Weight, kg (lb)	9867 (21,7	2503 (5518)

Figure 4-20. Movable Nozzle, Hybrid Booster

50289

FOLDOUT FRAME 1

FOLDOUT FRAME 2

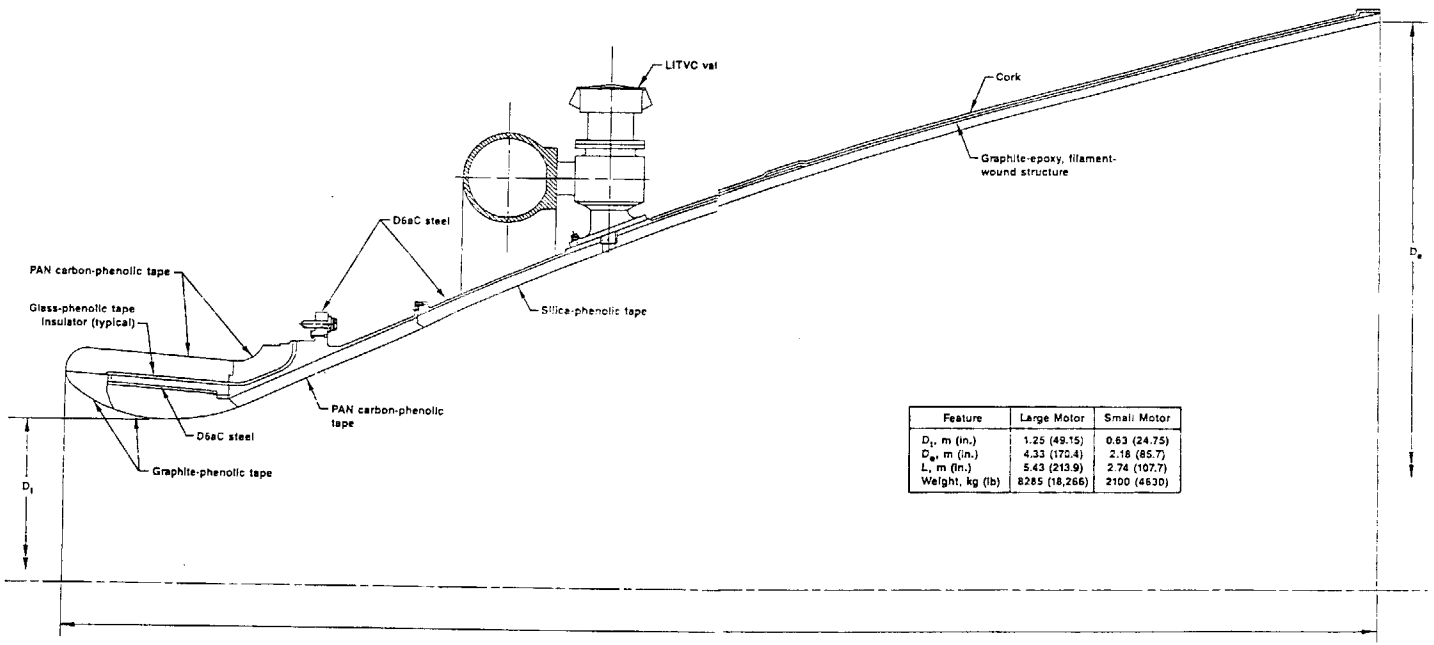

Feature	Large Motor	Small Motor
D_i, m (in.)	1.25 (49.15)	0.63 (24.75)
D_e, m (in.)	4.33 (170.4)	2.18 (85.7)
L, m (in.)	5.43 (213.9)	2.74 (107.7)
Weight, kg (lb)	8285 (18,266)	2100 (4630)

Figure 4-21. Fixed Nozzle, Hybrid Booster

50290

place of low-density carbon phenolic. This change was made to provide a liner material that would be compatible with the oxidizing environment of the LOX injectant proposed for the LITVC system. Silica phenolic was chosen based on its good performance in the similar oxidizing environment produced by the N_2O_4 injectant on the Titan nozzles. Carbon-phenolic materials perform poorly in highly oxidizing environments.

4.4.1 Nozzle Design Requirements

The main requirements from the MSFC statement of work affecting the nozzle design are (1) concepts shall use TVC (therefore, movable nozzles and fixed nozzles with LITVC are considered) and (2) concepts shall not use asbestos or asbestos-containing materials. No asbestos is used on the nozzle.

The CSD requirements affecting the nozzle design are the motor operating time, approximately 130 sec; average operating pressure, 5.17 MPa (750 psia); MEOP, 7.69 PMa (1115 psia); and exhaust environment. These requirements affect the choice of nozzle materials and, in effect, size the nozzle components from an ablative, thermal and structural standpoint.

4.4.2 Nozzle Configuration

Figures 4-20 and 4-21 show the movable and fixed nozzle configurations. The movable nozzle assembly includes the fixed housing, flexible bearing assembly with flexible thermal barrier, nose assembly supporting entrance and throat section insulators, a forward exit cone assembly and an aft exit cone assembly.

The fixed nozzle assembly includes the throat housing, which supports the entrance insulators and throat insert; the forward exit cone assembly, which includes the housing that provides for attachment of the nozzle to the motor aft closure; and the aft exit cone assembly, which consists of the liner, a steel housing with provisions for attaching TVC valve housings, an aft graphite-epoxy structural support and an aft external insulation of cork. On both nozzles the critical nose ring and throat ring insulators have been designed to minimize all potential contributors to "pocket erosion" to help

make nozzle performance reproducible. The material selected for these insulators is U.S. Polymeric FM-5014, which is the same graphite cloth/phenolic used in Titan Stage 0 SRM nozzles. FM-5014 has a low cross-ply thermal expansion characteristic that helps reduce the potential for "wedgeout" or uneven ablation. The insulator ply orientation is angled with the flow direction, the optimum orientation for uniform, minimum-rate ablation resistance.

The entrance cap, housing insulation, forward and mid exit cone liner, and forward and aft thermal seal rings are Fiberite K615, a PAN-based, continuous-fiber, carbon-cloth phenolic. This material is an eight-harness satin weave with Amoco's T-300-3K continuous fiber and the standard Borden S1008 resin system. The fabric is post-woven heat-treated to 2756° (4500°F). Preliminary data shows possible improvements in erosion to easily outweigh its higher density 1660 kg/m3 (1.66 g/cc) and higher thermal conductivity.

The aft exit cone liner on the movable nozzle is Fiberite MX 5926C, low-density, PAN-based, carbon-cloth phenolic. This is a prepreg which uses Amoco's T-300-3K continuous fiber in a square weave and the same resin as K615. This weave is not post-woven heat-treated. The liner is wrapped to a density of 1000 kg/m3 (1.0 g/cc) (although 0.97 has been reached) and a wrap angle parallel to the nozzle centerline.

The aft exit cone liner for the fixed nozzle is U.S. Polymeric FM 5504 silica phenolic, the same material that is used on the Titan Stage 0 SRM. It is a well characterized material that has demonstrated good performance in the LITVC oxidizing environment. The exit cone overwrap structure is a Fiberite system using Amoco T-40 graphite fiber with Fiberite's 982 low-temperature cure epoxy resin. This overwrap structure is wound over two back-to-back liners simultaneously. The overwrap uses layers of hoop and polar windings to achieve the necessary overall stiffness. The backside insulators for the throat and, in the movable nozzle, the forward exit cone liner are U.S. Polymeric FM 5755 glass cloth phenolic. This material uses an eight-harness satin weave cloth and has a cured density of 2000 kg/m3 (2.0 g/cc).

The compliance ring assembly, snubber assembly and actuator brackets on the movable nozzle are 7075-T73 aluminum. This aluminum has good forging mechanical properties and has been used extensively in aerospace applications including the Shuttle.

The external cork insulation is sprayable material. It is a CSD formulation of cork, adhesives, phenolic microballons, glass miscrospheres, chopped glass fibers and solvents. This is a room temperature cure material which is applied with automatic spray equipment.

The structural steel components on both nozzles are D6aC steel. This is a demonstrated, reliable, and well characterized material.

The movable nozzle flexseal reinforcements are HP-9-4-30 steel. The increased strength of this metal over D6aC was required for the shims.

4.4.3 Nozzle Development/Technology Acquisition

Nozzle analyses, performance predictions, and safety margins will have to be verified through a full series of materials characterization tests, subscale and component tests, and full-scale motor firings. Motor testing of a submerged and scaled-down nozzle will provide data on material properties, predictions, and, to a small degree, ease of manufacture. Cold flow studies should be used to optimize the nozzle inlet geometry and define aft closure/closure/nozzle operating environments.

TM-3 and 30% scale motor firings will provide early calibration of analytic techniques and design performance predictions. Finally, full-scale motor firings with fully instrumented nozzles will provide extensive data on full-scale nozzle analysis and performance.

4.5 THRUST VECTOR CONTROL (TVC)

Liquid injection and a turbohydraulic movable nozzle TVC concept were sized for the 4.57-m (180-in.) diameter motor. These two systems are the only types of TVC systems on motors over 3.05-m (120 in.) in diameter (Titan,

Shuttle) in use today. Titan uses nitrogen tetroxide LITVC and the Shuttle uses a movable nozzle with a redundant hydraulic TVA system. The movable nozzle TVC system would utilize conventional technology with experience gained from the shuttle system. Trade offs between the pump system and actuator feedback systems, along with redundancy requirements, will have to be made based on cost and reliability.

Cost and performance trade studies indicate that the movable nozzle TVC system is desired for a recoverable pump-fed hybrid and that the LITVC system may be more cost effective for an expandable pressure fed system.

For vehicles with multiple solid boosters (greater than 2), it is more cost-effective to eliminate TVC from the boosters altogether and provide control with the core engines, if possible.

4.5.1 Design Assumptions

The following design assumptions were made for the purpose of LITVC sizing:

- 6-deg vector angle (increased control moment for LITVC ignored)
- 1.5-deg average vector angle during flight
- Single valve out (per quadrant) redundancy
- LOX as injectant.

4.5.2 Performance

Considering the above assumptions along with the preliminary motor design characteristics (thrust, total impulse, etc.), LITVC systems for both motors were preliminarily sized. Table 4-13 summarizes each system's performance and weight estimates are presented in Table 4-14. The existing Shuttle SRB TVA system was used as the basis for the weight estimates of the movable nozzle system shown in the table. General performance characteristics of LITVC versus movable nozzle TVA systems are shown in Table 4-15.

TABLE 4-13. LITVC SYSTEM PERFORMANCE

T16921

Parameter	Diameter, (in.), m	
	(180) 4.57	(96) 2.44
Peak flow rate, total per quadrant, kg/s, (lb/sec)	662 (1460)	132 (290)
Number of valves/quadrant	4	2 (outboard quadrants only)
Injectant required (1.5-deg average vector angle), (lb)/kg	(30,000) 13,607.77	(7500) 3401.94
Axial impulse augmentation (1.5-deg average vector angle), %	0.63	0.63

LITVC inert weights are competitive with those for a movable nozzle. However, the LITVC system must carry a significant amount of injection fluid, which increases the total weight of the SRB. Fortunately, the additional LOX required is neither all inert nor all propellant. Therefore, its contribution of impulse augmentation must be considered when estimating vehicle payload capability. LOX injection provides 0.63% axial impulse augmentation, which offsets a portion of the weight penalty.

Flow control of liquid oxygen is well within the state-of-the-art. However, an LITVC system of this size using LOX has never been demonstrated. Testing will be required to determine injection performance and its effects on injection system and nozzle materials. By obtaining accurate side I_{sp} data along with more definition of vehicle geometry, mass properties, control and duty cycle requirements, better estimates can be made of total injection fluid required.

4.6 IGNITION SYSTEMS

The basic purpose of the hybrid ignition system is to provide the initial flame to start the vaporization process of the solid fuel so that it

TABLE 4-14. THRUST VECTOR CONTROL WEIGHT ESTIMATES

T16920

Item	Weight, kg (lb)		
A. 4.57m (180-in.) Diameter Motor			
LITVC			
Nozzle	8285.3	(18,266)	
Feed tube and manifold	648.6	(1430)	
Injector valves (16)	272.2	(600)	
Control system	9.1	(20)	
Total inert	9215.2	(20,316)	
Injectant fluid	13,607.8	(30,000)	
Duty cycle ullage	1088.6	(2400)	
Total	23,916.1	(52,726)	
Movable nozzle			
Nozzle	9866.5	(21,752)	
TVA system	725.8	(1600)	
Total	10,592.3	(23,352)	
B. 2.44m (96-in.) Diameter Motor			
Feed tube and manifold	81.7	(180)	
Injector valves (4)	45.4	(100)	
Control system	1.4	(3)	10.9 kg (24 lb)
Total inert	128.4	(283)	total/8 motors)
Injectant fluid	3401.9	(7500)	
Duty cycle ullage	172.4	(380)	
Total	3702.7	(8163)	

can continue burning with the injected oxidizer. A preliminary trade has been performed and the trade tree is shown in Figure 4-22. If fuel comes up to the injector face, individual igniters are required in every port. With such a configuration, failure to ignite any port will result in mission failure. Reliability can be improved by increasing the number of ignition sources per port at the expense of complexity and weight.

TABLE 4-15. LITVC/TVA CHARACTERISTICS

T16922

System	Description
LITVC	
• Relatively low acquisition cost (even with redundancy)	• $1.5 to 2.5M/motor
• Low launch support costs	• Simple checkout; no separate hydraulic power system • Large, short duration flow demands drive pump output requirements
Movable nozzle TVA system	
• Dependent on SRB weight, not duty cycle	• No injectant fluid
• Low development costs	• Mature technology (Shuttle, C4, D5, MX, Small ICBM)
• Higher acquisition costs	• $4 to 6M/motor
• Larger, heavier aft skirt required	• Must cary actuation loads and must be long enough to control nozzle aerodynamic loading to within TVA system capability

An alternate approach is to have a common plenum between the injection plane and the port entry. This can allow for a much smaller number of igniters for common ignition of all ports. This design, however, reduces the overall volumetric efficiency of the motor case. On the basis of improved reliability, this open head end plenum configuration is the CSD preferred approach at this time.

Whether single or multiple ports are simultaneously ignited, the basic ignition systems are similar. Potential ignition systems are:

- Injection of a pyrophoric material, i.e., TEA, pyrophoric methane, or silane
- Injection of supplemental gaseous fuel with an auxiliary flame, i.e., gas-gas igniter, pyrogen/pyrotechnic
- Ignition by means of a large pyrogen/pyrotechnic source.

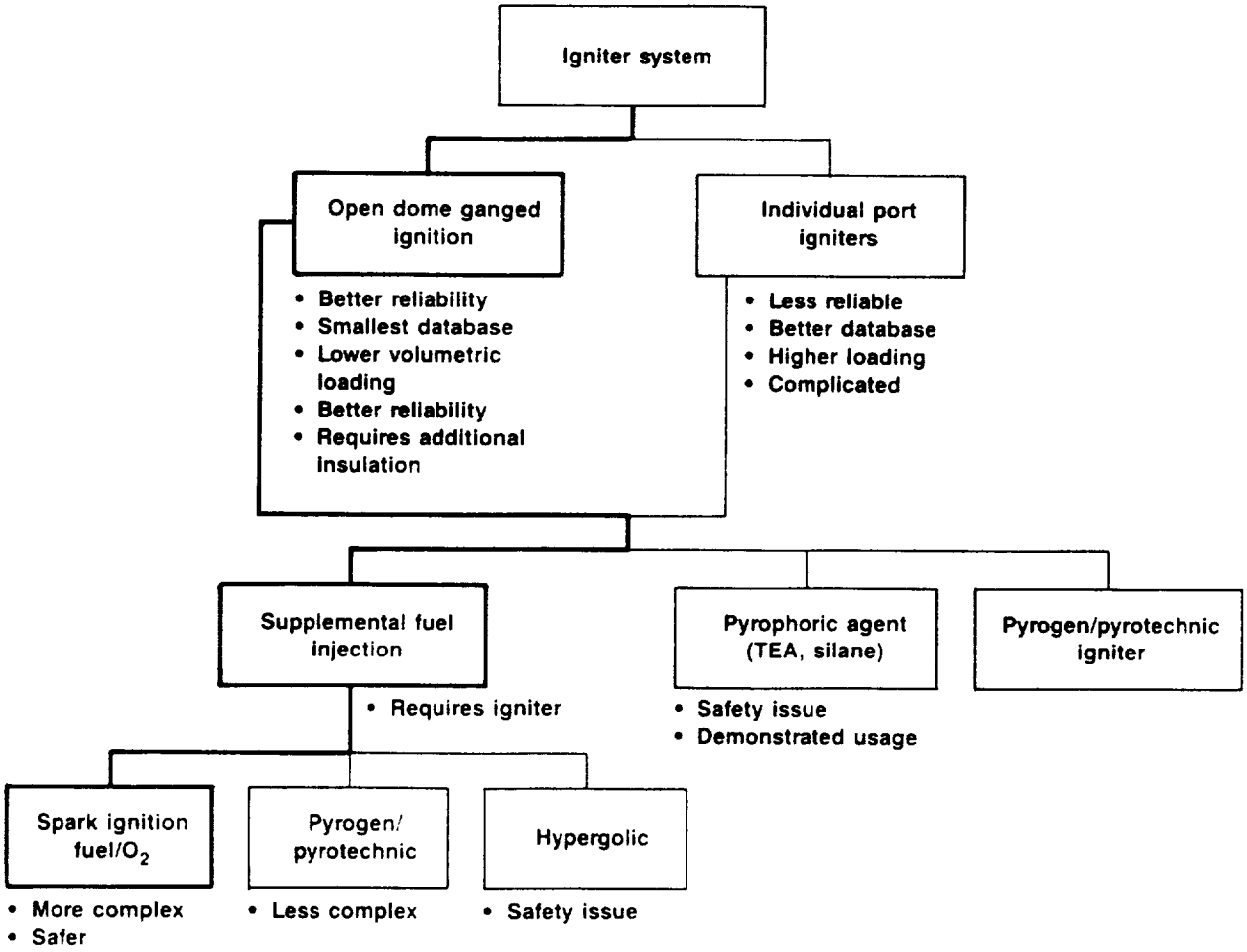

Figure 4-22. Igniter System Trade Study

50351

The last approach has been discarded as being unproven, bulky, and with lower safety than the first two approaches. The initial approach, pyrophoric injection, has been used in wind tunnels and for smaller scale ignition systems. The second technique, supplemental gas injection, is a safer approach and has been used on hybrids since their inception. The fuel used in a turbine-driven pump system or a hot gas pressurized LOX system can be utilized for the ignition process. The small quantity of fuel required for this ignition application can always be carried in a pressurized system. It has been chosen to use propane from the LOX pump drive system for the igniter fuel. The propane will be injected at a rate of 5% of the initial expected hybrid fuel flow for a duration of 200 to 300 msec. For uniform distribution, fuel injection ports will be provided in the vicinity of each oxidizer port.

On the basis of reduced complexity and better safety, the initial fuel/oxygen mixture will be ignited using redundant pyrogen igniters. A development issue is the required number of pyrogen igniters and sequencing and ramping of the oxygen, ignition fuel and pyrogen igniters.

4.7 FUEL GRAIN ANALYSIS AND PROCESSING

As part of the preliminary design and trade studies, structural analysis of both the large and small grains was performed to verify the grain adequacy and identify potential processing problems.

4.7.1 Grain Structural Analysis

The hybrid fuel grains are characterized as case-bonded cylinders with multiple perforations, symmetrically arranged circumferentially in two rows. The regions in such a grain that have the greatest potential for structural failure are the free surfaces and the bonded interface.

A schematic of the grain system is shown in Figure 4-23, which indicates the most critical structural locations. The analysis conducted was directed toward determining the stresses, strains, and margins of safety in these regions.

The principal method used in the grain structural analysis was the TEXGAP-2D[10,11] finite element computer code. An important feature of this code is its use of quadratic displacement continuum elements. In the TEXGAP-20 model far fewer elements are required than are necessary in codes that use constand strain elements. The code also has the capability of analyzing high material incompressibility, which is characteristic of propellant, fuel, and liner materials. Closed from solutions[12] also were used in the analysis to determine the induced stresses and strains; the analysis procedures that were used are consistent with those given in the Chemical Propulsion Information Agency (CPIA) handbooks[13,14] and, in particular, the standard analysis procedures of reference 15.

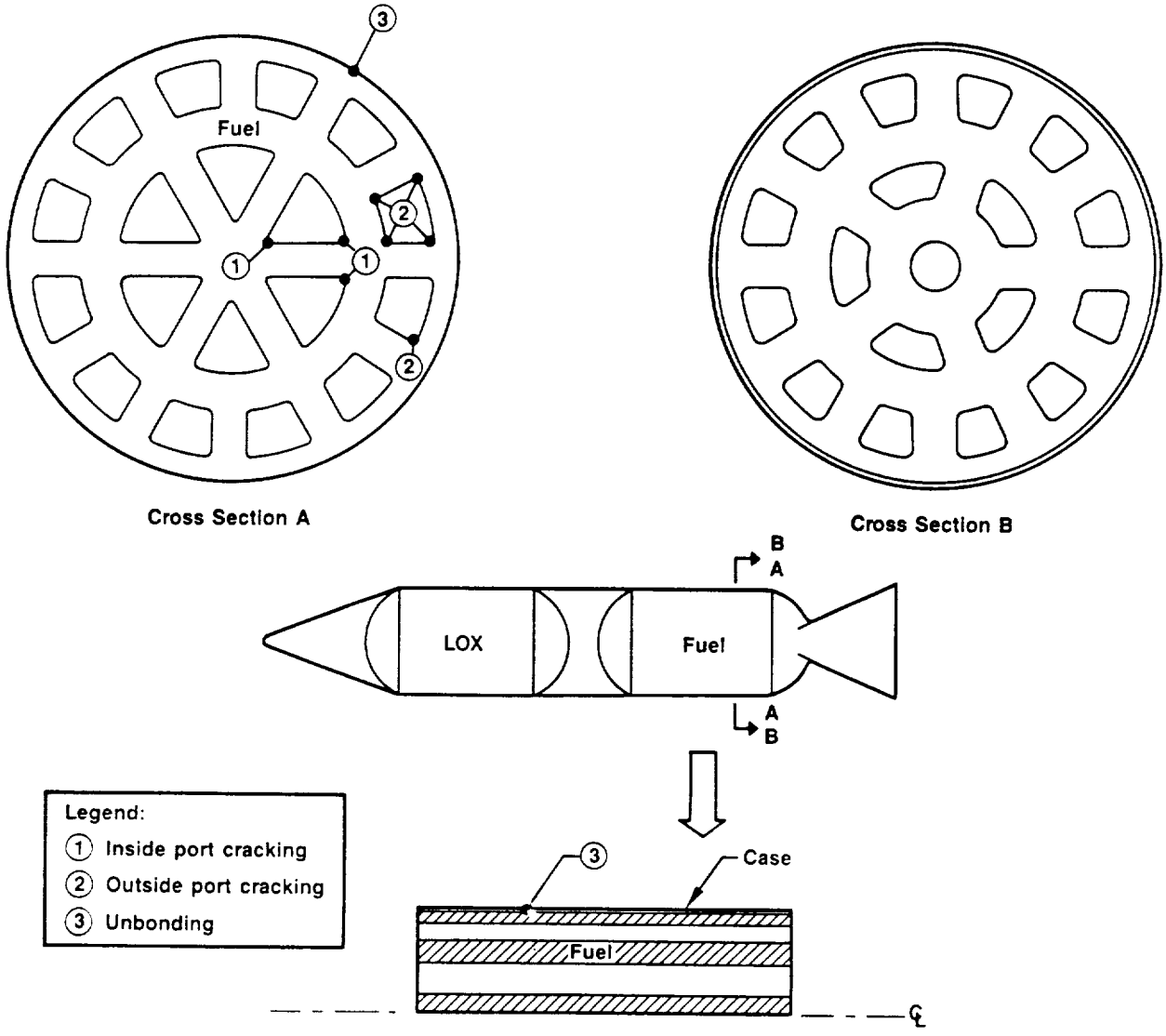

Figure 4-23. Schematic of 2.44-m (96-in.) Diameter Grain Indicating Potential Failure Modes

50292

The margin of safety (MS) is defined here are:

$$MS = \frac{\text{reduced allowable}}{\text{limit stress or strain x SF}} - 1$$

where SF is a prescribed safety factor (1.5 for nonoperational and 1.25 for operational loads). Measured allowables are degraded to account for batch-to-batch variation and aging.

A margin of safety of zero on a given failure mode thus satisfies the design requirements. Higher values indicate capabilities in excess of the requirements.

The given loads lead to stress and strain maxima that occur on the grain boundaries, which consist of both free and bonded surfaces. Hence, both strain- and stress-based failure criteria have been employed in the margin of safety calculations depending upon whether the grain surfaces or bonded interfaces are being examined. On the perforation surfaces, the maximum strain is tangential and in the plane of the cross section.

Margins are written using the maximum principal strain criterion, comparing the calculated value with the biaxial failure strain obtained (1) in an endurance test for the case of storage or (2) in a high rate, pressurized test for the case of ignition.

For bond failure, both maximum principal stress (MPS) and maximum deviatoric stress (MDS) are employed. The deviatoric stress is defined as:

$$\sigma_{dev} = \sigma_1 - 1/3 (\sigma_1 + \sigma_2 + \sigma_3), \text{ etc.}$$

and applies only to the normal components of stress. For pressurization, although the stress field is nearly compressive, the maximum deviatoric stress is tensile and can be compared with the deviatoric strength obtained in uniaxial high rate tests with pressure superimposed.

The MPS criterion is used for both thermal and acceleration loads. The laboratory sample for generating the strength is the rectangular bond-in-tension (BIT) specimen. A summary of loads, failure modes, critical stress/strain components, and the measured allowables with which they are compared is given in Table 4-16.

The finite element grid networks employed in the analysis of the 2.44-m (96-in.) grain design are shown in Figure 4-24. A characteristic 9.14-m

TABLE 4-16. GRAIN FAILURE MODES AND FAILURE CRITERIA

T16962

Failure Mode	Critical Stress or Strain Component	Measured Allowable
Cooldown, acceleration • Port cracking • Failure or unbonding near termination	• Tangential strain • Maximum principal stress	• Biaxial endurance strain • Bond endurance strength
Pressurization • Port cracking • Failure or unbonding near terminations	• Tangential strain • Maximum deviatoric stress	• Rate/pressure-dependent biaxial strain • Rate pressure-dependent uniaxial strength x 2/3

(30-ft) segment of the cross section was treated in the state of plane strain for cooldown and pres-surization loads, while an axisymmetric equivalent model, with suitable reduced shear modulus and density in the cavity regions, was used to determine axial slump.

Typical results, contours of maximum principal strain for storage at 278°K (40°F), are given in Figure 4-25. A summary of loads, failure modes, induced stress and strain, allowables and margins of safety are collected in Table 4-17. Note that mode 1 margins (Figure 4-23) may be increased by increasing fillet radii at the port corners.

A second design was also considered (Figure 4-26) with a full 180-deg sector of symmetry. Since the corners of the ports, once suitably rounded, have ample margin, only the bond is of structural interest and the FE grid only coarsely models the ports. The maximum principal stress in the fuel at the bond is indicated in Figure 4-26 for a 311°K (100°F) temperature decrease. This represents cure at 333°K (140°F) plus polymerization shrinkage followed by cooling to 289°K (60°F). The properties are listed in Table 4-17.

Note in Figure 4-26 that there are chords of fuel (from the center to the outside surface) "bridging" the cross section. The bond stress at the

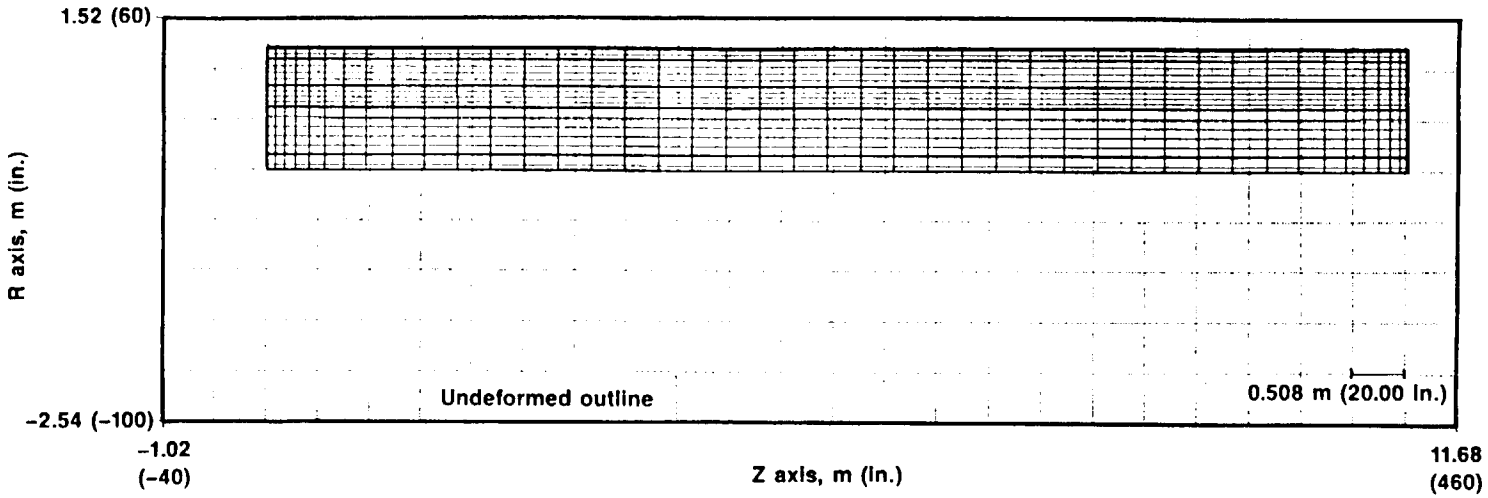

A. Longitudinal Grid

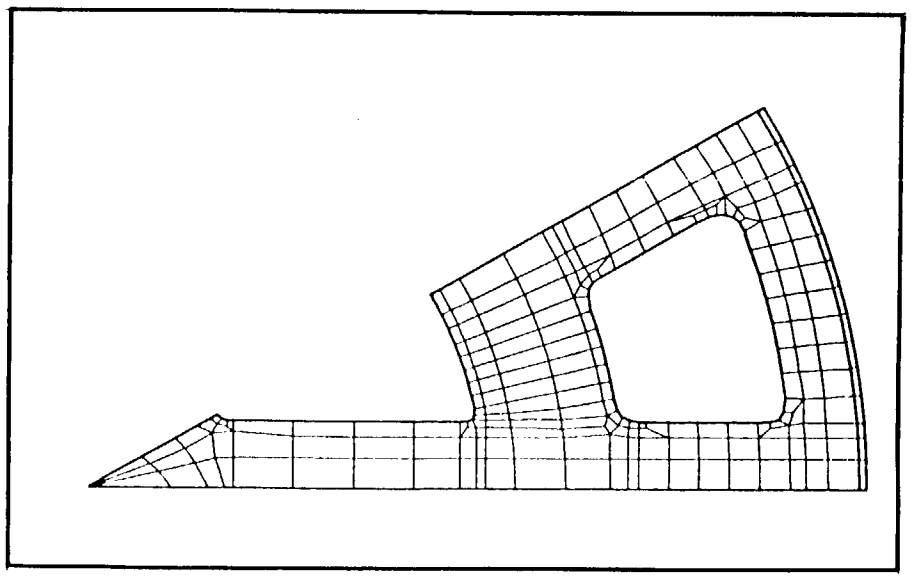

B. Cross Section Grid

Figure 4-24. Finite Element Grid Networks for 96-in-Diameter Hybrid Fuel Grain

50291

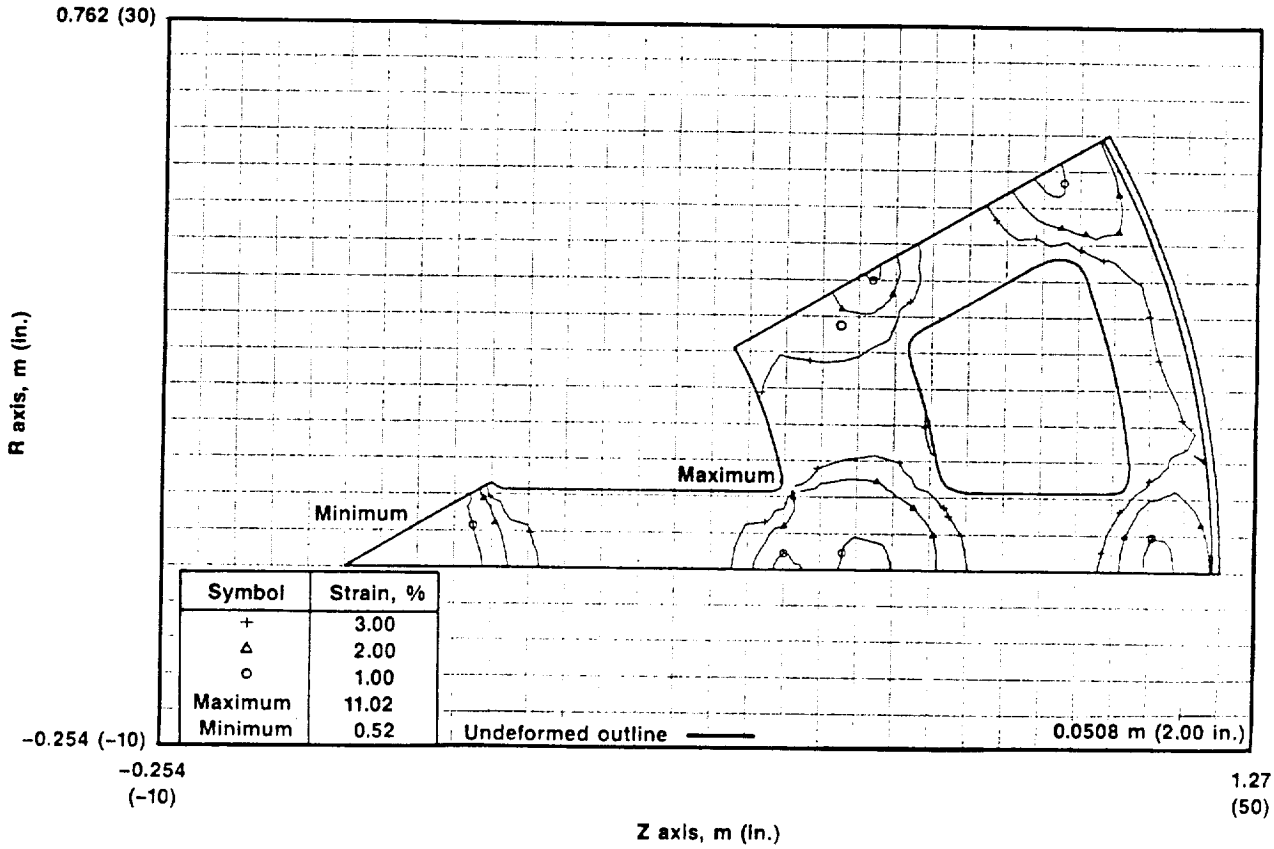

Figure 4-25. Contours of Maximum Principal Strain During Storage at 40°F
50293

ends of such a bridge exceed those at other locations where bridging is interrupted by a port.

Material properties can be divided into two categories: predictive properties and failure properties. Predictive properties are those required to determine the stresses and strains within the propellant grain. Failure properties consist of stress (strength) and strain capabilities.

Predictive properties include: rate modulus, relaxation modulus, Poisson's ratio, density, and coefficient of thermal expansion. The lowest margins of safety occurring in the fuel grain are written for the bond of the fuel to the motor case during storage. The stress induced in the fuel is directly proportional to modulus. Reducing modulus, however, increases the

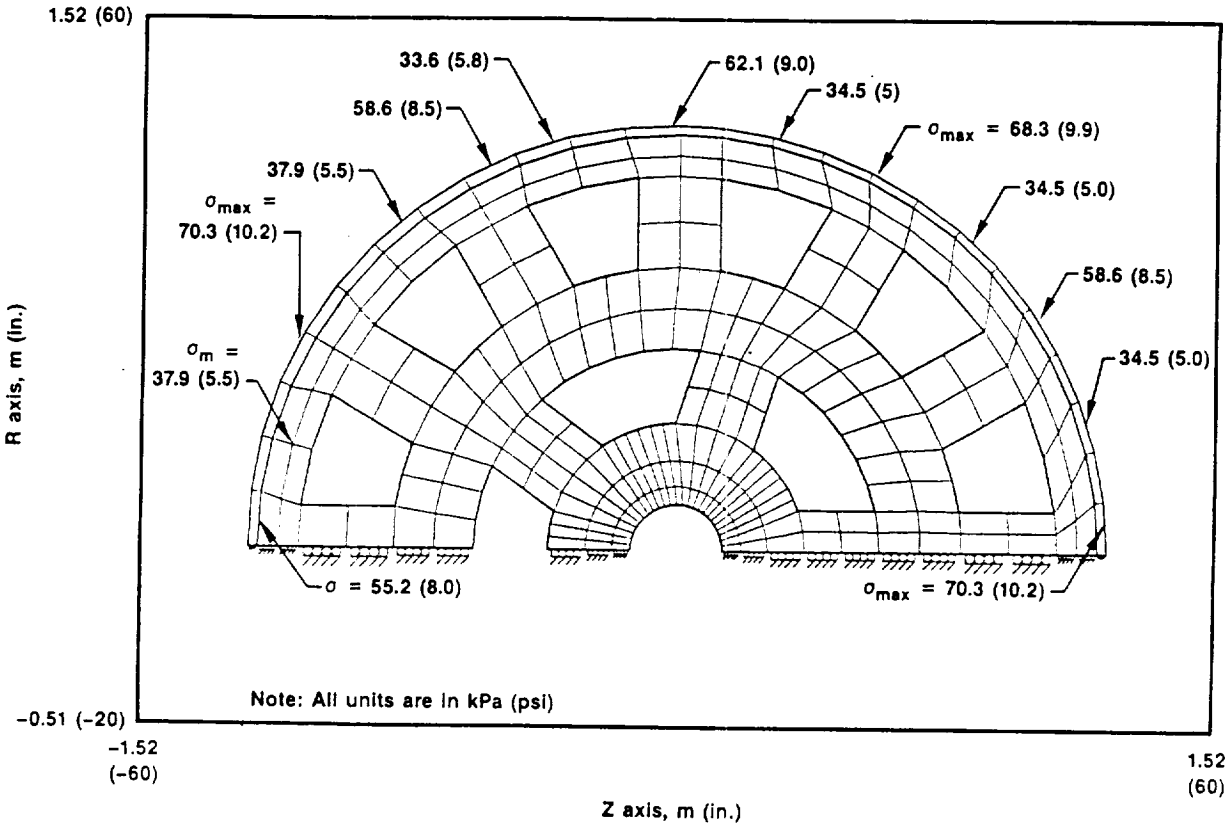

Figure 4-26. Coarse Finite Element Grid Network for 2.44-m (96-in.)-Diameter Fuel Grain with Bond Stress Indicated for ΔT = -100°F

50372

TABLE 4-17. MATERIAL PROPERTIES EMPLOYED IN FUEL GRAIN STRESS ANALYSIS UTF-26,858 400/2259

T16961

E = 1.14 MPa (165 psi) equilibrium modulus for cooldown and slump analysis
E = 6.9 MPa (1000 psi) equivalent elastic modulus during ignition at 40°F
E = 4.83 MPa (700 psi) equivalent elastic modulus during ignition at 70°F

ν = 0.499 (Poisson's ratio) during cooldown
ν = 0.4999 during ignition

α = 189 x 10^{-6} m/m/K (105 x 10^{-6} in./in./°F) coefficient of thermal expansion

ρ = 1.010 x 103 kg/m^3 (0.0365 lb/$in.^3$) density

T_f = -11K (-20°F) (equivalent temperature change to account for fuel polymerization shrinkage)

deformation due to slump. A compromise position on modulus is needed to optimize the structural integrity of the grain design.

There are some improvements to the design that would produce increased margins of safety at both the ports and the case bond. The fuel perforations require rounded (filleted) corners (an arc of 0.0254-m (1.0-in.) radius) to reduce strain concentrations. Because fuel has high strain capability, fillets will be small enough not to affect burnback profiles, yet large enough to avoid sharp corners.

The ends of the grain are regions of stress concentration requiring either an ample fuel fillet or a stress relief flap (boot). On large motors, relief boots are usually used. Typically, the boot length is 10% or more of the grain diameter, e.g., 0.25-m (10 in.) on Titan IV (3.05-m (120-in. diameter)) and 0.5-m (20 in.) on T34D (also 3.05-m (120-in.) diameter). At the tip of the boot, the insulation on the fuel side would be thickened locally to form a bulb to reduce the stress in the adjacent fuel. The bulb thickness will be tailored to control the peak stress and might be as high as 1 in. on a large grain.

As shown, the multi-ported configurations produce large circumferential variations in bond stress around the grain and at terminations or boot tips. Current demonstrated fuel bond strength capability is low; hence, the margins are low. The following steps can be taken to increase the bond margins:

- Raise the bond strength without a corresponding increase in modulus. This would require an investigation of alternate liners for those currently used for solid propellants.
- Orient the ports to avoid straight bridges of fuel across the grain. Interrupted bridging smooths out the induced bond stress. The average stress equals that for a circular port grain of the same cross sectional port area.
- Ambient or reduced cure temperatures can be used to produce a correspondingly reduced thermal load for storage.

- Consider other grain designs with dividing of the cross section into pie-shaped cells, partitioned from each other by stiff Kevlar sheets. Each cell would behave independently with central relief provided by one or more ports. Analysis would be conducted to determine induced stress advantages.

Man-rated solid propellant systems such as ASRM require a safety factor of two to be imposed on the calculated bond stress. The relative safeness of hybrid fuel compared to solid propellant suggests that the safety factor could be reduced to the conventional value of 1.5, since unbonded surfaces will not burn without oxidizer.

The finite element model representing an axisymmetric equivalent of the fuel grain was used to determine the relation between axial displacement and modulus under a gravitational load. For the 18-ported, 2.44-m (96-in.) diameter grain analyzed here,

$$u_{max} = 0.42 \frac{165}{E}$$

For the current formulation, the equilibrium modulus is 1.14 MPA (165 psi) and the peak axial displacement is 0.0107 m (0.42 in.). Should E be reduced for the purpose of decreasing the induced bond stresses, the displacement levels must be kept acceptable.

The 4.57-m (180-in.) diameter grain has the same problem area (low margins at the bond) as the 2.44-m (96-in.) diameter grain. Cracking of the port corners is con-trolled by appropriate corner radii.

Geometrically similar grains produce identical stress fields for cooldown and pressurization, while axial slump varies as the square of the scaling factor ($(180/96)^2 = 3.51$). The larger motor has a lower volumetric loading ratio, 60% compared to 68%. Therefore, it generates approximately 22% less bond stress than the smaller motor. With the same fuel, the axial

deflection of the larger motor is approximately 3.5 times that for the smaller grain, about 1.5 in. for an E of 1.15 MPa (165 psi).

4.7.2 Fuel Grain Processing

Both the large and small motors are ideal candidates for continuous mix operations. The inert fuels are particularly good candidates since the absence of oxidizers eliminates the safety problems inherent in a propellant system. New mix facilities would be required. However, the technology required is state-of-the-art in the chemical process industry.

As discussed in the preceding subsection, the grain margins would be improved by lowering the cure temperature to ambient levels. Techniques have been developed at CSD for ambient cures of ramjet fuels. These approaches could be applied directly to the related hybrid fuel grains. Higher cure temperatures (333°K (140°F)) are not a technology or facility issue since simple cure-oven buildings would be utilized for curing the segments.

The large number of ports, particularly in the large-diameter motor, and the lengths of the ports are of concern with respect to the casting operations. Mandre. removal requires a taper that will cause a variation of port area of about 7% in the large motor and 13% in the small motor. While the taper might be used to accommodate axial regression rate variations, an alternate approach might be to use cast-in-place consumable mandrels. These would be precured, fiber-reinforced, hollow structures with a port area equal to the design port area. With a wall thickness of approximately 3.81 x 10-3 m (0.15 in.), the man-drels would actually constitute the first portion of fuel grain during hybrid combustion. Pressurizing the mandrels or temporarily filling them during the fuel grain casting operation can make them strong enough to withstand the hydraulic loads of the fuel as it is cast into place.

Consumable mandrels are particularly attractive for the small motor using an overwrapped case approach. The overwrap must be done with the cartridge fuel grain in a vertical position. Although the center port can be used to

support and rotate the grain, additional stiffening is required. The cast-in-place consumable mandrels would easily be adapted to this process. Preferred materials for the mandrels are Spectra 1000 PT (plasma treated) polyethylene as the fiber and epoxy for the resin. These materials are also suitable for the cartridge outer layer (see Figure 4-27), which also should be consumable. This approach is an item which should be considered further in the subsequent phases of this program.

The fuel grain cartridge as well as the casting mandrel will be made from Spectra 1000 PT Fabric Style 988, and a wet lay-up epoxy resin suitable for cure at or below 394°K (250°F). Cloth lay-up on a reuseable male mandrel using vacuum bag and autoclave cure techniques can be used to make the low cost, consummable casting mandrels and cartridges. Positioning spiders will locate the mandrels with respect to the cartridge, according to the fuel grain

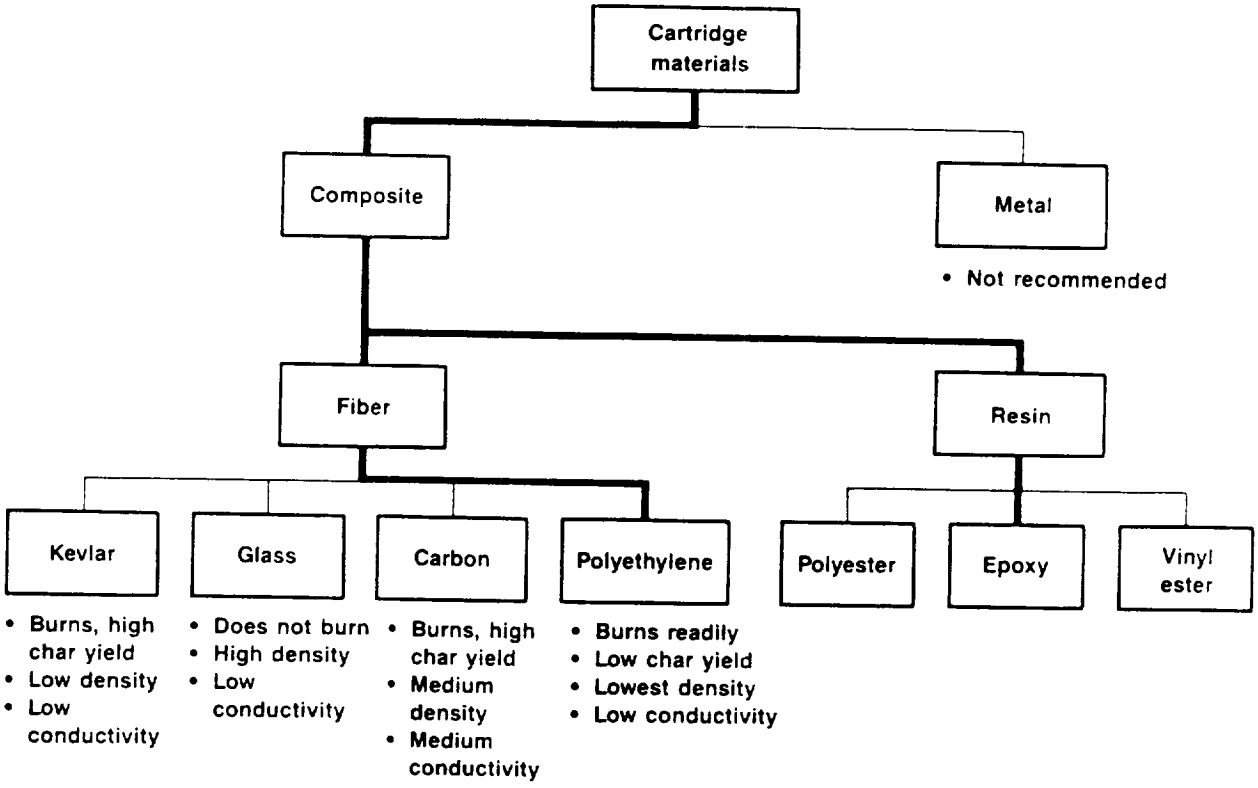

Figure 4-27. Cartridge Material Trade Study

50349

design, in preparation for casting. Once the fuel grain is cured, the reinforced grain can be positioned on the winding tooling for case overwind and cure. It is expected that the fuel grain mandrels will be 3.81 x 10-3 m (0.15 in.) thick and the cartridge 6.35 x 10-3 m (0.25 in.) thick in order to withstand fuel grain cast and cure loads, and subsequent case overwind and cure loads.

The two-segment large-booster design was selected on the basis of processing and reusability. Some consideration was be given to a welded throwaway system with no seals. A primary advantage of this approach is that it eliminates potential seal problems and might be done safely with the precast, inert fuel grain, which would not be feasible with a solid propellant motor. However, problems in verifying grain and case integrity led to discarding this approach.

Whether joints are used or not, the grains will be cast with a concave aft end and convex forward end that intersects the dome wall above the segment top. The aft convex end will similarly extend below the segment bottom in such a way that grain covers any potential joint or seam. EPDM boots will be used at all free ends to minimize termination bond stresses.

An additional item of concern is the potential need to support the fuel grain in the area of the residual fuel slivers. A preformed structure consisting of a nonconsumable fiber and a consumable resin would be used to ensure that the slivers do not exit through the nozzle. This is a complication that reduces the volumetric loading and complicates the grain casting. At this time ejection of the slivers is not considered to be a problem, but additional analysis and experimental verification is needed. Unlike a solid propellant motor, the passage of solid material through the nozzle does not cause a combustion problem. However it may be necessary to incorporate a retention system to improve the fuel utilization, particularly if there are large variations of fuel regression that could cause portions of the grain to be expelled prematurely.

The processing and loading of the 4.57-m (180-in.) diameter hybrid booster fuel grains will be of prime concern. The process starts with the receipt of the 4.57-m (180-in.) case segments and includes case insulation, lining, fuel mixing and casting, fuel grain inspection, final assembly and packaging for shipment. Three new processes have been selected for the hybrid fuel grain fabrication: 1) application of strip-wound insulation for the case and aft closure, 2) trowelable insulation for the forward closure (if required), and 3) continuous mixing of the UTF-29,901 hybrid fuel (designated UTF-29,901). The remainder of the processes and facility concepts selected for the fuel-grain fabrication have been proven in manufacturing solid rocket boosters. Because of their size, new or modified facilities will be required to process these fuel grains. The factory concepts presented here are modifications of standard solid rocket motor concepts with separate work stations for the insulation, mixing, casting, radiography, and final assembly of the grains. The fuel grains will be transported within and between stations using an in-plant rail system. However, since the fuel is inert, a facility with all of the work stations under one roof may be a better choice. Such a facility could use air bearing pallets to move the grains between the various work stations. Finally, water shipment of both the cases and fuel grain assemblies may be preferable to rail transportation because the case diameter exceeds the railroad clearances in many parts of the country.

Fuel grain process flow is depicted in Figure 4-28. Hybrid fuel grain processing starts with receipt of the case segments. They would be unloaded from the barge using a crane, placed upon a rail car, and taken to the receiving inspection station. After removal of the shipping covers, the cases will be visually inspected for shipping damage, corrosion, etc. Case manufacturing certifications will be reviewed and, if all inspection results are satisfactory, accepted and sent to stores to await the first process step, namely insulation of the case.

The first step in the insulation process is the cleaning of the case segments to remove the shipping preservative and visual inspection with ultraviolet light to insure that the case is clean and free from preservative and

other foreign matter. The cases will be placed onto a rotary insulation fixture and the insulation forming tooling will be installed onto each end. The insulation primer and adhesive will be applied to the case sidewalls using a numerically programmed spray lance. After the primer and adhesive have dried, the silica-loaded EPDM rubber insulation compound will be extruded and applied to the case wall in a continuous strip. Insulation fixture rotation and longitudinal axis positioning of the insulation extruder strip application boom will be numerically controlled in order to apply the correct insulation thickness for each location on the case wall. Scrim cloth and vacuum bag material will be applied over the insulation lay-up assembly and then the insulation will be cured in an autoclave. The autoclave pressure and temperature cure cycle will be programmed to cure the EPDM to achieve desired physical properties. After the cure cycle, the insulated case segment will be placed on the rotary platform of an ultrasonic inspection fixture. The insulation-to-case bond will be 100% ultrasonically inspected using this fixture.

The aft closure segment will be insulated with silica-loaded EPDM using the same process described above for the case segments. The forward closure segment will be insulated with a trowelable insulation material sufficiently viscous so that it may be applied with a machine similar to the strip extruder used for the case segments. The insulation forming tooling for the forward closure includes injector simulators which will be removed and replaced with the real injectors after the insulation cures. The closure will be placed on a rotary fixture and trowelable insulation will be pumped through a dispenser nozzle onto the closure in a continuous ribbon. This ribbon will be trowelled to the appropriate thickness contour by a heated doctor blade following the nozzle. The rotation of the fixture and the position and speed of the dispenser nozzle/doctor blade will be numerically controlled. The trowelable insulation will be cured in a heated oven and then inspected ultrasonically using the same automated technique described above for the case segments.

After acceptance of the insulation, the case segments are to be spray coated with UTL-0040 liner to prepare them for the fuel grain casting. The

FOLDOUT FRAME 1

FOLDOUT FRAME 2

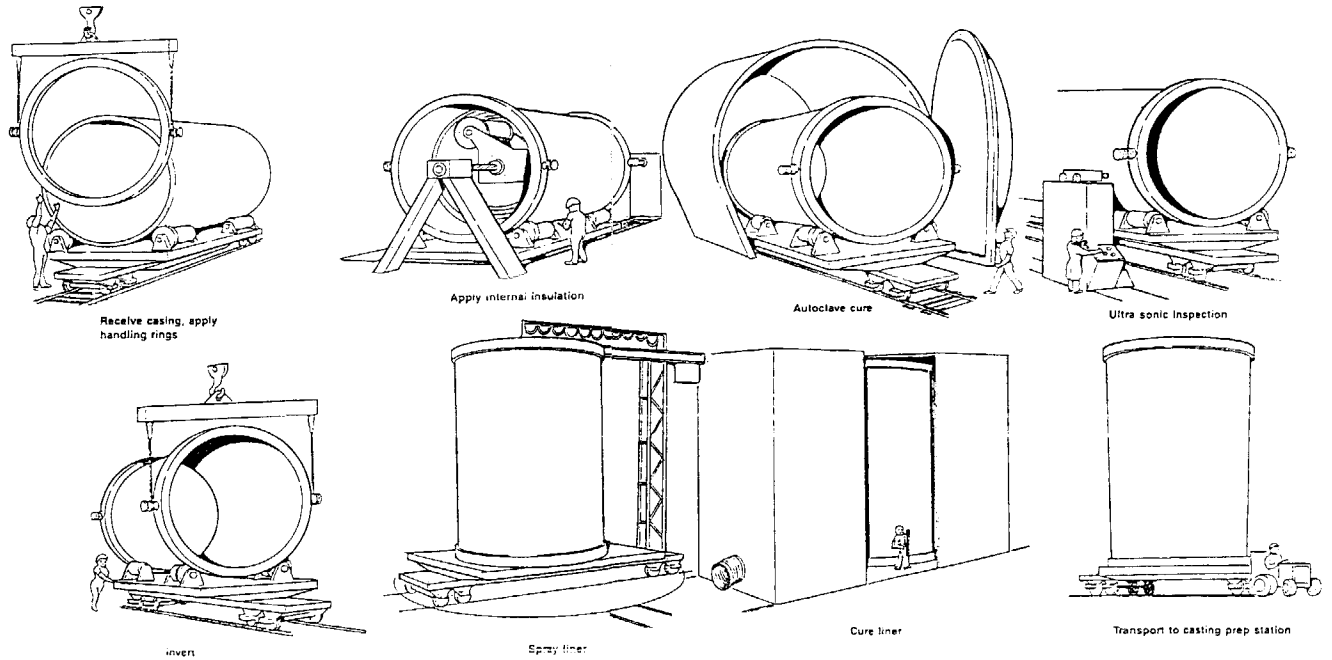

Figure 4-28. Hybrid Assembly Process
(Sheet 1 of 3)

50447

FOLDOUT FRAME 1

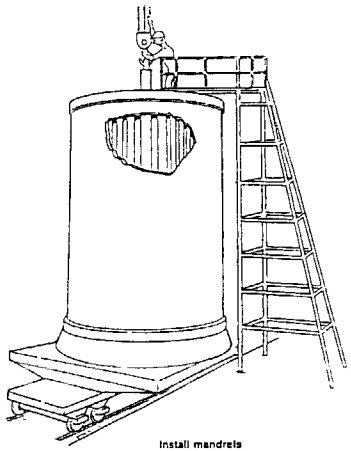

Install mandrels

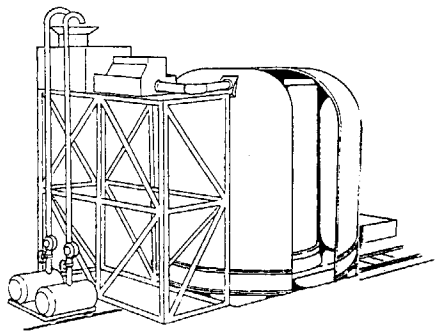

Mix and cast

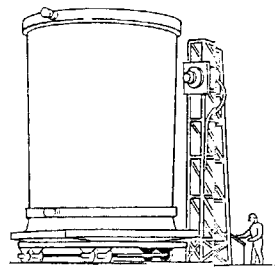

X-ray

FOLDOUT FRAME 2

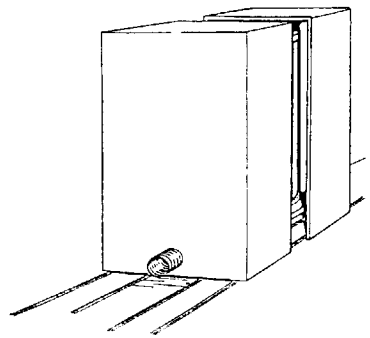

Cure fuel grain

Figure 4-28. Hybrid Assembly Process
(Sheet 2 of 3)

50447

FOLDOUT FRAME 1

FOLDOUT FRAME 2

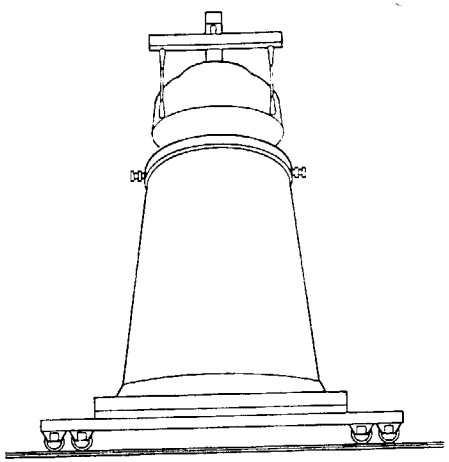

Install aft closure

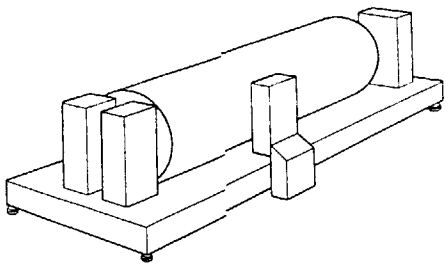

Weighnd CG

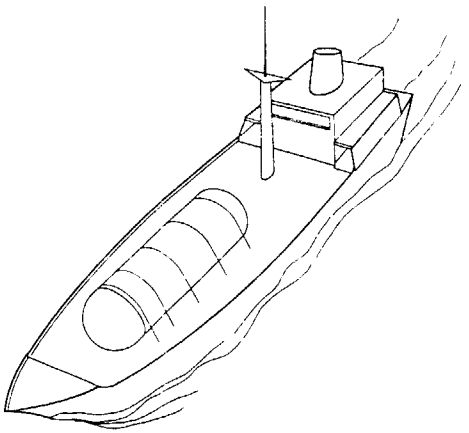

Transport by barge

Figure 4-28. Hybrid Assembly Process
(Sheet 3 of 3)

50447

4-67/4-68

segments will be turned to a vertical position and placed onto a rotary fixture with a crane. The UTL-0040 liner is sprayed onto the insulated case side wall using an automated spray lance. The rotation of the lining fixture and the position of the spray lance are numerically controlled to provide a uniform coat of liner over the case wall. After the liner coat is completed, it is cured in an oven at 333°K (140°F) for 16 to 18 hr.

The case now goes to the casting equipment assembly facility to prepare it for casting. The grain casting equipment consists of a baseplate, 34 separate mandrels and a top centering-plate. To enhance the assembly, the case segment is placed onto a baseplate with a crane. This baseplate forms the forward or aft grain contour and locates the fuel port mandrels. The fuel port mandrels, which form the internal grain configuration, are lifted and placed into the case and bolted onto the baseplate. After each of the 34 fuel port mandrels have been attached to the baseplate, the top centering plate will be installed onto the top of the case. The fuel port mandrels will then be attached to the centering plate, thereby fixing them in proper position, fore and aft, to form the fuel grain. Following the mandrel assembly, the case is pre-heated in an oven at 333°K (140°F) for 8 to 10 hr to prepare it for the fuel grain casting.

The hybrid fuel will be vacuum cast into the case/casting equipment directly form a continuous mixer. The case assembly will be transported from the casting equipment assembly station to a mixing and casting station. The case and its transport car will be placed in position and the two halves of the casting bell will be closed around it. The continuous mixer gantry will then be moved into position next to the bell. Fuel casting lines will be connected from the mixer through a port in the bell to a fuel distribution manifold positioned above the case/casting equipment assembly.

The mixer selected for the hybrid fuel is a co-rotating twin screw mixer extruder. One 4.57-m (180-in.) diameter fuel grain contains 138,348 kg (305,000 lb) of hybrid fuel. The motor will be cast in two mating halves,

each containing 169,174 kg (152,500 lb) of fuel. The fuel binder system is a hydroxy-terminated polybutadiene (HTPB) cured with an isocyanate. CSD's experience with the IUS propellant, which employs a similar system, shows that this polymer system must be placed into cure 36 hr after the isocyanate curative is added to the first batch. We therefore plan to cast the 4.57-m (180-in.) hybrid fuel grains within 36 hr on the basis of our IUS data. The required fuel production rate will be: 69,174 kg (152,500/36 = 1922 kg/hr (4300 lb/hr). Allowing for a mixing effectivity of 85%, this rate becomes approximately 2268 kg/hr (5100 lb/hr). Therefore, a 0.127-m (5-in.) diameter continuous mixer/ extruder having a variable throughput capacity of 1588 to 2495 kg/hr (3500 to 5500 lb/hr) has been selected to mix the UTF-29,901 hybrid fuel. Operating on a three-shift basis for five days per week one continuous mixer will produce two fuel grains each week. Therefore, two of these mixers would be required to support a launch rate of one flight per week.

Prior to the start of casting, the casting bell is evacuated to a pressure of 25 mm Hg. Next, the continuous mixer is started and brought up to a steady-state condition. Mixer start-up begins by filling the loss-in-weight feed hoppers with the three major fuel ingredients: HTPB polymer/ antioxidant/carbon black preblend, IPDI, and Escorez 5320. The mixer extruder screws are then started, followed in turn by the loss-in-weight feeders. The quality of the mixed fuel as it exits the mixer will be continuously monitored by on-line analytical instruments. When the mixed fuel output stream meets the specification as indicated by the on-line measurement, the mix operator opens the casting valve sending the fuel stream through the casting line and the distribution manifold into the case/casting equipment assembly.

The start-up of the mixer will be controlled by a process control computer which will employ real time data from the on-line analytical instruments in order to control the ingredient feed rates and the mixer screw speed as the major process variables. Off-specification material produced during start-up will be sent to a scrap hopper through a diverter valve. Loss-in-weightfeed hoppers will be refilled by pumping material from storage tanks located near the mixer gantry. Mixing and casting will continue until the grain is

completed. Fuel quality will be continuously measured and controlled by the closed loop process instrumented and control system. The system will also provide for instrument or control failure by an immediate shut down command which would close the casting valve and open the diverter valve.

After casting operation is finished, the fuel grain will be removed from the vacuum bell and transported to an oven where it will be cured for 5 days at 333°K (140°F). Following the cure, the fuel grain will be taken to a mandrel stripping station for removal of the casting tooling. The top centering plate is unbolted from the fuel grain mandrels and lifted from the grain. Each of the 34 fuel grain port mandrels will be unbolted from the casting base and "popped" loose from its fuel port using a hydraulic cylinder attached to the casting base. After popping each mandrel loose, it will be lifted from the grain with a crane. The final step will consist of lifting the case fuel grain assembly off the casting base and placing it onto a rail transport car.

The grain would then be placed into a storage building and allowed to cool from the cure temperature of 333°K (140°F) to ambient temperature, i.e., 289° to 306°K (60° to 90°F), prior to the X-ray inspection. The grain will be radiographically inspected to assure that it is free from voids and unbonded areas prior to final assembly.

After radiographic acceptance, the grain will be taken to the final assembly station. Final assembly consists of potting both fuel grain stress relief boots, assembly of the forward and aft closures to the appropriate fuel grains and assembly of electrical raceways and other final detailed parts. After assembly, the weight and center of gravity of the fuel grain will be measured using a special fixture. Finally, the shipping rings would be installed and the fuel grain placed on a rail car to be sent to the barge dock. There it is to be transferred onto shipping cradles on the barge using a special purpose crane. Shipping covers will be installed over the fuel grain end and closure boss. Finally, a shipping cover is placed over the fuel

TABLE 4-18. TROWELABLE INSULATION MATERIAL FORMULATION AND PHYSICAL PROPERTIES

T16783

A. Formulation		
Item	**Component**	**wt-%**
1	Trilene	51.0
2	Kevlar pulp	9.2
3	Peroxide curative	5.8
4	Other	34.0
5	EPDM polymer	42.8
6	SBR polymer	2.5
7	Silica filler	6.4
8	Kevlar	8.6
9	Phenolic	21.4
10	Peroxide curing agent	3.2
11	Other	15.1

B. Physical Properties	
Property	**Parallel/ Perpendicular**
Tensile strength, psi (kPa)	212/803
Elongation, %	<10/17
Specific gravity	1.05
Shore A hardness	95

grain to protect it from environmental exposure and shipping damage prior to the shipment to the launch site.

4.8 INSULATION

CSD's proposed hybrid booster insulation approach uses a simplified configuration, space shuttle booster specified derived safety factors, and greatly enhanced producibility to provide a reliable, low cost design.

The selected insulation material is a non-asbestos, EPDM elastomer containing Aramid pulp and fiber. Two different formulations are proposed. A trowelable material is recommended for the forward dome where insulation must be applied around and over the sides of a complex array of oxidizer inlet ports. In the cylindrical sections of the motor and in the aft dome, a windable strip material is recommended. As a backup for all areas of the motor, the windable strip material could be fabricated as calendered sheets and applied by standard hand lay-up and autoclave-cure techniques. The formulation and properties of this material are shown in Table 4-18. The trowelable material offers major improvements in processability, safety, reliability and cost effectiveness in comparison to currently available insulation materials for the forward dome. Previous internally funded CSD efforts have developed

high-performance, non-asbestos insulation materials suitable for conventional fabrication processes such as extrusion, strip winding or hand lay-up. It is proposed here to use a more producible, trowelable mastic insulation material by modifying previously identified non-asbestos insulation formulations, replacing solid EPDM polymer with a liquid EPDM polymer such as Uniroyal Trilene.

Trilene is a low-molecular-weight ethylene propylene terpolymer that can be processed like a liquid. It can be cured by either sulfur or peroxide cure systems. Like its high molecular weight counterparts, this material has good low-temperature properties, high-temperature proper ties, and oxidation resistance. The pounding is simplified because, as a liquid material, it is easier to blend higher quantities of fillers without adding plasticizers. The reduced need for plasticizers is a further advantage because plasticizers tend to migrate and can have adverse effects on insulation-to-propellant bonds.

An on-going CSD-funded laboratory/subscale motor test program has demonstrated the feasibility of the trowelable insulation system. Phase I of this proposed program will apply the CSD database to assess the scale-up issues and develop Phase II and III test plans for this material as a viable candidate for insulating full-size hybrid rocket motors.

As previously mentioned, automated and strip-wound insulation is proposed for the aft dome and cylinders. CSD has demonstrated extrusion and strip winding of non-asbestos, high-performance insulation in previous testing. The formulation and properties of the baseline material, CSD-NA-06, are shown in Figure 4-27.5. This material has specific ablation 23% lower than standard NBR-asbestos material. This material not only has the lowest ablation rate and lowest density among several similar materials tested, but also has better thermal and mechanical properties than the current carbon-filled EPDM used in the aft dome of the current shuttle SRM design. Parallel to the development of advanced, trowelable insulation material and process for use on the hybrid motor forward dome,

further evaluation of the automated strip wind approach will be conducted as a risk reduction back-up position.

4.8.1 Insulation Trade Studies

Insulation trade studies have been performed to select the optimum combination of materials and processes to meet the hybrid motor design objectives. A summary of the key trade studies, selection and rationale is provided in Table 4-19.

4.8.2 Insulation Development/Technology Acquisition

Development of the insulation systems is not critical for the hybrid development program, because alternative materials can be used and it is possible that parallel solid rocket efforts would be performed. If a program were performed, it should follow the outline discussed below. To develop a cost-effective and highly reliable insulation system, the insulation system must meet the following requirements: (1) provide material consistency and stability, (2) have minimal flow characteristics during cure, (3) have maximum ablation performance without increasing costs or decreasing reliability, (4) function as an impermeable membrane, (5) have sufficient elongation to accommodate case deformations during motor operation, and (6) have lot-to-lot consistency. The trowelable and strip windable insulation material will be compared to the standard Kevlar-filled EPDM and standard silica-filled EPDM materials. The initial phase of the program will evaluate five candidate trowelable formulations and at least two strip windable material formulations and compare them to the back-up material. Laboratory testing will be performed to determine those physical, thermal and ablation properties that will be needed to down-select to one trowable and one strip windable material. It is recommended that phase II consist of a complete materials characterization of the selected formulation.

A minimum of two lots of each material from a minimum of two vendors should be evaluated. Physical properties, thermal properties, cure characteristics and material composition will be evaluated. This information will

TABLE 4-19. INSULATION MATERIAL AND PROCESS TRADE STUDY

T16785

Material	Selection	Rationale
Trowelable Kevlar-filled EPDM	Baseline: forward dome	• High performance - Better ablation than asbestos-filled NBR - Good thermal and mechanical properties • Improved processing
Strip windable Standard Kevlar-filled EPDM	Baseline: cylinder aft dome	• High performance - Better ablation than asbestos-filled NBR - Good thermal and mechanical processing
Silica-filled EPDM		• Large database - Ablation rate greater than Kevlar- and asbestos-filled materials
Filament-wound Kevlar insulation		• Material stiffness is too high • Bond difficulties • Improved ablation over silica-filled material
Processing	**Selection**	**Rationale**
Automated troweling	Baseline: forward dome	• Improved reliability • Cost-effective • Homogeneous insulator • Improved insulation-to-insulation boundaries • Net final contour
Strip-winding	Baseline: cylinder aft dome	• Improved reliability • Cost-effective • Integrity dependent on knitting of strips during application • Final contour may need machining
Hand lay-up	Backup	• Proven reliability • Proven producability and performance
Filament-wound insulation		• Processing not as cost-effective as troweling or strip winding
Spray application		• Difficult to achieve specified thickness/contour with filled material • High potential for voids

be used to select the insulation material, and aid in selecting an optimum process and insulator design.

In the phase III motor demonstration part of the program it is recommended that at least three 1/3 scale motors with insulation from at least two lots of material be tested before going into a full-scale motor test.

4.9 CONTROL SYSTEMS

By combining features of both liquid and solid propellant rocket engines, the Hybrid Rocket Motor (HRM) provides an alternative propulsion source for earth-to-orbit transportation that is much more controllable than convention solid rocket boosters (SRBs). Coordination of the oxidizer delivery, thrust vector control, and thrust chamber systems in the HRM will be required to thoroughly exploit the benefits of HRM controllability. This section provides a description of some of the control system design issues which are particular to HRM control.

4.9.1 Background

An assessment of HRM control system design issues and techniques was performed for the two motor sizes being considered in this report; a large HRM duplicating the ASRM vacuum thrust-time profile and a smaller HRM with 1/4 the ASRM thrust level. HRM control system concepts and design issues have been identified and specific recommendations have been made where applicable. However, many of the HRM control system issues can only be answered after more detailed information is made available on mission requirements and HRM component models.

The HRM control system will be responsible for a number of actions, including motor start-up, shutdown, propellant tank pressurization, and safety monitoring and maintenance. The development of logic to support these specific HRM control functions is very hardware dependent and is thus not the focus of this preliminary assessment of HRM control concepts. The main focus in this report are concept formulations and design issues associated with the

development of logic which controls the magnitude and direction of the HRM produced thrust.

Control concepts and issues were examined for various combinations of HRM system component configurations. Both pump-fed and pressure-fed oxidizer delivery systems were considered in the analyses. In addition, two concepts for TVC are considered: a gimbaled nozzle and liquid injection.

The result of this section describes the HRM control system concepts and design issues. Control of the HRM has some unique features which will be elaborated on in the following subsections, such as

- Multiple pumping systems must be coordinated to achieve the global system oxidizer delivery requirements for pump-fed systems
- Health maintenance logic must be developed for oxidizer delivery pumps which provides an indication when a single pump shutdown is advisable
- Control logic must be developed for pump-fed systems to facilitate a smooth transition from nominal operation to a single pump-out condition while maintaining engine thrust
- Liquid injection TVC must be coordinated with the thrust chamber pressure control logic on systems utilizing LOX from the oxidizer delivery system for TVC injectant
- The feedback control of HRM chamber pressure requires a feedback loop to be closed around the thrust chamber dynamics, a non-stationary process.

These are some of the issues which will be discussed in the following subsections which describe the oxidizer delivery systems, the HRM control system architecture, control logic for nominal operation, and control logic for fault tolerance.

4.9.2 Oxidizer Feed System Configurations

The thrust of the HRM is controlled by modulating the flow rate of oxidizer into the thrust chamber. Two different high-pressure delivery systems are currently being considered. In the first option, the liquid oxygen (LOX) supply tank is maintained at a moderate pressure of about 0.41 MPa (60 psia) and a pump (or series of pumps) is utilized to deliver the required oxidizer flow to the 6.89+ MPa (1000+ psia) thrust chamber. A second alternative oxidizer delivery system is a pressure-fed system where the LOX supply tank is pressurized to a sufficient level, approximately 9.31 MPa (1350 psia), to push the LOX flow into the hybrid combustion chamber.

4.9.2.1 Pump-Fed Flow Schematic

Figure 4-29 shows a flow schematic of a pump-fed oxidizer delivery system which would be representative of those proposed for the HRM application. Fuel, such as propane, is mixed with a portion of LOX and combusted in the preburner to drive the turbo-pump which pumps LOX into the HRM thrust chamber. Design variables which are currently being examined are the number of pumps required, the oxidizer-fuel ratio in the preburner, and the porting of the turbine discharge.

Control of the pump-fed oxidizer delivery system will be initiated through the coordination of multiple flow control valves. Oxidizer is controlled with the following valves:

- Oxidizer supply (OSP) valve
- Oxidizer injection (OIJ) valve
- Oxidizer pressurization (OPR) valve
- "n" oxidizer TVC injector (TVC) valves.

The OSP valve will open prior to ignition to allow some LOX flow to chill the entire LOX pump system up to the preburner LOX injector. The OIJ and TVC valves will be used to control the LOX requirements to the injector and the TVC injection system. The OPR is used to modulate the amount of GOX flow returned to the LOX tank for repressurization. A predefined schedule of LOX

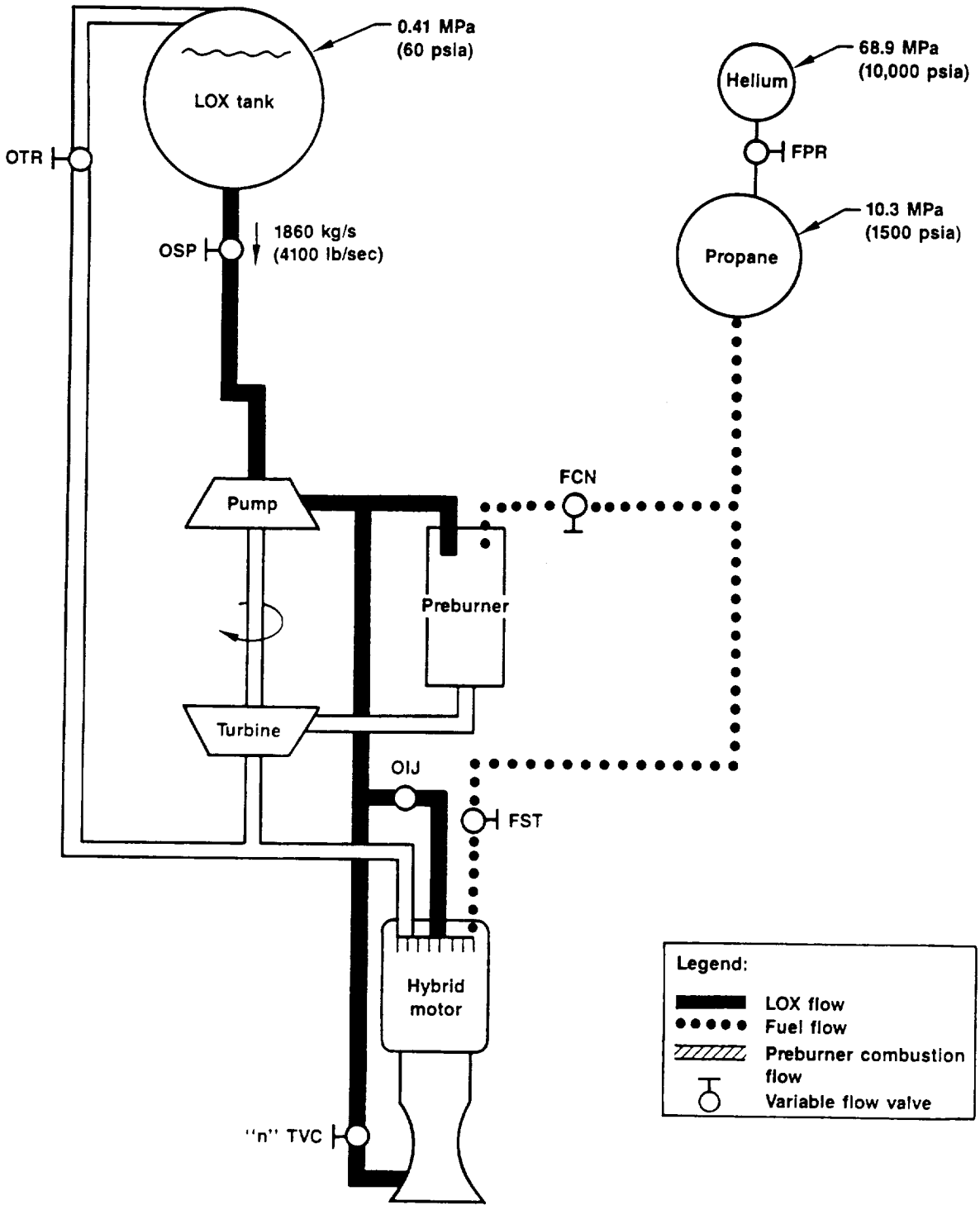

Figure 4-29. Pump-Fed Oxidizer Delivery System

50471

tank pressure, ranging from 0.41 MP (60 psia) at ignition to 0.21 MPa (30 psia) at shutdown, will be maintained. This LOX tank pressure regulation ensures that the LOX pump will not cavitate and that a minimum amount of GOX will be left as residual weight upon shutdown.

The on-board fuel supply is controlled with the following valves:

- Fuel start (FST) valve
- Fuel control (FCN) valve
- Fuel pressurization (FPR) valve.

The FST valve operates to supply fuel to the HRM during engine start up and ignition. The FCN valve controls of O/F ratio in the preburner, which will be utilized to control the amount of oxidizer injectant into the thrust chamber. This valve position will be modulated to control the HRM chamber pressure. The FPR is used to modulate the amount of pressurant (eg, helium) flow into the fuel tank to control its pressure.

The number of turbo-pumps per motor is a function of the required oxidizer flow rated and system reliability. The LOX requirements for the small HRM (approximately 934 kg/sec (2060 lb/sec)) can be handled with a single or multiple pump configurations while the large HRM, requiring LOX flow rates over 3629 kg/sec (8000 lb/sec), will utilize a multiple pump system, such as three pumps with a 50% margin in each pump to allow for a single pump-out capability.

4.9.2.2 Pressure-Fed Flow Schematic

The basic concept for a pressure-fed oxidizer delivery system is that the LOX tank is pressurized to a sufficient level where adequate oxidizer flow rates can be achieved by modulating control valves. Figure 4-30 shows a flow schematic of a system which would be representative of proposed pressure-fed delivery systems. This method of oxidizer delivery requires less components than the pressure-fed system, but it carries a large weight penalty due to the structural requirements on the LOX tank.

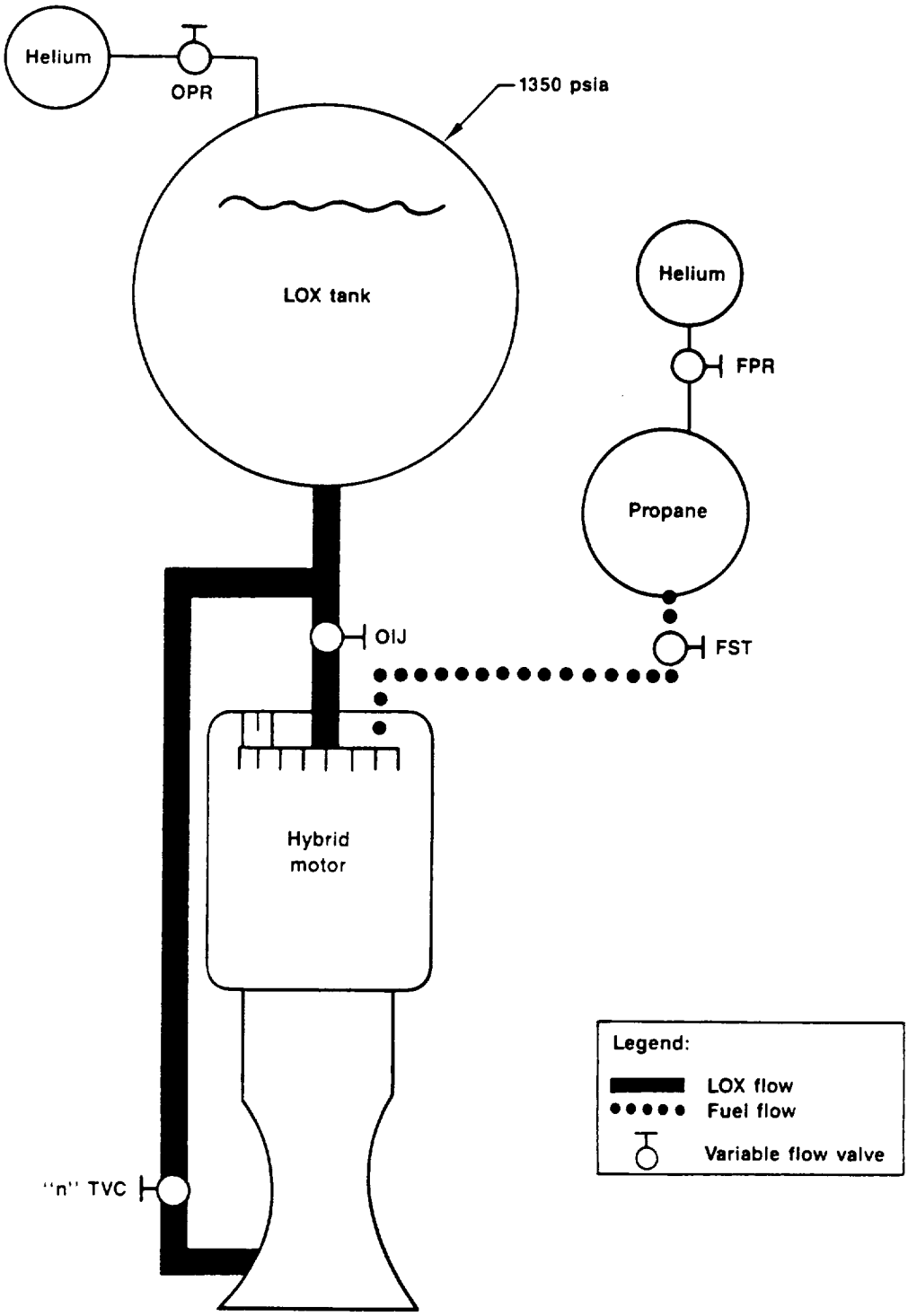

Figure 4-30. Pressure-Fed Oxidizer Delivery System

50472

The flow of LOX from the pressurized LOX tank to the HRM thrust chamber is controlled the OIJ valve. As with the pump-fed system, regulation of the LOX tank pressure is required which can be accomplished by using either a high pressure gas reservoir (as shown in Figure 4-29) or a separate turbopump system. One advantage of the pressure-fed system is that the flow of LOX can be rapidly modulated by adjusting the OIJ valve position. LOX flow changes in a pump-fed system require the creation of additional input energy (from pre-burner combustion) to alter the speed of the turbopumps.

The LOX flow rate and LOX tank pressure are related quantities, thus there could be adverse interactions between any control loops which attempt to regulate each of these separate parameters. However, it is envisioned that these control loops can be adequately separated in frequency range (high bandwidth flow control via the OIJ valve, low bandwidth LOX tank pressure control via the OPR valve) to ensure proper coordination.

4.9.3 System Control

4.9.3.1 Control System Architecture

The HRM control system regulates engine thrust magnitude and direction, and ensures safe and reliable engine operation. This subsection will focus on the design of control logic to control the HRM engine thrust during main-stage operation under nominal conditions, when all components in the system are functioning normally.

The configuration of this HRM control system will vary depending on the methods used to inject oxidizer and to provide TVC. Figure 4-31 shows a general block of the HRM control system when gimbaled nozzle TVC is utilized. In this configuration each HRM receives a thrust command, in the form of a requested thrust chamber pressure (Pcr), and gimbal angle commands from the core vehicle. For this configuration the chamber pressure and thrust vector are controlled with separate and non-interacting control loops.

Chamber pressure is controlled using a feedback controller which modulates the appropriate control valves in the oxidizer delivery system. For the

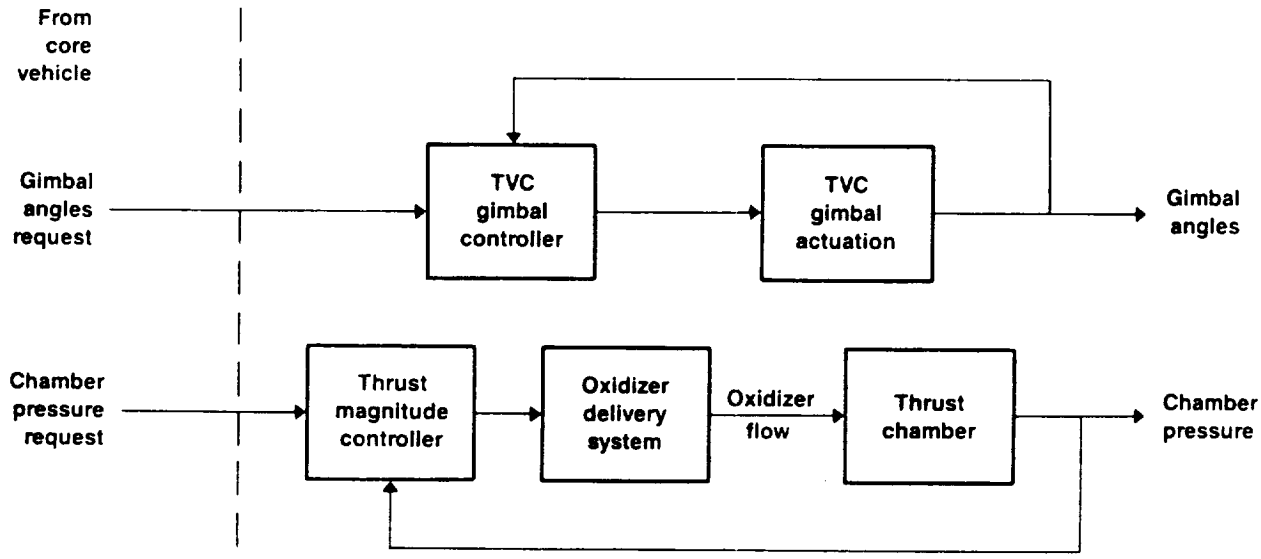

Figure 4-31. HRM Control System: Gimbaled Nozzle TVC

50473

pump-fed system this could be the FCN valve, which regulates the O/F ratio in the preburner. For the pressure-fed system this would be the OIJ valve, which meters the flow from the LOX tank into the injector. The direction of the thrust vector is controlled by closing a position feedback loop on the angular position of the gimbaled nozzle.

Figure 4-32 shows the HRM control system applicable with LOX injection TVC. For this configuration, the core vehicle commands are the chamber pressure and the desired mass flow rate for each of the four nozzle quadrants. The TVC injection controller adjusts the TVC nozzle injection valve positions. It is envisioned that a 16-valve configuration will be utilized (4 valves per quadrant). The total TVC LOX flow rate must be tapped off the oxidizer injection system. For this configuraiton there are now interactions between the two control functions. A level of coordination can be achieved by cross-strapping information between the separate loops.

The selection of the appropriate type of control logic for the various regulated HRM quantities must be based on an analysis of the associated system dynamics, process models and performance requirements. Some common control algorithm design issues include stability robustness, process and dynamic

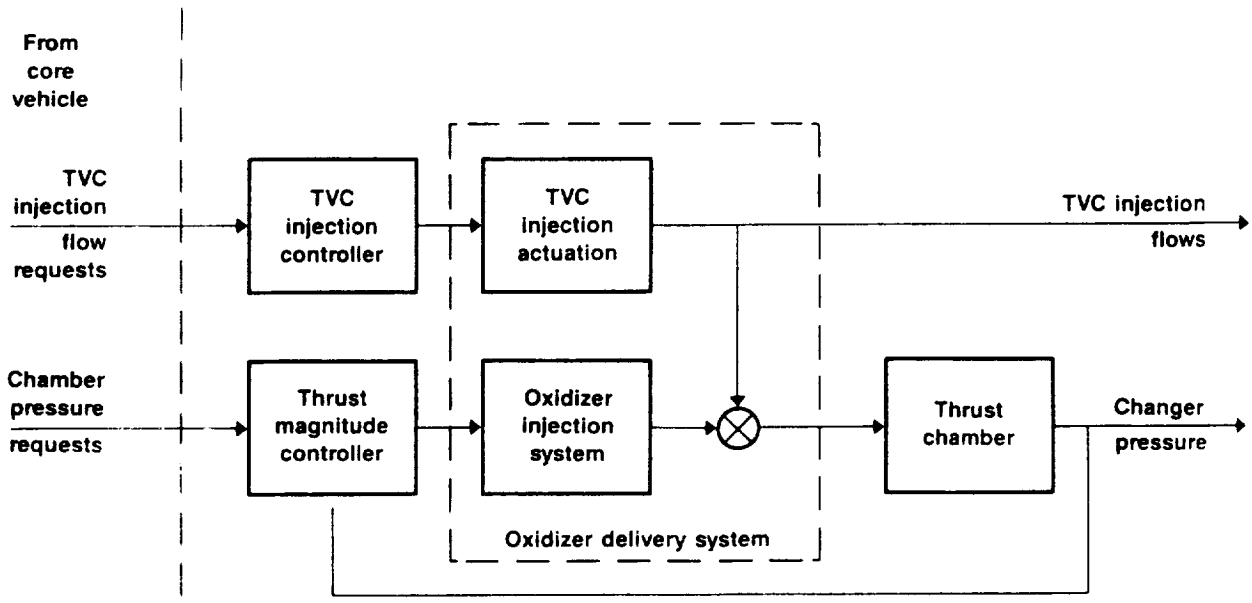

Figure 4-32. HRM Control System: LOX Injectant TVC

50474

system modeling, sensor and actuator characteristics, command response requirements, system disturbance characterization, and reliability requirements.

4.9.3.2 Thrust Chamber Response

One unique feature of the HRM control system is the time-varying dynamics of the thrust dhamber. Characterization of this non-stationary process is important in the assessment of HRM thrust magnitude control concepts. As shown in Figures 4-30 and -31, the input to the thrust chamber is the oxidizer flow rate, Wo. The output of interest is the thrust chamber pressure, Pc. The relationship between these two parameters during the entire burn time can be estimated using some simplifying assumptions.

An analytical expression can be obtained for the thrust chamber static sensitivity, dPc/dWo. The chamber pressure can be related to the oxidizer and fuel mass flow rates as

$$Pc = (C/At^*g)\ (Wf + Wo) \qquad (1)$$

where

c* = Characteristic exhaust velocity
At = Nozzle throat area m2 (in.^{2})
g = gravitational constant 9.8 m/sec2 (386 in./s^2)
Wo = oxidizer mass flow rate kg/s (lb/s)
Wf = fuel mass flow rate kg/sec (lb/s)

The mass flow of the fuel can be approximated by

$$Wf = \rho * As * r \tag{2}$$

where

ρ_f = density of fuel, kg/m3 (lb/in.^{3})
As = grain port surface area, m2 (in.^{2})
r = grain regression rate, m/sec (in./sec)

Experimental correlations have established that the fuel regression rate can be represented in the form

$$\dot{r} = a * (Wo/Ap)^n \tag{3}$$

where

Ap = grain port cross-sectional area, m2 (in.^{2})
a,n = empirical constants

Substituting equations (2) and (3) into equation (1) and differentiating with respect to the oxidizer flow, one can obtain an expression for the static sensitivity for the thrust chamber as

$$dPc/dWo = K1 * (1 + K2 * Wo)^{n-1} \tag{4}$$

where

$$K1 = C/At^*g$$

and

$$K2 = \rho_f{}^*a^*n^*As/(Ap^n)$$

The thrust chamber sensitivity from equation (4) was evaluated for the large 4.57-m (180-in.) diameter booster using the all-hydrocarbon inert fuel No. 7. Figure 4-33 is a plot of this calculated sensitivity. It can be seen that this sensitivity is approximately constant (less than 1% variation)

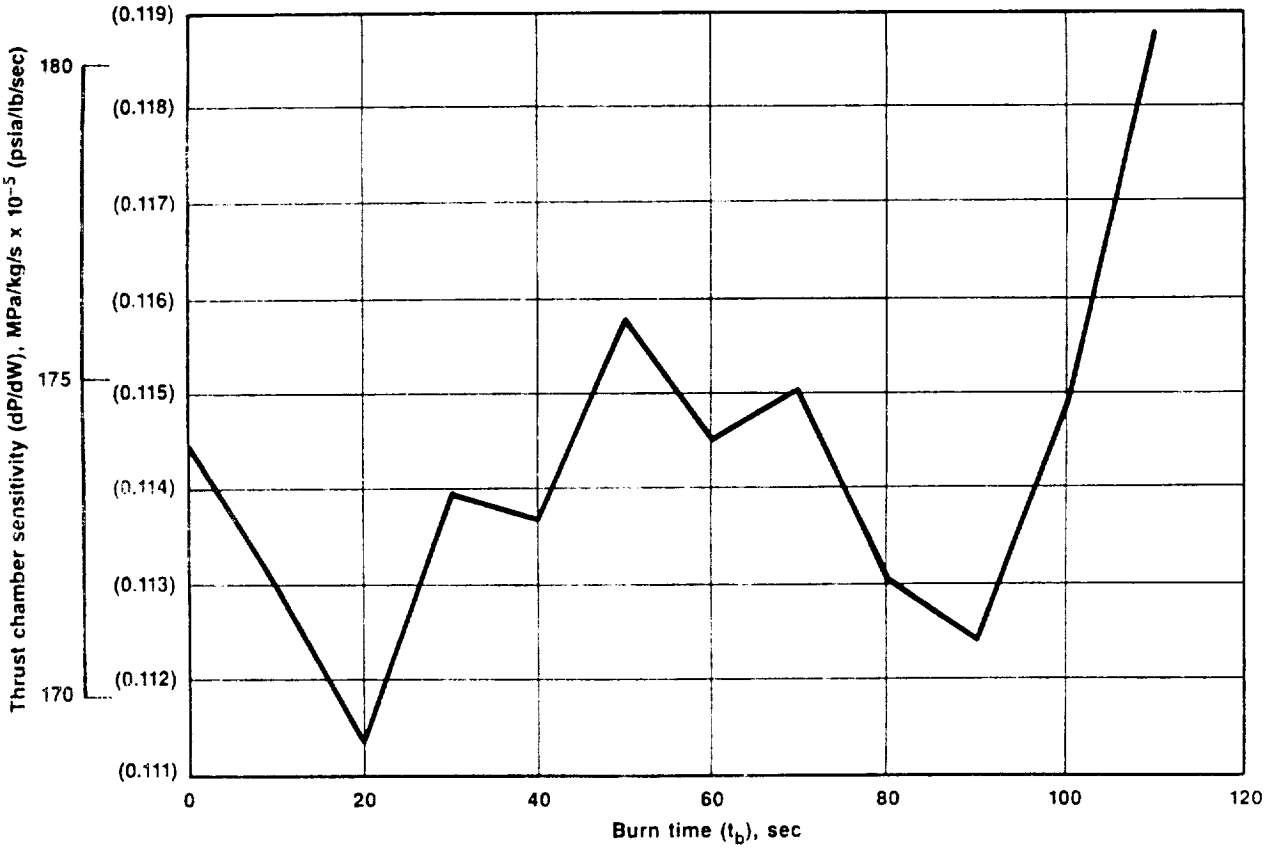

Figure 4-33. Thrust Chamber Sensitivity vs Burn Time

50475

during the entire burn time. Thus, even though the fuel regression rate, grain port volumes, and areas vary during the controlled process, the effective "gain" for this component block in the chamber pressure control system is constant.

The dynamics of the thrust chamber system can be approximated by assessing the magnitude of the transport delay associated the thrust chamber volume. This time constant, td in seconds, can be estimated as

$$td = \rho_g * Ap * Lg/(Wo+Wf) \qquad (5)$$

where

ρ_g = effective density of exhaust gas, kg/m3 (lb/in.$^{3)}$
Lg = length of grain, m (in.)

Figure 4-34 is a plot of the thrust chamber time constant for the large thrust booster. It can be seen that the approximated thrust chamber dynamics are of the order of a few tenths of a second. Also of note is that this response time increases by a factor of 2 during the burn time.

4.9.3.3 Thrust Magnitude Control

A feedback control which regulates chamber pressure by modulating oxidizer flow is proposed as the method of HRM thrust magnitude control. This is preferable to an open-loop control of oxidizer flow into the thrust chamber because of the inherent disturbance rejection and sensitivity reduction attributes of feedback.

As a baseline system, the control logic design for the thrust magnitude controller could be developed using single-input, single-output (SISO) design techniques. The modulate parameter value would be a valve position request in the oxidizer supply system (the OIJ valve position for the pressure-fed system, or the FCN valve positions on pump-fed systems).

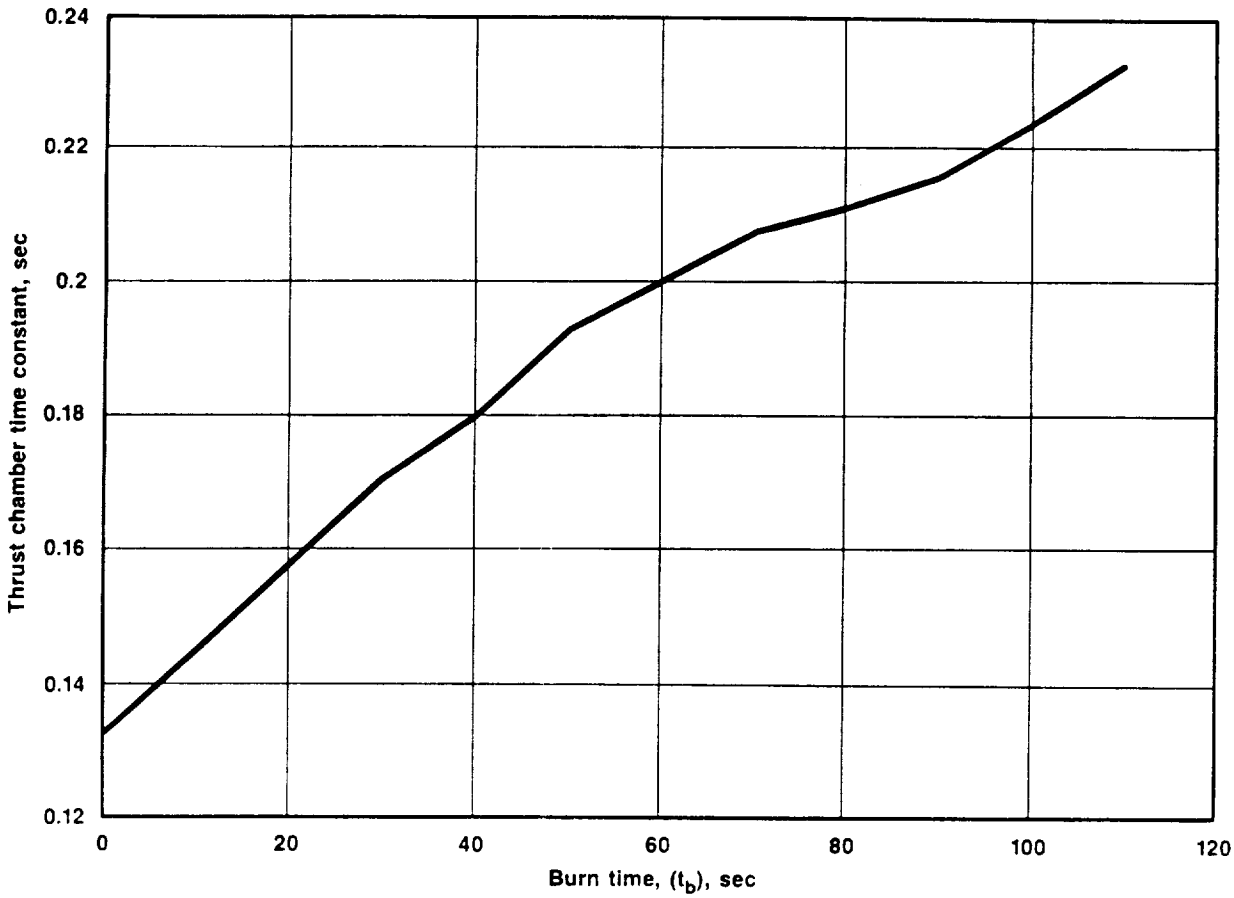

Figure 4-34. Thrust Chamber Constant vs Burn Time

50476

The design of the feedback logic will be based on considerations of the desired response characteristics of the closed-loop system and the dynamics of the oxidizer delivery system and thrust chamber. The standard design approach would be to develop dynamic models for the system components. Next, linear design models and transfer functions would be generated. Control logic would be developed at a series of operating points. The last step would be to simulate the performance of the closed-loop system.

The thrust chamber response characteristics vary during the burn time. Thus, gain schedules could be utilized to ensure consistent stability of the chamber pressure feedback system throughout the entire engine burn time. These gain schedules could be pre-computed parameter values as a function of time-of-flight or the integral of the measured chamber pressure. It is

anticipated that the control logic itself employ integrating action such that under nominal steady-state conditions, the chamber pressure is held to within the accuracy of the pressure sensors.

4.9.3.4 Thrust Vector Control

In addition to modulating the overall thrust magnitude of the hybrid motor, the HRM control system must also provide a mechanism for controlling the orientation of the thrust vector. Two methods have been considered for this system: (1) a gimbaled nozzle, and (2) a fixed nozzle with liquid injection thrust vector control (LITVC). This subsection will concentrate of the LITVC system, which will require more complex control logic than a gimbaled nozzle position servo-system. A conventional control approach would be used for a gimbaled nozzle.

For LITVC, the thrust vector is controlled by modulating the amount of injectant in each of four quadrants at the nozzle. Preliminary LITVC design studies have selected a 16-valve system (4 quadrants with 4 valves per quadrant). The commands to the TVC system from the core vehicle will be a mass-flow rate requirement for the injectant per quadrant.

$$TVC_{rq} = [\ Wi1,\ Wi2,\ Wi3,\ Wi4,\ lb/sec\ ] \qquad (6)$$

Preliminary system designs have been proposed which assume that LOX, supplied from the oxidizer delivery system, will be used as the TVC injectant. The settings of the LITVC valves will be determined based on the operational characteristics of the oxidizer delivery system. For the pressure-fed oxidizer system, the TVC valve positions can be determined from the TVC injectant request and the LOX tank pressure. For the pump-fed system, the calculation of TVC valve positions requires estimation of the LOX flow rate out of the pump and the relative flow resistant into the thrust chamber. In either case the TVC flow will be controlled with open-loop calibrations.

As shown earlier in Figure 4-32, the utilization of LOX for LITVC creates an interaction between the two major control loops in the HRM. The feasibility

of such a configuration will be dependent on the amount of TVC required. Preliminary analyses, based on a SRB TVC requirements analysis, indicate that a 6-deg adjustment in the thrust vector could be required which would result in a LOX flow request of 680 kg/sec (1500 lb/sec). For the large booster application this LOX flow diversion could result in a momentary loss of over 15% of the axial thrust in a pump-fed engine. A pressure-fed oxidizer delivery system would be better suited to handle the simultaneous chamber pressure and TVC LOX flow requirements, as no new energy must be created within the system. The LOX flow requests would be accommodated by metering the sets of LOX supply valves, not by adjusting the speed of turbo-pumps.

The adverse interactions between the LITVC and Pc controllers could be mitigated to a certain extent by cross-feeding information. A feedforward command could be added to the desired chamber pressure request based on the TVC LOX flow requirement and the thrust chamber sensitivity. For example, given the thrust chamber sensitivity, dPc/dWo, one can add a delta correction factor, delPc, to the chamber pressure request as

$$delPc(t) = (dPc/dWo)*(Wi1+Wi2+Wi3+Wi4) \qquad (7)$$

which would reduce the effect of LITVC interaction with pump-fed thrust chamber controller. An alternate control algorithm design approach would be to develop multivariable control (MVC) logic which would control both chamber pressure and LOX TVC flows through simultaneous and coordinated modulation of all control valves. In any case, a design issue that must be addressed for pump-fed LOX TVC systems is the reliability and maintanance issues associated with the imposed TVC duty cycle on the turbo-pumps.

The optimal configuration for the TVC system for the HRM can only be determined by analyzing the magnitude and frequency spectrum of distrubances which must be mitigated by TVC. Preliminary analyses has been conducted using TVC requirements from solid rocket motor systems. A vehicle powered by a set of HRMs also has the capability of generating thrust moments by modulating the

thrust output from each individual HRM. This capability has not yet been evaluated for the HRMs.

4.9.3.5 Multi-Pump Coordination

To achieve the flow requirements for the large pump-fed HRM booster, a multiple pump arrangement has been proposed. Coordination of these pumps will be required to meet the performance and reliability requirements for the HRM system.

Each pumping system supplies oxidizer to the thrust chamber for thrust control and GOX to the LOX tank to regulate its pressure, PLOX. (LOX injectant TVC would also be a required pump system output and would be handled in a similar manner to the coordination described here.) The Pc and PLOX feedback loops can probably be designed with minimal adverse interaction by providing adequate separation of their closed-loop bandwidths. The PLOX loop would only required to be low bandwidth and could be isolated from the high bandwidth Pc loop.

The overall controlled system is rank 2 in command inputs and measured outputs. However, internal to the controlled system there are six effective controlled quantities. Thus, there is the capability to control additional internal states in the pumping system. One control solution would be to simply generate the same command signals (eg., the FCN and OPR valve position requests) to each pump package. This approach will meet the global requirements for Pc and PLOX control. If all the pumps respond the same to these requests then the individual pump states (rotor speeds, pressure, temperatures and oxidizer flow rates) will be identical and will therefore be indirectly controlled. If there are significant pump-to-pump performance variations, then it would be possible to utilize the additional internal degrees-of-freedom in the multiple-pump system to control individual pump states. However, with the 50% flow margin design for each pump, it is likely that this simple control concept will be suitable.

4.9.4 Fault Tolerant Control Actions

The HRM control system must not only meet performance requirements under nominal conditions, it must also ensure system reliability in the face of component failures. This will be accomplished by utilizing fault tolerant control logic coupled with hardware redundancy.

The next subsections will consider the control system issues associated with sensor, actuator, and pump failure detection, isolation, and accommodation.

4.9.4.1 Sensor Failures

There will be a number of sensors which will be utilized by the HRM control system. Some would be appropriately classified as diagnostic sensors, such as rotor shaft speeds, vibration pickups, and thermocouples. These would be used to infer the general health of various HRM components. Another set of sensors would be used to directly alter control valve settings during normal operation. Failure of either type of sensor could results in a rapid degradation of system performance if appropriate measures are not taken.

Of main concern here would be the effect of failure of the thrust chamber pressure sensor which is used to regulate HRM thrust. The first level of fault tolerance would be hardware redundancy. For example, dual or triple redundant chamber pressure sensors could be used. Simple voting logic could be used to determine if any one of the sensor readings is in error. For the dual redundant case the two signals could be compared to each other. If there was a sufficient difference, then a synthesized value of chamber pressure could be derived (from the static sensitivity of the thrust chamber and a synthesized value for the oxidizer injection flow rate) and used as a referee to decide which sensor had failed. The level of hardware redundancy is a design detail that can be addressed by examining the reliability requirements and reliability data for the candidate pressure sensors.

In the event of the complete loss of all chamber pressure sensors, a back up mode of open-loop oxidizer flow control will be initiated. As shown

earlier, for the large boost HRM the thrust chamber sensitivity can be closely approximated as a constant. This means that an oxidizer flow rate request can be derived which corresponds to that required to maintain the core vehicle requested chamber pressure. A schedule of the control valve settings (either OIJ valve position for pressure-fed systems or FCN valve position for pump-fed systems) can then be derived based solely on the oxidizer delivery system characteristics. For the case where the thrust chamber sensitivity varied significantly during the burn time, these valve schedules would have to include an additional parameter, such as burn time, in the open-loop look-up tables.

4.9.4.2 Actuator/Valve Failures

The main control valves for the HRM will be dual redundant to allow fail-operational behavior. These valves have essentially dual redundant commands. The loss of one command signal does not significantly alter the performance of the valve. The second failure response would be to lock the valve in a fixed position.

Complete failure of a dual-redundant control valve could be tolerated in a multiple-pump system. The locked up pump would still provide flow and the remaining pumps would still provide feedback control of the thrust chamber pressure. However, complete control-valve failure could probably not be accommodated or permitted on a pressure-fed system. A fail-fixed condition of the OIJ would result in a fixed oxidizer injector line resistance. It would be doubtful whether the oxidizer flow could be controlled to any desirable bandwidth by modulating the LOX tank pressure. Thus, it will probably be a requirement that the likelihood of a complete OIJ valve failure in an pressure-fed system be extremely small.

A backup mode would probably also be required on all control valves to allow for safe engine shutdown in the event of loss of conventional valve control power (either hydraulic or electric). A separate pressurization system could be utilized which could close the appropriate valves in this condition.

4.9.4.3 Pump Failures

The multiple pump configuration proposed for the pump-fed large booster application will have the capability for pump-out operation. In its present form, a three pump system is proposed with each pump having a 50% flow margin. The HRM control system for such a system must thus be able to: (1) detect the presence of a failed or failing pump and (2) provide a safe pump shutdown and a smooth transition to a pump-out operating condition.

A series of diagnostic sensors will be utilized to assess the current condition of each pumping system. Rotor speed, preburner pressure, turbine inlet temperature, and pump vibration (from accelerometers) will be measured. Safe operational ranges will be established for each of these diagnostic sensors. Operation outside of these "redlines" will indicate unsafe pump conditions which will lead to pump shutdown.

The isolation of a failed pump can be accomplished by incorporating three additional valves per pump. A turbine discharge valve would be engaged to divert the flow overboard. At the same time, an oxidizer shutoff valve would seal the inlet to the pump system and a purge valve would be opened to purge the system with pressurized gas, such as helium. The control signals to each pump would then be increased by 50% to allow for continued operation. It might be necessary to deactivate integral terms in the thrust chamber control logic during this transition period to prevent excessive integral windup. A pump-out condition for any engine would be communicated to the core vehcile. If the vehicle was designed with an engine-out capability, then diagnostics would remain operational on the remaining running pumps on the pump-out HRM.

4.9.5 Technology Development Plan

The development of specific control logic for the HRM depends on detailed information on dynamic models of the system components, controlled system performance and reliability requirements, and specifications of sensor and actuator properties. Some of the these areas which are considered most important for HRM control system design are discussed below.

The response of the thrust chamber to variations in oxidizer injection flow rates needs to be further quantified. The preliminary analysis conducted in this report indicates that the thrust chamber static sensitivity is constant during the burn time for the large thrust booster application and that the characteristic time constant is on the order of a fraction of a second. Formulating this dynamic relationship using more precise models will illustrate the feasibility of the control concepts discussed in this report.

A second control system issue relates to multiple pump-fed oxidizer delivery system. In order to ensure safe operation it will be necessary to diagnose pump failures. A redline safety monitoring system has been proposed. The details of such a system, based on a pump failure mode and effects analysis (FMEA), will be required to develop a diagnostic sensor suite and algorithms. In addition, the pump shut-off sequence and transition logic for the pump-out operation is required.

The last major control issue which must be addressed is the TVC requirements for the vehicle. In all probability the assumed levels used in this report, based on solid rocket motor experience, are over-specified. A realistic specification of this requirement is especially critical in the development of control logic and coordinating actions between the LOX injectant TVC system and a pump-fed oxidizer delivery chamber pressure controller.

5.0 SYSTEM SELECTION

The final design and selection studies were based on considerations of reliability, safety, cost performance and "other" factors. These selection studies were performed for the oxidizer feed system and the TVC system, and for recoverability.

5.1 RELIABILITY AND SAFETY

While the SOW lists safety and reliability together, CSD believes these are two separate issues that must be addressed individually. This is particularly true if oxidized fuels are considered in any trades.

5.1.1 Reliability

The reliability evaluation of the different hybrid technology concepts are somewhat restricted due to a lack of reliability data for the specific hybrid booster components. The final CSD reliability approach for this study was to configure system level reliability trade-offs and qualitatively rank the systems. The system exhibiting the highest total score for reliability, safety, life-cycle-cost, performance and other factors, such as program risk, was then selected as the baseline concepts.

In the initial subcomponent trades for the preliminary concepts designs, fault tree analyses (FTA) were performed on selected subsystem technologies to identify major failure modes on a generic design basis. On a comparative subsystem basis, higher reliability is assumed for a subsystem with the lesser number of failure modes. The reliability rating was then calculated by deducting the number of failure modes from 100 and normalizing it to one by dividing it by the highest number of failure modes. The reliability rating was then obtained by multiplying the normalized value by the weighting factor.

5.1.1.1 Fault Tree Analysis

The case, igniter, and nozzle/TVC design configurations were evaluated by use of the fault tree analysis method. This methodology was chosen as a functional approach to reliability analysis due to the lack of detailed designs.

The fault trees were created to review failure combinations of generic designs down to the second level of indenture.

The subsystem evaluations were loaded chamber, monolithic vs segmented; igniter, a single redundant igniter system versus multiple cavities, with a redundant igniter or multiple igniters; and thrust vector control, fixed nozzle with injection and flexseal nozzle with electromechanical or electro-hydraulic actuation system.

Each design configuration, except for the igniter systems, was evaluated as follows:

- Count the number of failure modes associated with the appropriate FTA
- A = 100 - number of failure modes
- Normalize all values of A by dividing by the highest value of A to obtain a fractional rating
- Multiply the normalized values obtained by the weighting factor assigned to reliability.

Loaded Chamber. The monolithic and segmented chamber fault trees are shown in Figures 5-1 and -2. The monolithic chamber design produces fewer failure modes than the segmented design. The segmented design produces n times three plus (n-1) times two additional failure modes, where n is the number of segments. From a qualitative viewpoint, the monolithic chamber is the more reliable of the two alternatives.

Ignition System. Figures 5-3 and 5-4 depict the FTA for a single set of redundant igniters or multiple ports, with either single or redundant igniters. A direct comparison of the difference in the number of failure modes is complex, due to the redundant configurations. A qualitative evaluation was made to evaluate relative reliability.

FOLDOUT FRAME 1

FOLDOUT FRAME 2

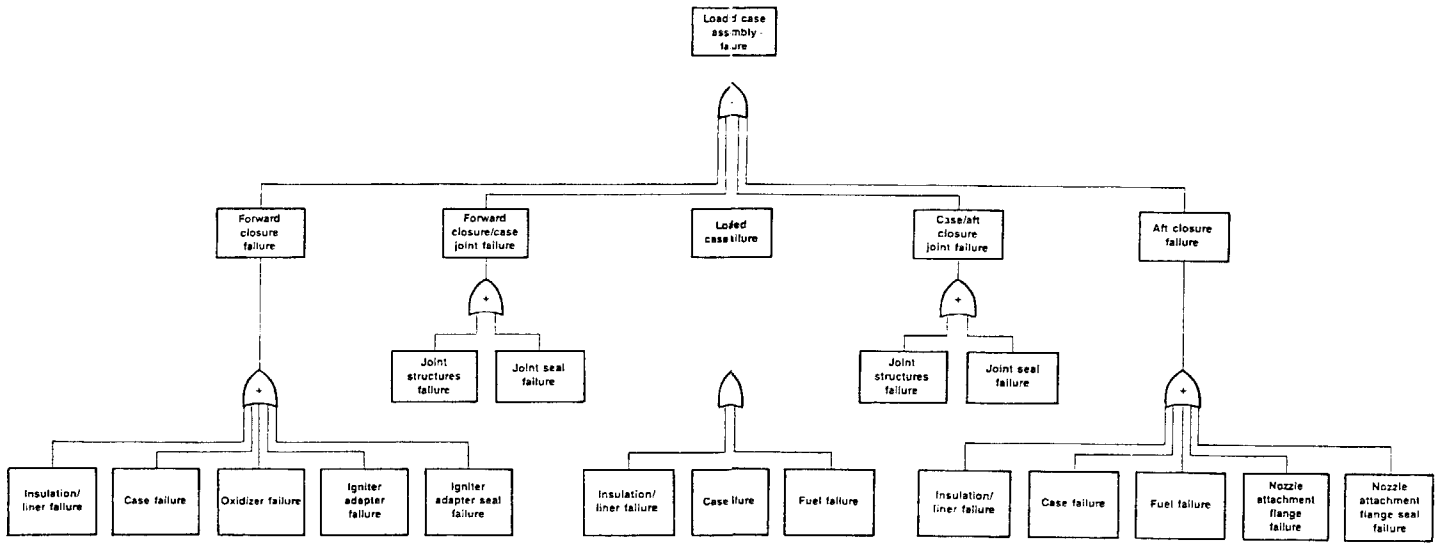

Figure 5-1. Monolithic Case Fault Tree

50300

FOLDOUT FRAME 1

FOLDOUT FRAME 2

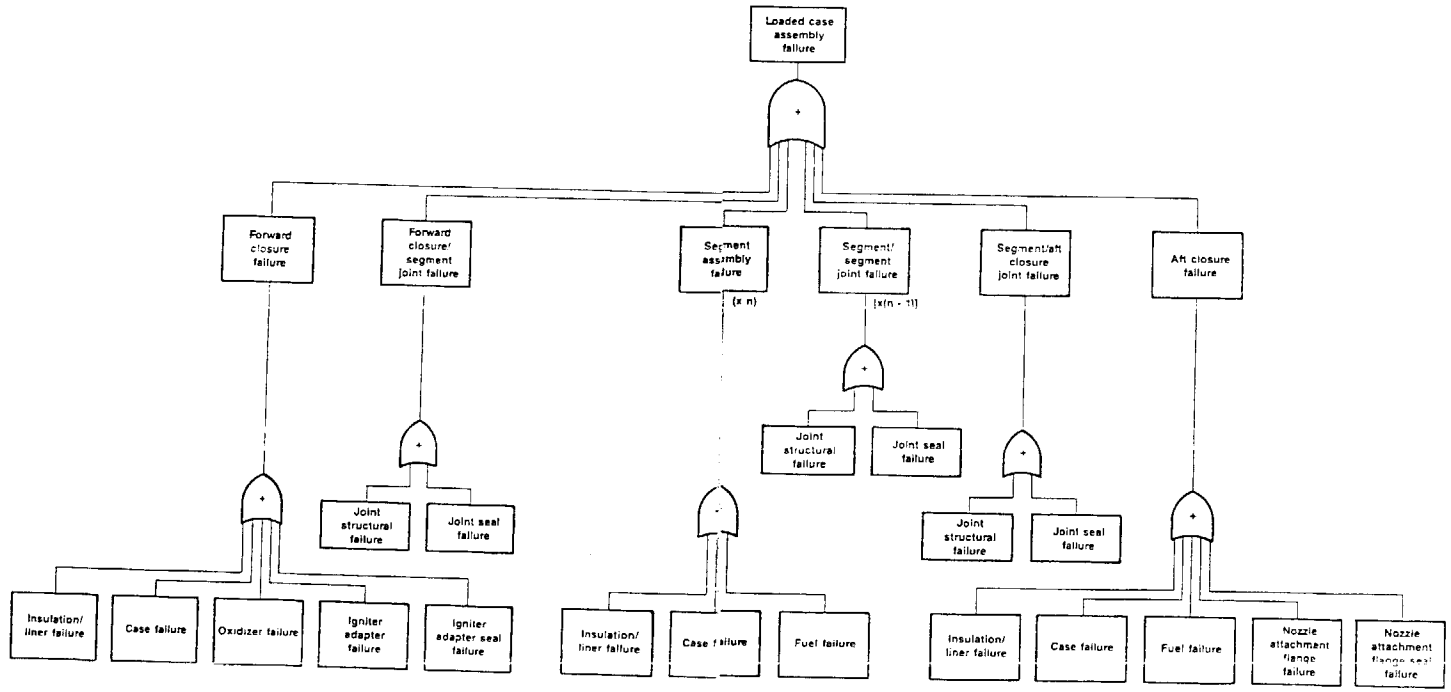

Figure 5-2. Segmented Case Fault Tree

50299

FOLDOUT FRAME 1

FOLDOUT FRAME 2

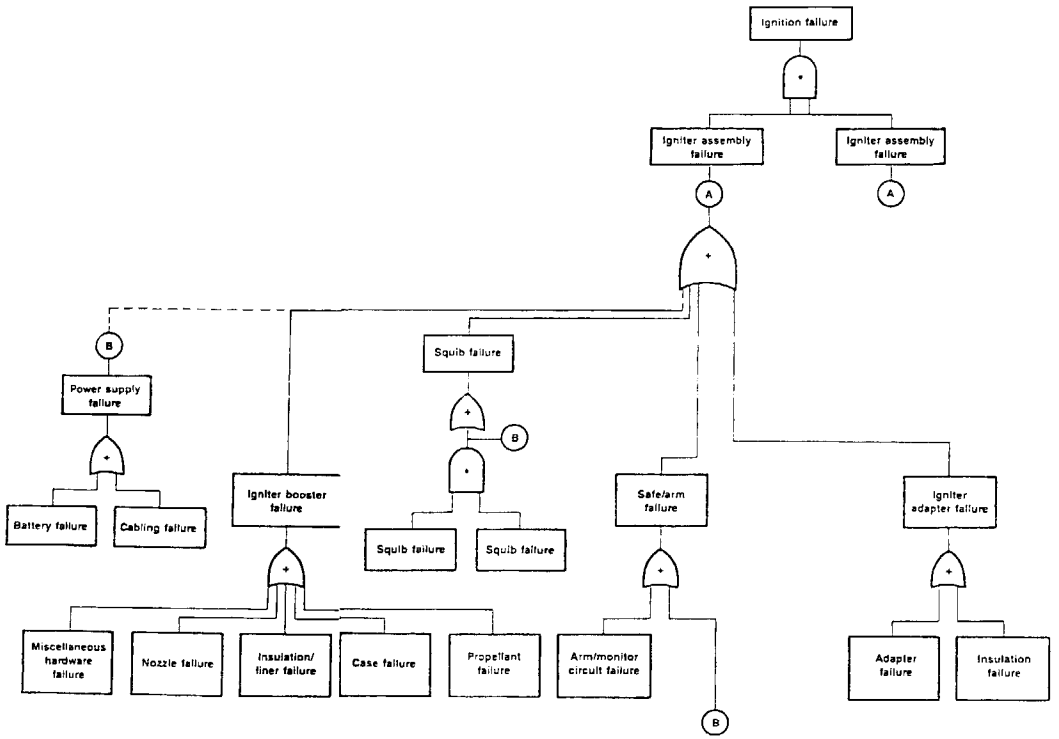

Figure 5-3. Single Set Ignition Fault Tree

50302

FOLDOUT FRAME /

FOLDOUT FRAME 2

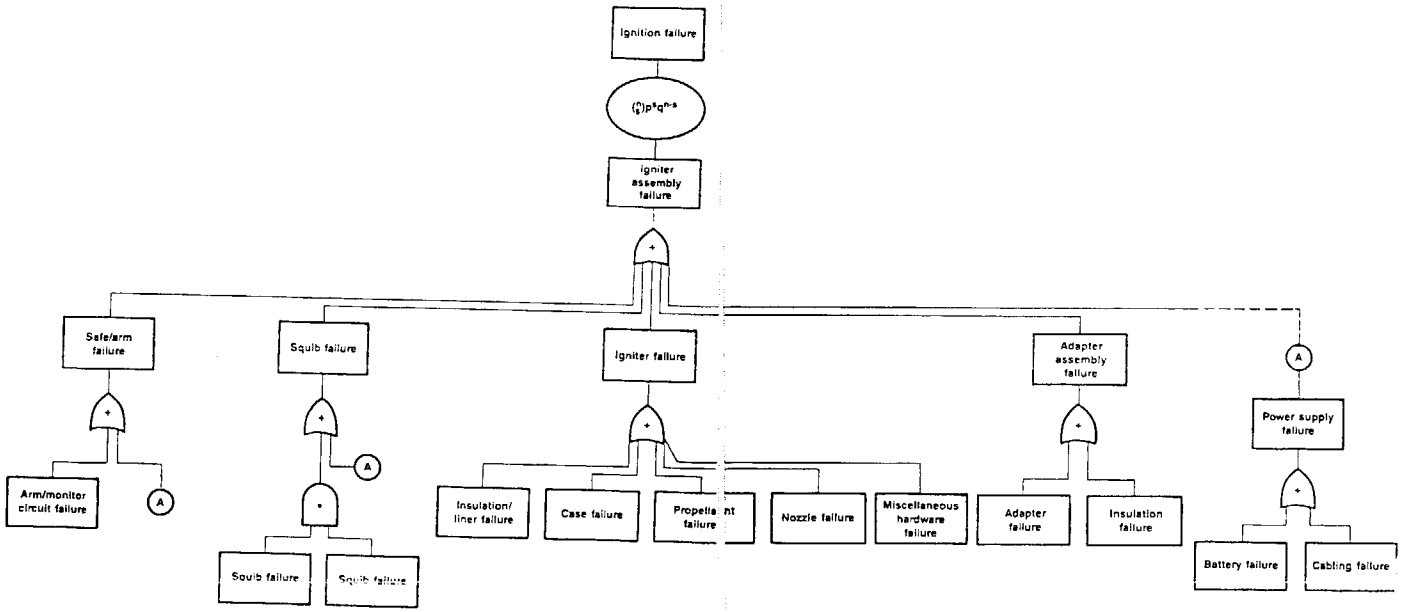

Figure 5-4. Multiple Ignition Fault Tree

50301

For the igniter evaluation, the following approach was used:

- Single redundant igniter design
  - Count the number of failure modes of one of the igniter systems
  - A = (100 - number of failure modes)/100
  - Let $R = 2A - A^2$
  - Normalize R and multiply by weight factor.
- Multiple cavities and igniters
  - Assume either 6 igniters for 6 cavities or one igniter per fuel port
  - A = (100 - number for failure modes)/100
  - Divide by R and multiply by weight factor.

Based on the failure modes analysis the single redundant configuration is much more reliable than the multiple igniters.

Thrust Vector Control. The thrust vector control design alternatives were evaluated in two parts. First, the different potential nozzle designs were modeled; then the different actuator systems were modeled. A complete evaluation would consist of the flexseal nozzle combined with actuators and the fixed nozzle with fluid injection. Both hydraulic and electromechanical actuator systems were evaluated for the flexseal nozzle.

Figures 5-5 and -6 show the FTA for the nozzle designs and Figures 5-7 and -8 depict the actuator system configurations. Following in ascending order by number of failure modes are:

- Fixed nozzle with fluid injection - 27 failure modes
- Flexseal nozzle with electromechanical actuators - 37 failure modes
- Flexseal nozzle with hydraulic actuators - 39 failure modes.

From the above, a qualitative evaluation indicates the fixed nozzle with fluid injection is the most reliable design, consequently, this approach was

selected for the preliminary concept designs. However, subsequent trades also considered life cycle costs, performance and development risk.

Tables 5-1 through 5-3 contain the weighted evaluations of reliability for the different preliminary subsystems evaluated as well as cost, performance and risk factors. Due to the lack of detailed designs with corresponding component failure rates, a relative ranking system was established to compare the alternative design configurations. The various parameters of concern were assigned a relative weight factor, which is a function of the importance of the parameter under consideration.

From the foregoing qualitative analysis the most reliable hybrid design configuration is determined to be the monolithic chamber with a single pair of redundant igniters and a fixed nozzle with fluid injection for thrust vectoring. If a flexseal nozzle were used, a hydraulic actuation system would be preferred.

5.1.1.2 Oxidizer Feed System Reliability Assessment

Two basic oxidizer feed systems were evaluated: pump feed and pressure feed. The schematics for these were shown earlier in section 4.0. Part counts reliability prediction method was employed to predict the reliability of these sytems. The point estimate reliability of pump-fed system with a redundant pump (three pumps with one-out capability) was estimated to be R = 0.999945. The point estimate reliability of the pressure fed system with a redundant main LOX valve is estimated to be R = 0.999956.

5.1.1.3 System Reliability Ranking

Since both oxidizer feed system exhibit very high reliability estimates, the overriding criteria are the reliability of the case design and the nozzle and TVC system. As the ignition system is the same for all the dsigns, it was not considered. Based on the fault tree studies the different systems were qualitatively ranked from 8 to 10 with the highest reliability score for the monolithic case with a fixed nozzle and secondary liquid injection. The segmented case with the flexseal nozzle was judged to have the lowest rating.

FOLDOUT FRAME 1

FOLDOUT FRAME 2

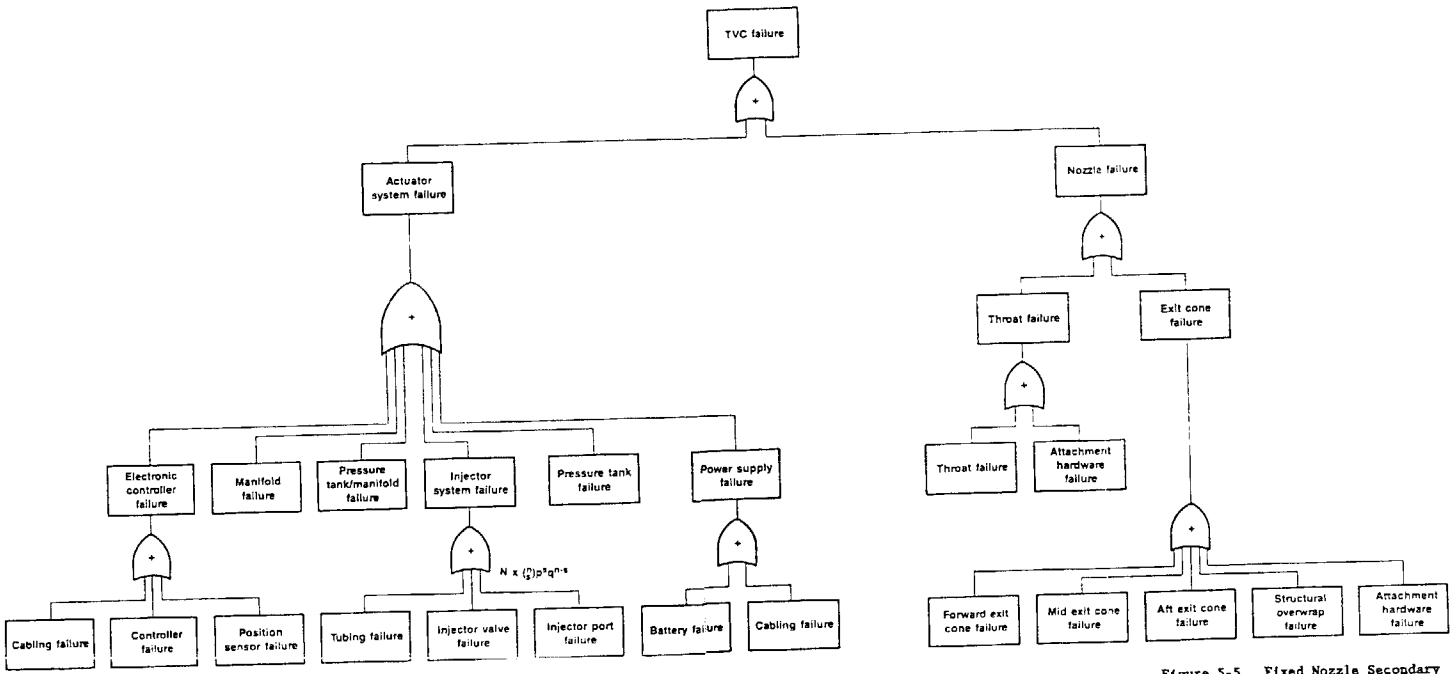

Figure 5-5. Fixed Nozzle Secondary Injection Fault Tree

50298

FOLDOUT FRAME 1

FOLDOUT FRAME 2

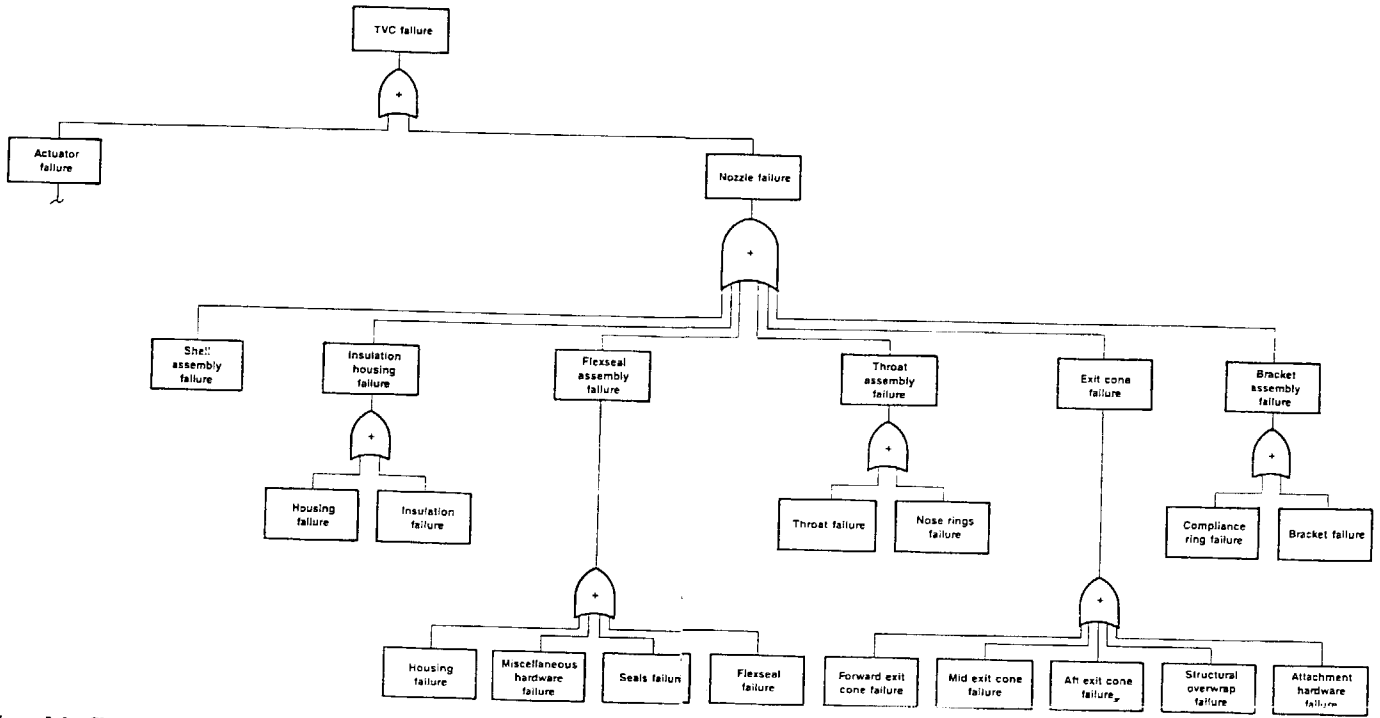

Figure 5-6. Flexseal Nozzle Fault Tree

50297

FOLDOUT FRAME 1

FOLDOUT FRAME 2

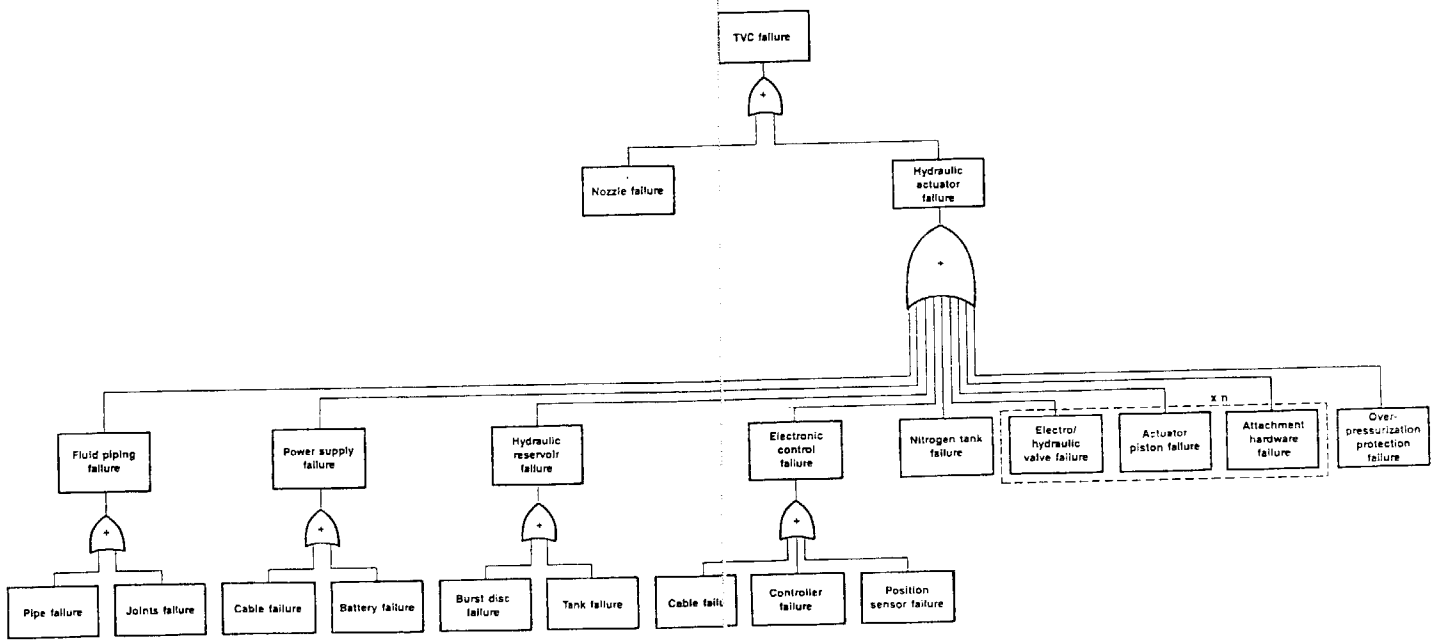

Figure 5-7. Hydraulic Actuators Fault Tree

50295

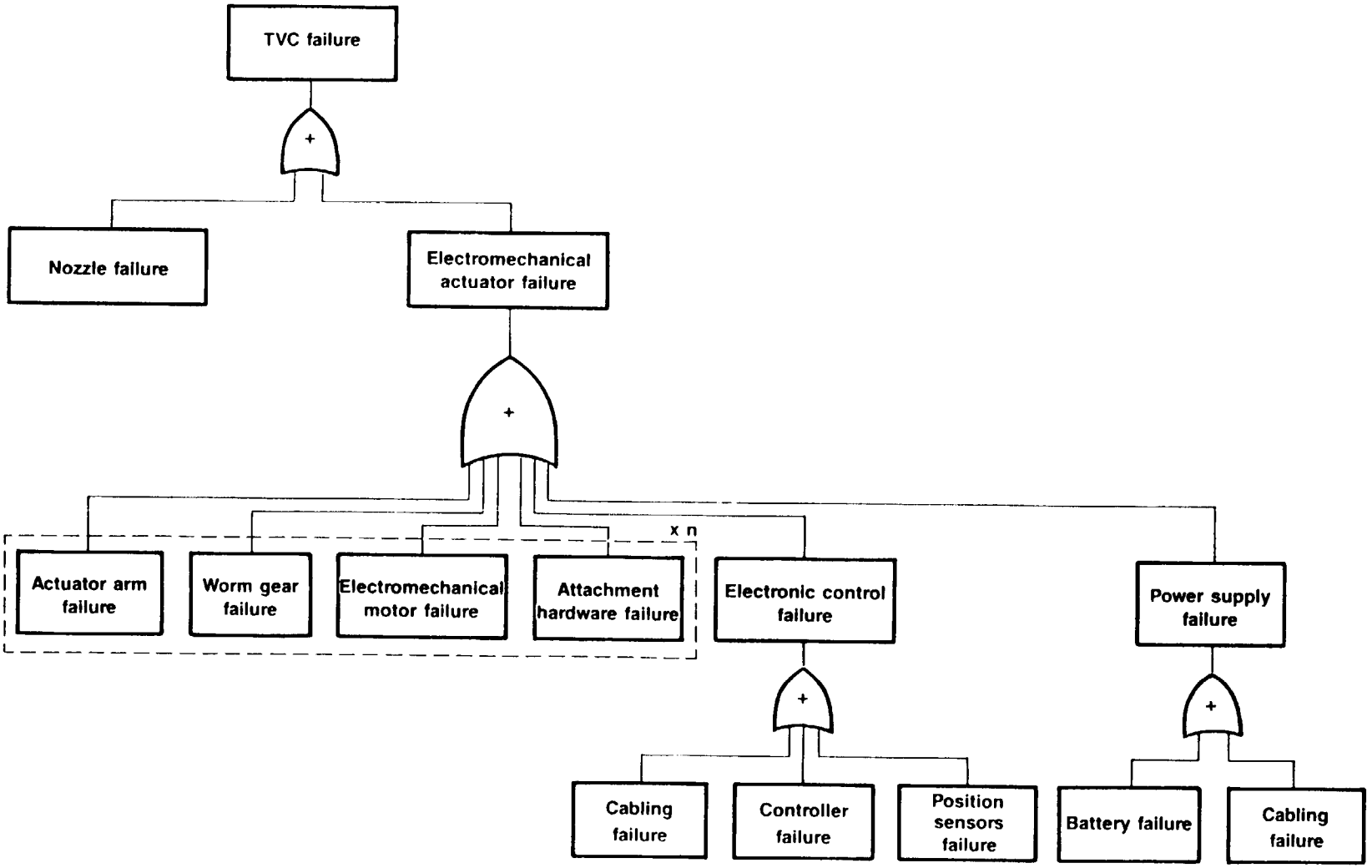

Figure 5-8. Electromechanical Actuator System Fault Tree

50294

TABLE 5-1. WEIGHTED COMPARISON, LOADED CHAMBER CONFIGURATIONS

T16897

Case Subsystem Trade Factor	Weighting Factor	Design Concept		
		Monolithic Composite	Segmented Steel	Monolithic Steel
		Weighted Rating	Weighted Rating	Weighted Rating
Reliability*	10	10	9.16	10
System safety	25	10	10	10
Cost	10	10	4	6
Performance: Δ payload	10	10	8	8
Risks/other	10	8	10	4
Total weighted ranking		48	41.16	38

* Rationale: 100 - number of failure modes = A. R = A/A maximum

TABLE 5-2. WEIGHTED COMPARISON, IGNITER CONFIGURATIONS

T16898

Igniter Subsystem Trade Factor	Weighting Factor	Design Concept: Single Redundant Igniter — Weighted Rating	Design Concept: Multiple Igniters (6) — Weighted Rating	Design Concept: Multiple Igniters (1 per Port) (34 Large, 18 Small) — Weighted Rating
Reliability	10	10	?	7.01
System safety	25	10	10	10
Cost	10	10	9	6
Performance: Δ payload	10	10	10	10
Risk/other	10	8	9	10
Total weighted ranking		48	41.4	36

Rationale: For single redundant igniter (100 - number of failure modes)/100 = A. $R = 2A - A^2$, normalized compartments.
Multiple igniters (6) assumes 6 ports (100 - number of failures modes)/100.

TABLE 5-3. WEIGHTED COMPARISON, NOZZLE CONFIGURATIONS

T16899

Nozzle Subsystem Trade Factor	Weighting Factor	Design Concept		
		Fixed Nozzle/LITVC Recoverable/ Nonrecoverable	Flexseal/ Hybrid Actuator Recoverable/ Nonrecoverable	Hot Ball and Socket Recoverable/ Nonrecoverable
		Rating	Rating	Rating
Reliability	10	9.55	9.32	Not applicable
System safety	10	10	10	-
Cost	8	10	6	-
Performance: Δ payload	6	8	10	-
Risk	6	9	9.5	-
Total weighted ranking		46.55	47.8	-

Rationale: 100 - number of failure modes = A. Normalize A to 1 by dividing by highest value. Multiply normalized value by weighting factor.

5.1.2 System Safety

MIL-STD-882B was used as a guideline to assess the potential system safety assessment. The hazard severity categories were used to evaluate the selected technology concepts. The quantitative probability of hazard associated with each subsystem presently cannot be derived due to the lack of a detailed component design. However, a qualitative hazard analysis, based on the hazard severity and hazard probability factors shown in Table 5-4 and the

TABLE 5-4. HAZARD LEVEL AND CATEGORY

T16958

A. Hazard Level		
Description	**Level**	**Specific Individual Item**
Frequent	A	Likely to occur frequently
Probable	B	Will occur several times in life of an item
Occasional	C	Likely to occur sometime in life of an item
Remote	D	Unlikely but possible to occur in life of an item
Improbable	E	So unlikely, it can be assumed occurrence may not be experienced
B. Hazard Category		
Description	**Category**	**Mishap Definition**
Catastrophic	I	Death or system loss
Critical	II	Severe injury, severe occupational illness, or major system damage
Marginal	III	Minor injury, minor occupational illness, or minor system damage
Negligible	IV	Less than minor injury, occupational illness, or system damage

criteria grouping of Figure 5-9 was performed. The analysis results indicate that basically, on a comparative basis, the selected technology concepts exhibit a similar system safety rating (for example, all loaded cases exhibit a similar ranking). Therefore, a rating of 10 (frequency of occurrence = 0.4 x weighting factor of 25 for system safety) is determined to be applicable to all subsystems and the overall systems. This is because of the choice of an inert fuel. If any oxidizer were used in the fuel, a score of 0.1 would apply. This would result in a weighted score of only 2.5 for the oxidized grains.

5.2 LIFE CYCLE COST STUDIES

Hybrid booster life cycle cost (LCC) studies were conducted to define the relative cost merits of the various design approaches examined. These cost studies were based on the Solid Technology Assessment and Cost Evaluation Model (STACEM). STACEM was developed by the Booz, Allen and Hamilton Co. under subcontract to CSD for the Air Force Astronautical Laboratory in an attempt to generate a life cycle cost estimating tool for solid rocket motor (SRM) cost trade studies. This model was supplemented with liquid feed system and associated tankage cost information to enable life cycle cost prediction of hybrid rocket motors.

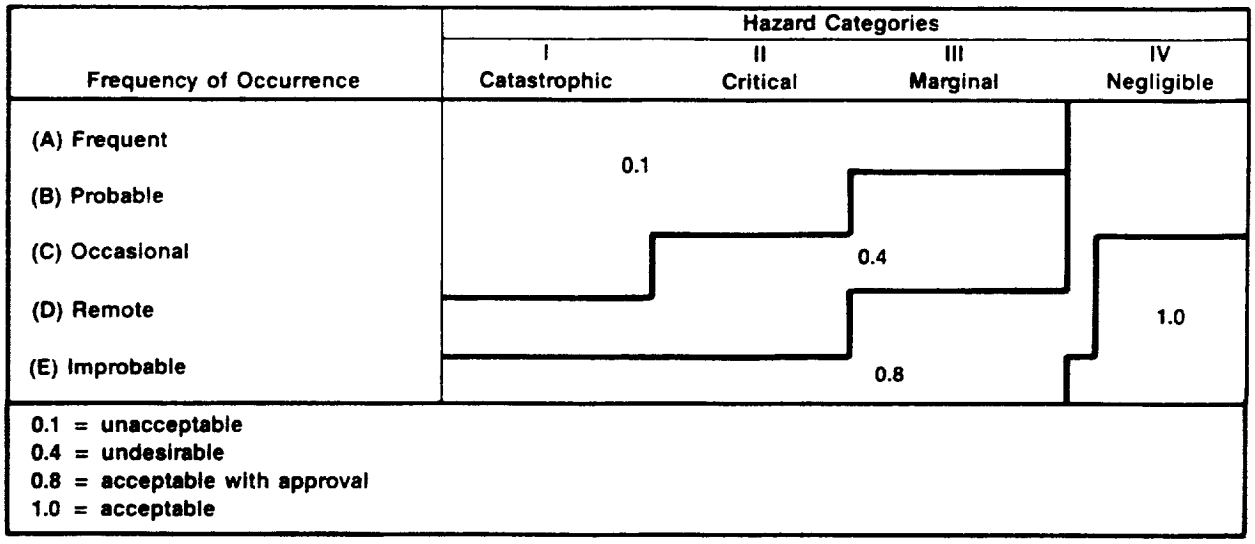

Figure 5-9. Qualitative Hazard Criteria Grouping

50382

5.2.1 Life Cycle Cost Model

STACEM defines costs into five life cycle phases: (1) research, development, testing and evaluation, (2) production, (3) launch support operations, (4) recovery operations, and (5) refurbishment. Each phase is further subdivided into a number of cost elements for which cost estimating relationships (CERs) were derived based on historical SRM cost information. These cost expressions are function of some component feature such as weight, size or operating characteristic, and have a certain degree of flexibility to account for changes in process or material cost.

Refurbishment CERs are a fraction of the production CERs for those components that are considered reusable, and are equal to production CERs for expendable components. Previous STACEM cost studies have shown that production and refurbishment cost phases dominate the LCC, depending on whether the booster analyzed is expendable or reusable. As such, CERs connected with these phases were correlated with cost information consistent with the technology and design approaches examined, to provide reasonable cost trade results. The cost information used to correlate CERs was generated at CSD in the case of solid fuel related components, and at both CSD and Space Flight Systems (SFS) in the case of booster structures. Additional CERs were generated to model liquid feed system and associated tankage cost from information generated by Pratt & Whitney (P&W). These costs addressed turbo-pumps; pre-burners; heat exchangers; igniters; valves and plumbing; and storage tanks for LOX, Propane, gaseous Helium and cryogenic Helium. Recovery costs CERs were also correlated with cost information obtained from SFS. Perhaps the LCC phase with the least estimated cost certainty is the launch support phase. These costs were based on the STACEM model, which are based on existing expendable launch vehicles, strategic missiles, and the STS solid rockets. Here the CERs are function of parameters such as manned versus unmanned, size of booster, boosters per vehicle and launch rate. The model here predicts launch support costs approximately ten times higher for a manned vehicle than for a comparable unmanned vehicle. All the vehicle configurations examined for cost in this report used the manned option.

5.2.2 Life Cycle Cost Mission Scenarios

Consistent with study requirements, two production rates were used to estimate LCC for all potentially promising hybrid booster configurations. Production phases consisting of 14 years with linear growth for the first four years and a steady rate for the remaining 10 years were used. Production schedules required to support 12 and 52 launches per year were defined for expendable and reusable boosters, as well as for the "eight small strap-ons" and "two large strap-ons" vehicle configurations. Table 5-5 shows a summary of the quantities required for each scenario and includes assumptions used to determine required quantities for the reusable scenarios. For development and qualification full-scale tests, it was assumed that 10 hybrid motors were required for static firings, and four flight sets were required to support an assumed four-flight test schedule prior to operational status (STS used four flight tests prior to being classified as operational). In the case of expendables, the number of HRBs produced is the minimum required to support the flight schedule. In the reusable mode, the cost analysis assumes a 90% recovery success and a maximum utilization rate of 20 uses with a one-year turnaround time per booster. Reusable hardware per booster include parts of the solid fuel combustor and liquid feed assembly. The combustor reusable hardware includes all items except for the obvious expendables such as fuel and insulation. The remaining hardware has various degrees of reusability (percent of part that is actually reused) which vary between 65 and 95%. These are all based on the STS solid motor experience data base. The feed assembly reusable hardware for the pump-fed configuration includes all items with exception of the tanks (LOX, Helium and fuel). Here it was assumed that the valving to the turbo-pumps and the recovery/decelerating system is such that the interior of the recovered turbo-pumps and associated hardware is not directly exposed to salt water. As a result, the cost to refurbish a feed assembly (not including fuel and tanks) is approximately 15% of what it costs to purchase a new unit. In the case of the pressure-fed configuration, all feed assembly items were assumed expendable except for the injector. It was judged that the tanks are too fragile, compared to the combustor's case, to be recoverable and repairable. Consequently they were considered expendable in all cases.

TABLE 5-5. COST QUANTITIES SUMMARY

T17016

Item	Large Hybrid Rocket Booster (HRB) (2-Vehicle)				Small Hybrid Rocket Booster (HRB) (8-Vehicle)			
	12-year		52-year		12-year		52-year	
	Expendable	Reusable	Expendable	Reusable	Expendable	Reusable	Expendable	Reusable
No. HRB produced for static and flight tests	18	18	18	18	42	42	42	42
No. HRB produced for operational flights	276	23	1196	111	1104	90	4784	442
Total No. HRB	294	42	1214	129	1146	132	4826	484
No. HRB recovered/ refurbished	0	253	0	1085	0	1014	0	4342
HRB service life (uses)	1	20	1	20	1	20	1	20
Recovery reliability, %	0	90	0	90	0	90	0	90
Turnaround time, years	0	1	0	1	0	1	0	1

5.2.3 Life Cycle Cost Trades

Tables 5-6 through 5-9 summarize the results of the hybrid booster life cycle cost trade study. In the case of the large hybrid, the use of a high launch rate mission did not affect the cost trades, the lowest cost configurations at the 12 launches/year rate also turned out to be lowest cost at the 52 launches/year rate. In the expendable versus reusable cost trade, the results show that if the large system has either pressure-fed or a pump-fed configuration, it is more cost effective to have a reusable system. This is true for the small pump-fed hybrid as well. However, if the small system is a pressure-fed configuration the lowest cost results from an expendable system.

A reusable pump-fed configuration is lower cost than an expendable pump-fed because the cost dominating hardware (feed assembly) represents more than 30% of the total booster cost, and therefore it pays to recover and refurbish the hardware. As the tanks represent approximately 10% of the total cost, their expendable costs are not as significant. An expendable pressure-fed system is either lower cost or cost comparable to a reusable pressure-fed system because the cost dominating hardware (the high pressure tanks) represent approximately 30% of the total booster cost and are not recoverable. Here the feed assembly (which is also not recoverable) represents approximately 5% of the total booster cost. Another configuration factor which affected the small booster expendable versus reusable trade is the combustor's case material. Here the expendable mode utilized a composite case which costs approximately 35% of the cost required to manufacture a recoverable metal case. This factor is attributed with balancing the lower costs in favor of an expendable configuration for the small booster.

In the thrust vector control cost trade, a liquid oxygen injection manifold in the nozzle exit cone was compared with an STS solid-motor-like, flexseal hydraulically gimballed nozzle. Here the higher per-unit costs of the flexseal configuraiton $5.3 versus $3.6 million) were traded against the higher booster costs of requiring an increased amount of LOX and associated tankage and plumbing to provide for the liquid injection thrust vector control. The results show a very small cost advantage in favor of the liquid

TABLE 5-6. LARGE HYBRID BOOSTER LCC SUMMARY (PUMP-FED LIQUID SYSTEM), $ x 10^6

T17017

Phase	12 Launches per Year				52 Launches per Year			
	Expendable		Reusable		Expendable		Reusable	
	LITVC	Flexseal	LITVC	Flexseal	LITVC	Flexseal	LITVC	Flexseal
DT&E	912	926	938	952	912	926	938	952
Production	5047	5307	621	645	17,626	18,611	2731	2837
No. units	276	276	23	23	1196	1196	111	111
Cost/unit	18.3	19.2	27.0	28.0	14.7	15.6	24.6	25.6
Recovery	0	0	169	169	0	0	640	640
No. launches	0	0	138	138	0	0	552	552
Cost/launch	0	0	1.2	1.2	0	0	1.2	1.2
Refurbishment	0	0	2701	2743	0	0	9194	9473
No. units	0	0	253	253	0	0	1085	1085
Cost/unit	0	0	10.7	10.8	0	0	8.5	8.7
Launch support	1101	1105	1495	1499	3352	3369	4545	4562
No. launches	138	138	138	138	552	552	552	552
Cost/launch	8.0	8.0	10.8	10.9	6.1	6.1	8.2	8.3
LCC	7060	7338	5924	6008	21,890	22,906	18,048	18,464

TABLE 5-7. LARGE HYBRID BOOSTER LCC SUMMARY (PRESSURE-FED LIQUID SYSTEM), $ x 10^6

T17018

Phase	12 Launches per Year				52 Launches per Year			
	Expendable		Reusable		Expendable		Reusable	
	LITVC	Flexseal	LITVC	Flexseal	LITVC	Flexseal	LITVC	Flexseal
DT&E	675	691	702	717	675	691	702	717
Production	4750	5056	561	585	17,227	18,472	2523	2631
No. units	276	276	23	23	1196	1196	111	111
Cost/unit	17.2	18.3	24.4	25.4	14.4	15.4	22.7	23.7
Recovery	0	0	169	169	0	0	640	640
No. launches	0	0	138	138	0	0	552	552
Cost/launch	0	0	1.2	1.2	0	0	1.2	1.2
Refurbishment	0	0	3428	3504	0	0	11,761	12,058
No. units	0	0	253	253	0	0	1085	1085
Cost/unit	0	0	13.5	13.8	0	0	10.8	11.1
Launch support	1228	1237	1669	1679	3894	3928	5286	5323
No. launches	138	138	138	138	552	552	552	552
Cost/launch	8.9	9.0	12.1	12.2	7.1	7.1	9.6	9.6
LCC	6653	6984	6529	6654	21,796	23,091	20,912	21,369

TABLE 5-8. SMALL HYBRID BOOSTER LCC SUMMARY (PUMP-FED LIQUID SYSTEM), $ x 10^6

T17019

Phase	12 Launches per Year				52 Launches per Year			
	Expendable		Reusable		Expendable		Reusable	
	LITVC	Flexseal	LITVC	Flexseal	LITVC	Flexseal	LITVC	Flexseal
DT&E	624	661	700	737	624	661	700	737
Production	6045	6648	862	917	20,754	23,020	3784	4030
No. units	1104	1104	90	90	4784	4874	442	442
Cost/unit	5.5	6.0	9.6	10.2	4.3	4.8	8.6	9.1
Recovery	0	0	338	338	0	0	1280	1280
No. launches	0	0	138	138	0	0	552	552
Cost/launch	0	0	2.4	2.4	0	0	2.3	2.3
Refurbishment	0	0	3608	3773	0	0	11,444	12,053
No. units	0	0	1014	1014	0	0	4342	4342
Cost/unit	0	0	3.6	3.7	0	0	2.6	2.8
Launch support	2106	2129	2966	2992	6380	6459	8991	9078
No. launches	138	138	138	138	552	552	552	552
Cost/launch	15.3	15.4	21.5	21.7	11.6	11.7	16.3	16.4
LCC	8775	9438	8474	8757	27,758	30,140	26,199	27,178

TABLE 5-9. SMALL HYBRID BOOSTER LCC SUMMARY (PRESSURE-FED LIQUID SYSTEM), $ x 10^6

T17020

Phase	12 Launches per Year				52 Launches per Year			
	Expendable		Reusable		Expendable		Reusable	
	LITVC	Flexseal	LITVC	Flexseal	LITVC	Flexseal	LITVC	Flexseal
DT&E	450	487	527	563	450	487	527	564
Production	5102	5836	619	684	18,323	21,199	2788	3086
No. units	1104	1104	90	90	4784	4784	442	442
Cost/unit	4.6	5.3	6.9	7.6	3.8	4.4	6.3	7.0
Recovery	0	0	338	338	0	0	1280	1280
No. launches	0	0	138	138	0	0	552	552
Cost/launch	0	0	2.4	2.4	0	0	2.3	2.3
Refurbishment	0	0	4248	4443	0	0	14,716	15,470
No. units	0	0	1014	1014	0	0	4342	4342
Cost/unit	0	0	4.2	4.4	0	0	3.4	3.6
Launch support	2389	2414	3368	3396	7545	7636	10,640	10,739
No. launches	138	138	138	138	552	552	552	552
Cost/launch	17.3	17.5	24.4	24.6	13.7	13.8	19.3	19.5
LCC	7941	8737	9100	9424	26,318	29,322	29,951	31,139

injection system (1 to 5%). This cost difference is considered unimportant when compared with other issues such as the availability of a large reusable flexseal data base. In addition, the liquid fuel for the pump drive system could be utilized for the actuator hydraulic drive, thereby further reducing the flexseal nozzle cost. In the lowest cost configuration (large pump-fed reusable booster), the cost difference is negligible (about 1%). Consequently the flexseal configuration was chosen as baseline. In the large vs small booster cost trade (i.e., two-booster vehicle versus eight-booster vehicle), the higher development costs inherent in the large-booster system were offset by the small booster systems's production, refurbishment and launch support costs, which are directly influenced by the much higher quantities.

5.3 PERFORMANCE

The final design studies were used to obtain predictions of component and system weights and packaging. using the partials described earlier, performance updates were performed to establish delta payloads for the alternative systems. These values were shown in section 3.4.

In performing the final selection studies, it was necessary to rank the systems using the delta payloads. As there is no clear performance requirement, it was necessary to rank the systems relative to one another. This was done using a normalized linear scale with the highest delta payload having a performance value of 10 and the lowest value of 8.

5.4 OTHER FACTORS

As part of the final ranking process, processing considerations, transportation concerns, handling constraints, development risks, environmental issues, etc., were included in the final selections. These factors were limited to only major design issues, primarily because of the lack of ultimate objectives. As system requirements become better defined, additional concerns must be considered, and these factors can be weighted better. For the purposees of this study a total score of 8 to 10 was used for the sum of the other factors.

The primary design issue is booster size as it impacts integration of the booster, manufacture, transportation, assembly and launch. Early in the selection process it was concluded that an inert fuel is the prefered baseline approach, because of inherent environmental issues, safety, and lower costs. Also the oxidized high regression rate fuels offered no performance improvement for a given diameter. Furthermore, as there was no launch platform or assembly building constraints, the choice of the inert fuel resulted in the 180-in. diameter being selected for the large booster. At this size the case is restricted to metal-segmented construction techniques, and all other approaches must be considered high risk. At 180-in. diameter the case is still of moderate risk. The only other important risk considerations are related to using either a flexseal nozzle system versus a fixed nozzle, and the risks inherent in the baseline gaseous oxygen feed systems.

The small diameter booster shares the same nozzle and feed system concerns. Another factor considered in the final trade was the risk of the composite, cartridge grain case system. This is a moderately risky area which should be reviewed in future studies as it does impact costs significantly and could impact the development schedule.

5.5 FINAL SYSTEM SELECTION

The final trade studies are summarized in Tables 5-10 and 5-11. These trades were performed for the two sizes of boosters, the launch rates of 12 and 52 per year, the oxygen feed system, the nozzle/TVC system and the issue of recovery versus non-recovery.

The selections are obviously influenced by the weightings for the different factors. Different cost or mission requirements could change the results, but given the current requirements and guide lines, the total scores favor a recoverable large booster with a pump-fed oxygens system. In the case of the small hybrid, the selection is not as straight forward. At the launch rate of 12 per year, an expendable pressure-fed LITVC system is favored overall because of a lower life cycle cost. However, the pump system shows better

TABLE 5-10. LARGE BOOSTER HYBRID BOOSTER TRADE

T17039

Criteria	Pump-Fed				Pressure-Fed			
	Flexseal Nozzle		LITVC		Flexseal Nozzle		LITVC	
	Reusable	Expendable	Reusable	Expendable	Reusable	Expendable	Reusable	Expendable
Reliability	8.00	8.00	9.00	9.00	8.00	8.00	9.00	9.00
Safety	10	10	10	10	10	10	10	10
LCC (12 launches/year)	9.76	6.0	10	6.79	7.93	7.00	8.29	7.94
LCC (52 launches/year)	9.67	6.15	10	6.95	7.37	6	7.73	7.03
Performance	10	10	8.80	8.80	9.41	9.41	8	8
Other	8.5	8.5	8.0	8.0	8.5	8.5	8.0	8.0
Total (12 launches/year)	46.26	42.50	45.8	42.59	43.84	42.91	41.29	40.94
Total (52 launches/year)	46.17	42.65	45.8	42.75	43.28	41.91	40.73	40.03

TABLE 5-11. Small Booster Hybrid Booster Trade

T17040

Criteria	Pump-Fed				Pressure-Fed			
	Flexseal Nozzle		LITVC		Flexseal Nozzle		LITVC	
	Reusable	Expendable	Reusable	Expendable	Reusable	Expendable	Reusable	Expendable
Reliability	9.50	9.50	10	10	9.50	9.50	10	10
Safety	10	10	10	10	10	10	10	10
LCC (12 launches/year)	7.82	6	8.56	7.77	6.04	7.87	6.90	10
LCC (52 launches/year)	9.20	6.81	10	8.73	6.00	7.47	6.96	9.90
Performance	9.3	10	8.70	9	8.70	9.30	8.0	8.7
Other	9.9	8.5	8.5	8.0	9.50	8.50	8.50	8
Total (12 launches/year)	45.62	44	44.76	45.07	43.24	45.17	43.40	46.70
Total (52 launches/year)	47.00	44.81	47.20	46.03	43.20	44.77	43.46	46.60

performance at 12 launches per year and has a higher overall score at 52 launches per year. These conclusions are based on using composite throwaway cases for the nonrecovery scenerio, and steel cases for the recoverable systems. If performance is the primary objective, the composite cases pump-fed system with a flexseal nozzle is the obvious choice. Upon these results, the pump fed small booster is the preferred design. This is based on the use of three small pumps for highest single booster reliability. The use of a single pump in each small booster for overall system reliability would change these conclusions.

While the flexseal nozzle is preferred for the large booster, the overall scores are not greatly higher than for a fixed nozzle with liquid oxygen injection. In the case of the pressure fed or the pump-fed small hybrid, a liquid injection system is preferred at the rate of either 12 launches per year or 52 launches per year and particularly if the system is expendable. These observations certainly warrant further evaluation of the liquid oxygen injection approach during phase II.

Life-cycle costs were specified as a selection parameter. If cost per pound of payload is used as a selection criteria, the selection is more specific. Delivered payload costs were computed for the systems described previously, using a current estimate of $3000 per pound of payload for the solid booster shuttle system. These costs per pound of payload for the hybrids are shown in Table 5-12. It is clear from these data that a reusable pump-fed system is preferred for the large booster and an expendable pump-fed system is optimum for the small hybrid. In both cases, the flexseal nozzle is preferred because of higher performance. However, this conclusion might change with consideration of the extra performance provided by LOX injection.

While these results are not as definitive as might be desired, they emphasize the versatility of the hybrid booster. A variety of configurations and subcomponents can be utilized. Optimization and final definition must be based on specific mission and performance requirments. Any phase II and III development studies must be paralled with additional system definition studies.

TABLE 5-12. COSTS ($) PER POUND OF PAYLOAD

T17086

Configuration	12 Launches per Year				52 Launches per Year			
	Expendable		Reusable		Expendable		Reusable	
	LITVC	Flexseal	LITVC	Flexseal	LITVC	Flexseal	LITVC	Flexseal
Large pump-fed liquid	2249	2107	2192	2032	2119	1986	2093	1943
Large pressure-fed liquid	2355	2175	2413	2200	2244	2069	2296	2093
Small pump-fed liquid	2365	2252	2536	2362	2182	2082	2338	2187
Small pressure-fed liquid	2490	2374	2866	2652	2340	2224	2680	2484

6.0 CONCLUSIONS AND RECOMMENDATIONS

6.1 CONCLUSIONS

The program considered fuel combinations and hardware design concepts capable of providing the hybrid propulsion advantages listed in Table 6-1 as well as some which sacrificed portions of a benefit to optimize another parameter.

It was found that more than one hybrid design offered the listed benefits while meeting all SOW (and informal) booster requirements. A 5.47 m (180-in.) diameter pump-fed engine with an inert fuel grian was found to best meet the large booster requirements. Life cycle costs favor reusability for either of the specified launch rates. A 2/44 m (96-in.) diameter overwrapped composite-case booster based on the same fuel and oxygen feed system was selected for the small booster application. These designs also provided a basis for the identification of technology issues and the recommendation for phase II and III technology acquisition.

Other detailed results are summarized below:

- The capability to throttle the hybrid booster and the passive feedback between the fuel regression rate and the oxidizer flow rate make the hybrid an extremely versatile propulsion system.
- The ability to throttle allows the hybrid to optimize the maximum g thrust-time profile for the same total impulse and increase the potential payload by an additional 2268 to 4536 kg (5,000-10,000 lb).
- The ability to throttle minimizes the effect of grain ambient temperature upon performance.
- The fuel composition has a major effect on the number of ports in the fuel grain. Low regression rate fuels require more ports than high regression rate fuels.
- An inert, clean exhaust hydrocarbon fuel offers the highest potential payload.

TABLE 6-1. BENEFITS OF HYBRID BOOSTERS

T17050

Benefits of Hybrid Boosters
• Low hazard manufacturing
• Low hazard assembly and pre-launch ops
• Benign failure modes (cracks, stable combustion)
• Controlled abort (shutdown) available
• Environmentally clean exhaust
• Competitively low life-cycle costs
• Competitive payload performance
• Simple throttling to match f-t curve and minimize thrust imbalance
• Possibility of flight readiness firing
• Can consider degrees of engine out
• Low cost refurbishing (if reuse chosen)

- The fuel composition has a major effect on the fuel grain length but a lessor effect on the overall booster length. High regression rate fuels result in 5 to 10% shorter booster lengths.
- Either pump-fed or pressure-fed oxygen delivery systems can be used with nearly identical performance.
- A GOX pump delivery system offers potentially the highest system performance but requires some development and verification.
- LOX pump design, composite LOX tank fabrication and flexseal nozzle optimization can be acquired from other parallel programs.
- Liquid propellant tankage and feed system technologies are directly translatable to the hybrid oxidizer delivery system.

6.2 RECOMMENDATIONS

It is recommended that the program continue into phase II to demonstrate as many as possible of the benefits at a scale credible for future applications, and that the following specific findings of the CDP be addressed:

- Specific mission requirements are needed to optimize any particular hybrid booster and the required subsystems. Additional optimization

studies should be performed in conjunction with the phase II technology acquisition studies.

- Large scale hybrid combustor studies are needed to fully define oxygen quality, injector configurations, port L/D, and port geometry effects.
- Dependent on TVC requirements, LOX injection TVC may be the best approach for maximum system performance (lowest cost and additional performance from LOX injection into the nozzle). Material and performance studies are required to fully evaluate performance gains, but are not required for the development of basic hybrid technology.
- Existing hybrid ballistic models need to be updated to better account for injector configuration and spray pattern effects, oxidizer vaporization, fuel port geometry, and minimization of fuel grain slivers.
- Solid propellant insulation and nozzle materials can be generally used for hybrid applications. Minimal characterization studies are required to define performance requirements unique to hybrids.

REFERENCES

1. Holzman A., and Jensen, G.E., "Hybrid Propulsion Technology Program" - Preliminary Design Report for Period 1989. Contract No. NAS8-37778, 5 July 1989.

2. "Investigation of Fundamental Phenomena in Hybrid Propulsion," Final Report No. UTC 2051-FR, Contract No. NOw-63-0737-C, Unitec Technology Center, 24 July 1964.

3. Lees, L., "Combustion and Propulsion," Third AGARD Colloquium, New York, Pergamon Press, 1958, p. 451.

4. Marxman, G. A., and M. Gilbert, Ninth Symposium (International) on Combustion, New York, Academic Press, 1963, p. 371.

5. Marxman, G. A., C. E. Wooldridge, and R. J. Muzzy, "Fundamentals of Hybrid Boundary Layer Combustion," AIAA Paper No. 63-505, presented at the Heterogeneous Combustion Conference, Palm Beach, Florida, Dec. 1963.

6. "Investigation of Fundamental Phenomena in Hybrid Propulsion," Final Technical Summary Report No. UTC 2007-FR, 6 June 1961 to 5 June 1963, Contract No. NOw 61-1000-c, United Technology Center, 5 July 1963.

7. "Investigation of Fundamental Phenomena in Hybrid Propulsion," Final Report No. UTC 2097-FR, Contract No. NOw-64-0659-c, United Technology Center, Nov. 1965.

8. "Hybrid Rocket Booster Assesment Study," CSD 2768-FR, Subcontract No. AS1-794105, Prime Contract No. NAS8-34183, United Technologies/Chemical Systems, March 1982.

9. "Demonstration of a High-Thrust Hybrid Thrust Chamber Assembly," Final Report No. UTC-2219-FR, Contract No. AF-04(611)-11618, United Technology Center, April 1968.

10. "Low Cost Hybrid," Final Report 2681-FR, AFRPL-TR-80-15, Contract No. F04611-78-C-0052, United Technologies/Chemical Systems, June 1980.

11. Becker, E. B., and R. S. Dunham, "Three-Dimensional Finite Element Computer Program Development, TEXGAP-2D Documentation," Volume I - Users Manual, AFRPL-TR-78-86, February 1979.

12. Allik, H., and J. Allik, "Three Dimensional Finite Element Structural Analysis Improvement, TEXGAP-2-D User's Manual Improvement," Analysis & Technology, Inc., Final Report AFRPL-TR-83-084, Dec. 1982.

13. Williams, M. L., et al., "Fundamental Studies Relating to Systems Analysis of Solid Propellants," Final Report, GALCIT 101, Guggenheim Aeronautical Laboratory, California Institute of Technology, Feb. 1961.

14. Fitzgerald, J.E., and W. L. Hufferd, Handbook for the Engineering Structural Analysis of Solid Propellants. Office of Naval Research, CPIA Publications, May 21, 1971.

Appendix A

DATA INPUT AND OUTPUT FOR HYBRID COMPUTER DESIGN PROGRAMS

```
ECHO=6
CONTROLS ::::::::::::::::::::::::::::::::::::::::::::::::::::::::::::::::::::::
NSC=6   IPT=2
IRSTRT=1
ITLIM=100
@@ IRSTRT=2
ITLIM=00
@@ ISENS=0  ISRCH=4  OPT=-1  OPTNAME="PAYOFF"   IPT=1
DELO=5.  RKO=.001  TOLR=.001   DELCUT=.2   DELMNO=.001  @@ ICOMB=1
DELTIN=1.0
DPRINT=2    IWAGPR=0
@
@ IOPT      OPTIMIZABLE PARAMETERS:
@           1= DMOTOR
@           3= LGODHY
@           4= WEBFR
@           8= ATAP
@           9= ARB
@
IOPT=4,8,3
IDES=0   @ WAGON WHEEL GRAIN - TANDEM TANKS
@IDES=1   @ SLOTTED GRAIN
@IDES=0   @ WAGON WHEEL GRAIN TANDEM TANKS
@IDES=3   @ CYLINDRICAL GRAIN AND OXIDIZER TANK
@-------------------------------------------------
@ ITHROT    THROTTLING OPTION FLAG
@           1 - CONSTANT OXIDIZER FLOW RATE (WDODES)
@           2 - CONSTANT ISP (WDODES,OFDES)
@           3 - CONSTANT ISP (FRQD,OFDES)
@           4 - CONSTANT THRUST (FRQD)
@           5 - INPUT THRUST TABLE (FTAB)
@-------------------------------------------------
@ITHROT=2  @ CONSTANT ISP WITH WDODES,OFDES
@ITHROT=3  @ CONSTANT ISP WITH FRQD,OFDES
@ITHROT=4  @ CONSTANT FRQD
ITHROT=5
@@@@@@@ NCTRP=0    @@ CIRCULAR CENTER PORT WITHOUT BURNING
@@@@@@@ NCTRP=1    @@ CIRCULAR CENTER PORT WITH BURNING
NCTRP=9     NOTRP=24
@@ NDEL=2    @ NUMBER OF PORTS SELECTION STEP INCREMENT; STEP IF)0
@@ NDEL=1    @ NUMBER OF PORTS SELECTION STEP INCREMENT
@@@@@@@@ NDEL=0  @ NO PORT SELECTION
NPAYOFF=5
END
CONSTRAINTS ::::::::::::::::::::::::::::::::::::::::::::::::::::::::::::::::::::
DHYLIM=41
PCRQD=750
PCTOL=3
TY=100
IMPRQD=324.0E6
GOL=.02   GOU=2.
DML=150.  DMU=200.
PLDTGT=22000.
OFL=0.5    OFU=3.14
RBL=.002
WEBL=0.05  WEBU=0.9
END
DESVAR ::::::::::::::::::::::::::::::::::::::::::::::::::::::::::::::::::::::::
```

```
DR=    0.571       @ DOME HEIGHT RATIO     1/1.75
NIS=   0.667       @ INTERSTAGE L/D
LMISC= 0.0
RHOINS=0.0414      @ CASE WALL INSULATION DENSITY
TCINS= 0.35        @ CASE WALL INSULATION THICKNESS
THINS= 2.00        @ HEAD/AFT END INSULATION
TWC=   1.0         @ COMPOSITE CASE OVERALL WALL THICKNESS
KWCASE=1.04
ALFNOZ=15.0
EPSNOZ=12     @@@ TEXTEND=21.5,50
RHOW=.105  TWOX=.50  SOX=43000.
RHOC=.283   SCASE=220000.      @@ STEEL MOTOR CASE CALC,
@@ RHOC=.06   SCASE=110000.      @@ COMPOSITE MOTOR CASE CALC
SAFACT=1.40   X3SIG=1.0
THRSTL=663200     @@ FULL SCALE
FRESID=0.06     ORESID=0.01034   @INCL 0.534% FOR LOX TANK PRESSURIZATION AT 70
                                 @PSIA, & 0.5% FOR RESIDUAL-FLEX SEAL NOZZLE
CCOMP=0.0 , 0.0      @@ FULL SCALE HYBRID
CNOZ=10450,  651.3  @@ FULL SCALE HYBRID FIXED NOZZLE
WPUMP=6100
CPUMP=0.01
WMISC=56491          @@ INJEC=1400,SUBSYSTEM=39518, 3-JOINTS=10800,IGN=500,
                     @@ FUEL TANK=450,HELIUM TANK=248,HELIUM=87,
                     @@ EXTRA FLEXSEAL NOZZLE=3487
########### DESIGN VARIABLES ################
ATAP=.194064
DMOTOR=180
LGODHY=40.2715
WEBFR=0.417559
########### REFERENCE MOTOR VALUES ##########
PARTIAL=0.143, -0.2, 885., -15.6
WTPREF=1116664. WINREF=193668.  ISPREF=265.8  @@ WINREF INCL UNBURNED WPROP+
AMREF=116.26                                  @@ INSULATION  8/10/89
END
PWOXTANK############################
RHOMET=0.29
RHOWRP=0.06
RHOXIN=0.00116
TOXMET=0.015
TOXWRP=0.084
TOXINS=1.00
KWCOMPW=1.25
KWMETSH=1.25
END
FUEL ::::::::::::::::::::::::::::::::::::::::::::::::::::::::::::::::::::::::
ARB=0.0756   NRB=0.53   @@ 5/15/89
RHOF=.03647
RHOOX=.0411
RCEXP=0.13   0.00   -0.2
RCREF=244   24   1.8
END
TABLES ::::::::::::::::::::::::::::::::::::::::::::::::::::::::::::::::::::::::
FFAC=1000.
FTTAB= 0.     @@@ 4/3/89 UPDATE
       0.9   1.2   2.0   2.9   3.9   4.9   5.9   6.9   7.8   8.8
       9.8  10.7  11.7  12.7  13.6  14.6  15.6  16.6  17.5  18.5
      19.0  19.5  19.7  19.9  20.1  20.5  20.9  21.1  21.5  21.8
      22.2  22.6  23.0  23.4  24.0  25.9  34.5  47.0  56.0  82.3
     115.5 119.1 123.0 126.1 127.1 128.1 129.1 130.1 131.1 132.1
     133.1 134.1 135.1 136.1
```

```
FTAB= 3147.7
3147.7 3161.1 3177.1 3192.5 3208.2 3235.3 3274.8 3314.6 3349.1 3378.4
3407.2 3417.1 3412.5 3399.4 3388.6 3377.7 3375.2 3381.3 3389.1 3398.5
3402.6 3406.2 3407.9 3408.6 3408.2 3408.5 3405.5 3403.9 3398.1 3382.4
3351.8 3321.6 3298.4 3275.6 3243.0 3158.5 2800.0 2475.0 2240.0 2624.8
2015.2 1950.0 1090.3  519.5  403.5  315.8  251.2  192.7  143.9  103.0
  72.6   50.1   32.9    0.0
ERTTAB=150*1.0
PCTAB= 100  250  500  750  1000  2000
OFTAB= 0.5  1.0 1.2 1.5 1.7
         1.9 2.0 2.1 2.2 2.3 2.4 2.5 2.6 2.7 2.8 2.9 3.0 3.1 3.2 3.3 4.0
ISPTAB=2*(200 248.5  260.4  290.3  304.5
          313.70 316.70 318.70 319.80 320.00 319.60 318.70 317.40
          315.9  314.4  312.80 311.20 309.60 308.00 306.40 300.00)
        200 250.00 261.5  290.4  304.8
          314.00 317.54 319.82 321.22 321.80 321.64 320.90 319.76
          318.38 316.87 315.28 313.67 312.04 310.43 308.83 300.00
        200 251.0  262.3  290.5  304.9
          314.62 317.97 320.41 321.98 322.73 322.75 322.15 321.10
          319.77 318.29 316.71 315.10 313.48 311.85 310.24 300.00
        2*(200 251.7  262.8  290.5  305.0
          314.82 318.26 320.80 322.48 323.36 323.50 323.00 322.03
          320.74 319.28 317.72 316.11 314.48 312.85 311.24 300.00)
CSTAB= 2*(4000 4583   4891   5489   5694
          5787   5800   5798   5784   5762   5736   5707   5677
          5646   5615   5585   5554   5524   5495   5467   5200)
        4000 4600   4892   5491   5707
          5814   5834   5838   5828   5809   5785   5757   5728
          5697   5666   5636   5605   5575   5545   5517   5200
        4000 4613   4894   5492   5713
          5828   5852   5859   5852   5836   5813   5786   5757
          5727   5696   5665   5634   5604   5574   5545   5200
        2*(4000 4623   4897   5493   5716
          5837   5864   5874   5869   5854   5832   5806   5778
          5748   5717   5686   5655   5625   5595   5565   5200)
EFFISP=0.93
EPSTAB=  2.0  5.0  7.0  9.0  10.  11.  12.  20. 200.
EISPTAB= 2*(251. 286.50 297.20 304.60 307.50 309.28 311.06 325.30  350.)
           252. 288.95 299.63 307.01 309.97 312.59 314.93 327.81  350.
           253. 290.34 301.04 308.43 311.39 314.01 316.35 329.24  350.
         2*(254. 291.32 302.03 309.42 312.39 315.01 317.35 330.24  350.)
REFISP=2*307.50  309.97  311.39  2*312.39
END ##########################################################################
RUN

 SHUTTLE HYBRID MOTOR STUDY - FUEL 7 - PCAVG=XXX  180*  PUMP-FED  FLEXSEAL                    19-AUG-89  13:16:10

)))) OPTIMIZED DESIGN:

PARAMETER  INITIALLY    OPTIMIZED    LOWER LIMIT  UPPER LIMIT       OPTION FLAG

WEBFR      0.417559     0.417559     0.500000E-01 0.900000          IOPT( 1)= 4
ATAP       0.194064     0.194064     0.100000E-06 0.670000          IOPT( 2)= 8
LGODHY      40.2715      40.2715     0.000000E+00  41.0000          IOPT( 3)= 3
```

SHUTTLE HYBRID MOTOR STUDY - FUEL 7 - PCAVG=XXX 180" PUMP-FED FLEXSEAL 19-AUG-89 13:16:10

TIME	THRUST	ISP	TOTIMP	O/F	GO	WDOTF	WDOTO	WDOTP	WTF	RREG	DWEB	PC	AT	EPS	ABURN
0.0	3147700.	304.3	0.0000E+00	2.506	0.73160	2876.27	7393.49	73.93	304839.	0.0486	0.00	948.	1961.2	12.00	1622740.
2.0	3177100.	305.3	0.6315E+07	2.449	0.71123	2943.30	7390.20	73.90	298970.	0.0493	0.10	959.	1961.5	12.00	1637658.
4.0	3210910.	305.1	0.1270E+08	2.484	0.70270	2945.69	7502.38	75.02	293082.	0.0489	0.20	968.	1961.8	12.00	1652489.
6.0	3278780.	304.8	0.1919E+08	2.528	0.70297	2971.43	7706.93	77.07	287171.	0.0489	0.29	988.	1962.1	11.99	1667247.
8.0	3354960.	304.5	0.2582E+08	2.575	0.70533	3002.92	7937.32	79.37	281196.	0.0490	0.39	1010.	1962.5	11.99	1682030.
10.0	3409400.	304.0	0.3259E+08	2.616	0.70263	3020.48	8112.34	81.12	275172.	0.0488	0.49	1025.	1962.8	11.99	1696806.
12.0	3408570.	303.7	0.3942E+08	2.639	0.68741	3002.71	8137.65	81.38	269143.	0.0481	0.59	1025.	1963.1	11.99	1711467.
14.0	3384240.	303.6	0.4621E+08	2.653	0.66762	2970.51	8096.97	80.97	263170.	0.0472	0.68	1017.	1963.4	11.99	1725870.
16.0	3377640.	303.3	0.5296E+08	2.673	0.65274	2950.65	8103.94	81.04	257253.	0.0465	0.78	1015.	1963.7	11.98	1740021.
18.0	3393800.	303.0	0.5973E+08	2.699	0.64349	2946.06	8173.11	81.73	251358.	0.0461	0.87	1019.	1964.0	11.98	1754007.
20.0	3408400.	302.6	0.6654E+08	2.725	0.63438	2941.16	8238.73	82.39	245470.	0.0456	0.96	1023.	1964.3	11.98	1767867.
22.0	3367100.	302.5	0.7334E+08	2.732	0.61387	2901.02	8146.89	81.47	239610.	0.0446	1.05	1010.	1964.7	11.98	1781553.
24.0	3243000.	302.7	0.7994E+08	2.710	0.57753	2809.28	7824.62	78.25	233903.	0.0429	1.14	973.	1965.0	11.98	1794783.
26.0	3154331.	302.8	0.8634E+08	2.698	0.55003	2741.04	7600.14	76.00	228352.	0.0416	1.22	946.	1965.3	11.98	1807562.
28.0	3070959.	302.8	0.9256E+08	2.686	0.52479	2676.92	7389.40	73.89	222932.	0.0403	1.30	921.	1965.6	11.97	1819951.
30.0	2987587.	302.9	0.9862E+08	2.673	0.50061	2613.37	7177.53	71.78	217640.	0.0391	1.38	896.	1965.9	11.97	1831969.
32.0	2904215.	303.0	0.1045E+09	2.658	0.47742	2550.32	6964.67	69.65	212475.	0.0379	1.46	871.	1966.2	11.97	1843624.
34.0	2820843.	303.1	0.1102E+09	2.642	0.45514	2487.68	6750.95	67.51	207435.	0.0368	1.54	846.	1966.5	11.97	1854927.
36.0	2761000.	303.2	0.1158E+09	2.633	0.43796	2440.66	6600.80	66.01	202510.	0.0359	1.61	828.	1966.9	11.97	1865909.
38.0	2709000.	303.2	0.1213E+09	2.627	0.42278	2399.11	6471.40	64.71	197669.	0.0351	1.68	812.	1967.2	11.96	1876640.
40.0	2657000.	303.2	0.1267E+09	2.619	0.40813	2357.90	6341.36	63.41	192911.	0.0343	1.75	797.	1967.5	11.96	1887130.
42.0	2605000.	303.3	0.1319E+09	2.611	0.39397	2317.00	6210.75	62.11	188235.	0.0335	1.82	781.	1967.8	11.96	1897383.
44.0	2553000.	303.3	0.1371E+09	2.601	0.38027	2276.38	6079.61	60.80	183641.	0.0327	1.88	765.	1968.1	11.96	1907406.
46.0	2501000.	303.4	0.1421E+09	2.591	0.36704	2236.14	5948.53	59.49	179127.	0.0320	1.95	750.	1968.4	11.96	1917202.
48.0	2448889.	303.4	0.1471E+09	2.581	0.35425	2196.17	5817.35	58.17	174694.	0.0313	2.01	734.	1968.7	11.95	1926777.
50.0	2396667.	303.4	0.1519E+09	2.569	0.34182	2156.32	5685.49	56.85	170340.	0.0305	2.07	718.	1969.1	11.95	1936135.
52.0	2344444.	303.5	0.1567E+09	2.557	0.32976	2116.64	5553.25	55.53	166066.	0.0298	2.13	703.	1969.4	11.95	1945279.
54.0	2292222.	303.5	0.1613E+09	2.543	0.31804	2077.11	5420.70	54.21	161872.	0.0291	2.19	687.	1969.7	11.95	1954213.
56.0	2240000.	303.6	0.1658E+09	2.529	0.30665	2037.69	5287.86	52.88	157756.	0.0285	2.25	671.	1970.0	11.95	1962941.
58.0	2269263.	303.4	0.1703E+09	2.551	0.30807	2052.34	5373.36	53.73	153666.	0.0285	2.31	680.	1970.3	11.94	1971575.
60.0	2298525.	303.2	0.1749E+09	2.573	0.30943	2066.89	5459.03	54.59	149548.	0.0286	2.36	688.	1970.6	11.94	1980235.
62.0	2327787.	303.0	0.1795E+09	2.595	0.31076	2081.31	5544.89	55.45	145400.	0.0287	2.42	697.	1970.9	11.94	1988918.
64.0	2357049.	302.8	0.1842E+09	2.617	0.31208	2095.83	5631.87	56.32	141223.	0.0288	2.48	705.	1971.3	11.94	1997625.
66.0	2386312.	302.6	0.1890E+09	2.639	0.31339	2110.29	5719.35	57.19	137018.	0.0288	2.54	714.	1971.6	11.94	2006356.
68.0	2415574.	302.3	0.1938E+09	2.660	0.31465	2124.65	5807.05	58.07	132783.	0.0289	2.59	722.	1971.9	11.93	2015110.
70.0	2444837.	302.1	0.1986E+09	2.682	0.31587	2138.90	5894.98	58.95	128520.	0.0290	2.65	731.	1972.2	11.93	2023886.
72.0	2474099.	301.9	0.2035E+09	2.704	0.31707	2153.07	5983.25	59.83	124229.	0.0290	2.71	739.	1972.5	11.93	2032684.
74.0	2503362.	301.6	0.2085E+09	2.725	0.31825	2167.27	6072.34	60.72	119909.	0.0291	2.77	748.	1972.8	11.93	2041503.
76.0	2532624.	301.3	0.2136E+09	2.747	0.31941	2181.42	6161.91	61.62	115561.	0.0292	2.83	756.	1973.1	11.93	2050344.
78.0	2561886.	301.1	0.2187E+09	2.769	0.32055	2195.49	6251.82	62.52	111185.	0.0292	2.88	765.	1973.5	11.93	2059205.
80.0	2591148.	300.8	0.2238E+09	2.790	0.32164	2209.46	6341.98	63.42	106780.	0.0293	2.94	773.	1973.8	11.92	2068087.
82.0	2620411.	300.5	0.2290E+09	2.812	0.32272	2223.41	6432.66	64.33	102348.	0.0294	3.00	782.	1974.1	11.92	2076988.
84.0	2593586.	300.5	0.2342E+09	2.809	0.31592	2202.23	6365.06	63.65	97917.	0.0289	3.06	774.	1974.4	11.92	2085851.
86.0	2556863.	300.6	0.2394E+09	2.802	0.30792	2174.97	6269.23	62.69	93539.	0.0285	3.12	763.	1974.7	11.92	2094571.
88.0	2520140.	300.6	0.2445E+09	2.794	0.30011	2147.84	6173.30	61.73	89215.	0.0280	3.17	752.	1975.0	11.92	2103151.
90.0	2483417.	300.7	0.2495E+09	2.786	0.29251	2120.90	6077.55	60.78	84946.	0.0275	3.23	741.	1975.3	11.91	2111590.
92.0	2446694.	300.7	0.2544E+09	2.777	0.28509	2094.07	5981.65	59.82	80730.	0.0271	3.28	730.	1975.7	11.91	2119892.
94.0	2409971.	300.8	0.2593E+09	2.768	0.27784	2067.32	5885.55	58.86	76568.	0.0266	3.34	719.	1976.0	11.91	2128058.
96.0	2373248.	300.9	0.2640E+09	2.759	0.27074	2040.64	5789.27	57.89	72459.	0.0262	3.39	708.	1976.3	11.91	2136090.
98.0	2336526.	301.0	0.2687E+09	2.749	0.26380	2014.04	5692.81	56.93	68404.	0.0258	3.44	697.	1976.6	11.91	2143991.
100.0	2299803.	301.0	0.2734E+09	2.739	0.25701	1987.50	5596.20	55.96	64402.	0.0253	3.49	686.	1976.9	11.90	2151761.
102.0	2263080.	301.1	0.2779E+09	2.728	0.25037	1961.02	5499.44	54.99	60453.	0.0249	3.54	674.	1977.2	11.90	2159403.
104.0	2226357.	301.2	0.2824E+09	2.717	0.24386	1934.58	5402.57	54.03	56556.	0.0245	3.59	663.	1977.6	11.90	2166917.
106.0	2189634.	301.3	0.2869E+09	2.705	0.23748	1908.18	5305.58	53.06	52713.	0.0241	3.64	652.	1977.9	11.90	2174306.
108.0	2152911.	301.4	0.2912E+09	2.693	0.23124	1881.86	5208.67	52.09	48922.	0.0237	3.69	641.	1978.2	11.90	2181570.
110.0	2116188.	301.5	0.2955E+09	2.681	0.22513	1855.59	5111.82	51.12	45184.	0.0232	3.74	630.	1978.5	11.90	2188712.

SHUTTLE HYBRID MOTOR STUDY - FUEL 7 - PCAVG=XXX 180" PUMP-FED FLEXSEAL 19-AUG-89 13:16:10

TIME	THRUST	ISP	TOTIMP	O/F	GO	WDOTF	WDOTO	WDOTP	WTF	RREG	DWEB	PC	AT	EPS	ABURN
112.0	2079465.	301.6	0.2997E+09	2.668	0.21913	1829.34	5014.90	50.15	41498.	0.0228	3.78	620.	1978.8	11.89	2195732.
114.0	2042742.	301.7	0.3038E+09	2.655	0.21325	1803.10	4917.92	49.18	37865.	0.0224	3.83	609.	1979.1	11.89	2202632.
116.0	2006144.	301.8	0.3078E+09	2.642	0.20749	1776.95	4821.23	48.21	34284.	0.0221	3.87	598.	1979.4	11.89	2209412.
118.0	1969922.	302.0	0.3118E+09	2.628	0.20189	1751.04	4725.54	47.26	30756.	0.0217	3.92	587.	1979.8	11.89	2216076.
120.0	1751607.	302.9	0.3156E+09	2.513	0.17546	1604.74	4136.22	41.36	27331.	0.0198	3.96	522.	1980.1	11.89	2222526.
122.0	1310736.	302.4	0.3187E+09	2.250	0.12656	1303.65	3001.31	30.01	24411.	0.0160	3.99	395.	1980.4	11.88	2228011.
124.0	906171.	296.9	0.3209E+09	1.964	0.08487	1009.28	2022.20	20.22	22097.	0.0124	4.02	278.	1980.7	11.88	2232349.
126.0	537913.	282.0	0.3223E+09	1.637	0.04951	711.54	1183.88	11.84	20357.	0.0087	4.04	168.	1981.0	11.88	2235606.
128.0	324571.	262.3	0.3232E+09	1.386	0.02999	511.45	718.97	7.19	19137.	0.0063	4.06	102.	1981.3	11.88	2237885.
129.9	204660.	244.3	0.3237E+09	1.191	0.01897	377.77	455.40	4.55	18290.	0.0046	4.07	64.	1981.6	11.88	2239467.

TFLGHT= 129.896 TARRVL= 129.896
ISTP= 6)) FUEL WEIGHT LIMIT

FUEL WEIGHT LIMIT (6.0% RESIDUAL) ACTUAL= 6.00%
OXIDIZER WEIGHT LIMIT (1.0% RESIDUAL)

SHUTTLE HYBRID MOTOR STUDY - FUEL 7 - PCAVG=XXX 180" PUMP-FED FLEXSEAL 19-AUG-89 13:16:10

DESIGN VALUES PAYOFF=-(DWPLD-PLDTGT)

IDES=	0	ITHROT=	5		
NPORT=	34	NOTRP=	24	NCTRP=	9

SIZES

DMOTOR=	180.0000	DGRAIN=	178.0527	DOX=	178.0527
LMTR=	1819.967	LGRAIN=	565.0254	LOX=	828.0266
LCASE=	642.1104	LDOMES=	102.7800	LINS=	565.0254
LIS=	120.0600	LNC=	221.4000	LNOZ=	229.7696
LBSTR=	1989.977				
TCREQ=	0.5981121	TWOX=	0.5000000		
DTO=	49.97080	DEXIT=	173.1039	TCINS=	0.3500000
ATO=	1961.203	AEXIT=	23534.43	THINS=	2.000000
ALFNOZ=	15.00000	EPSO=	12.00000		
AFORTO=	10105.96	ABURNO=	1622740.	WEB=	4.291939
RO1MIN=	8.256850	RO1=	8.256851	RO2=	16.84073
R1=	38.20830	R2=	46.79218	R3=	84.73443
R4=	89.02637				
A0=	214.1800	DOHYD=	16.51370	LG/DOH=	34.21555
A1=	226.2876	D1HYD=	14.03040	LG/D1H=	40.27150
A2=	327.2996	D2HYD=	14.03040	LG/D2H=	40.27150
VFCASE=	0.5528968	VFGRAIN=	0.5941269		
L/DCASE=	3.567280	L/DGRAIN=	3.173360		

WEIGHTS

WMOTOR=	1255546.	WPUMP=	6100.000	WNOZ=	18265.60
WINRT=	158480.1	WCASE=	59330.63	WOTANK=	5957.911
WMISC=	56491.00	WINS=	12334.99	PMF=	0.8737760
WTPROP=	1097066.	WTFUEL=	304838.8	WTOX=	784383.6
WPUMPF=	7843.836				

P&W METAL/COMPOSITE OXIDIZER TANK:

WMETSH=	2511.815	WCOMPW=	2910.241	WOXINS=	535.8540

REGRESSION EQUATION

```
  RREG=0.076*GO**0.53 *(PC/RCREF(1))**0.13
       *(LGRAIN/RCREF(2))**0.00 *(DHYAVG/RCREF(3))**-.20
```

FINAL FLIGHT VALUES

WDOMAX=	9245.098	WTFBRN=	286548.4	WTOBRN=	776273.1
PCAVG=	746.4625	MEOP=	1026.862	PCDES=	1437.607
O/FAVG=	2.637593	DT=	50.23045		
TOTIMP=	3.2367187E+08	FAVG=	2491785.	ISPAVG=	302.3320
IMPRQD=	3.2400000E+08	VEL=	18229.44		
DWP=	-53842.38	DWINRT=	-8705.938		
DISP=	36.53198	DAMREF=	60.45458	DWPLD=	25429.44

PFPCAVG= 0.513681
PFTOTIMP= 0.833005

NRAYOFF= 5 PAYOFF=-3.429441 SUMPEN= 1.346687 NRUN= 1

CPTIME= 7.37
EOF

```
ECHO=6
CONTROLS ::::::::::::::::::::::::::::::::::::::::::::::::::::::::::::::::::::
NSC=6   IPT=2
IRSTRT=1
ITLIM=100
@@ IRSTRT=2
ITLIM=00
@@ ISENS=0  ISRCH=4  OPT=-1  OPTNAME="PAYOFF"    IPT=1
DELO=5.  RKO=.001  TOLR=.001   DELCUT=.2   DELMNO=.01 @@@  ICOMB=1
DELTIN=1.0
DPRINT=2    IWAGPR=0
@
@ IOPT      OPTIMIZABLE PARAMETERS:
@           1= DMOTOR
@           3= LGODHY
@           4= WEBFR
@           8= ATAP
@           9= ARB
@
IOPT=4,8,3
IDES=0   @ WAGON WHEEL GRAIN - TANDEM TANKS
@IDES=1   @ SLOTTED GRAIN
@IDES=0   @ WAGON WHEEL GRAIN TANDEM TANKS
@IDES=3   @ CYLINDRICAL GRAIN AND OXIDIZER TANK
@-------------------------------------------------
@ ITHROT    THROTTLING OPTION FLAG
@           1 - CONSTANT OXIDIZER FLOW RATE (WDODES)
@           2 - CONSTANT ISP (WDODES,OFDES)
@           3 - CONSTANT ISP (FRQD,OFDES)
@           4 - CONSTANT THRUST (FRQD)
@           5 - INPUT THRUST TABLE (FTAB)
@-------------------------------------------------
ITHROT=5
@@@@@@@ NCTRP=0    @@ CIRCULAR CENTER PORT WITHOUT BURNING
@@@@@@@ NCTRP=1    @@ CIRCULAR CENTER PORT WITH BURNING
NCTRP=5     NOTRP=12
@@ NDEL=2    @ NUMBER OF PORTS SELECTION STEP INCREMENT; STEP IF)0
@@ NDEL=1    @ NUMBER OF PORTS SELECTION STEP INCREMENT
@@@@@@@@ NDEL=0  @ NO PORT SELECTION
NPAYOFF=5
END
CONSTRAINTS ::::::::::::::::::::::::::::::::::::::::::::::::::::::::::::::::::
DHYLIM=41
PCRQD=750
PCTOL=2
IMPRQD=81.0E6
GOL=.02   GOU=2.
DML=150.  DMU=200.
PLDTGT=10000.
OFL=0.5    OFU=3.14
RBL=.002
WEBL=0.05  WEBU=0.9
END
DESVAR ::::::::::::::::::::::::::::::::::::::::::::::::::::::::::::::::::::::
DR=    0.571      @ DOME HEIGHT RATIO    1/1.75
NIS=   0.8646     @ INTERSTAGE L/D
LMISC= 0.0
RHOINS=0.0414     @ CASE WALL INSULATION DENSITY
```

```
TCINS= 0.35        @ CASE WALL INSULATION THICKNESS
THINS= 2.00        @ HEAD/AFT END INSULATION
TWC=   1.0         @ COMPOSITE CASE OVERALL WALL THICKNESS
KWCASE=1.04
ALFNOZ=15.0
EPSNOZ=12     @@@ TEXTEND=21.5,50
RHOW=.105  TWOX=.50  SOX=43000.
@@ RHOC=.283    SCASE=220000.      @@ STEEL MOTOR CASE CALC, DELETE FOR COMPOSITE
SAFACT=1.40        X3SIG=1.0
THRSTL=165800     @@ 1/4 SCALE
FRESID=0.06      ORESID=0.01034    @INCL 0.534% FOR LOX TANK PRESSURIZATION AT 70
                                   @PSIA, & 0.5% FOR RESIDUAL
CCOMP=2058,     10.1 @@ 1/4 SCALE HYBRID  DELETE FOR METAL CASE
CNOZ= 2650,    165   @@ 1/4 SCALE HYBRID FIXED NOZZLE
WPUMP=3500           @@ 1/4 SCALE HYBRID
WMISC=14893      @@ INJECTOR=1350, SUBSYSTEM=12287,IGNIT=150,EXTRA FOR FLEXSEAL
                 @@ NOZZLE = 888,HELIUM TANK=71,HELIUM=23,FUEL TANK=124
CPUMP=0.01       @@ (ACUREX) RATIO OF WDOT PROPANE TO WDOT LOX
########## DESIGN VARIABLES ################
ATAP=.2722
DMOTOR=96
LGODHY=41
WEBFR=0.50085
########## REFERENCE MOTOR VALUES ##########
PARTIAL=0.572, -0.8, 885., -62.4
WTPREF=279166. WINREF=48417.   ISPREF=265.8  @@ WINREF INCL UNBURNED WPROP+
AMREF=29.065                                 @@ INSULATION
END
PWOXTANK##########################
RHOMET=0.29
RHOWRP=0.06
RHOXIN=0.00116
TOXMET=0.015
TOXWRP=0.045
TOXINS=1.00
KWCOMPW=1.25
KWMETSH=1.25
END
FUEL ::::::::::::::::::::::::::::::::::::::::::::::::::::::::::::::::::::::::
ARB=0.0756    NRB=0.53    @@ 5/15/89
RHOF=.03647
RHOOX=.0411
RCEXP=0.13    0.00    -0.2
RCREF=244     24     1.8
END
TABLES ::::::::::::::::::::::::::::::::::::::::::::::::::::::::::::::::::::::::
FFAC=250.
FTTAB= 0.      @@@ 4/3/89 UPDATE
       0.9   1.2   2.0   2.9   3.9   4.9   5.9   6.9   7.8   8.8
       9.8  10.7  11.7  12.7  13.6  14.6  15.6  16.6  17.5  18.5
      19.0  19.5  19.7  19.9  20.1  20.5  20.9  21.1  21.5  21.8
      22.2  22.6  23.0  23.4  24.0  25.9  34.5  47.0  56.0  82.3
     115.5 119.1 123.0 126.1 127.1 128.1 129.1 130.1 131.1 132.1
     133.1 134.1 135.1 136.1
FTAB= 3147.7
3147.7 3161.1 3177.1 3192.5 3208.2 3235.3 3274.8 3314.6 3349.1 3378.4
3407.2 3417.1 3412.5 3399.4 3388.6 3377.7 3375.2 3381.3 3389.1 3398.5
3402.6 3406.2 3407.9 3408.6 3408.2 3408.5 3405.5 3403.9 3398.1 3382.4
3351.8 3321.6 3298.4 3275.6 3243.0 3158.5 2800.0 2475.0 2240.0 2624.8
2015.2 1950.0 1090.3  519.5  403.5  315.8  251.2  192.7  143.9  103.0
```

```
  72.6   50.1   32.9    0.0
ERTTAB=150*1.0
PCTAB= 100  250  500  750  1000  2000
OFTAB= 0.5  1.0 1.2 1.5 1.7
         1.9 2.0 2.1 2.2 2.3 2.4 2.5 2.6 2.7 2.8 2.9 3.0 3.1 3.2 3.3 4.0
ISPTAB=2*(200 248.5  260.4  290.3  304.5
         313.70 316.70 318.70 319.80 320.00 319.60 318.70 317.40
         315.9  314.4  312.80 311.20 309.60 308.00 306.40 300.00)
       200 250.00 261.5  290.4  304.8
         314.00 317.54 319.82 321.22 321.80 321.64 320.90 319.76
         318.38 316.87 315.28 313.67 312.04 310.43 308.83 300.00
       200 251.0  262.3  290.5  304.9
         314.62 317.97 320.41 321.98 322.73 322.75 322.15 321.10
         319.77 318.29 316.71 315.10 313.48 311.85 310.24 300.00
       2*(200 251.7  262.8  290.5  305.0
         314.82 318.26 320.80 322.48 323.36 323.50 323.00 322.03
         320.74 319.28 317.72 316.11 314.48 312.85 311.24 300.00)
CSTAB= 2*(4000 4583   4891   5489   5694
         5787   5800   5798   5784   5762   5736   5707   5677
         5646   5615   5585   5554   5524   5495   5467   5200)
       4000 4600   4892   5491   5707
         5814   5834   5838   5828   5809   5785   5757   5728
         5697   5666   5636   5605   5575   5545   5517   5200
       4000 4613   4894   5492   5713
         5828   5852   5859   5852   5836   5813   5786   5757
         5727   5696   5665   5634   5604   5574   5545   5200
       2*(4000 4623   4897   5493   5716
         5837   5864   5874   5869   5854   5832   5806   5778
         5748   5717   5686   5655   5625   5595   5565   5200)
EFFISP=0.93
EPSTAB=  2.0  5.0  7.0  9.0  10.  11.  12.  20. 200.
EISPTAB= 2*(251. 286.50 297.20 304.60 307.50 309.28 311.06 325.30  350.)
           252. 288.95 299.63 307.01 309.97 312.59 314.93 327.81  350.
           253. 290.34 301.04 308.43 311.39 314.01 316.35 329.24  350.
         2*(254. 291.32 302.03 309.42 312.39 315.01 317.35 330.24  350.)
REFISP=2*307.50  309.97  311.39  2*312.39
END ##########################################################################
RUN

 SHUTTLE HYBRID MOTOR STUDY - FUEL 7 - PCAVG=XXX  96"   PUMP FED  FLEXSEAL                    19-AUG-89   13:13:19

)))) OPTIMIZED DESIGN:

PARAMETER  INITIALLY    OPTIMIZED    LOWER LIMIT  UPPER LIMIT       OPTION FLAG

WEBFR      0.500850     0.500850     0.500000E-01 0.900000          IOPT( 1)= 4
ATAP       0.272200     0.272200     0.100000E-06 0.670000          IOPT( 2)= 8
LGODHY      41.0000      41.0000     0.000000E+00  41.0000          IOPT( 3)= 3
```

SHUTTLE HYBRID MOTOR STUDY - FUEL 7 - PCAVG=XXX 96" PUMP FED FLEXSEAL 19-AUG-89 13:13:19

TIME	THRUST	ISP	TOTIMP	O/F	SC	WDOTF	WDOTO	WDOTP	WTF	RREG	DWEB	PC	AT	EPS	ABURN
0.0	786925.	302.0	0.0000E+00	2.711	1.08694	683.15	1903.82	19.04	74175.	0.0652	0.00	972.	476.8	12.00	287252.
2.0	794275.	303.7	0.1579E+07	2.635	1.02620	700.38	1895.62	18.96	72780.	0.0652	0.13	983.	476.9	12.00	294745.
4.0	802728.	303.3	0.3176E+07	2.670	0.99070	701.76	1925.26	19.25	71378.	0.0637	0.26	992.	477.1	11.99	302079.
6.0	819695.	302.8	0.4797E+07	2.716	0.96997	708.77	1978.68	19.79	69969.	0.0628	0.39	1013.	477.2	11.99	309270.
8.0	838740.	302.1	0.6456E+07	2.764	0.95370	717.20	2038.72	20.39	68543.	0.0622	0.51	1035.	477.4	11.98	316376.
10.0	852350.	301.5	0.8147E+07	2.804	0.93170	722.18	2083.65	20.84	67103.	0.0612	0.64	1052.	477.5	11.98	323386.
12.0	852143.	301.2	0.9854E+07	2.826	0.89475	718.61	2089.49	20.89	65661.	0.0597	0.76	1051.	477.7	11.98	330256.
14.0	846060.	301.0	0.1155E+08	2.838	0.85408	711.56	2078.24	20.78	64231.	0.0579	0.87	1043.	477.9	11.97	336927.
16.0	844410.	300.8	0.1324E+08	2.855	0.82169	707.47	2079.30	20.79	62813.	0.0565	0.99	1041.	478.0	11.97	343409.
18.0	848450.	300.4	0.1493E+08	2.880	0.79788	707.06	2096.43	20.96	61399.	0.0554	1.10	1045.	478.2	11.96	349752.
20.0	852100.	300.0	0.1663E+08	2.903	0.77533	706.52	2112.31	21.12	59985.	0.0544	1.21	1049.	478.3	11.96	355977.
22.0	841775.	300.0	0.1834E+08	2.906	0.74008	697.48	2087.74	20.88	58576.	0.0528	1.32	1036.	478.5	11.96	362069.
24.0	810750.	300.4	0.1999E+08	2.879	0.68723	675.82	2003.32	20.03	57204.	0.0504	1.42	998.	478.6	11.95	367907.
26.0	788583.	300.5	0.2158E+08	2.863	0.64686	659.92	1944.89	19.45	55868.	0.0484	1.52	970.	478.8	11.95	373501.
28.0	767740.	300.6	0.2314E+08	2.847	0.61042	644.96	1889.95	18.90	54563.	0.0467	1.61	944.	478.9	11.95	378884.
30.0	746897.	300.8	0.2466E+08	2.830	0.57633	630.09	1834.79	18.35	53287.	0.0450	1.71	918.	479.1	11.94	384071.
32.0	726054.	301.0	0.2613E+08	2.811	0.54434	615.29	1779.43	17.79	52041.	0.0434	1.79	893.	479.2	11.94	389069.
34.0	705211.	301.1	0.2756E+08	2.790	0.51426	600.57	1723.99	17.24	50825.	0.0418	1.88	867.	479.4	11.93	393886.
36.0	690250.	301.2	0.2895E+08	2.778	0.49068	589.62	1684.95	16.85	49636.	0.0406	1.96	848.	479.6	11.93	398540.
38.0	677250.	301.3	0.3032E+08	2.768	0.46990	579.96	1651.27	16.51	48466.	0.0395	2.04	832.	479.7	11.93	403065.
40.0	664250.	301.4	0.3166E+08	2.758	0.45017	570.36	1617.46	16.17	47315.	0.0384	2.12	816.	479.9	11.92	407465.
42.0	651250.	301.5	0.3298E+08	2.746	0.43142	560.81	1583.55	15.84	46184.	0.0373	2.20	800.	480.0	11.92	411746.
44.0	638250.	301.6	0.3427E+08	2.734	0.41356	551.31	1549.54	15.50	45072.	0.0363	2.27	783.	480.2	11.91	415911.
46.0	625250.	301.7	0.3553E+08	2.721	0.39653	541.84	1515.45	15.15	43978.	0.0354	2.34	767.	480.3	11.91	419965.
48.0	612222.	301.8	0.3677E+08	2.707	0.38024	532.39	1481.21	14.81	42904.	0.0344	2.41	751.	480.5	11.91	423911.
50.0	599167.	301.9	0.3798E+08	2.692	0.36469	522.99	1447.02	14.47	41848.	0.0335	2.48	735.	480.6	11.90	427751.
52.0	586111.	302.0	0.3917E+08	2.677	0.34981	513.62	1412.85	14.13	40811.	0.0326	2.54	719.	480.8	11.90	431491.
54.0	573056.	302.1	0.4032E+08	2.661	0.33554	504.27	1378.62	13.79	39793.	0.0318	2.61	703.	481.0	11.90	435131.
56.0	560000.	302.3	0.4146E+08	2.644	0.32183	494.93	1344.35	13.44	38794.	0.0309	2.67	687.	481.1	11.89	438675.
58.0	567316.	302.0	0.4258E+08	2.666	0.32175	498.79	1365.92	13.66	37800.	0.0309	2.73	695.	481.3	11.89	442170.
60.0	574631.	301.8	0.4373E+08	2.686	0.32164	502.62	1387.54	13.88	36799.	0.0309	2.80	704.	481.4	11.88	445665.
62.0	581947.	301.6	0.4488E+08	2.707	0.32152	506.44	1409.26	14.09	35790.	0.0309	2.86	712.	481.6	11.88	449158.
64.0	589262.	301.3	0.4605E+08	2.728	0.32140	510.26	1431.14	14.31	34773.	0.0309	2.92	721.	481.7	11.88	452652.
66.0	596578.	301.0	0.4724E+08	2.749	0.32126	514.06	1453.08	14.53	33749.	0.0309	2.98	730.	481.9	11.87	456144.
68.0	603894.	300.8	0.4844E+08	2.770	0.32110	517.83	1475.07	14.75	32717.	0.0309	3.04	738.	482.0	11.87	459636.
70.0	611209.	300.5	0.4966E+08	2.790	0.32092	521.58	1497.12	14.97	31678.	0.0309	3.10	747.	482.2	11.86	463126.
72.0	618525.	300.3	0.5089E+08	2.811	0.32075	525.33	1519.34	15.19	30631.	0.0309	3.17	756.	482.4	11.86	466616.
74.0	625840.	300.0	0.5213E+08	2.831	0.32058	529.08	1541.70	15.42	29577.	0.0309	3.23	764.	482.5	11.86	470105.
76.0	633156.	299.7	0.5339E+08	2.852	0.32039	532.81	1564.12	15.64	28515.	0.0308	3.29	773.	482.7	11.85	473593.
78.0	640472.	299.4	0.5466E+08	2.872	0.32019	536.51	1586.59	15.87	27446.	0.0308	3.35	782.	482.8	11.85	477080.
80.0	647787.	299.2	0.5595E+08	2.893	0.31997	540.20	1609.13	16.09	26369.	0.0308	3.41	790.	483.0	11.85	480566.
82.0	655103.	298.9	0.5725E+08	2.913	0.31974	543.87	1631.75	16.32	25285.	0.0308	3.47	799.	483.1	11.84	484051.
84.0	648396.	298.9	0.5856E+08	2.908	0.31176	538.93	1614.18	16.14	24201.	0.0303	3.54	790.	483.3	11.84	487512.
86.0	639216.	299.0	0.5985E+08	2.898	0.30269	532.50	1589.48	15.89	23130.	0.0297	3.60	779.	483.5	11.83	490910.
88.0	630035.	299.1	0.6112E+08	2.888	0.29392	526.08	1564.75	15.65	22071.	0.0292	3.66	768.	483.6	11.83	494244.
90.0	620854.	299.2	0.6237E+08	2.878	0.28543	519.68	1539.98	15.40	21025.	0.0286	3.71	756.	483.8	11.83	497517.
92.0	611674.	299.3	0.6360E+08	2.867	0.27720	513.29	1515.24	15.15	19992.	0.0281	3.77	745.	483.9	11.82	500729.
94.0	602493.	299.4	0.6481E+08	2.856	0.26923	506.93	1490.53	14.91	18971.	0.0276	3.83	733.	484.1	11.82	503882.
96.0	593312.	299.5	0.6601E+08	2.845	0.26150	500.58	1465.79	14.66	17964.	0.0271	3.88	722.	484.2	11.82	506978.
98.0	584131.	299.6	0.6719E+08	2.833	0.25399	494.24	1441.03	14.41	16969.	0.0266	3.93	711.	484.4	11.81	510016.
100.0	574951.	299.7	0.6835E+08	2.821	0.24670	487.90	1416.24	14.16	15986.	0.0261	3.99	699.	484.5	11.81	512999.
102.0	565770.	299.8	0.6949E+08	2.808	0.23960	481.57	1391.44	13.91	15017.	0.0256	4.04	688.	484.7	11.80	515927.
104.0	556589.	300.0	0.7061E+08	2.795	0.23270	475.24	1366.65	13.67	14060.	0.0251	4.09	677.	484.9	11.80	518801.
106.0	547408.	300.1	0.7171E+08	2.782	0.22600	468.92	1341.89	13.42	13116.	0.0246	4.14	665.	485.0	11.80	521622.
108.0	538228.	300.2	0.7280E+08	2.768	0.21946	462.61	1317.11	13.17	12184.	0.0242	4.19	654.	485.2	11.79	524391.
110.0	529047.	300.3	0.7387E+08	2.754	0.21310	456.29	1292.33	12.92	11265.	0.0237	4.24	643.	485.3	11.79	527109.

SHUTTLE HYBRID MOTOR STUDY - FUEL 7 - PCAVG=XXX 96" PUMP FED FLEXSEAL 19-AUG-89 13:13:19

TIME	THRUST	ISP	TOTIMP	O/F	GO	WDOTF	WDOTO	WDOTP	WTF	RREG	DWEB	PC	AT	EPS	ABURN
112.0	519866.	300.5	0.7492E+08	2.740	0.20689	449.96	1267.55	12.68	10358.	0.0233	4.28	631.	485.5	11.78	529777.
114.0	510686.	300.6	0.7595E+08	2.725	0.20084	443.64	1242.77	12.43	9465.	0.0228	4.33	620.	485.6	11.78	532394.
116.0	501536.	300.8	0.7696E+08	2.710	0.19494	437.32	1218.07	12.18	8583.	0.0224	4.37	609.	485.8	11.78	534963.
118.0	492481.	300.9	0.7795E+08	2.694	0.18924	431.07	1193.68	11.94	7715.	0.0220	4.42	598.	485.9	11.77	537484.
120.0	437902.	302.0	0.7891E+08	2.575	0.16405	395.08	1044.28	10.44	6872.	0.0201	4.46	532.	486.1	11.77	539921.
122.0	327684.	302.4	0.7967E+08	2.303	0.11779	320.50	755.60	7.56	6153.	0.0162	4.50	401.	486.3	11.77	541989.
124.0	226543.	297.9	0.8022E+08	2.007	0.07864	247.76	507.54	5.08	5585.	0.0125	4.53	282.	486.4	11.76	543620.
126.0	134478.	284.0	0.8058E+08	1.669	0.04567	174.41	296.10	2.96	5158.	0.0088	4.55	171.	486.6	11.76	544842.
128.0	81143.	264.5	0.8079E+08	1.413	0.02761	125.34	179.59	1.80	4859.	0.0063	4.56	104.	486.7	11.75	545696.
130.0	49638.	244.9	0.8092E+08	1.203	0.01698	90.87	110.68	1.11	4641.	0.0046	4.57	63.	486.9	11.75	546317.
132.0	26773.	229.7	0.8100E+08	0.959	0.00874	58.95	57.05	0.57	4491.	0.0030	4.58	34.	487.0	11.75	546745.
132.7	20888.	222.1	0.8102E+08	0.875	0.00672	49.73	43.90	0.44	4451.	0.0025	4.58	27.	487.1	11.75	546860.

TFLGHT= 132.740 TARRVL= 132.740
ISTP= 6)) FUEL WEIGHT LIMIT

FUEL WEIGHT LIMIT (6.0% RESIDUAL) ACTUAL= 6.00%
OXIDIZER WEIGHT LIMIT (1.0% RESIDUAL)

SHUTTLE HYBRID MOTOR STUDY - FUEL 7 - PCAVG=XXX 96" PUMP FED FLEXSEAL 19-AUG-89 13:13:19

DESIGN VALUES PAYOFF=-(DWPLD-PLDTGT)

IDES= 0 ITHROT= 5
NPORT= 18 NOTRP= 12 NCTRP= 5

SIZES

DMOTOR=	96.00000	DGRAIN=	93.30000	DOX=	93.30000
LMTR=	1382.114	LGRAIN=	399.9540	LOX=	744.7576
LCASE=	441.0660	LDOMES=	54.81600	LINS=	399.9540
LIS=	83.00160	LNC=	118.0800	LNOZ=	113.2883
LBSTR=	1472.786				
TCREQ=	0.0000000E+00	TWOX=	0.5000000		
DTO=	24.63819	DEXIT=	85.34920	TCINS=	0.3500000
ATO=	476.7684	AEXIT=	5721.221	THINS=	2.000000
ALFNOZ=	15.00000	EPSO=	12.00000		
APORTO=	1751.537	ABURNO=	287252.1	WEB=	4.803882
RO1MIN=	3.368969	RO1=	4.877487	RO2=	14.48525
R1=	22.31769	R2=	31.92546	R3=	41.84612
R4=	46.65000				
A0=	74.73812	DOHYD=	9.754975	LG/DOH=	41.00000
A1=	104.9375	D1HYD=	9.754976	LG/D1H=	41.00000
A2=	96.00930	D2HYD=	9.754977	LG/D2H=	40.99999
VFCASE=	0.7052962	VFGRAIN=	0.7438076		
L/DCASE=	4.594437	L/DGRAIN=	4.286752		

WEIGHTS

WMOTOR=	311358.4	WPUMP=	3500.000	WNOZ=	4630.000
WINRT=	35246.78	WCASE=	6097.536	WOTANK=	2170.764
WMISC=	14893.00	WINS=	3955.485	PMF=	0.8867968
WTPROP=	276111.6	WTFUEL=	74175.36	WTOX=	199936.9
WPUMPF=	1999.369				

P&W METAL/COMPOSITE OXIDIZER TANK:

```
WMETSH=    1183.608        WCOMPW=    734.6531        WOXINS=    252.5030

REGRESSION EQUATION

  RREG=0.076*60**0.53 *(PC/RCREF(1))**0.13
       *(LGRAIN/RCREF(2))**0.00 *(DHYAVG/RCREF(3))**-.20

FINAL FLIGHT VALUES

WDOMAX=    2113.715        WTFBRN=    69724.84        WTOBRN=    197869.5
 PCAVG=    748.0544          MEOP=    1053.258         PCDES=    1474.561
O/FAVG=    2.759551            DT=    24.90377
TOTIMP=  8.1016064E+07       FAVG=    610337.9        ISPAVG=    300.5348
IMPRQD=  8.1000000E+07        VEL=    18972.65
   DWP=   -11571.66        DWINRT=   -6631.656
  DISP=    34.73477        DAMREF=    21.20048         DWPLD=    28103.70

PFTOTIMP= 0.965731E-02


NPAYOFF= 5   PAYOFF=-1.810370        SUMPEN=0.9657309E-02    NRUN=     1


CPTIME=      7.36
EOF
```

Report Documentation Page

1. Report No.	2. Government Accession No.	3. Recipient's Catalog No.

4. Title and Subtitle
Hybrid Propulsion Technology Program
Volume 1 - Conceptional Design Package
Volume 2 - Technology Definition Package

5. Report Date
9-28-89

6. Performing Organization Code

7. Author(s)
Gordon E. Jensen, Allen L. Holzman, Steven O. Leisch, Joseph Keilbach, Randy Parsley, John Humphrey

8. Performing Organization Report No.
Proj 2027-FR

10. Work Unit No.

9. Performing Organization Name and Address
United Technologies Corporation/Chemical Systems Div.
P O Box 49028
San Jose, CA 95161-9028

11. Contract or Grant No.

12. Sponsoring Agency Name and Address
National Aeronautics and Space Administration
Washington, D.C. 20546-0001
Marshall Space Flight Center
Huntsville, AL

13. Type of Report and Period Covered
Final Report for period
March 6, 1989 to Sept 28, 1989

14. Sponsoring Agency Code

15. Supplementary Notes

16. Abstract

A concept design study was performed to configure two sizes of hybrid boosters - one which duplicates the advanced shuttle rocket motor vacuum thrust time curve and a smaller, quarter thrust level booster. Two sizes of hybrid boosters were configured for either pump-fed or pressure-fed oxygen feed systems. Performance analyses show improved payload capability relative to a solid propellant booster. Size optimization and fuel safety considerations resulted in a 4.57M (180 inch) diameter large booster with an inert hydrocarbon fuel. The preferred diameter for the quarter thrust level booster is 2.53M (96 inches). As part of the design study critical technology issues were identified and a technology acquistion and demonstration plan was formulated. The demonstration plan would culminate with test firings of a 3.05M (120 inch) diameter hybrid booster.

17. Key Words (Suggested by Author(s))	18. Distribution Statement
Hybrid booster, solid fuel, fuel regression, sizing study, oxidizer feed systems, test program, technology requirements.	Unclassified-unlimited

19. Security Classif. (of this report)	20. Security Classif. (of this page)	21. No. of pages	22. Price
Unclassified	Unclassified		

NASA FORM 1626 OCT 86